THÈSE

En vue de l'obtention du

DOCTORAT DE L'UNIVERSITÉ DE TOULOUSE

Délivré par :

Institut National Polytechnique de Toulouse (Toulouse INP)

Discipline ou spécialité :

Génie des Procédés et de l'Environnement

Présentée et soutenue par :

Mme NURUL NADIAH BINTI ABD RAZAK

le mardi 29 novembre 2022

Titre :

Hydrodynamique et cinétique de la synthèse catalysée par la lipase des diacylglycérols (DAG) dans les systèmes discontinus et continus

---

École doctorale :

Mécanique, Énergétique, Génie civil, Procédés (MEGeP)

Unité de recherche :

Laboratoire de Génie Chimique (LGC)

Directeur(s) de Thèse :

M. PATRICK COGNET

MME YOLANDE PERES

Rapporteurs :

MME KARINE DE OLIVEIRA-VIGIER, UNIVERSITE DE POITIERS

MME NGOH GEK CHENG, UNIVERSITY OF MALAYA

Membre(s) du jury :

M. MISRI GOZAN, UNIVERSITE D'INDONESIE, Président

MME GEW LAI TI, SUNWAY UNIVERSITY, Membre

MME YOLANDE PERES, TOULOUSE INP, Membre

M. MOHAMED KHEIREDDINE AROUA, SUNWAY UNIVERSITY, Membre

M. PATRICK COGNET, TOULOUSE INP, Membre

M. SULAIMAN AL-ZUHAIR, United Arab Emirates University, Membre

HYDRODYNAMIQUE ET CINETIQUE DE LA SYNTHESE DES DIACYLGLYCEROLS (DAG) CATALYSEE PAR LA LIPASE DANS LES SYSTEMES DISCONTINUS ET CONTINUS

Résumé

Les diacylglycérols (DAG) ont été largement utilisés dans les industries alimentaires, médicales, cosmétiques et pharmaceutiques grâce à leurs propriétés exceptionnelles en tant qu'émulsifiants, stabilisants et additifs nutritionnels pour l'homme. Comme alternative à l'utilisation de catalyseurs chimiques, cette étude a examiné la synthèse de dioléates de glycérol (GDO) par estérification du glycérol avec l'acide oléique par la *Candida antartica* lipase B (CALB 1) dans les systèmes batch et à flux continu. La première section de ce travail a examiné les effets de différents systèmes de solvants sur la conversion, le rendement et la sélectivité des oléates de glycérol. Les propriétés rhéologiques des systèmes sans solvant, ou utilisant comme solvants l'acétone, le tert-butanol ou un mélange, ont montré un comportement d'écoulement newtonien, et leurs viscosités ont diminué à des températures élevées. Par rapport aux monooléates de glycérol (GMO) et au trioléate de glycérol (GTO), la synthèse de GDO a conduit à un rendement et à une conversion plus élevées (70 %) avec une sélectivité de 54 %, à 40 ºC en 2 h dans un mélange acétone:*tert*-butanol. La deuxième section se concentre sur l'optimisation et la cinétique de la synthèse de GDO catalysée par les lipases en utilisant un réacteur discontinu. Une conversion élevée de l'acide oléique de 73% et une sélectivité du GDO de 77% ont été obtenues dans un mélange de acétone:*tert*-butanol 70:30 (v/v) à 45°C et avec une quantité d'enzyme de 0,15g. A 45°C, le modèle cinétique de Ping-Pong Bi-Bi, sans inhibition du substrat, donne le meilleur ajustement avec des valeurs de paramètres de Vmax = 1.21 M h^{-1}, K_m^G = 1.81 M et K_m^{OA}= = 6.81 M, pour les concentrations de glycérol et d'acide oléique entre 0.31 et 1.32 mol L^{-1} et 1.88 à 2.13 mol

L^{-1}, respectivement. La dernière section s'intéresse à la synthèse enzymatique de GDO dans un système à flux continu. La conversion maximale de l'acide oléique et la sélectivité du GDO ont atteint 85% et 74% respectivement, à 77 min de temps de passage (2×10^{-5} L min^{-1}) avec un rapport molaire 1,6:1 d'acide oléique:glycérol à une température constante de 45 ºC. Les études hydrodynamiques ont montré que la réaction d'estérification est cinétiquement contrôlée et non affectée par le transfert de matière externe et interne. En utilisant le modèle de Lilly-Hornby pour l'évaluation cinétique, les valeurs de Km augmentent avec le débit, tandis que Vmax semble être indépendant du débit. Les tests de réutilisation ont révélé que l'activité de la lipase immobilisée reste la même après 9 cycles de réaction successifs. Après 11 jours de fonctionnement, la stabilité de la lipase dans le milliréacteur à lit fixe continu n'a diminué que de 5 à 7 %, ce qui indique une opérabilité et une recyclabilité satisfaisantes. Les résultats globaux ont mis en évidence tout l'intérêt de l'utilisation de la lipase dans la synthèse du DAG dans des réacteurs discontinus et des réacteurs à flux continu. Ce travail a montré que la conversion de l'acide oléique et la sélectivité en GDO atteintes étaient de 73-85 % et 74-77 %, respectivement. Le temps de réaction optimal pour la synthèse de GDO dans un réacteur discontinu est de 2 h et peut être réduit à 1,3 h dans un réacteur à flux continu. Contrairement à l'approche du système discontinu, la lipase peut être facilement éliminée et efficacement recyclée de la colonne du réacteur à flux sans subir de changements de conversion appréciables. En utilisant les avantages de l'intensification des procédés, les résultats obtenus à partir des travaux pourraient être appliqués à la conception de procédés futurs et à l'extrapolation de la synthèse du DAG à des fins de commercialisation.

Mots-clés : Diacylglycérols, catalyseur vert, Candida antartica lipase B, intensification des procédés, cinétique enzymatique

HYDRODYNAMICS AND KINETICS OF LIPASE-CATALYSED SYNTHESIS OF DIACYLGLYCEROLS (DAG) IN BATCH AND CONTINUOUS FLOW SYSTEMS

ABSTRACT

Diacylglycerols (DAG) have been extensively used in food, medicine, cosmetic and pharmaceutical industries due to their outstanding properties as emulsifiers, stabilizers and nutritional benefits to human. To circumvent the use of chemical catalysts, this study investigated the synthesis of glycerol dioleates (GDO) through esterification of glycerol with oleic acid by *Candida antartica* lipase B (CALB 1) in the batch and continuous flow systems. The first section of this work examined the effects of different solvent systems on conversion, yield, and selectivity of glycerol oleates. The rheological properties of solventless, acetone, *tert*-butanol, and blended solvents systems exhibited Newtonian flow behavior, and their viscosities decreased at elevated temperatures. As compared to glycerol monooleates (GMO) and glycerol trioleate (GTO), GDO synthesis showed the highest yield (70%) and selectivity (54%) achieved at 40ºC within 2 h in the mixed solvents of acetone*:tert*-butanol at an enzyme load of 0.15 g. The second section focused on the optimization and kinetics of lipase-catalyzed synthesis of GDO using a batch reactor. A high oleic acid conversion of 73% and GDO selectivity of 77% were obtained in acetone: *tert*-butanol 70:30 (*v/v*) mixture at 45°C and an enzyme load of 0.15 g. At 45°C, the Ping-Pong Bi–Bi kinetic model with no substrate inhibition gives the best fit with parameter values of V_{max} = 1.21 M h^{-1}, K_m^G = 1.81 M and K_m^{OA} = 6.81 M, for glycerol and oleic acid concentrations between 0.31 to 1.32 M and 1.88 to 2.13 M, respectively. The final section studied the enzymatic synthesis of GDO under a continuous flow system. The maximum oleic acid conversion and GDO selectivity were achieved at 85% and 74% respectively, at 77 min of residence time (2×10^{-5} L min^{-1}) with 1.6:1 molar ratio of oleic acid:glycerol at a fixed temperature of 45ºC. The GDO content

started to decrease after the water content reached 5%. Hydrodynamic studies showed that the esterification reaction is kinetically controlled and unaffected by external and internal mass transfer. Employing Lilly–Hornby model for kinetic evaluation, K_m values increased with increasing flow rates, whereas, V_{max} appeared to be flow rate independent. Reusability tests revealed that the activity of immobilized lipase remained the same after 9 successive reaction cycles. This was accomplished by using the same enzyme repeatedly. After 11 days of storage, the stability of the lipase in the continuous packed bed millireactor decreased only 5 to 7%, indicating satisfying operational results and recyclability. The overall findings highlighted the successful application of lipase in the synthesis of DAG in batch reactor and continuous flow reactors. It was discovered that oleic acid conversion and GDO selectivity were attained at 73-85% and 74-77%, respectively. The optimum reaction time for GDO synthesis in a batch reactor was 2 h and decreased to 1.3 h in a continuous flow reactor. In contrast to the batch system approach, lipase enzyme can be recycled effectively without suffering any appreciable conversion changes. Utilising the benefits of process intensification, the results obtained from work could be applied for future process design and up scaling of DAG for commercialization purpose.

Keywords: Diacylglycerols, green catalyst, Candida antartica lipase B, process intensification, enzyme kinetis

ACKNOWLEDGEMENT

First and foremost, I would like to express my uttermost gratitude to my supervisors, Prof. Mohamed Kheireddine Aroua and Dr. Jane Gew Lai Ti from Sunway University, Malaysia and Prof. Patrick Cognet and Assoc. Prof. Dr. Yolande Pérès from Laboratoire de Génie Chimique, Institut National Polytechnique de Toulouse (INPT), Université de Toulouse, France for always being available and guiding me throughout the entire process. Without the invaluable assistance and opportunities provided, I would not be possible to carry out this Dual PhD programme. Your encouragement and guidance are something that I truly value.

I am also indebted and appreciative to Sunway University for the financial support of Studentship, Postgraduate Research Grant (PGSUREC 2019/005) and MyPAIR PHC-Hibiscus (MyPAIR/1/2019/TK10/SYUC//1) as well as the financial support for the Dual PhD candidate from French government sponsorship (Embassy of France in Malaysia). Thank you for giving me the privilege to work in a variety of research environments, including Department of Biological Sciences (Sunway University, Malaysia), Laboratoire de Génie Chimique (LGC, France) and Maison Européenne des Procédés Innovants (MEPI, France).

I also would like to thank my parents and my siblings for getting me through the hard times. No words could express how grateful I am to be blessed with wonderful family members, who have been showing their love and motivation during this project.

Last but not least, thanks to the helpful laboratory staffs and my friends for any big or small contributions - truly cherish having each and every one of you in my life. Thank you.

TABLE OF CONTENT

Résumé		II
ABSTRACT		IV
ACKNOWLEDGEMENT		VI
TABLE OF CONTENT		VII
LIST OF FIGURES		XI
LIST OF TABLES		XV
LIST OF ABBREVIATIONS		XVII
CHAPTER ONE : INTRODUCTION		1
1.1	Growing interest in diacylglycerols (DAG) compounds and their potential benefits	1
1.2	Chemical and enzymatic synthesis of DAG	3
1.3	Application of continuous flow bioreactor for DAG synthesis	7
1.4	Research design and scope	8
1.5	Problem statements	10
1.6	Objectives of research	12
1.7	Outline of the thesis	12
CHAPTER TWO : LITERATURE REVIEW		15
2.1	Rapid biodiesel development	15
2.2	Global glycerol status	16
2.3	Glycerol properties	18
2.4	Acylglycerols	20
	2.4.1 Monoacylglycerols (MAG)	21
	2.4.2 Diacylglycerols (DAG)	24
	2.4.3 Triacylglycerol (TAG)	27
2.5	Database search strategy	29
2.6	Distribution of acylglycerols articles	31
2.7	Role of lipase in the enzymatic production of acylglycerols	32
	2.7.1 Glycerolysis	36
	2.7.2 Esterification	41
	2.7.3 Interesterification	48
	2.7.4 Transesterification (Acidolysis)	53

2.7.5 Transesterification (Alcoholysis) 59
2.7.6 Hydrolysis/Partial hydrolysis 60
2.7.7 Deacidification 61
2.8 Bioreactor design for acylglycerol production 65
2.8.1 Batch Reactor 66
2.8.2 Packed Bed Reactor 67
2.8.3 Bubble Column Reactor 70
2.8.4 Microwave and Ultrasonic Reactor 71
2.8.5 Microreactor 72
2.9 Summary and research gap 73

CHAPTER 3 : MATERIALS AND METHODS 75

3.1 Materials 75
3.1.1 Lipase enzymes 75
3.1.2 Chemicals 75
3.2 Workflow of the study 76
3.3 Preliminary study in a batch system 77
3.3.1 Synthesis of glycerol oleates 77
3.3.2 Determination of lipase activity 79
3.4 Optimization of GDO synthesis 80
3.4.1 Optimization of GDO synthesis in a batch system using Response Surface Methodology (RSM) 80
3.4.2 Optimization of GDO synthesis in a continuous flow system using one-factor-at-a-time (OFAT) method 82
3.5 Mass-transfer limitation study in the batch and continuous flow systems 85
3.5.1 External mass transfer parameters 86
3.5.2 Internal mass transfer parameters 88
3.6 Kinetic studies of glycerol oleates synthesis 88
3.6.1 Kinetic study in a batch system 88
3.6.2 Kinetic study under continuous flow system 90
3.7 High Performance Liquid Chromatography (HPLC) analysis 91
3.7.1 HPLC conditions employed for the separation glycerol oleates in the preliminary study 91
3.7.2 HPLC conditions employed for the optimization of GDO in batch and continuous flow systems 92

3.8 Thermochemical analysis 93
3.9 Rheological analysis and log *P* for the solvents 95
3.10 Water content determination 96

CHAPTER 4 : RESULTS AND DISCUSSION 97

4.1 Preliminary study: Synthesis of glycerol oleates 97
4.1.1 Screening for a suitable lipase and its activity 97
4.1.2 Rheological properties and log P for the solvents 99
4.1.3 Yield profile for GMO, GDO and GTO in solventless vs. solvent systems 104
4.1.4 Conversion, selectivity & reaction rates of GMO, GDO and GTO. 109
4.1.5 Thermochemical analysis 113
4.1.6 Concluding remarks from the preliminary study 115
4.2 Batch reactor study: Investigation on GDO synthesis 116
4.2.1 Experimental data of the response surface methodology 115
4.2.2 Contour plot and surface plot on optimization of selected operating variables of oleic acid conversion (%) and GDO selectivity (%). 123
4.2.3 Optimization of oleic acid conversion (%) and GDO selectivity (%) and validation of the models 124
4.2.4 Proposed kinetic mechanism of GDO 127
4.2.5 Concluding remarks from the batch reactor study 135
4.3 Continuous flow reactor study: Investigation on GDO synthesis 136
4.3.1 Effect of enzyme concentrations and water contents 136
4.3.2 Effect of substrate concentrations 138
4.3.3 Effect of flow rates and residence times 140
4.3.4 Mass transfer limitation study 146
4.3.5 Kinetic parameters determination 150
4.3.6 Reusability and storage stability of *Candida antartica* lipase B (CALB 1) in the continuous flow reactor 153
4.3.7 Concluding remarks from the continuous flow reactor study 154

CHAPTER 5 : CONCLUSIONS 155

5.1 Conclusions 155
5.2 Study Limitations 156
5.3 Future Recommendations 156

5.4 Significance of the findings and future prospects 157

REFERENCES 160

LIST OF PUBLICATIONS & PAPERS PRESENTED 183

APPENDICES 184

LIST OF FIGURES

Figure 2.1	Schematic diagram of the transesterification of lipids.	16
Figure 2.2	Production of biodiesel and glycerol from 2003 to 2020. Adapted from Koranian *et al.*, (2022).	17
Figure 2.3	Illustration of the chemical structure of glycerol.	19
Figure 2.4	Illustration of the chemical structure of different isomeric forms of MAG.	21
Figure 2.5	Illustration of the chemical structure of different isomeric forms of DAG.	24
Figure 2.6	Illustration of the chemical structure of TAG.	27
Figure 2.7	Flow diagram of the systematic review information adopted with modification from PRISMA.	30
Figure 2.8	Yearly distribution of the acylglycerol compounds based on the selected articles.	32
Figure 2.9	Distribution of lipase catalysed reactions and type of lipases.	35
Figure 2.10	Distribution of lipase catalysed reactions and acylglycerol compounds.	36
Figure 2.11	Schematic diagram of glycerolysis reaction.	36
Figure 2.12	Schematic diagram of esterification reaction.	41
Figure 2.13	Schematic diagram of interesterification reaction.	48
Figure 2.14	Schematic diagram of acidolysis reaction.	53
Figure 2.15	Schematic diagram of alcoholysis reaction (a) TAG with alcohol (b) TAG with tri-fatty acids.	59
Figure 2.16	Schematic diagram of hydrolysis reaction.	60
Figure 2.17	Total studied number of reactors.	65
Figure 3.1	Schematic flow and organization of work on the study of the lipase-catalysed synthesis of GDO.	77
Figure 3.2	Schematic diagram of the preliminary study of glycerol oleates in a batch system.	79
Figure 3.3	Schematic diagram of the optimization and kinetic studies of GDO in a batch system.	81

Figure 3.4	Schematic diagram of the optimization, mass transfer and kinetic studies in a continuous flow system.	84
Figure 4.1	*Candida antartica* lipase B (CALB 1) activities assayed at different temperatures. *(The standard deviation of the triplicate measurements was <5 %)*	99
Figure 4.2	Evolution yield of GMO, GDO and GTO (%) as a function of time (h) performed in solventless (a-c) and *tert*-butanol (d-f) system at various temperatures (a, d) 35°C, (b, e) 50°C, (c, f) 65°C. Reaction conditions: 2 g of oleic acid; 0.26 g of glycerol; 1.2 g of solvent; 0.2 g of lipase enzyme; 1.28 g of 3 Å molecular sieves; and 200 rpm *(Symbol: ● yield of GMO; ○ yield of GDO; ▼ yield of GTO). (The standard deviation of the measurements of all graphs was <11 %)*	107
Figure 4.3	Evolution yield of GMO, GDO and GTO (%) as a function of time (h) performed in acetone (a-c) and in acetone:*tert*-butanol (d-e) at various temperatures (A, D) 35°C (b, e) 40°C (c, f) 45°C. Reaction conditions: 2 g of oleic acid; 0.26 g of glycerol; 1.2 g of solvent; 0.2 g of lipase enzyme; 1.28 g of 3 Å molecular sieves; and 200 rpm *(Symbol: ● yield of GMO; ○ yield of GDO; ▼ yield of GTO). (The standard deviation of the measurements of all graphs was <11 %)*	108
Figure 4.4	Percentage of conversion and selectivity of GMO, GDO and GTO as a function of temperature in different medium (a) solventless, (b) *tert*-butanol, (c) acetone, (d) acetone:*tert*-butanol. Reaction conditions: Reaction conditions: 2 g of oleic acid; 0.26 g of glycerol; 1.2 g of solvent; 0.2 g of lipase enzyme; 1.28 g of 3 Å molecular sieves; and 200 rpm.	111
Figure 4.5	Reaction rates of glycerol oleates as a function of temperature and solvent mixture (a) GMO, (b) GDO, (c) GTO. Productivity of glycerol oleates as a function of temperature and solvent mixture (d) GMO (e) GDO f) GTO. Reaction conditions: 2 g of oleic acid; 0.26 g of glycerol; 1.2 g of solvent; 0.2 g of lipase enzyme; 1.28 g of 3 Å molecular sieves; and 200 rpm *(Symbol: ● solventless; ○ tert-butanol; ▼ acetone; Δ tert-butanol: acetone).*	112
Figure 4.6	Standardized effects for oleic acid conversion (%) using a Pareto chart.	119
Figure 4.7	Residual plots for oleic acid conversion (%) (a) normality probability plot, (b) histogram plot, (c) standardized residual vs fitted value, and (d) standardized residual vs observation order.	120
Figure 4.8	Standardized effects for GDO selectivity (%) using a Pareto chart.	121

Figure 4.9	Residual plots for GDO selectivity (%) (a) normality probability plot, (b) histogram plot, (c) standardized residual vs fitted value, and (d) standardized residual vs observation order.	122
Figure 4.10	(a) Contour plot of conversion (%) (b) Surface plot of oleic acid conversion (%) (c) Contour plot of GDO selectivity (%) d) Surface plot of GDO selectivity (%).	123
Figure 4.11	(a) Time course of GDO synthesis (M) as a function of time (h) (b) Reaction rate of GDO synthesis as a function of oleic acid concentrations (M) at fixed glycerol concentration (M) (c) Reaction rate of GDO synthesis as a function of glycerol concentrations (M) at fixed oleic acid concentrations (M). Reaction condition: 45°C, 200 rpm and 0.15 g lipase enzyme.	128
Figure 4.12	Lineweaver–Burk plots. (a) Double reciprocal plot of 1/initial reaction rates of GDO *vs* 1/oleic acid concentrations (1/*v vs* 1/*s)* at various glycerol concentrations (b) Double reciprocal plot of 1/initial reaction rates of GDO *vs* 1/glycerol concentrations (1/*v vs* 1/*s)* at various oleic acid concentrations. Reaction condition: 45°C, 200 ppm and 0.15 g lipase enzyme.	129
Figure 4.13	Experimental and predicted initial rates (v_0) plots utilizing Ping-Pong Bi-Bi kinetic parameters model.	131
Figure 4.14	Reaction rate of GDO (M h^{-1}) at different oleic acid concentration (M) and temperatures.	132
Figure 4.15	Arrhenius plot of the lipase-catalyzed synthesis of GDO.	134
Figure 4.16	Effect of enzyme concentrations and water contents on esterification of oleic acid with glycerol. Reaction conditions: molar ratio of oleic acid:glycerol at 2.5:1; 1.1 g of molecular sieves; temperature at 45°C and flow rate of 5×10^{-5} L min^{-1}.	137
Figure 4.17	Effect of various ratio of substrates on esterification of oleic acid with glycerol. Reaction conditions: 0.15 g of lipase enzyme, 1.1 g of molecular sieves; temperature at 45°C and flow rate of 2×10^{-5} L min^{-1}.	139
Figure 4.18	Effect of flow rates and residence times on esterification of oleic acid with glycerol. Reaction conditions: 0.15 g of lipase enzyme, molar ratio of oleic acid:glycerol at 1.6:1; 1.1 g of molecular sieves; and temperature at 45°C.	141
Figure 4.19	Profiles of oleic acid conversion, GMO and GDO selectivity as a function of residence time under various ratio of oleic acid/glycerol. (a) Oleic acid conversion (b) GMO selectivity (c) GDO selectivity. Reaction conditions: 0.15 g of lipase enzyme; 1.1 g of molecular sieves; and temperature at 45°C. *(The standard deviation of the measurements of all graphs was 12 %)*	144

Figure 4.20 Profiles of Damköhler and Péclet number as a function of flow rates 149

Figure 4.21 Determination of kinetic parameters under continuous flow conditions (a) plot of Q ln (1-*f*) versus $fQ[OA]_0/K_m$ (b) K_m values as a function of Q. 151

Figure 4.22 Conversion of oleic acid during esterification with glycerol. (a) Reusability of CALB 1 (b) Storage stability of CALB 1. Reaction conditions: 0.15 g of lipase enzyme; molar ratio of oleic acid:glycerol: at 1.6:1; 1.1 g of molecular sieves; temperature at 45°C. 154

LIST OF TABLES

Table 1.1	Comparison of reaction condition from various studies in DAG production using chemical catalysts and biocatalysts	6
Table 2.1	Glycerol properties.	19
Table 2.2	Search string (SCOPUS Database)	29
Table 2.3	Enzymatic glycerolysis of the production MAG, DAG and TAG.	39
Table 2.4	Enzymatic esterification of the production MAG, DAG and TAG.	44
Table 2.5	Enzymatic interesterification of the production TAG	50
Table 2.6	Enzymatic acidolysis of the production TAG	55
Table 2.7	The production of MAG, DAG and TAG by other enzymatic techniques (a) alcoholysis (b) hydrolysis (c) partial hydrolysis (d) deacidification	62
Table 3.1	Summary of the variable levels in the reactions in RSM.	81
Table 4.1	Rheological characteristics of reaction medium at different temperatures.	103
Table 4.2	Gibbs energy change (ΔG), enthalpy (ΔH) and entropy change (ΔS) as a function of temperature of the reaction	114
Table 4.3	Box-Behnken Response Surface coded unit along with the experimental and predicted response of percentage of oleic acid conversion (%) and GDO selectivity (%)	117
Table 4.4	Values of model coefficients of oleic acid conversion	118
Table 4.5	Values of model coefficients of GDO selectivity	121
Table 4.6	Comparison of DAG production in batch system at its optimal condition	126
Table 4.7	Kinetic parameters for Ping Pong Bi-Bi model	130
Table 4.8	Reaction rate, apparent first-order rate constant, and V_{max} values obtained at different temperatures.	133
Table 4.9	Comparison of DAG production at its optimal condition using various reactors. Some of the information was adapted and modified from Abd Razak *et al.* (2021).	145
Table 4.10	The influence of flow rates on the hydrodynamic parameters of GDO determined from the esterification of oleic acid with glycerol in a continuous flow reactor catalyzed by immobilized CALB 1.	147

Table 4.11 Thiele modulus, external and internal effectiveness factors as a function of flow rates. 150

Table 4.12 Kinetic parameters of oleic acid and glycerol esterification under continuous flow system 153

LIST OF ABBREVIATIONS

Symbol & abbreviation	Unit	Description
ϕ		Thiele modulus
$[C]_0$	mol	Initial concentration of reactant which referring to [OA] or [Gly]
$[GO]$	mol L^{-1}	Concentration of glycerol oleates (M). Each [GO] is designated as follows; [GMO], [GDO] and [GTO] which represent the molar concentration of GMO, GDO and GTO respectively.
$[GO]_{total}$	mol L^{-1}	The sum concentration of glycerol oleates (M)
A	m^2	Area of the column
a_c	m^{-1}	Specific external surface area of the catalyst
C_R	mol L^{-1} min^{-1}	Reaction capacity
DAG		Diacylglycerols
d_{CALB}	m	Particle size of CALB 1 enzyme ($x10^{-4}$)
D_{mix}	m^2 s^{-1}	Diffusion coefficient
ε		Porosity of the bed column
$f_{[OA]}$		The proportion of reacted oleic acid.
GDO		Glycerol dioleates
Gly		Glycerol
GMO		Glycerol monoleates
GO		Glycerol oleates
GTO		Glycerol trioleate
K_{SL}	m s^{-1}	Solute - liquid mass transfer coefficient in solvent
l	m	Length of the column
log $P_{acetone}$		log P value of acetone
log $P_{t\text{-BuOH}}$		log P value of *tert*-butanol
M	m^3 mol^{-1}	Molar volume of solute (i.e. Glycerol or oleic acid) at its reaction temperature
MAG		Monoacylglycerols
η_E		External effectiveness factor
η_I		Internal effectiveness factor
OA		Oleic acid
ϕ		Association parameter of the liquid
ϕ_{mix}		Association parameter of mixed liquid
Q	L min^{-1} or m^3 s^{-1}	Volumetric flow rate
$r_{[GDO]}$	mol s^{-1}	Reaction rate of GDO
Re		Reynolds number
R_T	min	Residence time
Sc		Schmidt number
Sh		Sherwood number
T	°C	Absolute temperature in Kelvin
TAG		Triacylglycerols
U	m s^{-1}	Superficial velocity
V_R	L	Total volume of the reactor
V_{void}	L	Void volume
$W_{acetone}$	kg mol^{-1}	Molecular weight of the acetone
W_{mix}	kg mol^{-1}	Molecular weight of the mixed solvents

$W_{t\text{-}BuOH}$	kg mol^{-1}	Molecular weight of the *tert*-butanol
$x_{acetone}$		Mole fractions of acetone in reaction mixture
$x_{t\text{-}BuOH}$		Mole fractions of t-butanol in reaction mixture
z		Stoichiometric coefficients. For each [GO], z is calculated as follows: [GMO], z =1; [GDO], z =2 and [GTO], z =3.
μ_{mix}	kg m^{-1} s^{-1}	Mixture of fluid viscosity
ρ_{mix}	kg m^{-3}	Density of the liquid

CHAPTER 1 :

INTRODUCTION

Some information in Chapter 1 has been published in the following journals;

Abd Razak, N. N., Pérès, Y., Gew, L. T., Cognet, P., & Aroua, M. K. (2020). Effect of reaction medium mixture on the lipase catalyzed synthesis of diacylglycerol. *Industrial & Engineering Chemistry Research, 59*(21), 9869-9881.

Abd Razak, N. N., Gew, L. T., Pérès, Y., Cognet, P., & Aroua, M. K. (2021). Statistical optimization and kinetic modeling of lipase-catalyzed synthesis of diacylglycerol in the mixture of acetone/tert-butanol solvent system. *Industrial & Engineering Chemistry Research, 60*(39), 14026–14037.

Abd Razak, N. N., Cognet, P., Pérès, Y., Gew, L. T., & Aroua, M. K. (2022). Kinetics and hydrodynamics of *Candida antartica* lipase-catalyzed synthesis of glycerol dioleate (GDO) in a continuous flow packed-bed millireactor. *Journal of Cleaner Production*, 373, 133816.

1.1 Growing interest in diacylglycerols (DAG) compounds and their potential benefits

The prevalence of obesity problems, cardiovascular disease and high blood pressure due to high fat intake and the unfavorable effects of food lipids and oils in body have urged researchers to search for more desirable, functional and health-promoting lipids. Obesity is no longer affecting a few individuals but threatens global well-being. Growing worldwide data shows that many people including children are suffering from excessive body weight or obesity (James, 2004; Trasande *et al.*, 2012; Li *et al.*, 2018). The obesity level is declared as a "global epidemic" as the number nearly tripled since 1975 (World Health Organization**,** 2020). This global epidemic is resulted from combination factors such as genetic susceptibility, increasing consumption of high-energy foods such as food with high fat and sugar content as well as not getting enough physical activity in the lifestyle of modern society (Kopelman, 2000). Moreover, the latest studies suggest that obesity is farther complicated as it is linked with an increased risk of cancer (Vucenik *et al.*, 2012; Lega & Lipscombe, 2020) and also altered brain functions (Salsinha *et al.*, 2021).

DAG oil has attracted worldwide attention as it has the potential to overcome the accumulation of fat in body and subsequently is believed to be advantageous in the management and prevention of obesity. DAG exhibit a variety of biological functions such as suppressing accumulation of body fat (Matsuo & Tokimitsu, 2001; Meng *et al.*, 2004) and preventing the increase of body weight (Morita & Soni, 2009). Their positive effects on the health makes their production of considerable interest for pharmaceutical applications. The popular structured lipids that contains DAG are available commercially in Japan and the United States under the brand names "Econa" and "Enova," respectively. It was first established by Kao Corporation in Japan.

Studies also revealed that replacement with DAG oil in food products reduce 10 years risk of cardiovascular disease (Telle-Hansen *et al.*, 2012) and suppresses abdominal and visceral fat accumulation (Anikisetty *et al.*, 2018). In term of digestibility, the energy value of DAG are almost similar to triacylglycerols (TAG), however the biological functions of DAG in the human body differ from TAG. Many studies on animals and humans have been established to confirm the safety of DAG oil (Honda *et al.*, 2012; Bushita *et al.*, 2018; Honda *et al.*, 2018). Besides of its anti-obesity property, studies have shown that DAG possesses strong anti-oxidant activities (Waraho *et al.*, 2012) and it suppresses the postprandial increase in serum TAG (Lee *et al.*, 2019). It has been used in many fat-based food products and was found suitable as a Pickering emulsion for microencapsulation and microemulsion lipophilic active ingredients in food processes (Long *et al.*, 2015; Xue *et al.*, 2021).

DAG are basically processed by the similar digestive enzymes that break down TAG. Upon consumption, TAG are normally hydrolyzed to 1,2- and 2,3-DAG as intermediate products and further hydrolyzed to 2-MAG under the action of pancreatic lipase. They are then re-esterified to TAG and finally stored in the organism and significantly accumulate in the bloodstream as chylomicron complex. During TAG's

resynthetic process, they normally undergo 2-monoacylglycerol (2-MAG) pathway which involved two enzymes namely, DAG acyltransferase (DGAT) and MAG acyltransferase (MGAT) (Friedman & Nylund, 1980). These enzymes are responsible for the final synthesis step of TAGs using 2-MAGs as substrates.

Unlike TAG, DAG follow a different metabolic pathway after the absorption by the gastrointestinal epithelial cells due to the position of the fatty acid on the glycerol skeleton. Once DAG are hydrolyzed into 1-MAG, they are poorly re-esterified via the 2-MAG pathway as the DGAT and MGAT enzymes show low affinity toward 1-MAG (Yanai *et al.*, 2007; Phuah *et al.*, 2015). 1-MAG undergoes hydrolysis process, generating free fatty acids and glycerol. These compounds are required in the glycerol 3-phosphate pathway and then re-esterified to 1,3-DAG. Therefore, consumption of DAG causes the amount of free fatty acids in the portal vein increases due to a decrease in the enzyme activity associated with fatty acid production in the liver (Feltes *et al.*, 2013). This subsequently contributes to an increase in fatty acid β-oxidation that relates to the reduction in body fat and serum TAG levels (Meng *et al.,* 2004).

1.2 Chemical and enzymatic synthesis of DAG

The synthesis of DAG is an attractive option for the glycerol conversion as this material can be used for the products of commercial interest. Contributing about 75% of the worldwide production of emulsifiers, DAG known as an amphipathic molecule with hydrophilic and hydrophobic moieties that have various applications in many industries (Feltes *et al.*, 2013). At industrial scale, the production of DAG is commonly conducted by chemical glycerolysis of oils and fats. The reaction requires high temperatures nearly around 200 to 250°C, which contributed to the dark-colored, and burn tasted products (Sontag, 1982). It also involves the employment of alkaline catalysts such as sodium hydroxide (NaOH), potassium hydroxide (KOH), sodium methoxide ($NaOCH_3$) or

potassium acetate ($KC_2H_3O_2$) (Arpi *et al.*, 2016). Moreover, post purification step is required that is normally performed by molecular distillation (Sontag, 1982; Naik *et al.*, 2014). Enzymatic process offers an attractive approach as the reaction can be conducted under mild conditions. Moreover, it provides a promising route for DAG production by circumventing the application of hazardous chemicals and catalysts and toxic solvent. Enzymatic production of DAG can be carried out by direct esterification of glycerol with fatty acids, glycerolysis of oils or partial hydrolysis of oil (Feltes *et al.*, 2013; Phuah *et al.*, 2015).

Enzymes serve as an alternative catalyst to the industrial-made DAG due to its environmentally friendly nature. Lipases have been the important biocatalysts because of their excellent biochemical and physiological properties. Lipases can be found and extracted from diverse sources, including plants, animals, microbial (bacteria, fungus, and yeast) (Schmid & Verger, 1998; Sharma & Kanwar, 2014). Genetic engineering techniques have enabled the production of a growing variety of lipases from recombinant bacteria and yeasts as the main sources for industrial applications (Yucel *et al.*, 2018). Lipase works at milder and simple operating conditions and displays high selectivity to produce value added products. Among all the commercially available enzymes, lipase stands out as an important group of enzymes in biotechnology applications due to its versatilily; it catalyses a large number of reactions (Sarmah *et al.*, 2018).

There are numerous approaches in modifying lipase enzymes to make them suitable in organic solvent systems. Sharma *et al.*, (2019) studied and compared various immobilization techniques for *Candida rugosa* lipase. The immobilized lipases were synthesized using nanoparticle, cross-linked nanoparticles and conjugated magnetic nanoparticles formulations. They tested purified lyophilized *Candida rugosa* lipase and the other three formulations in different organic solvents namely, n-heptane, 1,4-dioxane,

and ter-butanol for biodiesel production. They discovered that the conjugated magnetic nanoparticles lipase showed better performance than the other formulation.

Recently, Li *et al.* (2021) obtained high purity DAG by combining partial hydrolysis and partial glyceride esterification by enzymatic approaches. Liu *et al.* (2021b) synthesized α-linolenic acid-enriched diacylglycerols (ALA-DAG) employing silkworm pupae oils as substrates. In another study, Zou *et al.* (2020b) produced docosahexaenoic acid-rich DAG-rich oil from microbial oil in a solvent-free system through enzymatic glycerolysis. Meanwhile Lakshmnarayanan *et al.* (2021) synthesized Fe_2O_3 nanoparticles from *Bauhinia tomentosa* leaf extract for the production of 1,3-DAG. Different reaction condition and techniques also have been established to improve miscibility of substrates and accelerate the lipase-catalyzed synthesis of DAG reactions, including the use of ionic liquids as solvents (Kahveci *et al.*, 2010), microwave irradiation (Matos et al, 2011; Hu *et al.*, 2013), and ultrasound irradiation (Fiametti *et al.*, 2012; Awadallak *et al.*, 2013).

A comparison of reaction conditions from various studies in DAG production using homogeneous, heterogeneous and enzyme catalysts is shown in Table 1.1**.** It is shown that biocatalysts offer effective ways for bypassing the conventional usage of extensive energy consumptions, high temperature and the risk of chemical catalyst leaching and poisoning (Amini *et al.*, 2017). There is still challenging efforts for researchers and technologists to make the enzymatic procedures economically appealing (Yang *et al.*, 2003). As compared to chemical catalysts, lipase requires a longer reaction time, which has raised severe criticism. Indeed, it is difficult to achieve a high conversion and selectivity of DAG in a short reaction time (Table 1.1).

Table 1.1. Comparison of reaction condition from various studies in DAG production using chemical catalysts and biocatalysts (Abd Razak *et al.*, 2020)

Homogenous/ heterogeneous catalyst	Type of reaction	Solvent	Substrate	Temperature (°C)	Time (h)	DAG composition (%)	Conversion (%)	Reference
hydrotalcite, layered double hydroxide	esterification	solventless	lauric acid	180	1	30[a]	99	Hamerski *et al.* (2014)
sulfuric acid	esterification	monoacylgycerol mixed with petroleum ether in 1:1 mass ratio	mixture of palmitic acid and oleic acid	70	20 min		88	Padzur *et al.* (2015)
mesoporous silica	esterification	supercritical carbon dioxide (SCC)	lauric acid	140	18	41[a]	93	Sakthivel *et al.* (2007)
functionalized organosilica	esterification	solventless	lauric acid	140	20 min	73[b]	45	An *et al.* (2016)
carbon-based heterogeneous ionic liquid	esterification	ionic liquid	lauric acid	140	1	77[a]	91	Sun *et al.* (2017)
Biocatalyst (lipase)	**Type of reaction**	**Solvent**	**Substrate**	**Temperature (°C)**	**Time (h)**	**DAG composition (%)**	**Conversion (%)**	**Reference**
Thermomyces lanuginose	esterification	hexane	oleic acid	55	72	30[a]	90	Tripathi *et al.* (2006)
Candida antarctica	esterification	*tert*-butanol	oleic acid	60	8	40[a]	75	Duan *et al.* (2010)
Candida antarctica	glycerolysis	*tert*-butanol	olive oil	55	12	57[a]	~75	Voll *et al.* (2011)
Rhizomucor miehei	glycerolysis	solvent free	lard	62	65°C for 2 h and then transferred to 45°C for 8 h	62[a]	76	Diao *et al.* (2017)
Candida antarctica	glycerolysis	solvent free	virgin coconut oil; consists mainly of lauric acid and myristic acid	50	24	3.6[a]	N/A	Derawi *et al.*, (2017)

[a]DAG yield (%) [b]DAG selectivity (%) N/A = not available

1.3 Application of continuous flow bioreactor for DAG synthesis

Application of flow chemistry for rapid transformations of organic synthesis has been extensively involved in the past decade (Gourdon *et al.*, 2015; Smith & Baxendale, 2018; Yasukouchi *et al.*, 2019; Mathieu *et al.*, 2020). However, innovation of continuous flow-bioreactions through the fusion of flow-chemistry and implementation of biocatalysts in the system has raised its attention only recently (Kecskemeti & Gaspar, 2018; Tamborini *et al.*, 2018; Britton *et al.*, 2018). As reviewed by De Santis *et al.* (2020), this significant interest of flow-bioreactions arose from two factors; efficient synthesis achieved in flow chemistry and excellent selectivities obtained in biocatalysis. During the continuous flow process, the reaction medium is pumped throughout the column at a particular flow rate, which determines the residence time.

A continuous reactor has the advantage over a batch reactor, as it does not require unloading, cleaning, and reloading after each batch. The usage of lipase enzyme in continuous flow reactor have received considerable interest in developing new reaction methodologies and some of these studies have focused on the kinetic resolution of alcohols (Csajagi *et al.*, 2008), regioselective hydrolysis of sugar (Bavaro *et al.*, 2018), synthesis of esters compounds (Denčić *et al.*, 2013; do Nascimento *et al.*, 2019), biodiesel production (Šalić *et al.*, 2018; Aloitabi *et al.*, 2019) and the production of synthetic fragrances (Salvi *et al.*, 2017; Tentori *et al.*, 2020). Except for sugar fatty acid ester studies (Watanabe *et al.*, 2001; Ye & Hayes, 2012; Du & Luo, 2012; Ruela *et al.*, 2013; Sutili *et al.*, 2015), the literature on lipase-catalyzed synthesis of emulsifier or surfactant in continuous flow system is still in its infancy and clearly lacking (Matos *et al.*, 2013; Junior *et al.*, 2012; Bavaro *et al.*, 2020).

1.4 Research design and scope

The present works examined the production of DAG by enzymatic esterification that was conducted in two different types of reactors, namely batch reactor (217 mm length × 18 mm ID) and continuous flow packed bed millireactor (100 mm length × 6.6 mm ID). The enzymatic esterification of glycerol with oleic acid is chosen as a model reaction. Glycerol with 90% purity was used in this study. Crude glycerol with purity less than 90% was not employed in this reaction because there are multiple contaminants present in crude glycerol, such as methanol and fatty acid methyl esters. As reviewed by Samul *et al.*, (2014), high impurities in crude glycerol can limit the yield of the targeted compounds. The proportions of chemical constituent in crude glycerol samples vary substantially depending on the raw material, type of catalyst used, recovery efficiency of the biodiesel (Yang *et al.*, 2012, Tian *et al.*, 2021). Furthermore, for the enzyme kinetic determination, lipase requires relatively high purity starting materials to eliminate inhibitory effects by other chemical such as methanol. Oleic acid, represents relevant industrial properties such as good fluidity with its unique double bond due to its *cis*-double bond in hydrocarbon chain. As oleic acid is a heat-sensitive compound, enzymatic esterification process appears to be a suitable alternative to the chemical process.

The reaction between glycerol with oleic acid is known to produce glycerol oleates which consists of glycerol monooleates (GMO), glycerol dioleates (GDO) and glycerol trioleate (GTO) that represent acylglycerols namely MAG, DAG and TAG, respectively. A suitable solvent system to improve the miscibility of substrates will result in homogeneous system and enhance the conversion of substrate, the reaction rate, and the product distribution, particularly in favor of DAG formation. Therefore, different types of solvent systems namely solvent, solvent blend and solvent-free systems were studied on the distribution of acylglycerols formation. Two solvents, *tert*-butanol and acetone were chosen as the reaction medium that represent polar and aprotic solvents respectively.

Since GDO exhibits an intermediate polarity between GMO and GTO, thus a mixture of acetone and *tert*-butanol was also tested. Besides facilitating the enzymatic reaction, both solvents can be certainly eliminated from the products during down-stream processes due to their low boiling points (acetone = 56ºC, *tert*-butanol = 82ºC). Acetone has been applied in the extraction of organic and non-organic compounds and shows no toxicity in an animal model (Anyaehie, 2009; Helen *et al.*, 2017). Meanwhile, *tert*-butanol has been studied and used for over 50 years as a co-solvent in many drugs in medical field (Bhatnagar *et al.*, 2020). *tert*-butanol serves as an organic co-solvent which seems appropriate for freeze-drying injectable drugs. It has been incorporated to increase the solubility of hydrophobic drugs (Kunz *et al.*, 2018; Kunz *et al.*, 2019).

As the reaction is being under the influence of thermodynamic equilibrium, optimization for enzymatic processes is essential in order to drive the reactions towards formation of a more desirable product such as GDO. There is a need to achieve a high conversion and GDO selectivity in a short reaction time at the optimal conditions using biocatalyst. Hence, the current research investigated the key factors that influence the efficiency of GDO production in the selected solvent system. With a goal to achieve the optimal response, a sequential set of experiments can be designated using a statistical technique namely Response Surface Methodology (RSM). RSM can be categorized into two designs; Central Composite Designs (CCD) and Box–Behnken designs (BBD) (Ferreira *et al.*, 2007). Experimental levels of CCD are comparable to factorial design with the exception that CCD comprising several central points with the range of extreme value. Unlike CCD, BBD are placed at the middle points of the particular extreme value (Said & Amin, 2015). Both modelling designs establish a correlation between the input and output factors which make them useful for analyzing and optimizing the behavior of any system (Chew *et al.*, 2015; Haq et al, 2020; Saat & Annuar, 2020). These techniques are convenient, reduce time and money as they cut off the required number of tests

considering the domain of the experimental set up. Thus, for the batch reaction system, BBD was employed to design a sequential set of experiments in order to achieve the optimal responses. Then, the optimized parameters obtained in a batch system were adopted in the continuous flow reactor for process intensification purpose. The optimization of the operating parameters for a continuous flow system was performed by changing one-factor-at-a-time (OFAT) for the enhancement production of DAG. OFAT is a technique that examines the effects of changing one parameter while holding all the others constant. This approach was used since it allows for the flexibility and customization of experimentation based on the circumstances.

In addition, the formation and distribution of GDO are associated with the fluid behavior and enzymatic performance. Therefore, the hydrodynamics and kinetics of immobilized enzyme were studied in both reactors. Understanding these aspects are essential for the rational design of DAG synthesis using the enzymatic method. The hydrodynamics works comprises a study of the rheological characteristics of the mixture, substrate movement from the bulk solution to the immobilized lipase's outer surface (external mass transfer limitation), and also a study of substrate diffusion into the inner part of immobilized lipase (internal mass transfer limitation). The enzyme kinetics data from the experimental works of the batch system were fitted to a proposed model involving two substrates reaction. Meanwhile for the continuous flow system, the kinetic data were fitted Lilly-Hornby model which accounted the residence time and hydrodynamic of the reaction.

1.5 Problem statements

It is crucial to examine the selection of organic solvent to increase the miscibility between oleic acid and glycerol. An appropriate solvent system will result in homogeneous system, improve substrate conversion, and enhance GDO formation. There

is no comprehensive comparative studies have been done on solventless, solvents and blended solvents. The role and effect of different solvent systems need to be explored. Thus, the current work evaluates the selectivity and yield of GDO production using enzymatic approach tested in various solvent systems and examines the composition of glycerol oleates as the polarity and viscosity of the reaction medium changed.

With regards to DAG production, an efficient process should be developed using a new methodology and recent technology. Making enzymatic methods commercially viable remains a difficult task as it requires long reaction time (Tripathi *et al.*, 2006; Amini *et al.* 2017). The study on different reactors (batch and continuous flow reactors) is indeed relevant for defining the suitable and advanced technology that can be employed to improve lipase-catalyzed synthesis of DAG. Once the suitable solvent system has been selected, the optimization of GDO is essential to maximize reaction yield and subsequently reduce the by-products. This can be done by evaluating various reaction parameters, including substrate concentration, reagents and solvent compositions, temperature and enzymes. Thus, employing statistical designs for the batch and continuous flow systems is necessary to achieve a high conversion and GDO selectivity in a short reaction time by using biocatalyst.

Fluid behavior and enzymatic efficiency both affect how DAG are formed and distributed. However, the study on fluid dynamic such as rheological properties of solvent concerning the enzymatic synthesis of DAG has been inadvertently overlooked. In this work, the rheological behaviors of each tested system are investigated. Rheological study is intended to examine the liquid behavior of different solvents at elevated temperatures and these properties becomes essential for determining mass transfer and diffusion limitations in enzymatic esterification. Meanwhile enzymatic efficiency is determined by the kinetic model of lipases in the selected solvent used in the reaction systems. Analysis on these areas would be useful for the rational design using the enzymatic method.

Understanding these areas provide a perfect insight into what an enzymatic synthesis is particularly doing in the both systems, particularly when dealing with immiscible substrates and producing multiple end products.

1.6 Objectives of research

The primary goal of this research is to develop a novel process for the production of GDO from glycerol. To deliver a coherent vision of the study, the objectives are systematically developed as follows:

1. To investigate the effect of solvent, solvent blend and solvent-free systems in esterification of glycerol with oleic acid in a batch system;
2. To optimize selected key parameters involved in the enzyme-catalyzed synthesis of glyceryl oleate in batch system and millireactor.
3. To compare the efficiency of milli-reactor with a batch reactor based on mass transfer and kinetics relationship of the optimized enzyme reaction.

1.7 Outline of the thesis

Generally, this thesis consists of five chapters. Overall, the thesis body comprised the introduction, literature review, methodology, results and discussion and the final conclusion. The contents of each chapter are described as below:

Chapter 1: Introduction

This chapter overviews aspects associated with DAG. The aspects include the growing interest in DAG compounds and their potential benefits, alternative catalyst of DAG synthesis and application of continuous flow bioreactor for DAG synthesis. This chapter also demonstrates the research design and scope of the current study, problem statements and the outline of the thesis.

Chapter 2: Literature review

This chapter includes a brief background on biodiesel development, global glycerol status, glycerol properties, and acyclglycerols properties (MAG, DAG and TAG). This chapter also specifically focusing on the systematic review method which was analyzed using Preferred Reporting Items for Systematic Review and Meta-Analyses (PRISMA) standard. The distribution of acylglycerols articles based on the given Database Search string are examined and discussed according two main area; lipase catalyzed reactions and bioreactor designs for acyclglycerols production.

Chapter 3: Materials and Methods

This chapter consist of the type of enzymes, chemicals and materials used in this research. The workflow, general methods and procedures are illustrated in schematic diagrams. The methods of esterification and the experimental set up in batch and continuous flow reactors are concisely described. Analytical procedures for determination of glycerol oleates, oleic acid and water contents as enzyme properties are explained in this chapter. All the hydrodynamics and mass transfer calculations are included in Chapter 3.

Chapter 4: Results and Discussion

In this chapter, the results are discussed in three sections. The first section focuses on the preliminary results consisting of the selection of the solvent system for GDO production, hydrodynamics, mass transfer effects, thermo-chemical results in a batch reactor system. The optimization of selected parameters and the development of the immobilized enzyme kinetic mechanism, kinetic model of GDO in the batch system are elaborated in the second section. The final section explains about the optimization, mass transfer limitations for both external and internal diffusivity, kinetic of GDO under a continuous flow system.

Chapter 5: Conclusion and future recommendations

The last chapter concludes all findings achieved based on the research objectives. The study limitations, recommendations for future works, significance contributions and future prospect are incorporated in this section.

CHAPTER 2 :

LITERATURE REVIEW

2.1 Rapid biodiesel development

Growing in energy consumption, increasing in the crude oil prices, global warming caused by greenhouse gas emissions, environmental degradation, and a rapid dwindling resource of fossil fuels have prompted the development of alternative fuels. Moving towards a greener society, biofuels stand out as one the promising substitution sources of energy for the current fossil fuels with low economic cost and high-energy output. Biofuels are sustainable fuels made from biomass and are divided into four categories: biodiesel, bioethanol, biogas, and biohydrogen (Amini *et al.*, 2017). Among them, biodiesel is the most viable option for effectively reducing our reliance on fossil fuels for transportation. The biodiesel industries have garnered much interest as they are abundant, cheap, eco-friendly, and renewable. It also has the ability to reduce greenhouse gas emissions by 41% during the combustion process, likely to lessen pollutants in a closed environment, and requires no modifications to be used in diesel engine, thus making it an environmentally friendly diesel substitute (Mahbub *et al.*, 2019).

A wide range of raw materials, catalysts, and technologies can be employed to obtain this promising fuel (Ayoub & Abdullah, 2012; Amini *et al.*, 2017). Due to its environmentally friendly and non-toxic nature, many scholars, industries players, and governments all over the world have taken interest in biodiesel. Biodiesel consists of long-chain alkyl esters that produced from edible and non-edible plants sources, animal fats, waste cooking or cultivation of algae or microorganism. Generally, with the presence of a catalyst, biodiesel is made through lipid transesterification with an alcohol that produces a mixture of alkyl esters as shown in Fig. 2.1. Biodiesel can be synthesized using a variety of procedures, including batch processing, supercritical, ultrasonic, and

microwave treatment (Vivek *et al.*, 2017). Biodiesel production is expected to raise by 4.5% each year in the future, reaching 41 Mm^3 in 2022 (Monteiro *et al.*, 2018). The European Union is likely to remain the primary producer and user of biodiesel, along with the United States, South America (Argentina, Brazil), and South East Asia (Thailand and Indonesia) dominating the current market (Nda-Umar *et al.*, 2019).

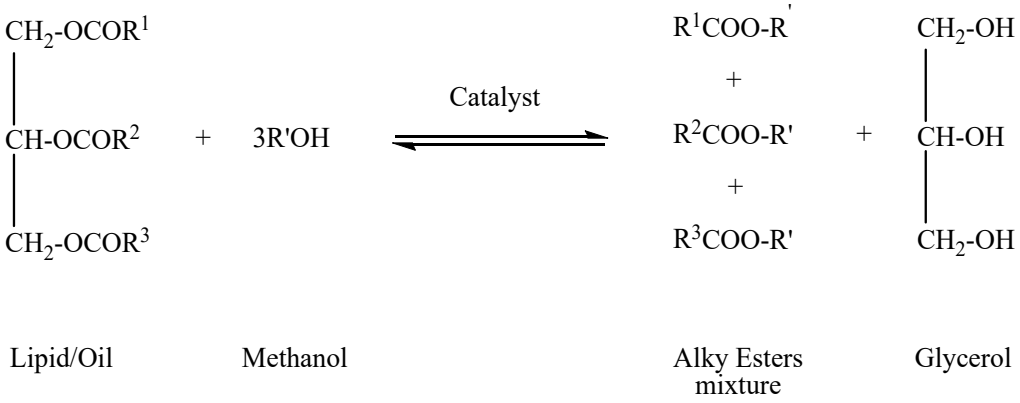

Figure 2.1. Schematic reaction diagram of the transesterification of lipids

2.2 Global glycerol status

Due to increasing research on biodiesel technology worldwide, current high production yielded a surplus amount of crude glycerol generated as a by-product, estimated at 10% (*w/w*) of the total biodiesel production (Ilham & Saka, 2016; Nda-Umar *et al.*, 2019). The greatest impediments to biodiesel commercialization is that the co-product glycerol's market has become saturated, resulting in a drastic drop in pricing and negatively impacting the biodiesel economy.

From the late 1990s to 2003, global glycerol production remained largely steady and at a very low level. In 2004, biodiesel production skyrocketed, accompanied by a massive surge in crude glycerol produced (Ayoub & Abdullah, 2012). Biodiesel production in European Union (EU) countries was estimated to be 1.93 million tonnes. Within ten years, it was estimated to be 10.37 million tonnes in 2013, rising to 11.58 million tonnes in 2016, with Germany and France leading the way. Fig. 2.2 clearly

illustrates the growing trend of the biodiesel production, crude glycerol production and crude glycerol price.

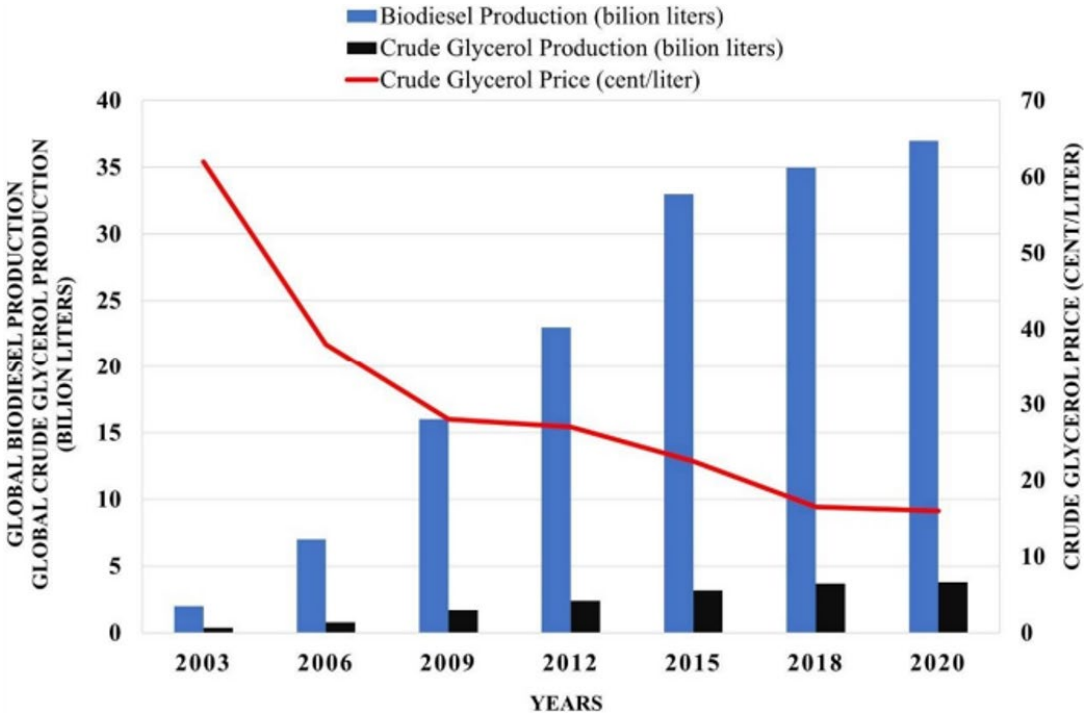

Figure 2.2. Production of biodiesel and glycerol from 2003 to 2020. Adapted from Koranian *et al.*, (2022).

The increased production of biodiesel was undoubtedly attributable to the increased output of glycerol. Consequently, some EU biodiesel producers are having significant difficulties disposing of extra glycerol due to the high cost of disposal (Samul *et al.*, 2014). It was ultimately proven when Dow Chemical halted its synthetic glycerol factory in Texas in 2007. Meanwhile in England, Procter & Gamble Chemicals shut its glycerol refinery in 2006 (Ciriminna *et al.*, 2014).

The current market is now unable to absorb all of the excessive glycerol generated from biodiesel which resulted in a very steep decrease in glycerol price accompanied by imbalance supply/demand imbalance for this chemical (Gholami *et al.*, 2014; Vivek *et al.*, 2017). Therefore, strategies for handling this surplus raw resource are urgently needed. One possible approach is through the conversion of glycerol into high-value and

useful products which has been the subject for many research. GRAIL, or "Glycerol Biorefinery Approach Towards the Production of High Quality Products of Industrial Value," was launched in 2013 by a European consortium with 15 associates from various countries with the aim of developing solutions as well as technologies to utilise glycerol and transform it into valuable products using a biorefinery technique (Anitha *et al.*, 2016). According to researchers and industry leaders, these transformation will improve biodiesel's economics by minimizing its production costs.

Transformation reactions turning biodiesel-derived glycerol into value-added compounds would be an effective and economically viable technique to explore. Being a building block in a wide range of processes, glycerol can be converted to different value-added derivatives such as acrolein, propylene glycerol (Gonzalez-Garay *et al.*, 2017), succinic acid (Efthymiou *et al.*, 2021), polyester (Velario *et al.*, 2018), acylglycerols (Abd Razak *et al.*, 2021), hydrogen gases (Carrero *et al.*, 2017), glycerol carbonates (Olivares *et al.*, 2020), acroleins (Pala Rosas *et al.*, 2017) and ethanol (Kostyniuk *et al.*, 2020) using chemical and enzymatic catalysts. Glycerol is an outstanding material that possess 2000 established utility as a high-valued starting material. It is used in a variety of products, including cosmetics, toiletries, sweeteners, softening agents, cough syrups, surface coatings, paints, and more (Díaz-Álvarez *et al.*, 2011).

2.3 Glycerol properties

Glycerol was discovered in 1779 by Swedish chemist, CarlWilhelm Scheele. Several years later in 1823, the French chemist, Michel Eugene Chevreul named the compound as ‘glycerin’. In 1855, the molecular formula of $C_3H_5(OH)_3$ was given by Charles-Adolphe Wurtz. Glycerol is the simplest trihydric alcohol with the IUPAC name of propane-1,2,3-triol (Fig. 2.3).

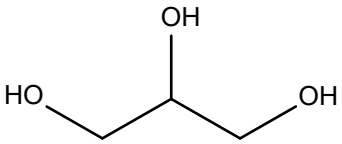

Figure 2.3. Illustration of the chemical structure of glycerol.

It is also commonly known as 1,2,3-propanetriol, 1,2,3-trihydroxypropane, glyceritol or glycyl alcohol. Glycerol is an oily liquid, water-soluble, sweet taste, clear, colorless, odourless, viscous and hygroscopic liquid with a high boiling point. The presence of its three hydroxyl groups make it easily dissolves in water, stable and can be employed in diverse reactions. A list of physical and chemical properties are shown in Table 2.1.

Besides transesterification process in biodiesel production, glycerol can be produced through saponification and hydrolysis processes in fatty acid and soap factories. Glycerol is generally divided into three types on the market: crude, purified, and synthetically produced glycerol. Both crude and purified glycerol are the byproduct of biodiesel manufacturing, however synthetic glycerol is achieved in a different way. Crude glycerol is different from refined and manufactured glycerol as it has a lower purity.

Table 2.1. Glycerol properties (Gholami *et al.*, 2014).

Property	Unit	Glycerol
Molecular formula	-	$C_3H_8O_3$
Molecular weight	g mol^{-1}	92
Density	g ml^{-1}	1.256
Dynamic viscosity	Pa.s	1
Refractive index	-	1.472
Dielectric constant	-	46
Boiling point	ºC	290
Heat of dissolution in water	J g^{-1}	-62
Specific heat capacity	J g^{-1} K^{-1}	2.38
Thermal conductivity	W m^{-1} K^{-1}	0.29
Thermal expansion coefficient	ºC	0.00052 (20-60ºC)
Flash point	ºC	199
Fire point	ºC	204
Autoignition	ºC	370

The low degree of purity of crude glycerol limits the option of its application. Many contaminants and other compounds are found in the crude glycerol produced by biodiesel, including methanol, organic and inorganic salts, water, vegetable colours, mono and diglyceride traces, and soap (Yang *et al.*, 2012, Tian *et al.*, 2021). As a result, large-scale biodiesel manufacturers may process crude glycerol to produce refined glycerol with higher purities ranging from 95.5 to 99 %, to be practically used and applied in a wide range of industries (Ayoub & Abdullah, 2012). Glycerol has diverse applications and its distribution of usage comprise categories such as textile (24%), food (21%), pharmaceutical (18%), cosmetic (18%), tobacco (6%) and paper and printing (5%) (Lima *et al.*, 2021).

2.4 Acylglycerols

Glycerol esterification produces a variety of valuable chemicals and has been a subject of great interest in recent years. Acylglycerols are primarily generated from the reaction between natural fats or oils. The reaction produces monoacylglycerols (MAG), diacylglycerols (DAG), and triacylglycerols (TAG), as well as a minor amount of unreacted glycerol. Due to versatility of lipids, the term 'Structured lipids' has been widely used which include acylglycerols (MAG, DAG, TAG) and phospholipids (Kim & Akoh, 2015). Structured lipids refer to a new type of functional lipids that can be synthesized by chemical, or enzymatic means. It can be achieved by altering the configuration and/or distribution of fatty acids in the glycerol backbone (Guo *et al.*, 2020).

MAG and DAG have distinct molecular structures than TAG, with MAG having two free hydroxyl groups and DAG having only one free hydroxyl group. Moreover, MAG and DAG have different physical and chemical properties than TAG as a result of

their structural variations. The differences include the following properties such as crystallization polymorphism, melting points, solid fat content, texture and rheology.

2.4.1 Monoacylglycerols (MAG)

The emulsifiers most widely employed by the worldwide are MAG and DAG as well as their organic acid derivatives. Among the acylglycerols, the MAG are the simple and most polar molecules comprising trihydric alcohol glycerol with only one hydroxyl group esterified with a long-chain fatty acid. They can be found in three different stereochemical forms as illustrated in Fig. 2.4.

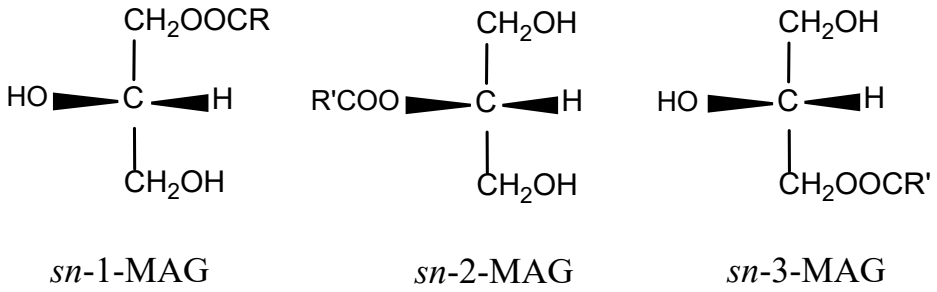

Figure 2.4. Illustration of the chemical structure of different isomeric forms of MAG.

1- or 3-MAG are referred to as 'α-monoacylglycerols,' while the 2 MAG are referred to as ' β-monoacylglycerols.'

2.4.1.1 Physico-chemical properties of MAG

In term of physico-chemical properties of MAG, Vereecken *et al.* (2009) studied the crystallisation and melting behaviour of both saturated and unsaturated MAG with various chain lengths with two isomers. The study was performed using DSC and X-ray diffraction (XRD). They found that the saturated MAG samples had higher crystallisation and melting temperatures with the increased of the chain length (Vereecken *et al.*, 2009). Three polymorphs comprising β, α, and sub-α with decreasing melting temperatures have been discovered for purified saturated MAG (1-MAG and 2-MAG). On the other hand,

the crystallisation and melting behaviour of unsaturated MAG was less complex. The XRD result confirmed that it was the stable β polymorph as one peak in the crystallisation and melting curves were obtained. It has been shown that the addition of MAG (monopalmitin) to refined, bleached and deodorized palm oil produced a rougher crystal structure (Verstringe *et al.*, 2013). In another investigation, it was revealed that MAG have the fastest crystal formation followed by DAG and then TAG. The experiments were conducted and analyzed using differential scanning calorimetry (DSC) (Basso *et al.*, 2010). It was hypothesized that the presence of distinct acylglycerols structures (MAG, DAG, and TAG) was the main cause of variances in crystallisation profiles.

Another physico-chemical characteristic is known as solid fat content (SFC). Fatty acid profiles, acylglycerols composition, and temperature are the key factors that determine the SFC. With the temperature range of 0 to 40°C, lard-MAG has been found to have the highest SFC, followed by lard-DAG and lard TAG, determined through SFC-temperature curves (Cheong *et al.*, 2009). The application of 3-5 % MAG enhanced the SFC of structured chicken fat and reduced induction period of crystallization (IP_{cryst}) (Naderi *et al.*, 2016). Meanwhile, Romain *et al.* (2013) isolated MAG from *Nephelium lappaceum L*. oil and found that MAG fractions had markedly increased SFC at all temperatures tested, regardless of purification level.

The rheological properties are normally determined using shear viscosity, viscoelasticity, and texture analysis. Shakerardekani *et al.* (2013) revealed that the addition of 1.5% MAG resulted in an increase in shear force, suggesting a strong spreadability of pistachio spread. Whereas adding distilled-MAG to sesame paste enhanced its viscosity with 8% distilled-MAG was suitable in minimising oil separation (Al-Mahasneh *et al.*, 2017).

2.4.1.2 Rational application of MAG

MAG are mostly employed as emulsifiers because they have higher emulsification activity than DAG. Due to their superior emulsifying qualities compared to the other acylglycerols, MAG with a high degree of purity are chosen for commercial application in the food sectors. Animal fats such as lard, tallow and hydrogenated vegetable oils obtained from soybean, rapeseed, and cottonseed are the most often utilised raw ingredients (Krog, 2018). Due to their emulsifying, stabilising, and conditioning qualities, they are commonly employed in bakery products, margarines, dairy products, and confectionary. In the food processing sector, MAG is used to stabilise both water-in-oil (such as margarine) and oil-in-water (such as artificial cream) emulsions (Subroto, 2020). A concentration of 0.5% is typically enough to produce a stable emulsion (Feltes *et al.*, 2013).

MAG are used to reduce the rate of crystallisation of palm stearin and to minimize the graininess of palm-based margarine (Saadi *et al.*, 2011). Naderi *et al.* (2018) demonstrated that the use of MAG from canola oil in creating liquid margarine and shortening resulting in good bakery products. They are commonly employed as emulsifiers and stabilisers in cookies (Goldstein *et al.*, 2011) and they can also be utilised to extend the shelf life of bread and cheese (Buňková *et al.*, 2010; Hauerlandová *et al.*, 2014). The effects of MAG such as 1-monocaprylin, and 1-monocaprin on spoiling inhibition on bread were investigated by Buňková *et al.* (2010). They found that application of microfilm of MAG (65 mg L^{-1}) over the bread surface inhibited fungus growth up to 14 days of storage. It was suggested that membranes are destabilised by 1-monocaprylin, which promotes membrane fluidity and the occurrence of phase boundary defects (Hyldgaard *et al.*, 2012). It also has been shown that MAG at a dose of 0.15% inhibited the growth and multiplication of both *Bacillus* species in processed cheese samples during the storage period (Hauerlandová *et al.*, 2014). When MAG such as

monolaurin and monocaprin were added to apple juice, the total viable counts of bacteria and yeasts decreased (Doležálková *et al.*, 2012).

In the recent study, Truong *et al.*, (2019), fabricated oil foams from oleogels by a whipping action and using MAG and native phytosterols (NPS) as co-gelators. The lipidic crystal network was altered by the addition of NPS, resulting in thinner, needle-like crystal morphologies. The result highlights the impact of lipidic crystal size on oleogel sample whippability, which is important for oleogel applicability on aerated food products.

2.4.2 Diacylglycerols (DAG)

DAG are much less polar than MAG. DAG are esters of the trihydric alcohol glycerol consisting of two of the hydroxyl groups are esterified with fatty acids. Owing to the existence of hydrophilic polar groups, DAG can be easily emulsified and possess better interfacial characteristics. Similar to MAG, DAG present in two configurations, 1,3-DAG and 1,2(2,3)-DAG (Fig. 2.5).

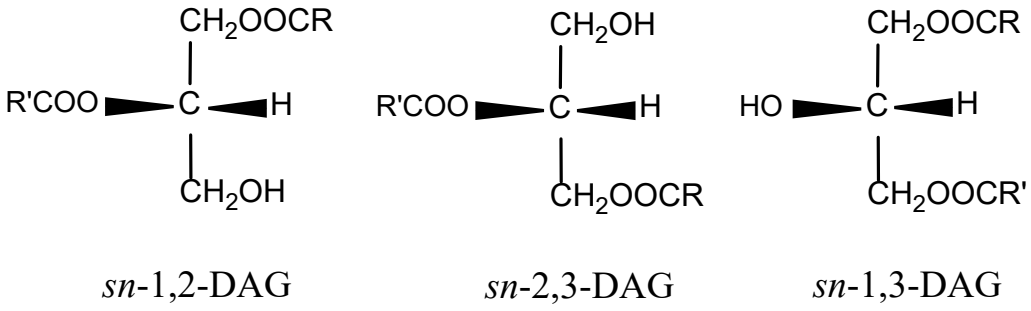

Figure 2.5. Illustration of the chemical structure of different isomeric forms of DAG.

2.4.2.1 Physico-chemical properties of DAG

Under the same composition of fatty acid, 1,3-DAG molecules crystallise faster and have a higher melting point than 1,2-DAG molecules. This is likely due to their different lamellar conformation, with 1,3-DAG forming a V-shaped structure and 1,2-

DAG forming a hairpin-shaped structure, respectively. The chemical structure and fatty acid chain lengths had a significant impact on crystal polymorphism of DAG. The effect of various purifying processes on crystal polymorphism and morphology was affected by the purity of the medium chain DAG, medium-long-chain DAG, and long-chain DAG end products (Wang *et al.*, 2020a). Saitou *et al.* (2012) observed that the DAG fractions crystallise in order, with high-melting molecules like 1,3-disaturated DAG crystallizing first, followed by 1,3-saturated-unsaturated and 1,3-diunsaturated DAG. 1,3-DAG likely to crystallize into β-form polymorph, wherease 1,2-DAG typically display α and β' form (Saitou *et al.*, 2012; Xu & Dong, 2017).

Saberi *et al.* (2011) examined the SFC profile of palm-derived DAG in variety fractions with palm-derived oils. It was discovered that palm-based DAG had a greater SFC profile than palm-based oils, specifically at temperatures beyond 15°C. Meanwhile, the SFC of long-chain-DAG was higher than medium-long-chain-DAG followed by medium-chain-DAG correlated to the high melting point of C18 and high crystallization onset temperature (Wang *et al.*, 2020a).

Ng *et al.* (2014) showed that increasing the amount of palm olein-based-DAG in the DAG emulsions had a significant impact on the rheological properties. High thixotropy was observed when 30% of palm olein-DAG was introduced. The yield stress, storage modulus, and loss modulus of rheological characteristics were all significantly affected by the palm olein--DAG content. The rheological parameters of palm kernel-based DAG-enriched mayonnaise were examined by Phuah *et al.* (2016a). They discovered that the mayonnaise exhibited similar gel-like behaviour, with a higher storage modulus and a loss tangent of less than 0.3. The viscoelastic characteristics were unaffected by storage time. In another study, physical characteristics revealed that combining DAG and polyglycerol polyricinoleate significantly increased the emulsion viscoelasticity which resulted in a higher deformation yield (Yang *et al.*, 2020).

2.4.2.2 Rational application of DAG

Like MAG, DAG are often used oil-in-water type emulsion foods and water-in-oil foods (Lo *et al.*, 2008). In the oil-in-water food application, Phuah *et al.* (2016a) replaced soybean oil in mayonnaise with palm kernel-based diacylglycerols (PK-DAG) at various concentration of 5–20%. Due to the decreased degree of unsaturated fatty acid, mayonnaise including PK-DAG has been observed to have higher oxidative stability. The findings indicated that up to 10% PK-DAG could be used in a healthy mayonnaise composition.

Meanwhile, in water-in-oil emulsion foods, blending ratio of 50 wt% of palm-based DAG with 35 wt% of sunflower oil and 15 wt% of palm kernel olein produced saturated fatty acids that are lesser compared to commercial soft tub margarine. Multiple iso-solid diagrams were adopted and analysed to find the best formulation conditions (Saberi *et al.*, 2012).

Liu *et al.* (2019) reported that the whipping properties, textural characteristics, and sensory evaluation were satisfactory within the range of DAG substitution from 10–30%. On the contrary, the end product's quality reduced at the greater DAG substitution of 40%. DAG showed considerable prospects as a partial replacement for hydrogenated palm kernel oil in whipped cream. Emulsions with higher DAG content favored higher lipolysis (Liu *et al.*, 2021a).

The effect of DAG concentration (2-10 wt%) on oleogel and foam properties was examined by Lei *et al.* (2020). The whipping and foaming stability of an oleogel containing 10% DAG was similar to that of a 6% fully hydrogenated palm oil. As a result, DAG can be potentially utilized as a substitute for fully hydrogenated palm olein (FHPO) in the production of thermo-responsive oil foams.

In the investigation of DAG emulsion stabilized by L-theanine and β-lactoglobulin complex, Xue *et al.* (2022) reported that by binding β -lactoglobulin as a surface stabiliser,

L-theanine was found to increase the droplet size, distribution emulsification stability and antioxidant capability of DAG.

2.4.3 Triacylglycerols (TAG)

Triglycerols (TAG) comprise three fatty acids esterified with a glycerol backbone. TAG are the form in which fat energy is stored in adipose tissue. The simplest is TAG with three identical fatty acids which is quite uncommon in nature. Mixed TAG contain two or three different fatty acids and constitute the majority of the fat in the body. Three carbons on glycerol permits stereochemically unique fatty acid bond positions: *sn*-1, *sn*-2, and *sn*-3 (Fig. 2.6). The melting point of TAG is determined by the physical characteristics and location of the fatty acids esterified to glycerol which include their chain length, number, position, and conformation of the double bonds, and the stereochemical position (Farfán *et al.*, 2013).

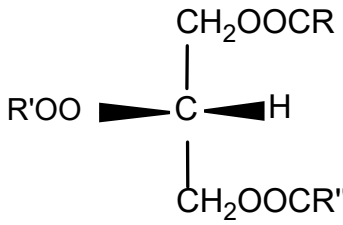

TAG

Figure 2.6. Illustration of the chemical structure of TAG

2.4.3.1 Physico-chemical properties of TAG.

TAG can exist in three polymorphic forms, α, β and β'. Using DSC and X-ray diffraction, the crystallisation and polymorphism characteristics of eight fat blends with the same saturated fat concentration (50%) but different TAG compositions were examined by Vereecken *et al.* (2010).The two-step crystallisation seen during DSC-stop and return studies which attributed by a polymorphic transition of the unstable α

polymorph to the more stable β′. The distribution of the β′ or β polymorph differed between blends, which can be explained by the fact that their TAG compositions differed. Pang *et al.* (2019) showed that the interesterified TAG had a high concentration of β' polymorph crystals and a high solid fat content, as well as moderate antioxidant activities. They esterified fats of beef tallow, palm stearin and camellia oil blends. In case of roll-in shortenings which consist of trisaturated and unsaturated TAG, they displayed similar crystal characteristics (β′ or mixed β′ and β) with other shortenings (Macias-Rodriguez & Marangoni, 2016).

As investigated by Oliviera *et al.* (2017), the SFC of TAG composition should not below than 10% for the optimal shape retention. The stability and resistance of fat products to oil exudation are normally determined by SFC between 20 and 22°C. The plastic fats contain plasticity and spreadability at 4-10°C to preserve their forms for certain period at ambient temperature (20-22°C) without oil effusion. To get this condition, total SFC of 15%–35% should be used (Pang *et al.*, 2019).

2.4.3.2 Rational application of TAG

Integrating fatty acids with varying chain lengths or adjusting their locations on the glycerol molecule, can change the nutritional value and metabolic activity of the lipid. Many studies have done on the esterified lipid/oil containing omega 3-polyunsaturated fatty acids **(**PUFAs), conjugated linoleic acid and/or other special fatty acids because of their advantageous effects such as antioxidative and low calories (Bakir *et al.*, 2018; Zou *et al.*, 2020a). Eicosapentaenoic acid (EPA) and docosahexaenoic acid (DHA) are incorporated into TAG due to their original diverse health benefits including the ability to reduce the risk of cardiovascular and neurological illnesses (Siriwardhana *et al.*, 2012). However, these structured TAG are ideal for the manufacturing of margarines, spreads,

and dressings. Bakery margarines and frying shortenings seem to be inappropriate due to the high vulnerability of omega-3 PUFAs to thermal oxidation (Osório *et al.*, 2009).

TAG comprise more than 96% of milk fat in butter (Staniewski *et al.*, 2021). The major disadvantage of milk fat is its high saturated fatty acid content, which has been associated to an increased risk of cardiovascular disease. Paula *et al.* (2015a) produced structured lipid by interesterification of milk fat butter with soybean oil in continuous fluidized bed reactor. The structured lipids obtained was rich in PUFAs and displayed higher spreadability than butter.

.

2.5 Database search strategy

In order to examine the acylglycerols articles which are related to the current study, the systematic review method was conducted by referring to the Preferred Reporting Items for Systematic Review and Meta-Analyses (PRISMA) standard. The study was identified on March 14, 2022, using the Scopus database. The systematic review process in selecting a number of relevant articles consisted of three main stages namely identification, screening, and eligibility. The first stage is the identification of keywords, followed by the process of searching for related and similar terms based on the thesaurus, dictionaries, encyclopaedia, and past research. Other terms combined with Boolean operators AND and OR. The search terms or keywords used is shown in Table 2.2.

Table 2.1. Search string (SCOPUS Database).

((("glycerol monooleate*" OR "GMO" OR "monoacylglyc*" OR "MAG" OR "diacylglyc*" OR "DAG" OR "glycerol dioleate*" OR "GDO" OR "Triacylglyc*" OR "TAG" OR "glycerol trioleate*" OR "GTO") AND ("lipase*") AND ("reactor*")))

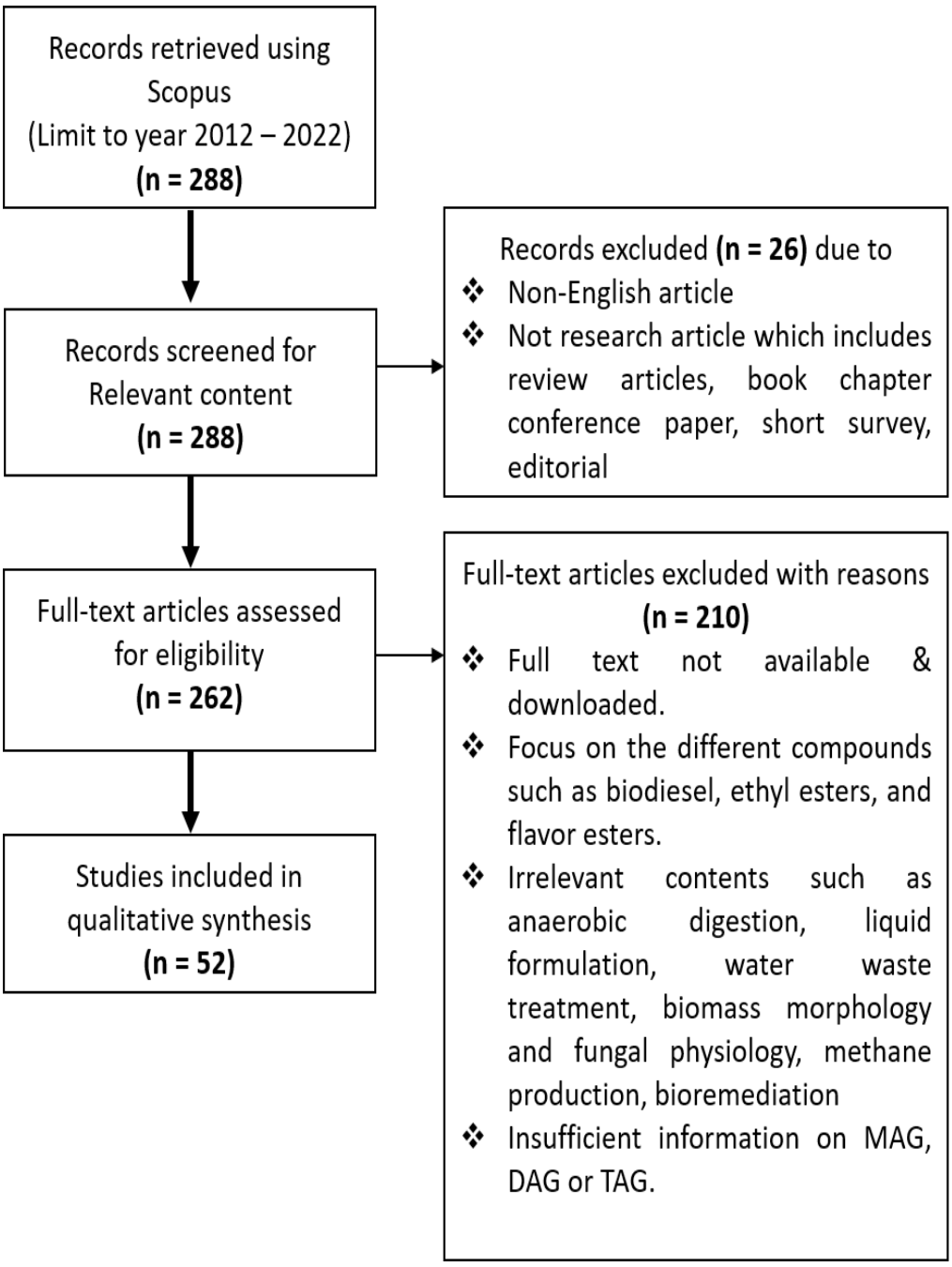

Figure 2.7. Flow diagram of the systematic review information adopted with modification from PRISMA.

The studies comprised those articles published in the year 2012 to 2022. Articles considered suitable for inclusion were downloaded and assessed before a final decision was made. If any of the applicable exclusion criteria were found in the abstract, the study was eliminated. Articles were included if 1) article not written in English and 2) conference abstracts, reviews, editorials, letter to the editor and case reports. When the decision to include a study based on the title and abstract was ambiguous, the whole text was read and checked for inclusion and exclusion criteria. The eligibility screening process was carried out for 262 articles. For eligibility screening, the title, abstract and the main contents of all 262 articles were examined thoroughly to ensure that relevant and sufficient information fit the objectives of the review. Hence, 210 articles were excluded. Ultimately, the remaining 52 articles were selected for the qualitative synthesis as shown in Fig. 2.7.

2.6 Distribution of acylglycerols articles

Out of 52 full-text articles were considered for inclusion in the systematic review, 9 articles specifically investigated on lipase-catalysed synthesis of MAG, 9 articles on DAG production and TAG being the most studied compound with the total number of 29 articles. The remaining 5 articles examined the mixture of MAG, DAG or/and TAG. Fig. 2.8 showed the yearly distribution of the selected articles varied during the analyzed period. There is no obvious pattern in term of number of articles for MAG synthesis. The most active year for DAG synthesis is in 2016 with 4 articles were observed. It can be found that 2012, 2013, 2015, 2016 and 2020 were the most active publication years for the production of TAG.

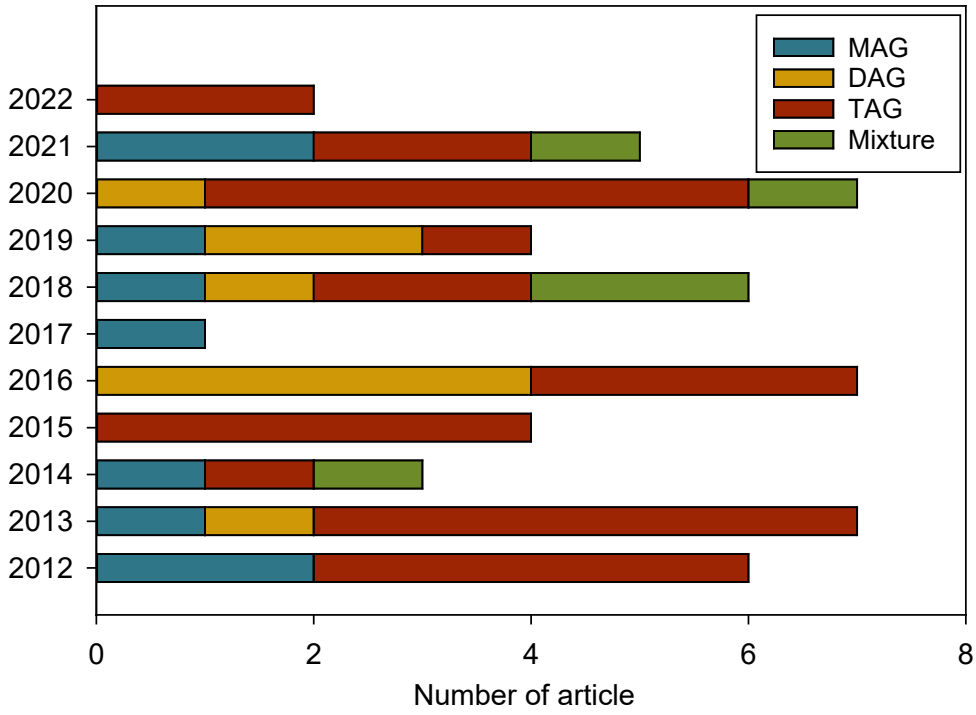

Figure 2.8. Yearly distribution of the acylglycerols compounds based on the selected articles.

2.7 Role of lipase in the enzymatic production of acylglycerols

Enzymes are non-toxic biocatalysts that speed up reactions and are extremely versatile in catalysing a wide range of reactions under mild conditions. Lipase-catalyzed synthesis of acylycerols increasingly being studied as possible substitutes to the classical method. The key reasons are higher yields and milder reaction conditions, which result in higher-quality products and lower energy requirements. Many microorganisms are known as potential producers of extracellular lipases including bacteria, yeast and fungi (Yücel et al, 2018). According to Yücel *et al.* (2018), the main terrestrial species of yeasts that were found to produce lipases are *Aspergillus niger, Candida antarctica, Candida rugosa, Chromobacterium viscosum, Mucor miehei, Pseudomonas cepacia, Pseudomonas fluorescens, Photobacterium lipolyticum, Rhizopus oryzae, Streptomyces sp., and Thermomyces lanuginose.*

Lipases (triacylglycerol acylhydrolases, EC 3.1.1.3) belong to the class of serine hydrolase that act on the carboxylic ester bonds. Lipases have common pentapeptide sequence of Gly-X_1-Ser-X_2-Gly (glycine sometimes is substituted by other small residues) where Gly, Ser, X_1 are referred to glycine, serine, histidine respectively and X_2 represents glutamic or aspartic acid (Sarmah *et al.*, 2018). The structural elements of lipase composed of lid, binding pocket, oxyanion hole, and disulfide bond. Lipase-catalyzed reactions occur at the interface between the insoluble substrate and the aqueous phase as the movement of the lid permits substrate to reach the catalytic site. The external side of the lid is hydrophilic, while the internal side facing the active site is hydrophobic. The lid is closed and covers the enzyme's active site in aqueous media. The lipase transforms into an activated form, which is referred to as "interfacial activation" once the lid is in open state at the oil-water interface (Sarmah *et al.*, 2018; Xiao *et al.*, 2018). Due to these special characteristics, lipases are distinguished from other esterases because of their ability to hydrolyze insoluble esters.

Lipases can be categorized into three groups based on their specificity namely nonspecific lipases, 1,3-specific lipases and fatty acid-specific lipases (Ribeiro *et al.*, 2011).

i. Nonspecific lipases cleave acylglycerol molecules randomly producing free fatty acids, glycerol, MAG and DAG as intermediates.
ii. 1,3-specific lipases catalyze the hydrolysis of TAG at C1 and C3 positions generating fatty acids, 2-MAG and 1,3 or 2,3 DAG.
iii. Meanwhile fatty acid-specific lipases hydrolyze esters having long chain fatty acids with double bonds on C9.

Lipase-catalyzed reactions are typically divided into two groups namely hydrolysis and synthesis. Synthesis reactions can be categorized as esterification, aminolysis, interesterification and transesterification that consists of alcoholysis, and acidolysis

(Sarmah *et al.*, 2018). As presented in Fig. 2.9, the production of acylglycerols by lipase can be achieved from various reaction mechanisms involving glycerolysis (n=10), esterification (n=12), interesterification (n=11), acidolysis (n=10), transesterification (alcoholysis) (n=3), hydrolysis (n=4), partial hydrolysis (n=1) and deacidification (n=1). Most commercially important immobilized lipases used in the synthesis of acylglycerols are Lipozyme RM IM (*Rhizomucor miehei* lipase) Lipozyme TL IM (*Thermomyces lanuginose* lipase), and Novozym 435 (*Candida antarctica* lipase B) with the number of reported article of 18, 9 and 12 respectively (Fig. 2.9). Lipozyme RM IM was employed in all reaction except for glycerolysis. Meanwhile Novozyme 435 was the most preferable enzyme for glycerolysis and esterification reactions. Other commercialized lipases were *Rhizopus oryzae* produced by recombinant *Pichia pastoris* (Ornla-ied *et al.*, 2022) and Lipolase containing *Thermomyces lanuginosus* lipase (Čech *et al.*, 2012) which were employed in interesterification and hydrolysis reaction, respectively.

Both Lipozymes act favourably on ester bonds at the *sn*-1 and *sn*-3 position of the TAG which normally targeted for the development of tailor-made fatty acid composition in modifying commodity oils and fats. Meanwhile Novozym 435 is a nonspecific or random lipases that equally reacts with the three glycerol bonds. The chemical structure of the substrate and the reaction medium have an impact on Novozym 435 regioselectivity (Ortiz *et al.*, 2019). In term of carrier materials, Lipozyme RM IM, Lipozyme TL IM and Novozym 435 are immobilized on an anionic resin, gel of granulated silica and macroporous acrylic resin, respectively (Pedro *et al.*, 2018). Different immobilization methods have been established for lipases utilized in acylglycerols production such as adsorption (Gu *et al.*, 2016; Yadav *et al.*, 2017; Subroto *et al.*, 2020; Dom *et al.*, 2014), entrapment (Savickaite *et al.*, 2021) and covalent bonding (Freitas *et al.*, 2013, Teixeira *et al.*, 2014; Paula *et al.*, 2015b; Zhoa *et al.*, 2019; Bavaro *et al.*, 2020; Vilas Bôas *et al.*, 2021).

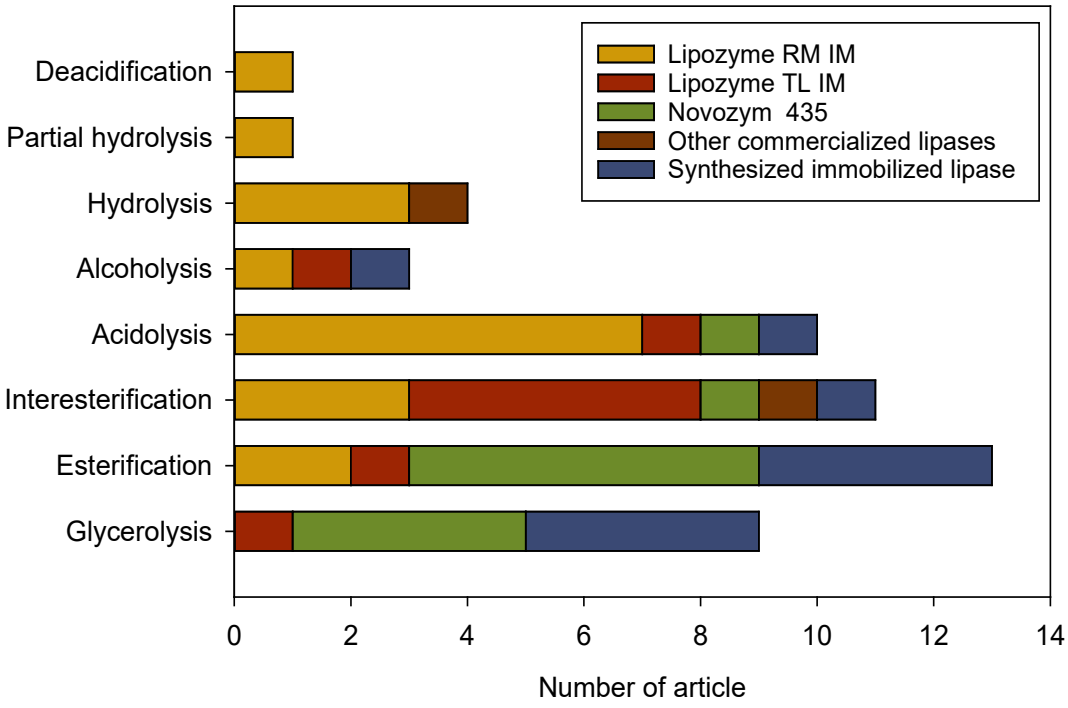

Figure 2.9. Distribution of lipase catalysed reactions and type of lipases.

Distribution of lipase catalysed reactions based on the targeted acylglycerols or the highest production of MAG, DAG or TAG is shown in Fig. 2.10. The synthesis of MAG is normally conducted through glycerolysis and esterification reaction with 5 and 4 number of reported articles, respectively. Meanwhile for DAG synthesis, the esterification reaction being the most favourable method (5 articles). For the other DAG synthesis methods such as glycerolysis, acidolysis, partial hydrolysis and deacidification only one article reported for each category. Interesterification is most common employed reaction for TAG synthesis with a total number of 11 published articles followed by acidolysis (10 articles), glycerolysis and alcoholysis (3 articles each), hydrolysis (2 articles) and esterification (1 article). In contrast to DAG synthesis, esterification is the least common method used to produce TAG. The mixture of MAG, DAG and/or TAG are obtained through three methods namely glycerolysis, esterification and hydrolysis reaction. Depending on the targeted products, it is also possible to produce MAG, DAG

and TAG using a combination of these techniques. The details of the synthesis using each technique are discussed in the next subtopic.

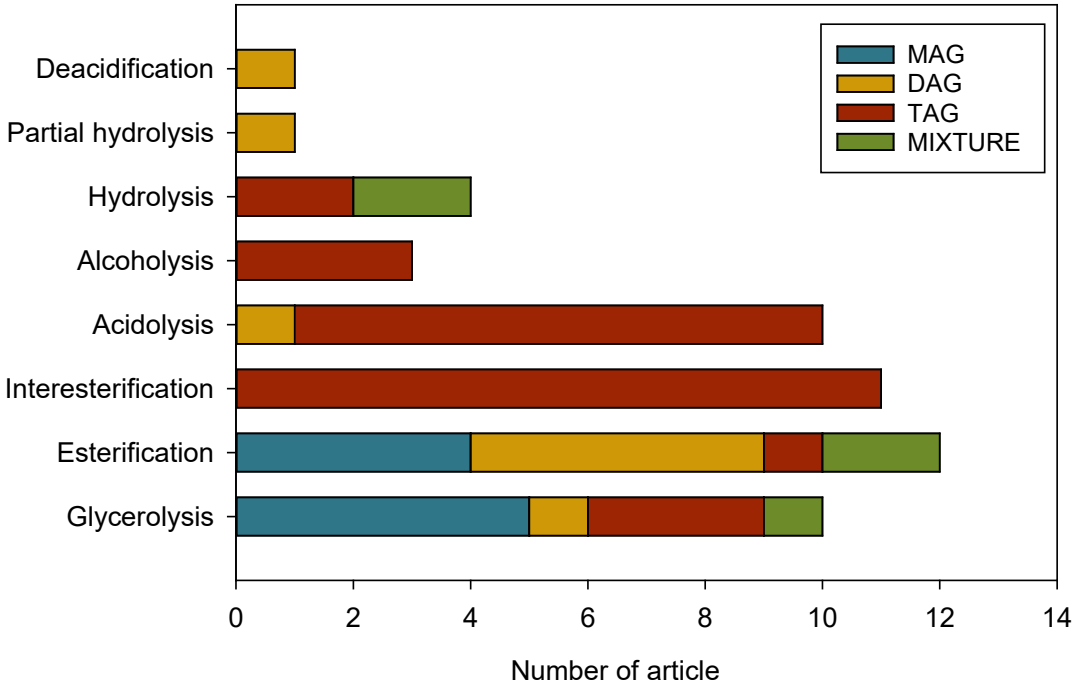

Figure 2.10. Distribution of lipase catalysed reactions and acylglycerols compounds.

2.7.1 Glycerolysis

Glycerolysis is referring to the transfer of the fatty acyl group from the edible oil or TAG molecule to the backbone of glycerol (Fig. 2.11).

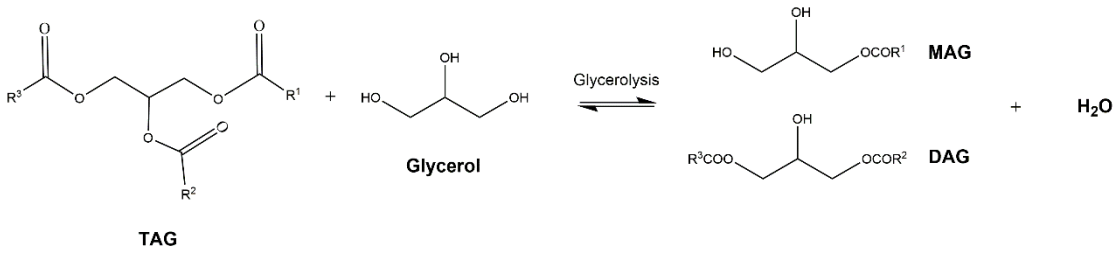

Figure 2.11. Schematic diagram of glycerolysis reaction.

As can be observed in Table 2.3, glycerolysis of oils is a commonly used method to produce high contents of MAG, ranging from 31.5 to 90% (Fiametti *et al.*, 2012; Freitas

et al., 2013, Teixeira *et al.*, 2014; da Silva *et al.*, 2018; Vilas Bôas *et al.*, 2021). Glycerolysis of babassu oil, which contains more than 90% saturated fatty acids, was performed using Burkholderia cepacia lipase immobilised on polysiloxane-poly(vinyl alcohol) (Freitas *et al.*, 2013, Teixeira *et al.*, 2014; Vilas Bôas *et al.*, 2021). Utilizing babassu oil is an economic substrate as it is inexpensive and does not compete with the food supply (Song *et al.*, 2012). The modification of fats and oils reactions are particularly vulnerable to oxidative conditions. In order to prevent the lipid feedstock oxidation during the glycerolysis of babassu oil, Freitas *et al.* (2013) and Teixeira *et al.* (2014), studied the incorporation of different antioxidants and emulsifiers during the production of MAG. The addition of emulsifiers or surfactants to the reaction medium may improve the system's homogeneity, enhance the surface area and lipase efficiency. Both studies were conducted with the aim to find an alternative of substituting inert environment, N_2 in the medium during the glycerolysis reaction. Although the best performance was obtained using N_2, they observed that soy lecithin (Freitas *et al.*, 2013) and buriti oil (Teixeira *et al.*, 2014) were found to be effective in inhibiting the oxidation of babassu oil. In contrast, Vilas Bôas *et al.* (2021) obtained comparable inhibition results for cocoa butter in an inert environment using a continuous packed bed reactor. The optimal molar ratio of babassu oil to glycerol appeared to be at 1:9 with the reaction proceeding for 9.8 h. They reported that the highest productivity and selectivity of MAG obtained at 52.3 ± 2.9 mg g^{-1} h^{-1} and 31.5 ± 1.8%, respectively. As a result, this natural antioxidant can be potentially used as a substitution to inert atmosphere. Alternatively, recycling nitrogen is another possible approach to avoid the oxidation of product while reducing the continuous use of inert atmosphere. Recycled nitrogen was applied in the production of DAG by glycerolysis of soybean oil in a packed bed reactor (Zhang *et al.*, 2016). Using a slightly high temperature (80°C) as compared to other glycerolysis studies, the highest content of DAG was achieved at 49.4 % and 63.5% after purification.

While most of the MAG research focused on various emulsion-based foods, da Silva *et al.* (2018) examined the synthesis of andiroba oil polyol for polyurethane foams production. The andiroba oil polyol at 50°C with 150% *tert*-butanol, yielded the highest amount of MAG (66.47 %), making it the best choice for polyurethane foams synthesis.

On the other hand, the kinetics of glycerolyis were investigated by Choong *et al.* (2018) and Arranz-Martínez *et al.* (2018). TAG synthesis through glycerolysis was done using palm olein IV56 with glycerol and successfully modelled and fits on complex ping-pong bi-bi mechanisms (Choong *et al.*, 2018). Arranz-Martínez *et al.*, (2018) used glycerol, ratfish liver oil and cyclopentanone as substrates. They discovered that glycerolysis rate of TAG was more than 1.5 times faster than that of diacylglyceryl ethers.

Table 2.3. Enzymatic glycerolysis of the production MAG, DAG and TAG.

Targeted compound	Substrate	Enzyme	Reactor	Reaction conditions	Analytical Instrument	Highlights	Reference
MAG	babassu oil, glycerol	*Burkholde-ria cepacia* lipase immobilized on SiO_2-PVA	batch and continuous packed bed reactor	babbasu oil:glycerol at a molar ratio of 1:15, 12 h, 50°C, antioxidant agents or emulsifier (30-100 ppm)	Gas chromatogram -phy (GC)	• MAG concentrations achieved at 60 and 24% in batch and continuous mode, respectively. • Soy lecithin was found to be efficient emulsifier but limited performance to be used in continuous runs.	Freitas *et al.* (2013)
MAG	babassu oil, glycerol	*Burkholde-ria cepacia* lipase immobilized on SiO_2-PVA	batch and continuous packed bed reactor sparging with N_2.	babbasu oil:glycerol at a molar ratio of 1:15, 12 h (batch), 6 h (packed bed reactor), 50°C, antioxidant agents (30-100 ppm)	GC	• In preventing oxidation of MAG, an inert atmosphere, N_2 showed best performance (60 %) followed by buriti oil (57.6 %) and cocoa butter (56.6 %)	Teixeira *et al.* (2014)
MAG	babassu oil, glycerol	*Burkholde-ria cepacia* lipase immobilized on SiO_2-PVA particles	continuous packed bed reactor	babasu oil:glycerol at a ratio of 1:9, 9.8 h, 50.15°C, cocoa butter as an antioxidant agent	GC	• The highest MAG selectivity (31.5%) and productivity (52.30 mg g^{-1} h^{-1})	Vilas Bôas *et al.* (2021)
MAG	olive oil, glycerol	Novozyme 435	mechanically stirred reactor under ultrasound irradiation	Olive oil:glycerol at a molar ratio of 1:2, irradiation power supply 130 W, 2 h, 60 - 70°C.	GC	• Ultrasound irradiation in solvent-free system yielded high contents of reaction products, especially MAG.	Fiametti *et al.* (2012)
MAG	andiroba oil, glycerol, t-butanol	Novozyme 435	tubular fixed bed reactor	andiroba oil:glycerol at a ratio of 2:1; 50°C.	HPLC	• The highest content of MAG achieved at 66.47 %. • Functionality of andiroba oil polyol increased in mixture with 50 % of glycerol.	da Silva *et al.* (2018)

Table 2.3. Enzymatic glycerolysis of the production MAG, DAG and TAG (continued).

Targeted compound	Substrate	Enzyme	Reactor	Reaction conditions	Analytical Instrument	Highlights	Reference
DAG	soybean oil, glycerol	Lipozyme 435 (Novozym 435)	bubble column reactor	soybean oil:glycerol at a molar ratio of 1:20, 2.5 h, 80°C.	GC	• The highest content of DAG achieved at 49.4 % and 63.5% after purification.	Zhang *et al.* (2016)
TAG	palm olein IV56, glycerol	Lipozyme TL IM	conical flask batch reactor	palm olein:glycerol at a molar ratio of 1:1, 55°C.	HPLC	• Glycerolysis reaction fits a complex ping-pong bi-bi model.	Choong *et al.* (2018)
TAG	ratfish liver oil, cyclopenta-none, glycerol	Novozyme 435	basket reactor	128 g ratfish liver oil, 304 g Cyclopentanone, 12.8 g glycerol, 48 h, 40°C.	HPLC	• Glycerolysis of TAG is more than 1.5 times faster compared to that of diacylglyceryl ethers.	Arranz-Martínez *et al.* (2018)
MAG, DAG	palm stearin and palm olein, glycerol	*Candida antarctica* lipase B immobilized on macro-porous, Amberlite IRA-96 free base.	stirred tank reactor	oil:glycerol at a ratio of 1:1.5, 24 h, 50°C.	Thin Layer Chromatogra-phy (TLC)	• The highest content of MAG, DAG and TAG achieved at 7.86%, 27.34% and 62.49% respectively.	Subroto *et al.* (2020)

2.7.2 Esterification

The most direct mechanism of producing MAG or DAG is esterification, which involves free fatty acids esterify with either glycerol or MAG (Fig. 2.12). In this reaction, water is produced as a by-product.

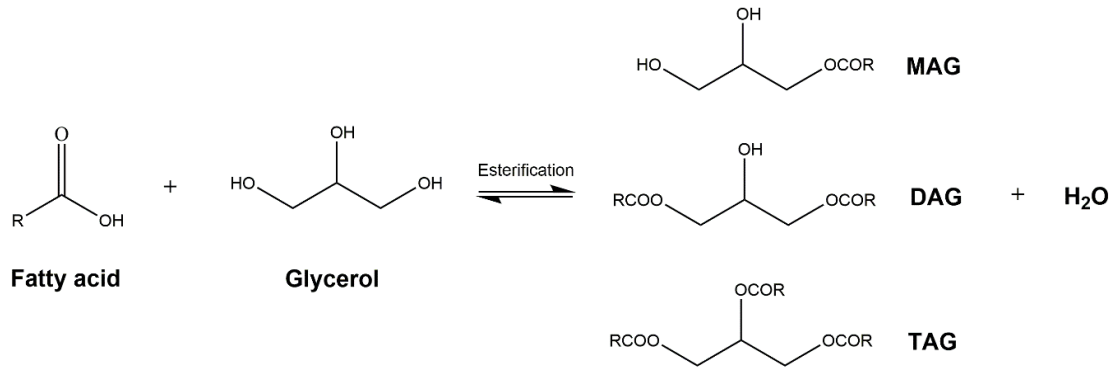

Figure 2.12. Schematic diagram of esterification reaction.

Junior *et al.* (2012) tested two commercial lipases namely, Lipozyme RM IM and Lipozyme TL IM.for the enzymatic esterification of (R,S)-1,2-isopropylidene glycerol with stearic acid that derived from palm oil refining process. They observed that Lipozyme RM IM showed better result than Lipozyme TL IM. High yield of MAG was achieved (70–95%) at equivalent molar ratio of substrates (1:1) at 60°C using a statistical model namely, Central Composite Design. The optimal temperature achieved at 60°C which is in line with similar MAG studies (Yadav *et al.*, 2017; Guajardo *et al.*, 2019, Satyawali *et al.*, 2021). However, Yadav *et al.*, (2017) obtained the optimal MAG production when excessive amount of glycerol to undecylenic acid (5:1) was applied in the reaction containing *tert*-butanol as a solvent. MAG of undecylenic acid can be applied as emollient and emulsifier in skin care products, moisturizer, liquid soap, sunscreen lotion, body washes and anti-ageing creams (Yadav *et al.*, 2017).

Deep eutectic solvent (DES) have attracted much interest as a green solvent that can be used instead of organic solvents. DES shares many of the same properties as ionic liquids, including being liquid at room temperature, having a high vapour pressure, and

having a good thermal stability. Conversely, DES is made from inexpensive resources, has a high dissolving capability, biodegradable, and it is easier to create. Utilizing the advantage of DES, Guajardo *et al.* (2019) used choline chloride:glycerol (ChCl:Gly) as both a reaction medium and a substrate. The molar ratio of ChCl:Gly was set at 1:2 for the preparation of DES. Different concentrations of benzoic acid (60-300 mM) was employed with the present of water as a co-solvent. With increasing concentrations of benzoic acid, Novozyme 435 lipase was observed to be highly inactivated.

Based on Table 2.4, it shows that out of 9 articles, 5 articles reported on esterification reaction that favour on DAG formation (Hu *et al.*, 2013; Liu *et al.*, 2016; Das & Ghosh, 2019; Zhoa *et al.*, 2019; Chen *et al.*, 2020). Expect for the study conducted by Zhoa *et al.* (2019), Novozyme 435 was found to be more effective, suitable and preferred lipase in catalyzing the esterification of oil or fatty acid with glycerol (Hu *et al.*, 2013; Liu *et al.*, 2016; Das & Ghosh, 2019; Chen *et al.*, 2020). Zhoa *et al.* (2019) immobilized the lipase enzyme from *Rhizopus oryzae* on nanosized magnetite particles. The immobilised enzyme demonstrated good activity and 97% regioselectivity for 1,3-DAG production. They also found that even after 55 reaction cycles, the immobilised enzyme still had 70% residual activity. Hu *et al.* (2013) found that as compared to glycerolysis reaction, esterification provided significantly greater acyl donor conversion calculated at 74.21% and 94.42%, respectively. The comparative study was carried out using the commercial enzyme, Novozyme 435 which was tested in two different reaction conditions namely glycerolysis of TAG and esterification of glycerol with caprylic acid. For DAG synthesis *via* esterification reaction, the optimal substrate ratio of oil:glycerol was in range of 2:1 to 3:1 (Hu *et al.*, 2013; Das & Ghosh, 2019; Zhoa *et al.* 2019). On the other hand, Liu *et al.* (2016) and Chen *et al.* (2020) observed that surplus amount of glycerol should be employed to reach maximum DAG yield.

Rodriguez *et al.* (2013) and Kang *et al.* (2015) demonstrated the production of TAG through two-step lipase-catalyzed reaction. In the finding reported by Rodriguez *et al.* (2013), MAG was initially produced and purified through alcoholysis reaction by lipase. Then, MAG obtained from the first step was subsequently esterified with caprylic acid. At the end of the synthesis, 93% pure TAG was achieved with 38% DHA at *sn*-2 position and 60% caprylic acid at *sn*-1,3 positions. However, because highly purified MAG is expensive, this process is less appealing to industry (Zhang *et al.*, 2016). Kang *et al.* (2015) studied two step esterification processes employing *Candida rugosa* lipase and Novozym 435 in the first and second step, respectively. First step was done with the esterification of conjugated linoleic acid dodecan-1-ol and the product obtained was then reacted with glycerol in the second step achieving 93.7 g/100 g of final TAG.

Instead of aiming of one particular compound, Dom *et al.* (2014) and Guebara *et al.* (2018) discussed the mixture of MAG, DAG and TAG. Both authors used response surface methodology to optimize the reaction parameters. The highest acylglycerols yield of was found to be at 75.4% through esterification of glycerol with palm oil fatty acid distillate to produce medium-chain acylglycerols (Dom *et al.*, 2014) and 88% was attained using caprylic acid and glycerol (Guebara *et al.*, 2018).

Table 2.4. Enzymatic esterification of the production MAG, DAG and TAG.

Targeted compound	Substrate	Enzyme	Reactor	Reaction conditions	Analytical Instrument	Highlights	Reference
MAG	(R,S)-1,2-isopropylidene glycerol, Stearic acid	Lipozyme RM IM, Lipozyme TL IM.	batch and continuous flow packed bed reactor	(R,S)-1,2-isopropylidene glycerol: stearic acid at a molar ratio of 1:1, 4 h, 60°C.	GC	• Batch and continuous flow conditions can lead to high yield (70–95%). • High yield achieved at 73 % in 1 minute in a continuous flow reactor.	Junior *et al.* (2012)
MAG	undecylenic acid, glycerol	immobilized *Candida antarctica* lipase B preparation (named as PyCal)	batch type reactor, packed bed reactor	undecylenic acid:glycerol at a molar ratio of 1:5, 2 h, 60°C.	HPLC	• MAG and DAG content achieved at 92% and 8%, respectively. • High conversion achieved at 86% in 10 minute in a packed bed reactor.	Yadav *et al.* (2017)
MAG	benzoic acid, deep eutectic solvents (choline chloride:glycerol 1:2)	Novozyme 435	batch, fed-batch reactor, recirculated continuous packed-bed reactor.	200 mM of benzoic with deep eutectic solvents, 24 h, 60°C.	Ultra HPLC	• Highest conversion achieved at 90% in fed batch reactor with 59% higher compared to the batch. • 67% conversion in recirculation in packed-bed bioreactor at 7 cycles of operation.	Guajardo *et al.* (2019)
MAG	caprylic acid, lauric acid, glycerol	Lipozyme 435 (Novozyme 435), *Candida antarctica* lipase B, *Rhizomucor miehei* (Novozyme 40,086)	shake flasks, packed bed reactor was coupled with pervaporation	fatty acid:glycerol at molar ratio of 1:1, 24 h, 50-65°C.	HPLC	• Highest conversion achieved at 90%, with range of 55-70% of MAG, 30-35% of DAG and 1–10% of TAG in various reactors tested.	Satyawali *et al.* (2021)

Table 2.4. Enzymatic esterification of the production MAG, DAG and TAG (continued).

Targeted compound	Substrate	Enzyme	Reactor	Reaction conditions	Analytical Instrument	Highlights	Reference
DAG	caprylic acid, glycerol, TAG	Novozyme 435	batch and packed bed reactor	caprylic acid:glycerol at a molar ratio of 2:1, 10 h, 60°C (batch), 7 h, 65°C (packed bed reactor).	GC	• Batch reactor: highest conversion achieved at 94.42% with 45.45% of DAG content. • Packed bed reactor: highest conversion achieved at 82.30% with 77.26% DAG content. • Microwave irradiation can speed up the glycerolysis and resulted higher DAG content than the conventional heating.	Hu *et al.* (2013)
DAG	palm oil deodorizer distillate, glycerol	Novozyme 435	bubble column reactor	palm oil deodorizer distillate :glycerol at a molar ratio of 1:7.5, 30 min, 60°C.	GC	• Highest contents achieved at 57.94 ± 1.60% of DAG, 24.68 ± 2.08% of MAG, 2.67 ± 1.72% of TAG and 14.69 ± 1.22% of fatty acid. • 91.30 ± 1.10% of DAG was obtained after purification using molecular distillation step.	Liu *et al.* (2016)
DAG	caprylic acid, capric acid, glycerol	Lipozyme RM IM, Novozyme 435	batch reactor under vacuum	Lipozyme RM IM: fatty acid:glycerol at a ratio of 3:1, 18 h, 60°C. Novozyme 435: fatty acid:glycerol at a ratio of 3:1, 6 h, 60°C.	High Performan-ce Thin Layer Chromatograp hy (HPTLC)	• Caprylic acid-DAG yield attained at 58.86±4.05% for Lipozyme RM IM and 53.77±3.74% for Novozyme 435. • Capric acid-DAG yield attained at 55.41 ±3.95%, for Lipozyme RM IM and 51.89 ±2.6 for Novozyme 435.	Das & Ghosh (2019)

Table 2.4. Enzymatic esterification of the production MAG, DAG and TAG (continued).

Targeted compound	Substrate	Enzyme	Reactor	Reaction conditions	Analytical Instrument	Highlights	Reference
DAG	oleic acid, glycerol	*Rhizopus oryzae* immobilized on nanosized magnetite particles	batch reactor with vacuum	oleic oil:glycerol at a ratio of 2.8:1, 8 h, 30°C.	HPLC	• 1,3-DAG content achieved at 76% • 95% of 1,3-DAG was obtained after purification.	Zhoa *et al.* (2019)
DAG	caprylic acid, capric acid, glycerol.	Novozyme 435 (immobilized Candida antarctica lipase *B*)	bubble column reactor	Fatty acid:glycerol at a ratio of 1:7.5, 30 min, 60°C.	GC	• Caprylic acid-DAG and capric acid-DAG content achieved at 41% and 44%, respectively. • After purification, the concentrations of caprylic acid-DAG and capric acid-DAG were increased to 80 and 83%, respectively.	Chen *et al.* (2020)
TAG	MAG production: Cod liver oil, ethanol, 1-butanol. TAG production: MAG, caprylic acid	Novozyme 435, *Rhizopus oryzae* (lipase DF-DS)	small & large stirred-batch type reactor	MAG production: 75 g cod liver oil, 300 g ethanol, 48 h, 35°C. TAG production: caprylic acid:2-MAG at a molar ratio of 3:1, 0.5 h, 37°C.	TLC, GC	• After synthesis and purification, 93% pure TAG was obtained consists of 38% DHA at *sn*-2 position and 60% caprylic acid at *sn*-1,3 positions	Rodriguez *et al.* (2013)
TAG *trans*-10, *cis*-12 conjugated linoleic acid (t10,c12-CLA-enriched TAG)	conjugated linoleic acid, dodecan-1-ol, glycerol	*Candida rugose* lipase (immobilized on Immobead 150), Novozyme 435	recirculating packed bed reactor (first step), vacuum batch reactor system (second step)	conjugated linoleic acid:dodecan-1-ol at a molar ratio of 1:1, 12 h, 20°C.	GC	• TAG content reached 93.7 g 100 g^{-1}.	Kang *et al.* (2015)

Table 2.4. Enzymatic esterification of the production MAG, DAG and TAG (continued).

Targeted compound	Substrate	Enzyme	Reactor	Reaction conditions	Analytical Instrument	Highlights	Reference
MAG, DAG	palm oil fatty acid distillate, glycerol	Oil palm mesocarp lipase	packed bed reactor	palm oil fatty acid distillate:glycerol oil at a molar ratio of 10:1, 135 min, 65°C.	TLC, Alkaline titration	• The highest acylglycerols yield achieved at 75.4% based on actual experimental run which is close to the predicted yield of 75%.	Dom *et al.* (2014)
MAG, DAG, TAG	caprylic acid, glycerol	Lipozyme RM IM	batch type reactor	caprylic acid:glycerol at a ratio of 2:1, 6 h, 50°C.	GC	• The total acylglycerols yield achieved at 88% (MAG, DAG, TAG)	Guebara *et al.* (2018)

2.7.3 Interesterification

Enzymatic interesterification involves the exchange of fatty acids within and between TAG as shown in Fig. 2.13. It normally conducted using a combination of two or three different oils with the presence of lipase enzyme.

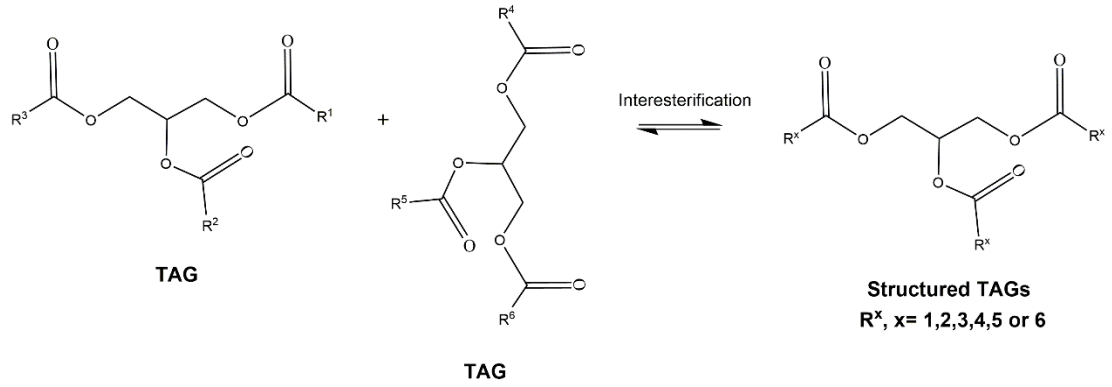

Figure 2.13. Schematic diagram of interesterification reaction.

Most edible fats and oils are limited in their potential application because of the natural TAG structures unable to impart desirable properties to fat products. Therefore, the enzymatic interesterification method has been widely studied to modify the physicochemical properties of fats and oils. This process was carried out to improve the quality of low-cost, saturated fats as well as commercial oils and fats (Mohamed, 2012; Shin *et al.*, 2013). Table 2.5 shows that cocoa butter substitutes, milkfat-based substitutes, structured lipids enriched with essential fatty acids are among the most prominent applications of lipase-catalyzed interesterification from various oil sources. Most of the findings have been reported on the application of commercial lipases such as Lipozyme TL IM (Jenab *et al.*, 2013, Saw *et al.*, 2014; Lee *et al.*, 2015; Zhang *et al.*, 2020a; Zhang *et al.*, 2020b) and Lipozyme RM IM (Shin *et al.*, 2013; Zhang *et al.*, 2021a; Zhang *et al.*, 2021b) for the development of a new type of structured lipid. Both Lipozyme TL IM and Lipozyme RM IM are 1,3-specific lipases, therefore, desired acyl group can be directed to a specific place on the glycerol back bone of TAG during the interesterification reaction. The arrangement of fatty acid was calculated and determined through

interesterification or incorporation degree. Depending on the composition mixture of the substrates, the temperature range for the TAG synthesis through interesterification process appears to be between 45°C to 80°C (Table 2.5).

Numerous studies reported on the use of combination of fats and oils that derived from the palm fruit such as palm olein, palm stearin and palm kernel oil to produce structured TAG through interesterification method (Mohamed, 2012; Saw *et al.*, 2014; Zhang *et al.*, 2020b Zhang *et al.*, 2021b). These oils also can be modified through the mixture with the other source of oils such as flaxseed oil (Shin *et al.*, 2013) and coconut oil (Ornla-ied *et al.*, 2022). Palm oil present in the form of refined, bleached and deodorized palm oil (Mohamed, 2012; Lee *et al.*, 2015) or fully hydrogenated palm oil (Zhang *et al.*, 2021a; Ornla-ied *et al.*, 2022). Besides palm oil, several articles also have reported on the interesterification reaction using soybean oil. Paula *et al.* (2015b) reported that the mixture of soybean oil and milk fat resulted in reduction of saturated fatty acid content, and it showed to be more spreadable at cooler temperatures. A mixture of soybean oil and caprylic/capric TAG was conducted to TAG produce with high medium- and long-chain triacylglycerols content (Zhang *et al.*, 2020b).

Table 2.5. Enzymatic interesterification of the production TAG

Targeted compound	Substrate	Enzyme	Reactor	Reaction condition	Analytical Instrument	Highlights	Reference
TAG	palm olein oil, palmitic and stearic fatty acid mixture	Lipozyme RM IM	batch reactor	Palm olein oil:palmitic and stearic fatty acid mixture at a molar ratio of 1:3, 3 h, 60°C.	GC	• Produced cocoa butter equivalent using substrates that were obtained from palm oil physical refining process. • TAG compositions of cocoa butter equivalent achieved at 26.6% of 1,3-dipalmitoyl-2-oleyl-glycerol, 42.1 % of 1(3)-palmitoyl-3(1)-stearoyl-2-oleoyl-glycerol, 7.5% of 1-palmitoyl-2,3-dioleoyl-glycerol, 18% of 1,3-distearoyl-2-oleoyl-glycerol, 5.8% of 1-stearoyl-2,3-dileoyl-glycerol.	Mohamed (2012)
TAG	fully hydrogenated canola oil, canola oil.	Lipozyme TL IM	high pressure batch stirred reactor under $SCCO_2$	fully hydrogenated canola oil: canola oil at a ratio of 30-50% (w/w), 2h, 65°C.	GC	• Produced base-stock for zero-*trans* margarines in equilibrium with $SCCO_2$. • The amounts of saturated and triunsaturated TAG decreased while the amounts of mixed TAG increased.	Jenab *et al.* (2013)
TAG	refined, bleached, and deodorized palm olein of iv 62	Lipozyme TL IM	laboratory scale and pilot scale batch type reactor	30 g of palm olein (conical flask), 90 kg of palm olein (pilot scale batch reactor), 8 h, 65°C	HPLC	• Trisaturated TAG attained at 4.5%.	Saw *et al.* (2014)
TAG	palm kernel oil, refined, bleached, and deodorized palm oil	Lipozyme TLIM	stirred batch reactor	palm kernel oil: palm oil at a molar ratio of 90:10, 7.26 h, 50°C.	HPLC	• The highest yield of TAG attained at 60% with 20% increase in yield was obtained via Response Surface Methodology.	Lee *et al.* (2015)

Table 2.5. Enzymatic interesterification of the production TAG (continued)

Targeted compound	Substrate	Enzyme	Reactor	Reaction condition	Analytical Instrument	Highlights	Reference
TAG	milkfat, soybean oil	Rhizopus oryzae immobilized on polysiloxanepoly-(vinyl alcohol) (SiO_2–PVA)	basket-type stirred, batch system	milkfat:soybean oil at a mass ratio of 65:35, 12 h, 45°C.	GC	• The milkfat-based product is more spreadable under cooling temperature having lower saturated fatty acids contents • Potential use of basket-type stirrer.	Paula *et al.* (2015b)
TAG	palm olein, palm stearin	Lipozyme TL IM	packed-bed reactor	palm olein: palm stearin at a mass ratio of 9:1, 46 min, 80°C.	GC	• Interesterification degree attained at 94.41%	Zhang *et al.* (2021a)
TAG	palm olein: palm kernel oil: palm stearin.	Lipozyme TL IM	pilot scale packed-bed reactor	palm olein:palm kernel oil:palm stearin at a ratio of 5:3:2, 60°C.	GC	• Enzymatic interesterification TAG had lower solid fat content tendency compared to that of chemical interesterification TAG.	Zhang *et al.* (2021b)
TAG	fully hydrogenated palm kernel oil, coconut oil and fully hydrogenated palm stearin	*sn*-1,3-specific lipase from *Rhizopus oryzae* (rProROL)	batch type reactor	fully hydrogenated palm kernel oil:coconut oil:fully hydrogenated palm stearin at a ratio of 70:10:20, 6 h, 60°C.	HPLC	• SFC profile and microstructure profile of cocoa butter substitute similar to the commercial one.	Ornla-ied *et al.* (2022)
TAG	anhydrous butterfat, palm stearin, flaxseed oil	Lipozyme RM IM, Novozyme 435	stirred-batch type reactor	anhydrous butterfat:palm stearin: flaxseed oil at a weight ratio of 6:6:8 and 4:6:10, 24 h, 60°C.	GC, HPLC	• Total saturated fatty acids of the modified butterfats attained a range of 41.4% to 47.4%. • The 6:6:8 and 4:6:10 modified butterfats contained 21.7% and 26.5% α-linolenic acid, respectively.	Shin *et al.* (2013)

Table 2.5. Enzymatic interesterification of the production TAG (continued)

Targeted compound	Substrate	Enzyme	Reactor	Reaction condition	Analytical Instrument	Highlights	Reference
TAG	palm kernel oil, palm olein, fully hydrogenated palm oil	Lipozyme RM IM	packed bed reactor	palm kernel oil:palm olein:fully hydrogenated palm oil at a ratio of 4:3:3, 65°C.	HPLC	• Interesterification degree attained at 97.10%	Zhang *et al.* (2020a)
TAG	caprylic:capric, soybean oil	Lipozyme RM IM	pilot scale packed bed reactor	caprylic:capric TAG to soybean oil at a ratio of 45:55, 75°C, 16 min.	GC	• TAG compositions achieved at 80.07% of medium- and long-chain TAG, 9.03% of medium - chain TAG, and 10.89 % pf long-chain TAG.	Zhang *et al.* (2020b)

2.7.4 Transesterification (Acidolysis)

Acidolysis is a form of transeresterification that involves the interchange of acyl groups between a free carboxylic acid (fatty acid) group and an ester from oil or fats (Fig. 2.14).

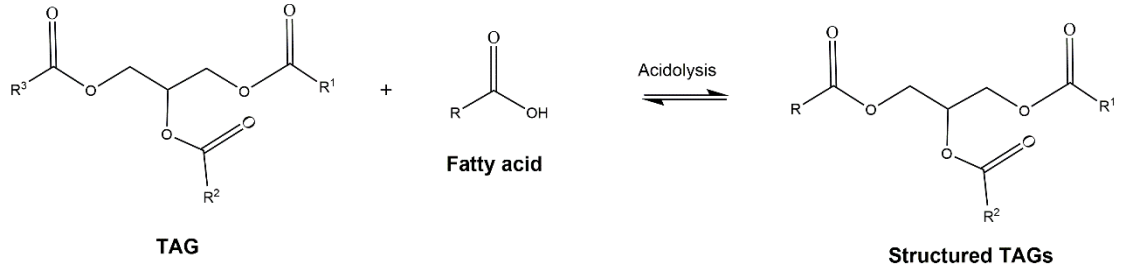

Figure 2.14. Schematic diagram of acidolysis reaction.

As can be seen from Table 2.6, acidolysis reaction was widely conducted to produce structured TAG which is similar to interesterification reaction. None has reported on MAG synthesis and only one article investigated on DAG synthesis via this route (Kim *et al.*, 2018). Kim *et al.* (2018) studied the enzymatic synthesis of structured monogalactosydiacylglycerols enriched in pinolenic acid. Monogalactosyldiacylglycerols composed of one *D*-galactopyranosyl residue attached to the *sn*-3 position of 1,2-DAG. Having a sugar molecule, this compound can act as non-ionic emulsifier in food products. The authors managed to obtain structured monogalactosydiacylglycerols containing ~42 mol % PLA under optimal reaction conditions using Lipozyme RM IM lipase.

When performing an acidolysis process, selecting the proper enzyme is crucial since various types of enzyme will alter the yield. Table 2.6 shows that Lipozyme RM IM lipase is more typically employed than Lipozyme TL IM lipase, while nonspecific enzymes like Novozyme 435 may also be applied. While the other studies utilized the commercial enzymes, Gu *et al.* (2016) reported a procedure for preparation of immobilized *Aspergillus oryzae* L03 lipase on a macroporous adsorption resin D3520 to produce structured TAG. They found that the immobilized lipase exhibited improvement in term of TAG-52 carbon number content (45.65%) as compared to the commercial

lipase, Lipozyme TL IM (33.24%). It was concluded that immobilized *Aspergillus oryzae* L03 has the potential for a cheap alternative lipase.

Canola oil, palm oils (palm stearin, palm mid fraction oil), pine oil, mustard oil, terebinth fruit oil, grape seed oil and silkworm pupae oil are among the tested oil for the acidolysis process. These native oils were employed in acidolysis because they included essential fatty acids such as linoleic acid (LA), alphalinoleic acid (ALA), eicosapentanoic acid (EPA), docosahexanoic acid (DHA), and y-linolenic acid (GLA) which promote body health. The production of structured TAG was achieved through the incorporation of medium chain length fatty acids such as capric, caprylic and lauric acids (Savaghebi *et al.*, 2012; Choi *et al.*, 2013; Sengupta *et al.*, 2015; Kocak Yanik *et al.*, 2016; Bassan *et al.*, 2019; Cozentino *et al.*, 2022). The effect of the fatty acid chain length on acidolysis process was also investigated. Sengupta *et al.* (2015) discovered that the incorporation of caprylic acid was the highest as compared to capric and lauric acids which mainly due to its viscosity. Meanwhile pinolenic acid, palmitic, oleic and stearic are the example of long chain length fatty acids that have been exploited so far (Kim *et al.*, 2018; Choi *et al.*, 2013; Mohamed 2013; Gu *et al.*, 2016; Kocak Yanik *et al.*, 2016; Wang *et al.*, 2020b). Except for the work done by Bassan *et al.* (2019) all the authors observed that an excess of the fatty acid in the reaction mixture (range from 2 to 30 times higher than oil) significantly increased the incorporation of the TAG to establish the optimal operating parameters.

Table 2.6. Enzymatic acidolysis of the production TAG

Targeted compound	Substrate	Enzyme	Reactor	Reaction conditions	Analytical Instrument	Highlights	Reference
DAG	Monogalacto-sydiacylglycerols, pinolenic acid from pine nut oil	Lipozyme RM IM, Lipozyme TL IM, Novozym 435, *Candida rugose* lipase (immobilized on Immobead 150)	stirred batch reactor.	Monogalac-tosydiacyl-glycerols: pinolenic acid at a ratio of 1:30, 26 h, 25°C.	TLC, GC	• The highest incorporation degree of pinolenic acid achieved at 42% using Lipozyme RM IM. • 96.6% of structured monogalactosydiacyl-glycerols was obtained after purification using silica column chromatography.	Kim *et al.* (2018)
TAG	canola oil, caprylic acid	Lipozyme TL IM, Novozyme 435	batch reactor	canola oil:caprylic acid at a molar ratio of 1:3, 15 h, 55°C.	GC	• The highest incorporation of caprylic acid achieved at 37.2 mole % and 38.5 mole % with Lipozyme TL IM and Novozyme 435, respectively. • Structured medium-long-medium TAG achieved at 21.2% and 9.9% with Lipozyme TL IM and Novozyme 435, respectively.	Savaghebi *et al.* (2012)
TAG	modified pine nut oil, capric acid	Lipozyme RM IM	continuous packed bed reactor	modified pine nut oil: capric acid at a molar ratio of 1:5, 240 min, 60°C.	GC	• Structured TAG with carbon number of 38 (medium-long-medium or medium-medium long) and 46 (medium-long- long or long-medium-long) achieved at ~30% and >45%, respectively.	Choi *et al.* (2013)

Table 2.6. Enzymatic acidolysis of the production TAG (continued)

Targeted compound	Substrate	Enzyme	Reactor	Reaction conditions	Analytical Instrument	Highlights	Reference
TAG	palm mid fraction oil, palmitic and stearic fatty acid mixture	Lipozyme RM IM	batch reactor	palm mid fraction oil:palmitic and stearic fatty acid mixture at a molar ratio of 1:2, 3 h, 60°C.	GC	• TAG compositions of cocoa butter equivalent achieved at 30.7% of 1,3-dipalmitoyl-2-oleyl-glycerol, 40.1 % of 1(3)-palmitoyl-3(1)-stearoyl-2-oleoyl-glycerol, 9% of 1-palmitoyl-2,3-dioleoyl-glycerol, 14.5% of 1,3-distearoyl-2-oleoyl-glycerol, 5.7% of 1-stearoyl-2,3-dileoyl-glycerol.	Mohamed (2013)
TAG	capric, caprylic and lauric acids, mustard oil	Lipozyme RM IM, Lipozyme TL IM, Novozyme 435.	stirred tank batch reactor, packed bed bio reactor	fatty acid:mustard oil at a molar ratio of 6:3, 24 h, 60°C.	GC	• The highest incorporation achieved with caprylic acid at 32.43%, followed by capric acid 30.45% and lauric acid achieved and 28.66% in a packed bed reactor using Novozyme 435.	Sengupta *et al.* (2015)
TAG	terebinth fruit oil, palmitic acid, caprylic acid.	Lipozyme RM IM	recirculating packed bed reactor	terebinth fruit oil: palmitic acid: caprylic acid at a mole ratio of 1:3.10:2.07, 5.9 h, 45°C.	HPLC	• Maximum structured TAG achieved at 52.23% with minimal caloric value of 38.96 $kj \cdot g^{-1}$ at optimal condition using central composite rotatable design (CCRD).	Kocak Yanik *et al.* (2016)

Table 2.6. Enzymatic acidolysis of the production TAG (continued)

Targeted compound	Substrate	Enzyme	Reactor	Reaction conditions	Analytical Instrument	Highlights	Reference
TAG	palm stearin, oleic acid	*Aspergillus oryzae* L03 lipase, Lipozyme TLIM	stirred tank reactor, packed bed reactor	palm stearin:oleic acid at a molar ratio of 1:7.13, 3 h, 62.09°C.	GC	• Synthesized *Aspergillus oryzae* L03 lipase showed higher C52 content (TAG with a carbon number of 52) compared to the commercialized Lipozyme TLIM. • The highest C52 content achieved at 48.60 ± 2.36 %, with 57.46 ± 1.72 % total palmitic acid at the *sn*-2 position and 74.21 ± 2.45 % oleic acid at the *sn*-1,3 positions in packed bed reactor.	Gu *et al.* (2016)
TAG	grape seed oil, capric acid	Lipozyme TL IM, Lipozyme RM IM, Novozym 435	packed bed reactor	grape seed oil:capric acid at a ratio of 2:1, 24 h, 45°C.	GC	• The highest incorporation degree achieved at 34.53 ± 0.05 mol% using Lipozyme RM IM.	Bassan *et al.* (2019)
TAG	silkworm pupae oil, oleic acid	Lipozyme RM IM	microwave irradiation and under conventional shaker bath	**s**ilkworm pupae oil :oleic acid at a ratio of 1:5, 1 h, 60°C.	HPLC	• The relative content of polyunsaturated fatty acids glyceride and oleic acid in silkworm pupae oil increased from 51.1% to 81.0% and 3.9% to 35.8%, respectively in the microwave reactor. • The relative content of glycerol trioleate was twice as high as that in the shaker reactor	Wang *et al.* (2020b)

Table 2.6. Enzymatic acidolysis of the production TAG (continued)

Targeted compound	Substrate	Enzyme	Reactor	Reaction conditions	Analytical Instrument	Highlights	Reference
TAG	grape seed oil, capric acid	Lipozyme RM IM	packed bed reactor	grape seed oil:capric acid at a ratio of 1:3, 120 h, 45°C.	GC	• The highest incorporation degree at 39.91%.	Cozentino *et al.* (2022)

2.7.5 Transesterification (Alcoholysis)

Transesterification is known as alcoholysis which involves an exchange of an ester group from TAG with another alcohol (Fig. 2.15a). Transesterification is also sometimes referred as esterification of oil/fat with TAG that derived from the formal acylation of the three hydroxy groups of glycerol such as tripalmitin (Wang *et al.*, 2016a) and tricaprylin (Utama *et al.*, 2020) (Fig. 2.15b).

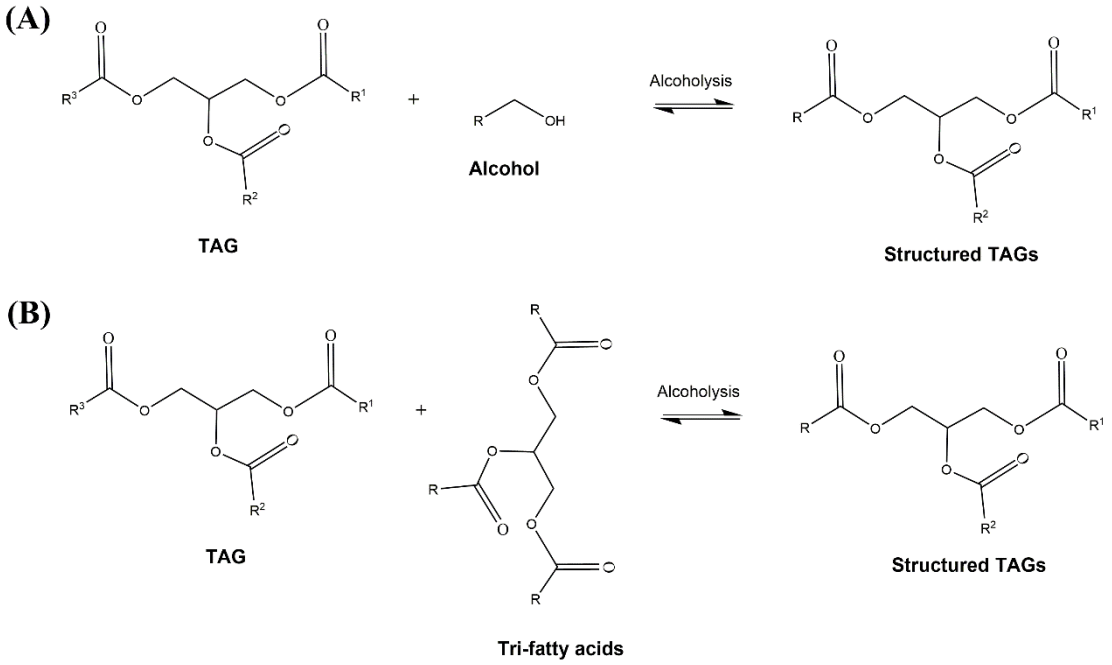

Figure 2.15. Schematic diagram of alcoholysis reaction (a) TAG with alcohol (b) TAG with tri-fatty acids.

It can be seen from Table 2.7(a), as compared to the other two commercial immobilized enzymes (Lipozyme TL IM and Novozyme 435), Lipozyme RM IM displays superior performance had the highest polyunsaturated fatty acids incorporation to tripalmitin (Wang *et al.*, 2016a). Polyunsaturated fatty acids was obtained from microalgal oil and the incorporation were attained at 33.4% (Novozyme 435), 42.6% (Lipozyme TL IM), and 49.8% (Lipozyme TL IM). Utilizing similar Lipozyme TL IM, Utama *et al.* (2020) discovered that the optimal esterification of refined bleached deodorized palm olein with tricaprylin yielded 13% of medium-long medium structured lipid namely 1,3-dicapryoyl-2-oleoyl-*sn*-glycerol. Meanwhile, Savickaite *et al.* (2021)

conducted the investigation of continuous transesterification (alcoholysis) of the selected oils (avocado or sunflower oil) with alcohol (ethanol or methanol) as substrates. They tested three different enzyme namely, GD-95RM lipase, GDEst-95 esterase and fused GDEst-lip lipolytic enzyme. Having more than 50% biocatalytic activites, all three immobilized enzymes exhibited long-term preservation capability for at least 3 months.

2.7.6 Hydrolysis/Partial hydrolysis

Partial hydrolysis includes the hydrolysis of TAG with the presence of water to produce a combination of DAG, MAG, and free fatty acids (Fig. 2.16).

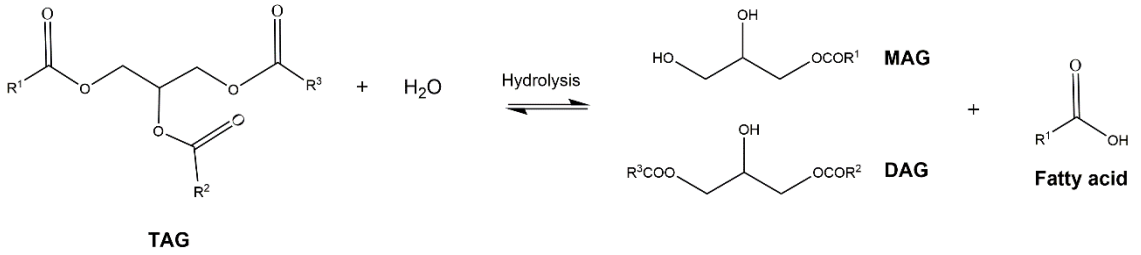

Figure 2.16. Schematic diagram of hydrolysis reaction.

This hydrolysis method is advantageous since it is a straightforward reaction, requires no addition of glycerol and inexpensive to carry out. However, when water is added into the reaction, it may damage the quality of the edible oil, especially if it contains a lot of polyunsaturated fatty acids (Phuah *et al.*, 2015). Bavaro *et al.* (2020) observed the hydrolysis of hempseed oil using *Pseudomonas cepacia* lipase immobilized on Sepabeads EC-EP with the addition of *tert*-butanol. The reaction yielded 40% mixture of MAG and DAG with linolenic acid and oleic acid compositions calculated at 82% and 16% respectively. Using triolein as substrate, Hares Júnior *et al.* (2018) calculated the fraction composition of MAG and DAG attained at 9.2–21.4% and 37.6–40.2%, respectively. Meanwhile, TAG conversions were reported using virgin coconut oil (Chua *et al.*, 2012) and soybean oil (Čech *et al.*, 2012) during the hydrolysis reaction. In addition, refined, bleached and deodorized palm oil was also used as substrate in partial hydrolysis process

targeted for DAG compound (Phuah *et al.*, 2016b). As compared to other hydrolysis studies, Phuah *et al.* (2016b) conducted the partial hydrolysis reaction in a packed bed reactor at 3.8 mL min^{-1} obtaining 29.5 % of DAG yield.

2.7.7 Deacidification

Another method used in the synthesis of DAG is deacidification of the high content of acid in oil such as rice bran oil. This oil may contain as much as 30 to 40 % free fatty acid (Song *et al.*, 2012). Deacidification method is similar to glycerolysis, however, its purpose is to reduce the amount of acid in the oil, which was accomplished by adding glycerol. Deacidification of the mixture of glycerol and high-acid rice bran oil through continuous dehydration was established using a series of three packed-bed columns (Lu *et al.*, 2016). Crude Before starting the enzyme-catalyzed procedure, rice bran oil had undergine three process called degumming, dewaxing, and bleaching. In the experiment, column 1 and column 3 were filled with Lipozyme RMIM and used for the first and second deacidification, respectively. Molecular sieves were occupied in column 2 for dehydration of the first-deacidification rice bran oil. Column 2 afforded 85.22% maximal dehydration rate with 20.0 g of molecular sieves and a flow rate of 0.3 mL min^{-1}. The optimization conditions for the first deacidification column (Column 1) were attained at a flow rate of 0.3 mL min^{-1}, molar ratio of glycerol: rice bran oil at 5.52:1 and at 66.10°C. While the conditions of secondary deacidification (Column 3) were also optimized as 0.2 mL min^{-1}, molar ratio of glycerol: rice bran oil at 5 and at 65°C. The product had 39.55% DAG and 3.16% free fatty acids when tested under these conditions.

Table 2.7. The production of MAG, DAG and TAG by (a) Transesterification (alcoholysis) (b) Hydrolysis (c) Partial hydrolysis (d) Deacidification

Targeted compound	Substrate	Enzyme	Reactor	Reaction conditions	Analytical Instrument	Highlights	Reference
(a) Transesterification (alcoholysis)							
TAG	polyunsaturated fatty acids, tripalmitin	Lipozyme RM IM, Lipozyme TL IM, Novozym 435.	batch reactor, packed bed reactor microreactor	Polyunsatu-rated fatty acids: tripalmitin at a molar ratio of 7:1, 21 h (batch), 2.5 h (microreactor), 60°C.	TLC	• The highest incorporation attained at 54.2%, with incorporation at *sn*-1, 3 up to 81.3% in microreactor using Lipozyme TL IM.	Wang *et al.* (2016a)
TAG	refined bleached deodorized palm olein, tricaprylin	Lipozyme TLIM	packed bed reactor	refined bleached deodorized palm olein:tricaprylin at a ratio of 1:1, 15 min, 50°C.	HPLC	• The highest yield of equivalent carbon number of 32 attained at 13% with incorporation degree of 71%.	Utama *et al.* (2020)
MAG, DAG, TAG	avocado oil, sunflower oil, ethanol, methanol	GD-95RM lipase, GDEst-95 esterase and fused GDEst-lip lipolytic enzyme	packed bed column reactor	30.3 ml of oil, 12.1 ml of alcohol, 7.6 ml of 50 mm tris-HCL (pH 8) buffer	TLC	• All the synthesized enzymes were able to react with the oils generating free fatty acids, MAG, DAG and TAG.	Savickaite *et al.* (2021)

Targeted compound	Substrate	Enzyme	Reactor	Reaction conditions	Analytical Instrument	Highlights	Reference
(b) Hydrolysis							
MAG, DAG	Hempseed oil, water	*Pseudomonas cepacia* lipase immobilized on Sepabeads EC-EP.	packed-bed reactor	hempseed oil 1.6 ml, 2 h, room temperature	GC	• The highest yield of the mixture of MAG and DAG attained at 40% with linolenic acid and oleic acid composition of 82% and 16%, respectively.	Bavaro *et al.* (2020)
MAG, DAG	triolein, water	Lipozyme RM IM	batch type reactor	20% oil:water, 1-6 h, 50-60°C.	TLC, HPLC	• The fraction of MAG and DAG achieved at 9.2–21.4% and 37.6–40.2%, respectively.	Hares Júnior *et al.* (2018)
TAG	virgin coconut oil, water	Lipozyme RM IM	batch reactor	40% of VCO, 240 min (4h), 50°C.	GC	• The highest production of free fatty acids achieved at 4.56 mM	Chua *et al.* (2012)
TAG conversion	soybean oil, water	*Thermomyces lanuginosus* lipase (Lipolase)	batch reactor and a slug-flow microreactor	oil:water at a molar ratio of 2:1, 10 min to 1 h, 35°C.	GC, HPLC	• The triglyceride conversion achieved at 25-30% and almost 50% for the residence time of 10 min and 1 h, respectively.	Čech *et al.* (2012)

Targeted compound	Substrate	Enzyme	Reactor	Reaction conditions	Analytical Instrument	Highlights	Reference
(c) Partial hydrolysis							
DAG	refined, bleached and deodorized palm oil, water	Lipozyme RM IM	packed bed reactor	refined, bleached and deodorized palm oil:water at a molar ratio of 20:1, 6 h, 55°C.	HPLC	• The highest DAG yield achieved at 29.5 % DAG.	Phuah *et al.* (2016b)

Targeted compound	Substrate	Enzyme	Reactor	Reaction conditions	Analytical Instrument	Highlights	Reference
(d) Deacidification							
DAG	rice bran oil, glycerol	Lipozyme RM IM	packed bed reactor	rice bran oil:glycerol at a molar ratio of 1:5.52, 40 min, 66°C.	HPLC	• The highest DAG and FFA content achieved at 38.99% and 3.04%, respectively.	Lu *et al.* (2016)

2.8 Bioreactor design for acylglycerols production

Apart from reaction parameters, another essential characteristic for enzymatic processes is the enzyme reactor. The reactor chosen should optimize reaction efficiency, as well as product yield and quality; facilitate enzyme recyclability; improve enzyme stability; and enhance productivity with the least amount of capital investment (Phuah *et al.*, 2015). Fig. 2.17 provides an overview on the reactors used in the synthesis of MAG, DAG, and TAG by lipase enzyme. Packed bed reactor being the most preferred reactor employed for MAG and TAG production with the total studies of 8 and 12, respectively. This is followed by stirrer tank reactor and shake flask reactor which are commonly operated in either batch or continuous modes. For DAG synthesis, it is hard to draw conclusion on the favored reactor as no discernible trend was observed due to a small number articles that research on DAG. Lipase-catalyzed reactions are also carried out in bubble column reactor (Liu *et al.,* 2016; Zhang *et al.,* 2016; Chen *et al.,* 2020), microwave (Hu et al., 2013; Wang *et al.,* 2020b), ultrasonic reactor (Fiametti *et al.,* 2012) and microreactor (Čech *et al.,* 2012; Wang *et al.,* 2016a).

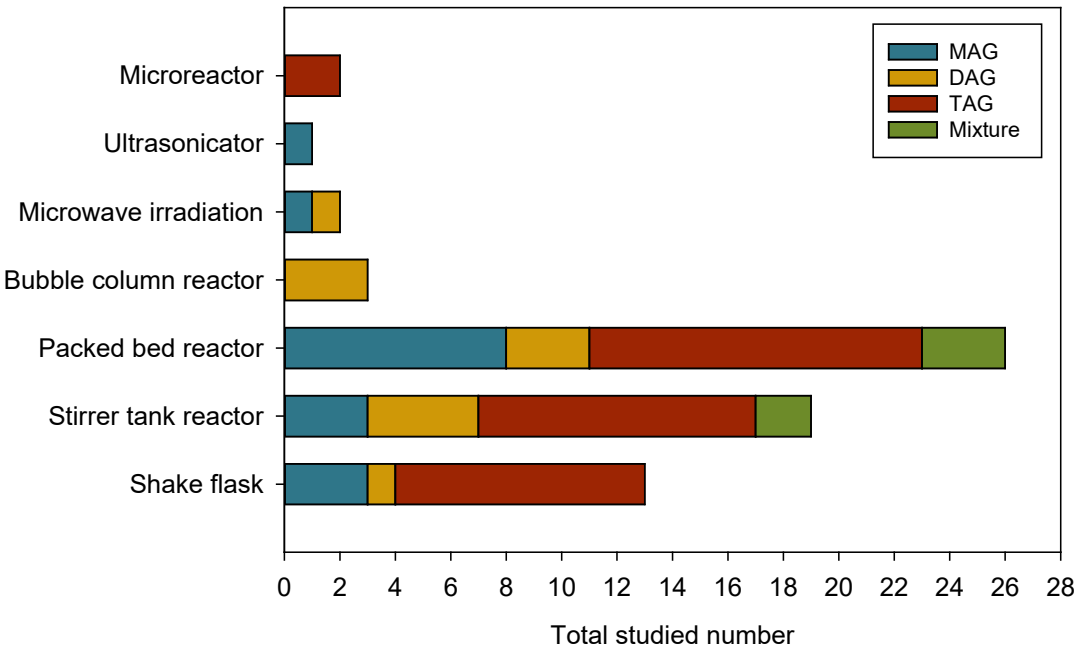

Figure 2.17. Total studied number of reactors.

2.8.1 Batch Reactor

In bioprocess engineering, the shake flask is the most basic bioreactor type. It is the simplest reaction vessels used for screening and process development. The system's simplicity allows it to be employed for a wide range of activities. This reactor has been extensively used for the synthesis of TAG in the laboratory (Mohamed, 2012; Savaghebi *et al.*, 2012; Mohamed, 2013; Rodriguez *et al.*, 2013; Saw *et al.*, 2014; Lee *et al.*, 2015; Wang *et al.*, 2016a; Choong *et al.*, 2018). Only a few reported on the synthesis of MAG (Junior *et al.*, 2012; Yadav *et al.*, 2017; Satyawali *et al.*, 2021) and DAG (Hu *et al.*, 2013) using this type of reactor. Besides shake flask, the reaction is also can be conducted in screw-cap glass vials (Ornla-ied *et al.*, 2022). Shake flasks are commonly used for reaction optimization because they are simple and easy to handle. The optimum conditions obtained from shake flask (batch laboratory-scale) can be further utilized in the pilot-scale reactor for a larger batch production (Rodriguez *et al.*, 2013; Saw *et al.*, 2014; Lee *et al.*, 2015 Satyawali *et al.*, 2021).

Another type of batch reactor is stirrer tank reactor which consists of a propeller, or magnetic stirrer that mechanically agitates reactant mixtures. Stirrer tank reactor has a number of advantageous features such as easy temperature control and suitability for multiphasic system. Furthermore, it provides a highly regulated environment for slow reactions, allowing the composition of reaction medium to be precisely monitored (Doran, 2012). Stirrer tank reactor operated under vacuum was also applied for water removal (Guebara *et al.*, 2018; Das & Ghosh, 2019; Zhoa *et al.*, 2019). Batch stirrer tank reactors are commonly used for preliminary research, determining operating parameters, and generating kinetic data (Arranz-Martínez *et al.*, 2018) due to their convenience of use and affordable cost. Besides, they are also suitable to be used for the examination of novel or diverse supports and lipase immobilisation strategies (Freitas *et al.*, 2013; Teixeira *et al.*, 2014; Paula *et al.*, 2015b; Zhoa *et al.*, 2019).

The high quality of mixing and homogeneity is essential in stirred tank reactor. Homogeneity is influenced by a variety of parameters, including the stirrer type and the design of the stirred tank reactor (with or without baffles). Subroto *et al.* (2020) investigated the glycerolysis-interesterification in a stirred tank reactor using a rectangle, fin, and concave at the middle (‘‘V”) stirrers. They found that the difference between fin-type and "V" type stirrers was not significant but superior to rectangle stirrers. MAG, DAG and TAG obtained were 7.86%, 27.34% and 62.49% respectively. The physical agitation, however, would destroy the enzyme carrier due to shear stress. The high shear stress of stirring imposed to the immobilized enzyme by the mechanical agitation. Therefore, the immobilized enzymes may not be able to be employed again for a long time. To reduce these effects, Paula *et al.* (2015b) designed a stirrer tank containing a central basket and compared with the performance attained in a lateral basket. The authors used *Rhizopus oryzae* immobilized on polysiloxane-poly(vinyl alcohol) in the production of structured TAG through interesterification of milkfat with soybean oil. During 10 batch runs with 60 h total operation time, non-notable deactivation of the biocatalyst was observed which highlighted the potential use of both reactors.

To ensure excellent product consistency, intensive mixing is essential, which results in significant energy usage. As a result, many attempts have been made to replace the mechanical agitator and reduce energy consumption using other forms of continuous reactors. Another drawback of a batch reactor is its low productivity, which comes from the requirement to empty, wash, and reload the reactor for each new batch.

2.8.2 Packed Bed Reactor

Packed bed reactor can solve the difficulties found in the batch reactor. Unlike the batch reactor, the substrates are pumped through the column that filled with the catalyst. Solid packing materials of nearly comparable size are used to fill the packed bed reactor

(Doran, 2012). The accessible surface area and void space as well as functionality of the system are influenced by the catalyst size distribution and bed structure. Lipozyme TL IM, Lipozyme RM IM and Novozym 435 are widely utilized immobilized enzymes in packed bed reactor due to their small particle sizes and recyclability efficiency (Kocak Yanik *et al.*, 2016; da Silva *et al.*, 2018; Utama *et al.*, 2020). Lower-particle-size catalysts have more surface area, which could boost the rate of reaction and subsequently eliminating the mass transfer effects. Some immobilized carrier or support for lipase such as polystyrene-based hydrophobic resin (Gu *et al.*, 2016), polystyrene divinylbenzene beads (Yadav *et al.*, 2017), Sepabeads EC-EP (Bavaro *et al.*, 2020), calcium alginate-enzyme beads (Savickaite *et al.*, 2021) and silica–polyvinyl alcohol (Freitas *et al.*, 2013; Teixeira *et al.*, 2014; Vilas Bôas *et al.*, 2021) have been successfully synthesized for the production of aclyglycerol in the packed bed reactors. As a packed bed reactor is made from a fixed bed of catalyst, it is also known as fixed bed reactor (Freitas *et al.*, 2013; da Silva *et al.*, 2018). A packed bed reactor system has various advantages over a batch system, including ease of operation and excellent separation of reaction products and enzymes. The immobilized enzyme can be recovered, recycled, and incorporated again in a packed bed reactor system. Due to the lack of mechanical agitation, problems such biocatalyst shear, which are typical in batch reactors can be eliminated resulting in good catalyst stability and long-term use (Teixeira *et al.*, 2014; Gu *et al.*, 2016, Cozentino *et al.*, 2022).

In packed bed reactor system, flow rate is a critical operating parameter that must be carefully monitored in order to reduce mass transfer resistance while maintaining overall reaction rate. (Phuah *et al.*, 2015). It has a significant impact on reaction kinetics as well as volumetric productivity (Subroto *et al.*, 2020). Moreover, flow rate is necessary factor to determine the residence/reaction time in a packed bed reactor. The reaction time in batch reaction is the time determined after the reaction is finished and downstream

processing is performed on the mixture afterward (Shuler & Kargi, 2002). On the other hand, the residence time for a continuous reaction is calculated by dividing the reactor volume by the flow rate (Rønne *et al.*, 2005). Besides flow rate, the capillary length also can be used to study the effect of residence time of the reaction mixture (Čech *et al.*, 2012). Depending on the reactor configuration and the column length, various flow rates have been established ranging from 0.0003 mL min^{-1} (0.018 mL h^{-1}) even up to 2000 mL min^{-1} (Freitas *et al.*, 2013; Teixeira *et al.*, 2014; Kocak Yanik *et al.*, 2016; Dom *et al.*, 2014; Bavaro *et al.*, 2020; Utama *et al.*, 2020; Cozentino *et al.*, 2022).

Several authors investigated the comparative studies of the acylglycerols catalysed by lipase in stirrer tank reactor and packed bed reactor (Junior *et al.*, 2012; Sengupta *et al.*, 2015; Yadav *et al.*, 2017; Guajardo *et al.*, 2019). Packed bed reactor stands out for its high efficiency as high conversion can be achieved in shorter residence time. Employing Lipozyme RM IM, continuous flow reactor afforded a high yield of 73% within 1 min at 0.6 mL min^{-1} during the production of MAG (Junior *et al.*, 2012). In a packed-bed reactor utilising PyCal lipase, Yadav *et al.* (2017) discovered a high conversion of 86% within a 10-minute residence time. Besides its efficiency, less migration of acyl groups was also observed during the synthesis of structured TAG in packed bed bioreactor (Sengupta *et al.*, 2015). Productivity of the fed-batch and packed bed reactor systems achieved similar results (Guajardo *et al.*, 2019).

Having interesterification degree more than 90% (Kang *et al.*, 2015; Zhang *et al.* 2020b, Zhang *et al.*, 2021a), packed bed reactor showed a promising system for industrial processes of structured TAG products. The incorporation of fatty acids to the oils can improve the nutritional content of foods as well as provide functional qualities with higher nutritional value (Sengupta *et al.*, 2015). The low cost and broad applicability are key features for industrial applications of packed bed reactors, especially when compared to batch systems. Therefore, more progression is required in order to make enzymatic

synthesis of large-scale acylglycerols to be economically practicable. Zhang *et al.* (2020a, 2020b) assessed the feasibility of enzymatic TAG production in a self-made pilot scale packed bed reactor. A pilot-scale test was conducted in a 5 kg scale packed bed reactor containing 783 g Lipozyme TL IM. The packed bed reactor's daily output was expected to be 100 kg on a pilot scale. They observed that the biocatalytic efficiency was maintained, allowing a single batch of Lipozyme TL IM to be employed in 25 successive batches, resulting in interesterification of 125 kg of substrates (Zhang *et al.*, 2020b).

2.8.3 Bubble Column Reactor

The establishment of vacuum reactor is one of the strategies used to limit the presence of water in the reaction medium. Therefore, vacuum-driven air bubbling and vacuum-driven nitrogen bubbling reactor were established with the purpose to reduce the water content and enhance the mass transfer in the mixture particularly during the production of DAG using Novozym 435 lipase (Liu *et al.*, 2016; Zhang *et al.*, 2016 and Chen *et al.*, 2020). Liu *et al.* (2016) and Chen *et al.* (2020) conducted the esterification reactions at 60°C and 30 min reaction time with N_2 gas flow of 10.6 cm min^{-1}. The esterification of glycerol with a mixture of fatty acid (60% palm oil deodorizer distillate, 40 wt% oleic acid) was performed achieving the DAG purity of 91.30 ± 1.10% using one-step purification (Liu *et al.*, 2016). Meanwhile with double-step purification, Chen *et al.*, (2020) obtained 99% DAG purity. They conducted the synthesis of high purity medium chain DAG using a mixture of glycerol with dicaprylin and dicaprin as reaction substrates. In another study, Zhang *et al.*, (2016) investigated the production of DAG-enriched soybean oil in bubble column reactor by glycerolysis reaction and compared its thermal properties with soybean oil. They also found that DAG-enriched soybean oil has a higher melting point and crystallization onset than soybean oil. Unlike in a packed bed system, the mass transfer problem is reduced in the bubble column system as gases are blown

from the bottom up and increases interaction between immiscible substrates and lipase. However, the nitrogen gas must be purged throughout the reaction, resulting in substantial operational costs.

2.8.4 Microwave and Ultrasonic Reactor

It is important to update existing procedures and further leverage emerging technology. Performance of existing reaction can be improved by newer operational methods such as microwave irradiation (Hu *et al.*, 2013; Wang *et al.*, 2020b) and ultrasonication irradiation (Fiametti *et al.*, 2012). The principle of ultrasonic irradiation which is also referred as sonochemisty lies on the acoustic cavitation phenomena. The bubbles collapsing creates localised supercritical conditions, such as high temperature and pressure. DAG content was notably higher than that obtained via conventional heating and the reaction rate was boosted to a degree by microwave irradiation performed at 500 W for 1 h of reaction (Hu *et al.*, 2013). Similar reaction time is also required to redistribute fatty acids in the silkworm pupae oil transesterification to produce the novel structured lipid at 50 W (Wang *et al.*, 2020b). As compared to the products from the shaker reactor, Wang *et al.* (2020b) observed that the relative content of oleic acid was increased from 3.9% to 35.8% under microwave irradiation. The exposure of ultrasonic power at mild irradiation power supply in solvent-free glycerolysis of olive oil for 2 h reaction yielded a high content of reaction products, especially MAG (Fiametti *et al.*, 2012). Enzymatic ultrasound-assisted glycerolysis reaction was conducted using an ultrasonic water bath equipped with a longitudinal vibration transducer operating at 37 kHz frequency and 132 W output power. To depict the experimental data, two simple kinetic modelling methods focus on the ordered-sequential bi bi mechanism and reaction stoichiometry were used. However, the attention should be given either on the use of

probe or additional energy input for both microwave and ultrasonic reactors. These factors incurred extra costs for the overall production process.

2.8.5 Microreactor

Process intensification is an approach for converting traditional chemical processes into more cost-effective, productive, and environmentally friendly techniques. According to Stankiewicz & Moulijn (2000), process intensification can be simply defined as any chemical engineering development that leads to a substantially smaller, cleaner, and more energy efficient technology. As reviewed by many literatures, application of biocatalyst in continuous flow processing in milli- and microstructured reactors now becoming popular as it opens powerful process over conventional reactors (Tamborini *et al.*, 2018; Britton *et al.*, 2018; Woodley *et al.*, 2019; de Santis *et al.*, 2020). Being a part of process intensification, flow processing potentially speed up biotransformations due to greater mass transfer, allowing large-scale production to be done with substantially less equipment and a significant reduction in reaction time as compared to batch processes. The literature concerning the synthesis of TAG under continuous flow condition using microreactor system was examined by Čech *et al.* (2012) and Wang *et al.* (2016a).

Čech *et al.* (2012) investigated the TAG production by hydrolysis of soy bean oil in water using free *Thermomyces lanuginosus* lipase (Lipolase) in a microfluidic flow system. The system was equipped with microfluidic devices namely the slug flow generator, primary microseparator and secondary microseparator for complete separation of the oil and water phases. Each system was made using a separate technology. TAG conversion attained at 25-30% and almost 50% at 10 min and 1 h residence time, respectively. They discovered that energy consumption can be greatly reduced when compared to traditional agitated reactor. Due to the low characteristic velocities utilised

in their slug flow studies, the mass transfer coefficient is likewise lower. The findings suggest that the invented technology could be effective for producing fine compounds with a high substrate conversion.

By using a design of a packed-bed microreactor, Wang *et al.* (2016a) reported on the restructuring of polyunsaturated fatty acids-TAG using microalgae oil from Schizochytrium sp. mixed with tripalmitin in n-hexane. The microreactor channel was filled with Approximately 90 mg of Lipozyme RM IM beads before being covered with a glass pane. Then, a glass cement was used to seal the stainless steel plate and the glass pane. They examined that Lipozyme RM IM could be recycled in microreactor at least 18 times while maintaining its catalytic activity and selectivity. In contrast to batch reactor, Lipozyme RM IM only maintained 90% of its original activity. They studied that the main cost can be reduced from $212.3 to $14.6 per batch with the microreactor. At 2.5 h of reaction time, the maximum incorporation of total polyunsaturated fatty acids achieved was 54.2%, consisting 81.3% of *sn*-1,3 of polyunsaturated fatty acids.

2.9 Summary of literature review and research gap

It can be summarized that lipase-catalyzed synthesis of acylglycerols have made significant progresses and several technologies and methods have been studied and applied in a cost-effective and efficient way. The use of lipase enables the various reactions to be performed under mild environments while improving or retaining the product's quality. As compared to TAG synthesis, the rational design for MAG and DAG synthesis using lipase enzyme are relatively unexplored. This opens up a research gap and need to be studied. It was found that 3 out of 7 processes are suitable for DAG production namely glycerolysis, esterification and partial hydrolysis.

Concerning the acylglycerols synthesis, the most widely applied reactor in processes involving immobilized lipases is a batch reactor, followed by a packed bed

reactor. The success of a bioprocess does not depend solely on the catalytic efficiency of lipases and it is necessary to explore the bioreactor systems. Efficient reactors should be able to reduce capital costs, energy consumption, space necessity, reaction time, waste streams, and environmental problems. Therefore, it highlights the need of investigating the capacity of new reactors to improve acylglycerols reaction productivity.

Lastyly, most of the examined articles studied about the optimization and physiochemical properties of the targeted acylyglycerols. Potential developments for a new experimental design study should include the aspects such as mass transfer and kinetic model which are relatively scarce. With further advancements, industrial enzymatic of acylglycerols could become a realistic option in the future could potentially reduce the total production cost.

CHAPTER 3 :

MATERIALS AND METHODS

The information in Chapter 3 has been published in the following journals;

Abd Razak, N. N., Pérès, Y., Gew, L. T., Cognet, P., & Aroua, M. K. (2020). Effect of reaction medium mixture on the lipase catalyzed synthesis of diacylglycerol. *Industrial & Engineering Chemistry Research, 59*(21), 9869-9881.

Abd Razak, N. N., Gew, L. T., Pérès, Y., Cognet, P., & Aroua, M. K. (2021). Statistical optimization and kinetic modeling of lipase-catalyzed synthesis of diacylglycerol in the mixture of acetone/tert-butanol solvent system. *Industrial & Engineering Chemistry Research, 60*(39), 14026–14037.

Abd Razak, N. N., Cognet, P., Pérès, Y., Gew, L. T., & Aroua, M. K. (2022). Kinetics and hydrodynamics of *Candida antartica* lipase-catalyzed synthesis of glycerol dioleate (GDO) in a continuous flow packed-bed millireactor. *Journal of Cleaner Production*, 373, 133816.

3.1 Materials

3.1.1 Lipase enzymes

Four lipases (EC 3.1.1.3) including (1) lipase *Candida antarctica* B immobilized in acrylic resin, ≥5,000 U/g, recombinant, expressed in *Aspergillus niger* (CALB 1, also known as Novozyme 435), (2) lipase *Candida antarctica* B, immobilized on immo-bead 150, recombinant from *Aspergillus oryzae* (CALB 2), (3) Amano lipase PS, from *Burkholderia cepacia* and (4) Lecitase® Ultra, a phospholipase were purchased from Sigma Aldrich (Sigma Aldrich, USA).

3.1.2 Chemicals

The molecular sieve 3 Å, acetone, heptane, *tert*-butanol, glycerol (Gly) (approximately 99%), oleic acid (OA) (technical grade, 90%), monoolein (GMO) (1-oleoyl-*rac*-glycerol, approximately 99%), diolein (GDO) (mixture of 1,2- and 1,3-dioleoyl-*rac*-glycerol, approximately 99%), triolein (GTO) (glyceryl trioleate, ≥99%), 4-nitrophenyl palmitate (*p*NPP), sodium hydroxide solution (NaOH) were purchased from Sigma–Aldrich (USA). HPLC grade solvents such as *n*-heptane, methanol, acetonitrile, tetrahydrofuran were sourced from Merck (Darmstadt, Germany). Karl Fischer (KF)

reagents were sourced from Fischer Scientific Co. KF reagent HYDRANAL-composite 5 (Honeywell-Fluka®) was used as the titrant and HYDRANAL Methanol dry (Honeywell-Fluka®) acted as the medium. Karl Fischer Aqualine water standard was initially used to standardize the KF titration.

3.2 Workflow of the study

Lipase-catalysed esterification of oleic acid with glycerol was studied in batch and continuous flow reactors. Fig. 3.1 shows the overall flow and organization of the experiments that comprises preliminary study, batch system study and continuous flow system study. Initially, in the preliminary study, four different types of lipases were chosen as the biocatalyst of reaction. The effect of different solvent systems at various temperatures, rheological characteristics, mass transfer and thermodynamic studies were investigated during the synthesis of glycerol oleates.

To further improve the selectivity of GDO production, rigorous optimization of the reaction operating variables is essential. Therefore, in the second section of study, the effects of operating parameters in one selected solvent system were examined for the optimization of GDO synthesis by using Box–Behnken designs (BBD) in the batch reactor. Based on the optimized condition, the investigation on the reaction mechanism and the kinetic parameters were carried out. In this study, various fixed initial quantities of oleic acid were reacted with different initial concentrations of glycerol and *vice versa*.

The final part of the experiments were focusing solely on the continuous flow system. In this section, the optimization of GDO production was performed using one-factor-at-a-time (OFAT) method. Mass transfer limitation and kinetics of lipase under continuous flow were examined at the optimized conditions. The enzyme kinetics were calculated using the experimental data achieved at different flow rates at various oleic acid concentrations with fixed concentration of glycerol.

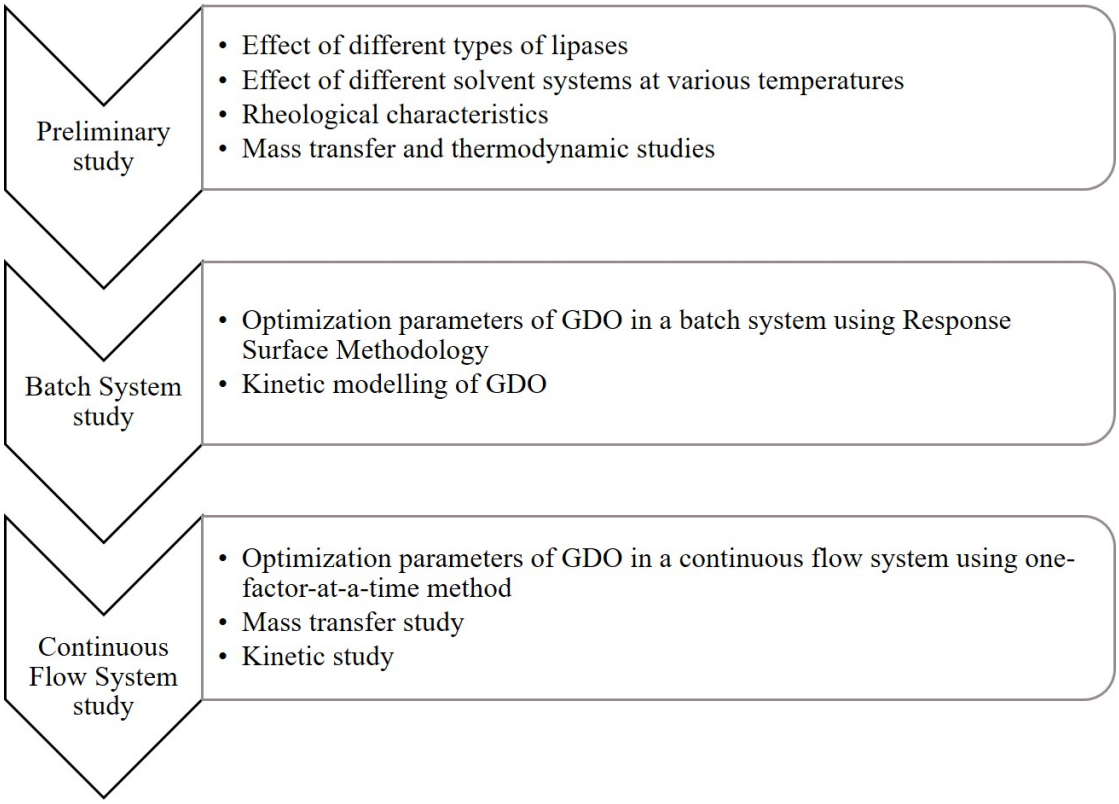

Figure. 3.1. Schematic flow and the organization of work on the study of the lipase-catalysed synthesis of GDO.

3.3 Preliminary study in a batch system

Synthesis of glycerol oleates

Preliminary study was performed in order to investigate the profiles of glycerol oleates and to study pretreatment conditions which could improve GDO production. Four commercially available lipases were screened for their ability to esterify oleic acid with glycerol. The operating mode of the esterification reaction of glycerol with oleic acid was adapted from Duan *et al.* (2010). In order to standardize and maintain batch-to-batch consistency, all the solvents used were pre-incubated at least 24 h prior reaction using excess of molecular sieve. The molar ratio OA:Gly was fixed at 2.5:1 and the composition of the reaction mixtures were as follows: oleic acid (2 g), glycerol (0.26 g), solvent (1.2 g) and lipase enzyme (0.2 g). 3 Å molecular sieves (1.28 g) were added into the reaction mixture to remove water produced during the reaction. The enzymatic esterification was

performed in screw-capped glass tubes and stirred using magnetic stirrer bar with hemispherical ends at 200 rpm. Considering the viscosity of reaction medium, miscibility of glycerol and oleic acid, the presence of molecular sieve and immobilized lipase enzyme, the most suitable agitation speed to achieve a good mixing and homogeneity for this system was found to be at 200 rpm. Moreover, studies have shown that 200 rpm was the optimum agitation speed for esterification reaction involving immobilized lipase (Garlapati *et al.*, 2013, Kabbashi *et al.*, 2015, Subroto *et al.*, 2020). Four different type of solvent systems were employed namely solventless, acetone, *tert*-butanol and blended mixture of acetone*:tert*-butanol. The boiling point of acetone and *tert*-butanol are quite low, estimated at 56 ºC and 82 ºC, respectively. Since the recovery and purification of GDO are normally conducted at 100 to 200 ºC using molecular distillation (Naik *et al.*, 2014; Chen *et al.,* 2020), both solvents can be certainly eliminated from the products during down-stream processes. Glass tubes were used for the reaction, which was placed in a beaker of water that was heated on a hot plate. Depending on the boiling point of the solvent used, a constant reaction temperature (35 to 65ºC) was applied at different combination of experimental run**.** The schematic diagram of the preliminary study in a batch system in shown in Fig. 3.2. In order to monitor the progress of the reaction, samples (100 µl aliquot each) for analyses were taken at regular intervals such as 0.5 h, 1 h, 2 h, 4 h, 6 h and 24 h. Two independent replicates were made for every experiment conducted. Blank experiments (without catalyst) were also conducted in parallel.

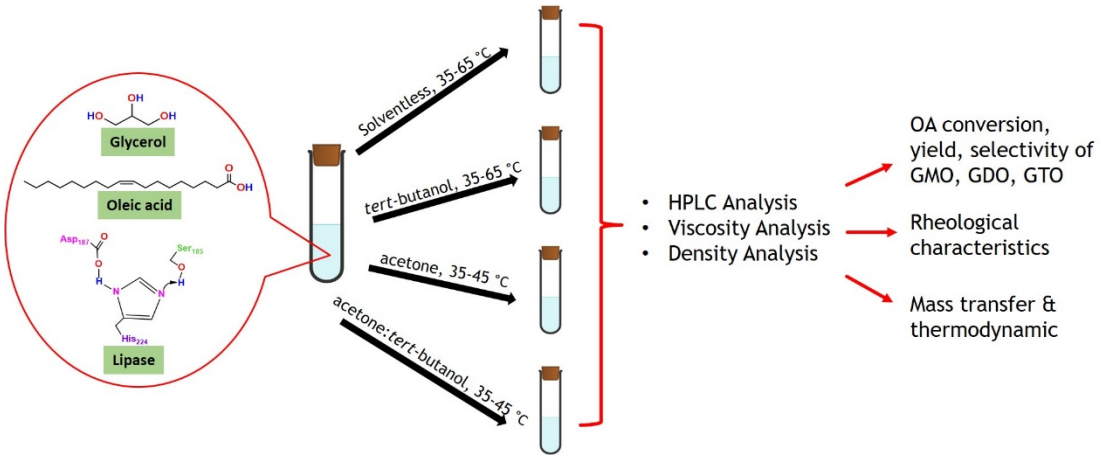

Figure 3.2. Schematic diagram of the preliminary study of glycerol oleates in a batch system.

3.3.1 Determination of lipase activity

Lipase activity was measured by monitoring the rate of hydrolysis of *para*-nitrophenyl palmitate (*p*Npp) (Pencreac'h & Baratti 1996). Approximately, 20 mM *p*Npp was dissolved in *n*-heptane and used as a substrate for lipase. The hydrolysis reaction was carried out in a two-phase solution where immobilized lipase partitioned between heptane and 0.1 M NaOH solution interphase. The assay was done by adding 2.5 mL of 0.1 M NaOH and 0.5 mL of 20 mM*p*Npp in *n*-heptane into a cuvette. Two immiscible solutions were formed where *p*Npp in *n*-heptane was in the upper part and 0.1 M NaOH was in the lower part. Then, 10 mg of immobilized lipase was added and the spectrophotometric absorbance was monitored immediately at 410 nm for 20 minutes. The reaction was measured using UV/VIS Spectrophotometer Jasco V-630 (Japan) equipped with a temperature controller system. To ensure proper mixing of the solutions, a tiny magnetic stirrer bar (9 mm diameter × 8 mm high) was located at the bottom of the cuvette (10 mm diameter). Hydrolysis of *p*Npp released *p*-nitrophenol and resulted in yellow coloration in the 0.1 M NaOH solution. Reactions within the temperature range of 30 to 80°C were performed in order to investigate the effect of temperature on lipase activities. The range of temperatures is considered the ideal range to study the stability of enzymes

since changes in the physical and chemical properties of the lipase could possibly be observed (Duan *et al.,* 2010; Anand *et al.,* 2020; Skliar *et al.,* 2020). By employing Beer-Lambert relationship, lipase activity, U_E was calculated using Eq. (3.1);

$$U_E\ mL^{-1} = \Delta Abs_{410nm} \times \frac{1}{l_c} \times \frac{1}{\xi_{410}} \times \frac{V_{TA}}{V_{pNpp}} \tag{3.1}$$

where ΔAbs_{410nm} is the absorbance difference at 410 nm at for a specific interval (min^{-1}), l_c is the light path length in cuvette (cm), ξ_{410} is the extinction coefficient of *p*-nitrophenol i.e. 1070.43 M^{-1} cm^{-1}, V_{TA} is the total assay volume (mL) and V_{pNpp} is the *p*Npp volume (mL).

3.4 Optimization of GDO synthesis

3.4.1 Optimization of GDO synthesis in a batch system using Response Surface Methodology (RSM)

The use of acetone: *tert*-butanol mixtures for the synthesis of glycerol oleates showed a positive effect on selectivity for GDO based on the preliminary studies in Section 3.3 (Abd Razak *et al.*, 2020). Therefore, the experiments were carried out at various percentages of acetone to *tert*-butanol ranging from 30 to 70% in the mild temperature range 35 to 45°C and enzyme loading of 0.1 to 0.2 g. Since moderate temperature was applied during the reaction, it is believed that use of lipases may lower the overall cost. The optimal and reasonable amount of lipase enzyme employed for the synthesis of DAG appears to be between 5-10% based on the oil weight (Duan *et al.*, 2010; Voll *et al.*, 2011). In this work, the enzyme load of 0.1 g (2.51 × 10 g L^{-1}), 0.15 g (3.78 × 10 g L^{-1}) and 0.2 g (5.03 × 10 g L^{-1}) used correspond to the mass percentage of 5, 7.5 and 10% based on the weight of oleic acid (i.e. 2 g), respectively. Based on the progression curve obtained, sampling (100 µL aliquot each) for analyses was fixed at 2 h

of reaction. Each combination of variables was conducted in triplicates. The schematic diagram of the optimization study in a batch system in shown in Fig. 3.3.

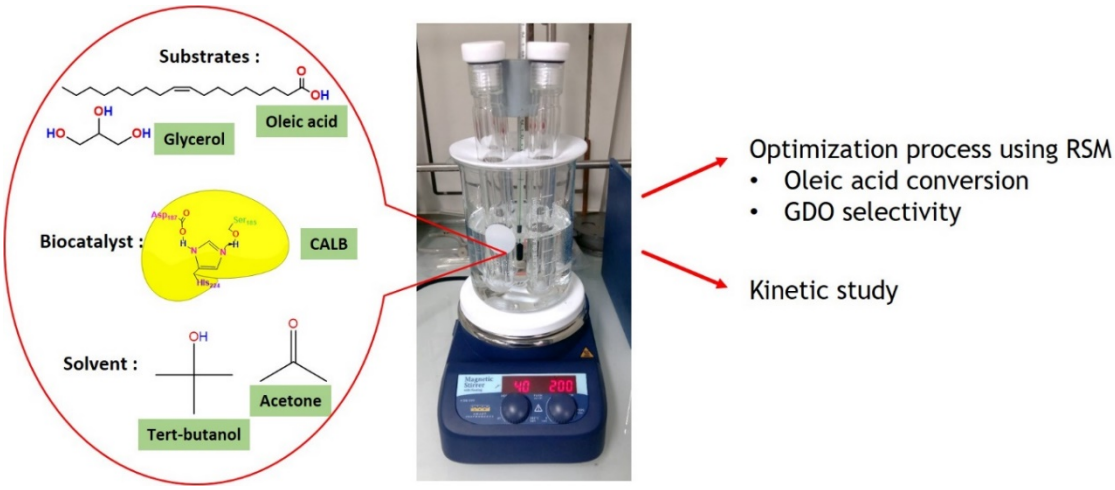

Figure 3.3. Schematic diagram of the optimization and kinetic studies of GDO in a batch system.

In this work, being a part of RSM, BBD was established to optimize the particular variables employed in the reaction. An orthogonal array design was constructed using MINITAB® 18 software. Applying three factors at three level design, each independent variable was coded at three levels between -1, 0 and +1. Table 3.1 illustrates the variable values with their respective design codes.

Table 3.1. Summary of the variable levels in the reactions in RSM

Label	Variables	Level (coded)		
		(-1)	(0)	(+1)
A	Percentage of acetone to *tert*-butanol (*v/v* %)	30	50	70
B	Temperature (°C)	35	40	45
C	Enzyme loading (g)	0.1	0.15	0.2

Coded values compare the coefficient sizes in order to determine which variable has the strongest influence on the response. If a design is analyzed in actual factor values, it might no longer be orthogonal. Coded value of each factor was calculated using Eq. (3.2) (Myer, 2016);

$$Coded\ value\ =\ \frac{actual\ factor\ value - \left(\frac{highest\ factor\ value + lowest\ factor\ value}{2}\right)}{\left(\frac{highest\ factor\ value - lowest\ factor\ value}{2}\right)} \qquad (3.2)$$

Employing a second order polynomial equation, the correlation between the independent variables and the predicted response (Y) is shown in Eq. (3.3);

$$Y = \beta_0 + \beta_1 A + \beta_2 B + \beta_3 C + \beta_{11} A^2 + \beta_{22} B^2 + \beta_{33} C^2 + \beta\alpha_{12} AB + \beta_{13} AC + \beta_{23} BC \qquad (3.3)$$

where Y is the predicted response variable; β_1, β_2, and β_3 are the linear terms coefficients; β_{11}, β_{22}, and β_{33} are the quadratic terms coefficients; and β_{12}, β_{13}, and β_{23} are the interaction terms coefficients. The coded forms of the input variables are represented by A, B and C. The statistical results and response surfaces were generated using the design software. The analysis of variance (ANOVA) was used for the various statistical evaluation of regression model.

3.4.2 Optimization of GDO synthesis in a continuous flow system using one-factor-at-a-time (OFAT) method

A commercially available continuous flow system, VapourTec R2C/R4 was used in the process intensification of glycerol oleates. An Omnifit column (100 mm length × 6.6 mm ID) was loaded with 1.1 g of molecular sieve of 3 Å size followed by the addition of commercial immobilized CALB as a biocatalyst. The column resembles a packed bed millireactor (Fig 3.4). The particle size of the polymeric resin of immobilized CALB was estimated to be 315-1000 μm, with a surface area of 130 $m^2\ g^{-1}$ and a pore diameter of 150 Å (Ortiz *et al.*, 2019). Denčić *et al.* (2013) and Chowdhury & Mitra (2015) observed that the average particle size distribution was between 420-500 μm. Due to this variation,

the mean size of 500 μm lipase was selected for result evaluation. Acetone was initially pumped to rinse the instrument until it had reached a stable condition and ready for the reaction. A solution of oleic acid (1.9 to 2.1 M) and glycerol (0.8 to 1.3 M) were independently prepared in a reagent bottle containing mixture of acetone:*t*-butanol (70:30 v/v). Due to high viscosity, premixed solution of glycerol was submerged in a stirring water bath at 45°C. Both stock solutions were pumped from the reagent bottles and then combined in a T-mixer before entering the inlet of the column. The mixture was fed in upward direction at various flow rates (2×10^{-5} to 1.5×10^{-3} L min^{-1}) and the maximum pressure was kept at 20 bar. The peristaltic pumps were used to control the flow rate of both reactants and the temperature for heating jacket was set at 45ºC.

The amounts of immobilized lipase were varied from 0.05 to 0.25 g. As compared to the range of lipase applied in the batch system, the range of lipase used in a continuous flow system is broader since the OFAT approach was employed in the synthesis of GDO. To study the effects of residence time, both substrates were introduced into the column at different rates ranging from 2×10^{-5} to 1.5×10^{-3} L min^{-1}. To investigate the effect of molar ratio of substrates on esterification, the molar ratio oleic acid to glycerol were set at 1.4 to 2.5. Samples were taken at predetermined residence time to monitor the reaction progress. All experiments were repeated in triplicate to determine the reproducibility of data. Both reagent tubes were dipped into the acetone flask and rinsed for 15 min in order to clean any residual reaction mixture after processing.

The residence time, *R*t (min^{-1}) was calculated from the following formula given by Rønne *et al.* (2005) as shown in Eq. (3.4);

$$Rt = \frac{V_R \times \varepsilon}{Q} \tag{3.4}$$

where V_R is the volume of the reactor (L), ε is the bed porosity of the immobilized enzyme and Q is the volumetric flow rate (L min^{-1}). The bed porosity, ε is referring to the ratio of the reactor void volume, V_{void} to the total reactor volume, V_R. V_{void} specifically refers to

the volume of the liquid phase contained inside a column, which was estimated by weighing the mass differential of added particles (i.e. CALB and molecular sieve) in a reactor with and without the presence of solvent. Then, the subtracted value obtained was divided with solvent's density. Based on the Eq. (3.5), the value of V_{void}, V_R and ε were estimated at 1.54 mL, 2.44 mL and 63.23% respectively.

$$\varepsilon = \frac{V_{void}}{V_R} \tag{3.5}$$

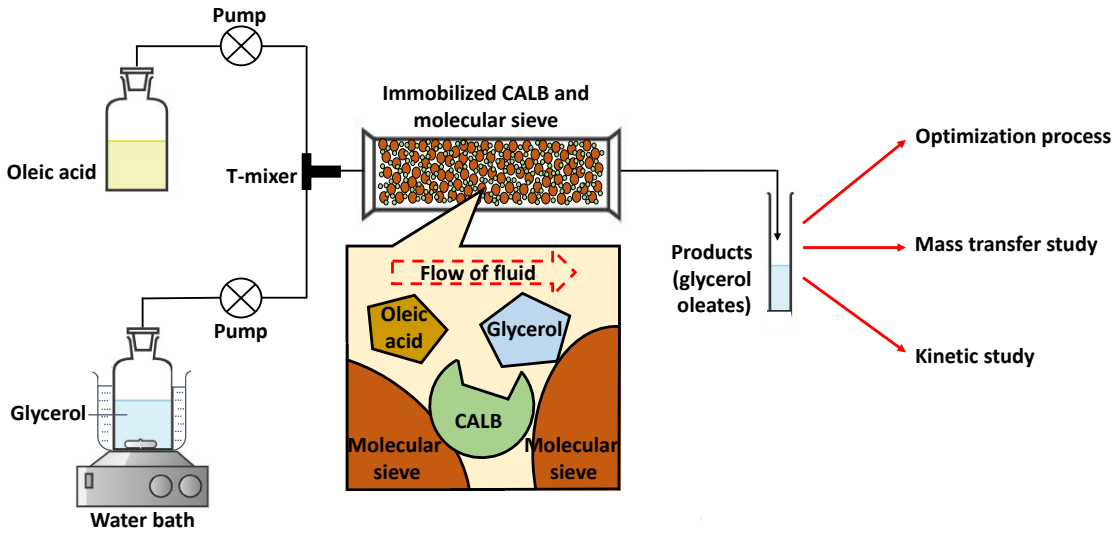

Figure 3.4. Schematic diagram of the optimization, mass transfer and kinetic studies in a continuous flow system

Reusability of CALB 1 was tested by repeatly using the same enzyme in the production of glycerol oleates in a continuous flow system. The flow rate of the reaction system was set from 2×10^{-5} to 5×10^{-5} L min^{-1} at 45°C and the reaction time was set according to its residence time. After this time, approximately 2 mL of sample was collected in a collecting vial. Then, the enzyme was washed with acetone for 15 min and fresh reaction substrates were then introduced for the next run. The sample was determined through HPLC analysis for each cycle.

Meanwhile the storage stability of CALB 1 was investigated after continuously reused for each cycle. After the reusability experiment was done, the enzyme was washed with acetone for 15 min, unloaded from the column and kept at -4°C to be reused for other

esterification processes. After storage, the reused enzyme was then loaded into the column and fresh reaction substrates were pumped into the column. The sample was collected at the outlet and subjected to HPLC analysis. The stability of reused lipase was observed for 11 days of storage.

3.5 Mass-transfer study in the batch and continuous flow systems

The concentration differential between the bulk solution and the particle interior drives mass transfer of substrate to reaction sites in the solid catalyst. The reaction rate depends on the mass transfer rate of reactant outside and inside the particle. Basically, there are two types of transport mechanisms that are commonly occur. The first process is known as external mass transfer in which substrate are transferred from bulk liquid phase to the surface of the immobilized biocatalyst, while the internal mass transfer is referring to simultaneous diffusion and reaction of substrate within the biocatalyst. The mass transfer rates and the effectiveness factors are depending on the reactor hydrodynamics and also the properties of the liquid such as density, viscosity, and diffusivity. It is important to understand the diffusional effects in the system since the reaction rate depends on the mass transfer rate of the reactant inside and outside the particle.

Adapted from Wilke and Chang (1955) correlation, the diffusion coefficient of glycerol and oleic acid in a blended mixture were calculated using Eq. (3.6) to (3.7) as proposed by Safi *et al.* (2007).

$$D = 7.4\times10^{-8}\frac{(\Phi W)^{1/2}}{\mu M_V^{0.6}}T \tag{3.6}$$

$$D_{mix} = 7.4\times10^{-8}\frac{(\Phi_{mix}W_{mix})^{1/2}}{\mu_{mix}M_V^{0.6}}T \tag{3.7}$$

$$\Phi_{mix}W_{mix} = x_{t-BuOH}\Phi W_{t-BuOH} + x_{acetone}\Phi W_{acetone} \tag{3.8}$$

The diffusivity, D (m^2 s^{-1}) was calculated using Eq. 3.6 in which ϕ is the association parameter of the solvent, W is the molecular weight of the solvent (kg mol^{-1}), μ is the solvent viscosity (kg m^{-1} s^{-1}) and M_V is the molar volume of reactants (m^3 mol^{-1}) and T is the absolute temperature (K).

The diffusivity in blended solvents, D_{mix} (m^2 s^{-1}) was determined using Eq. (3.7) where ϕ_{mix} is refer to the association parameter of blended solvents, W_{mix} is the molecular weight of the blended solvents (kg mol^{-1}) and μ_{mix} is the viscosity of blended solvents (kg m^{-1} s^{-1}).

Association parameter of the blended liquids and the molecular weight of the blended solvents represented in Eq. (3.8) where $x_{acetone}$ is the mole fraction of acetone in reaction mixture, $x_{t\text{-}BuOH}$ is the mole fraction of t-butanol in reaction mixture, $W_{acetone}$ molecular weight of acetone (kg mol^{-1}) and $W_{t\text{-}BuOH}$ is the molecular weight of the *t*-butanol (kg mol^{-1}). Considering the association of glycerol and oleic acid and the unavailability of ϕ values, 2.60 (ϕ of water) and 1.0 (ϕ of hydrocarbons), are used in the calculation, respectively (Guo and Sun, 2007).

3.5.1 External mass transfer parameters

External mass transfer study requires determination of the external mass transfer coefficient, K_{SL} (m s^{-1}) that is correlated with variables such as flow rate, reactor diameter and fluid properties. The dimensionless numbers Reynolds (*Re*), Schmidt (*Sc*) and Sherwood (*Sh*) were calculated by Eqs. 3.9 to 3.11 as shown below;

$$Re = \frac{d_{CALB} U \rho_{mix}}{\mu_{mix}} \tag{3.9}$$

$$Sc = \frac{\mu_{mix}}{\rho_{mix} D_{mix}} \tag{3.10}$$

$$Sh = \frac{K_{SL} d_{CALB}}{D_{mix}} \tag{3.11}$$

where d_{CALB} is the diameter of CALB 1 enzyme, U is the superficial velocity (m s^{-1}), ρ_{mix} is the density of liquid mixture (kg m^{-3}), U is superficial velocity (m s^{-1}).

Superficial velocity, U in flow system was determined using Eq. (3.12);

$$U = \frac{Q}{A} \tag{3.12}$$

where Q is flow rate (m^3 s^{-1}), A is cross sectional area of the column (m^2).

In this work, *Sh* number was determined by means of Moo-Young and Blanch (1981) correlation for Sherwood number applied for the range $10 < Re < 10^4$ as shown in Eq. (3.13);

$$Sh = 0.95\ Re^{0.5} Sc^{0.33} \tag{3.13}$$

K_{SL} values (m s^{-1}) were then used to describe the external mass transfer effect in the form of Damköhler (*Da*) dimensionless number. *Da* serves as an index of controlling mechanism in the system in order to assess the relative importance of reaction kinetics and solute transport.

$$Da = \frac{r_{[OA]}}{K_{SL} a_C [OA]_0} \tag{3.14}$$

where $r_{[OA]}$ is the reaction rate of OA, and a_c is external surface area per volume of catalytic bed (m^{-1}) and $[OA]_0$ is the surface concentration of OA (M).

The specific external surface area of the catalyst, a_c was determined from the porosity and the diameter (d_{CALB}) of the catalyst particles, as shown in Eq. (3.15) (Fogler, 2016).

$$a_c = \frac{6(1-\varepsilon)}{d_{CALB}} \tag{3.15}$$

The external effectiveness factor (η_E) or the interphase effectiveness factor is defined as the ratio of the reaction rate for the condition at the surface to the reaction rate

surrounding the particle. The values of the external effectiveness factor were calculated in order to verify the existence of an external mass transfer limitation. The external effectiveness factor was determined by Eq (3.16) as outlined by Carberry (2001).

$$\eta_E = \left[\frac{1}{2Da} (\sqrt{1 + 4Da} - 1) \right] \tag{3.16}$$

Peclet number (*Pe*) was calculated according to the Eq. (3.17). This number measures the relative importance of advection with respect to diffusion.

$$Pe = \frac{U \times l}{D_{mix}} \tag{3.17}$$

where *l* is the length of packed bed reactor (m).

3.5.2 Internal mass transfer parameters

Meanwhile, the internal mass transfer diffusion was evaluated by the Thiele modulus (Shuler & Kargi 2002; Doran, 2012) as shown in Eq. (3.18).

$$\phi = \frac{r_{[OA]}}{D[C]_0} (\frac{d_{CALB}}{3})^2 \tag{3.18}$$

where $[C]_0$ is the surface concentration of substrate (M) i.e. glycerol $[Gly]_0$ or oleic acid $[OA]_0$ in organic phase.(Diffusivity value must check)

The internal effectiveness factor (ηI) or the intraphase efficiency in terms of the Thiele modulus (Φ) was subsequently determined using Eq. (3.19).

$$\eta_I = \frac{3}{\phi} (\frac{1}{\tanh \phi} - \frac{1}{\phi}) \tag{3.19}$$

3.6 Kinetic studies of glycerol oleates synthesis

3.6.1 Kinetic study in a batch system

Initial reaction rate was calculated from the slope of the polynomial equation of glycerol oleates synthesis for each set of experiment as embodied in Eq. (3.20).

$$r_{[GO]} = \frac{\Delta[GO]}{\Delta t_{[GO]}} \tag{3.20}$$

where Δ[GO] is the changes in the molar concentration (M) of glycerol oleates and Δ*t* is the changes of time for each [GO] (h). Each [GO] is designated as follows; [GMO], [GDO] and [GTO] which represent the molar concentration (mol L^{-1}) of GMO, GDO and GTO respectively.

Kinetic experiments were carried out following the procedure described in Section 3.5. For kinetic model investigation, experiments were conducted by maintaining the concentration of one of the substrates constant and varying the concentration of the other and *vice versa*. In the first set of experiments, glycerol concentrations were varied from 0.31 M to 1.32 M at a fixed concentration of oleic acid. Whereas, in the second set, the concentration of oleic acid was varied from 1.88 M to 2.13 M at a fixed quantity of glycerol. The plots shown in the present work were constructed from all the experimentally determined reaction rates utilizing Lineweaver–Burk reciprocal analysis (Segel, 1975). The reaction rates obtained at various oleic acid and glycerol concentrations focusing on GDO synthesis were fitted to kinetic model using non-linear regression (Polymath® software).

For activation energy determination, the initial reaction rate of GDO synthesis was studied in the range of 35 to 55°C. Activation energy is the minimum energy required to convert a normal stable molecule into a reactive molecule and it reflects the rapidity of chemical reactions. The activation energy (E_a, J mol^{-1}) of GDO synthesis was calculated using the linearized Arrhenius equation;

$$\ln k' = \frac{E_a}{RT} + \ln A_F \tag{3.21}$$

where *R* is the gas constant (8.3145 J mol^{-1} K^{-1}) and A_F is the frequency factor or Arrhenius factor (min^{-1}). To calculate k_1', the rate of GDO synthesis was plotted against

different initial oleic acid concentration for each temperature tested (35 to 55°C). The rate constant k_1' was obtained from the slope of the resulting linear plot.

3.6.2 Kinetic study under continuous flow system

When working with continuous flow reaction system, flow rate playing a major role on enzyme kinetics. Therefore, the Michaelis–Menten constant, *Km*, were calculated using the experimental data achieved at different flow rates (2×10^{-5} L min^{-1} to 1.5×10^{-3} L min^{-1}) at various oleic acid concentrations (1.85 M to 2.08 M) with fixed concentration of glycerol (1.30 M). In this experiment, amount of immobilized lipase was fixed at 0.15 g and was loaded in the packed bed reactor. Employing Eq. (3.22), the apparent kinetic parameters in packed-bed enzyme reactors were evaluated with the underlying assumptions of Michaelis–Menten kinetics and plug-flow behavior under steady state conditions (Lilly *et al.*, 1966). As outlined by Marangoni (2003), rearrangement term of Lily-Hornby equation leads to Eq. (3.23).

$$f_{[OA]}[OA] = \frac{C_R}{Q} - K_m \ln(1 - f_{[OA]}) \tag{3.22}$$

$$Q\ln(1 - f_{[OA]}) = \frac{f_{[OA]} Q[OA]_0}{K_m} - \frac{C_R}{K_m} \tag{3.23}$$

where $f_{[OA]}$ is the fraction of oleic acid converted, C_R is the reaction capacity and K_m is the Michaelis-Menten constant (M). K_m was calculated from the slope of the linear plot, and the maximum reaction rate, V_{max} was measured from reaction capacity value, C_R which was obtained from the intercept of the plot. The relationship between C_R and V_{max} shown in Eq. (3.24),

$$C_R = k_{cat}[ET]\varepsilon, \quad V_{max} = k_{cat}[ET] \tag{3.24}$$

In this study, the reacted oleic acid concentration, f was experimentally determined by subtracting the oleic acid in the outlet stream from the inlet stream of the reactor (Seong *et al.*, 2003) as shown in Eq. (3.25),

$$f_{[OA]} = 1 - \frac{[OA]}{[OA]_0} \tag{3.25}$$

where [OA] is the oleic acid concentration (M).

The reaction rate under continuous flow condition of GDO was determined according to Eq. (3.26) (Csajági *et al.*, 2008; Wang *et al.*, 2014; Zambelli *et al.*, 2016; Bavaro *et al.*, 2018).

$$r_{[\mathrm{GDO}]} = [GDO] \times Q \tag{3.26}$$

3.7 High Performance Liquid Chromatography (HPLC) analysis

3.7.1 HPLC conditions employed for the separation glycerol oleates in the preliminary study

The glycerol oleates and oleic acid in the reaction mixture was analyzed by a Thermo Scientific HPLC-RI through an isocratic method, equipped with Gemini C18 11OA column (100 mm × 2 mm × 3 μm). Prior to analysis, reaction samples were dissolved into appropriate amount of acetone and mobile phase. For OA and GMO analysis, the sample was mixed with 50% of acetone and 50% of mobile phase (v/v). Meanwhile for GDO and GTO analysis, the sample was mixed with 80% of acetone and 20% of mobile phase (v/v). The sample was filtered through a 0.20 μm PTFE filter for subsequent analysis by HPLC. OA and GMO were separated using a mobile phase consisted of acetone/water (80:20 v/v) with 0.1% trifluoracetic acid, TFA (v/v of total mobile phase); GDO and GTO were separated using acetonitrile/methanol/ tetrahydrofuran (40:40:20 v/v/v) (Lee *et al.*, 2013; Kong *et al.*, 2018). The injection volume was 10 μL and the diluted samples were eluted at a 220 μL min^{-1} flow rate. The column and RI detector temperatures were set at 40°C and 45°C respectively.

3.7.2 HPLC conditions employed for the optimization of GDO in batch and continuous flow systems

For Response Surface Methodology (RSM) experiment in a batch system, glycerol oleates and oleic acid in the reaction mixture was analyzed by an Agilent HPLC-RI meanwhile for one-factor-at-a-time (OFAT) experiment using continuous flow system, the analysis was examined using VWR Hitachi Chromaster HPLC-RI. The analysis was carried out using an isocratic method, equipped with Kinetex XB-C18 column (100 mm × 4.6 mm × 2.6 μm).

Each 100 μL sample was withdrawn and mixed 1 mL of acetone:acetonitrile (60:40 v/v). The sample was filtered through a 0.20 μm PTFE filter for subsequent analysis by HPLC. OA and GMO were separated using a mobile phase consisting of acetonitrile/water (80:20 v/v) meanwhile GDO and GTO were separated using acetone:acetonitrile (60:40 v/v). The injection volume was 20 μL and the diluted samples were eluted at a 1 mL min^{-1} flow rate. The column and RI detector temperatures were set at 40°C and 45°C respectively.

External calibration curves of GMO, GDO and GTO were constructed based on the specific area obtained for each HPLC used. The calculation for conversion, yield, selectivity in term of percentage and productivity were determined using Eq. (3.27) to (3.30), respectively.

$$Conversion = f_{[OA]} \times 100\% \tag{3.27}$$

$$Yield = \frac{z[GO]}{[OA]_0} \times 100\% \tag{3.28}$$

$$Selectivity = \frac{[GO]}{[GO]_{total}} \times 100\% \tag{3.29}$$

$$Productivity = \frac{[GO]_{max}}{t_{[GO]_{max}}} \tag{3.30}$$

where z is the stoichiometric coefficients of [GO]. For each [GO], z is calculated as follows: [GMO], z =1; [GDO], z =2 and [GTO], z =3. $[GO]_{total}$ is the total concentration of glycerol oleates (mol L^{-1}) and $[GO]_{max}$ is the maximum molar concentration of glycerol oleates (mol L^{-1}) at its maximum time i.e. 24 h, $t_{[GO]max.}$

3.8 Thermochemical analysis

Oleic acid (OA) undergoes a reversible reaction with glycerol (Gly) to form GMO, GDO, GTO and water (H_2O) with lipase as a biocatalyst. The esterification occurs based on three consecutive reaction steps as reflected in Eq. (3.31) to (3.33).

$$OA + Gly \rightleftharpoons GMO + H_2O \; ; K_{GMO} \tag{3.31}$$
$$OA + GMO \rightleftharpoons GDO + H_2O \; ; K_{GDO} \tag{3.32}$$
$$OA + GDO \rightleftharpoons GTO + H_2O \; ; K_{GTO} \tag{3.33}$$

At equilibrium, there is no net driving force for further change in which the reaction has reached the limit of its capacity for chemical transformation. The apparent equilibrium constant K_{eq} was subsequently estimated using Eq. (3.34).

$$K_{eq} = K_{GMO}.K_{GDO}.K_{GTO} \tag{3.34}$$

where $K_{GMO,}$ K_{GDO} and K_{GTO} represent each apparent equilibrium constant value. The calculation conditions for $K_{GMO,}$ K_{GDO} and K_{GTO} are shown in Eq. (3.35) to (3.37) (Lortie *et al.*, 1993).

$$K_{GMO} = \frac{[GMO]_{eq}[H_2O]_{eq}}{[Gly]_{eq}[OA]_{eq}} \tag{3.35}$$

$$K_{GDO} = \frac{[GDO]_{eq}[H_2O]_{eq}}{[GMO]_{eq}[OA]_{eq}} \tag{3.36}$$

$$K_{GMO} = \frac{[GTO]_{eq}[H_2O]_{eq}}{[GDO]_{eq}[OA]_{eq}} \tag{3.37}$$

where $[GMO]_{eq}$, $[GDO]_{eq}$, $[GTO]_{eq}$, $[OA]_{eq}$, $[Gly]_{eq}$ $[H_2O]_{eq}$ are the concentration of GMO, GDO, GTO, OA, Gly and water at equilibrium, respectively.

K_{eq} was measured at various temperatures. The temperature dependence of K_{eq} is expressed according to van't Hoff equation as embodied in Eq. (3.38),

$$\ln K_{eq} = -\frac{\Delta H}{RT} + \frac{\Delta S}{R} \tag{3.38}$$

where ΔH is van't Hoff enthalpy (J mol^{-1}) and ΔS is entropy (J mol^{-1} K^{-1}).

At constant pressure and temperature, Gibbs free energy change (ΔG, J mol^{-1}) for the reaction at non-standard conditions was calculated using Eq. (3.39),

$$\Delta G = \Delta H - T\Delta S \tag{3.39}$$

Gibbs free energy at standard condition (ΔG^o, J mol^{-1}) was calculated as shown in Eq. (3.40),

$$\Delta G - \Delta G^0 = RT \ln K_{eq} \tag{3.40}$$

3.9 Rheological analysis and log *P* for the solvents

Rheological measurements were performed using an AR2000ex rheometer (TA Instruments). Shear stress (τ) and viscosity (μ) of initial reaction mixture were measured using a cone-and-plate geometry with a diameter of 60 mm. The angle and the gap between the cone and plate are 2º and 65 μm, respectively. Samples were placed in the measurement plate of the viscometer at the intended temperature ranges from 35 to 65ºC. The shear stress of the sample was measured in the range of shear rate 0.1 to 2000 s^{-1}. Determination of liquid viscosity and its flow behaviour was based on Herschel–Bulkley model (Barnes *et al.*, 1989) as shown in Eq. (3.41).

$$\tau = \tau_0 + b\gamma^n \tag{3.41}$$

where *b* is the consistency coefficient ($Pa.s^n$), γ is the shear rate (s^{-1}), τ is the shear stress (Pa), τ_0 is the yield stress (Pa) and n is dimensionless flow behavior index.

The density of each mixture at different temperatures was measured using Anton Par DMA-4500 density meter. Density measurements were carried out at temperatures from 30 to 65ºC with three replicates for each reading.

Hydrophobicity is reflected by log *P*, where *P* is the partition coefficient for a given solvent between *n*-octanol and water. The log *P* values for *tert*-butanol and acetone were obtained from the literature (Laane *et al.*, 1987; Narayan & Klibanov, 1993; Kuo & Parkin, 1996). The log P_{mix} of the blended mixture of *tert*-butanol and acetone was calculated as proposed by Fu and Vasudevan (2010) in Eq. (3.42).

$$\log P_{mix} = x_{t-BuOH} \log P_{t-BuOH} + x_{acetone} \log P_{acetone} \tag{3.42}$$

where log P_{acetone} is the log P value of acetone and log $P_{t\text{-BuOH}}$ is the log P value of *tert*-butanol. Hydrophobicity was included because it was hypothesized polar solvents were believed to favour partially acylated glycerol species as products, whereas apolar solvents were expected to prefer a complete acylation of glycerol (Kuo & Parkin, 1996).

3.10 Water content determination

Water content analysis was conducted using a TitroLine Karl-Fischer analyzer (Schott Instruments, Germany). Prior to sample measurement, a calibration titration was established using a water standard. The sample was loaded in a syringe and added into the titration vessel. The syringe weight was quickly measured (before and after the injection) to estimate the amount of sample added. The water content percentage was measured from the utilization of KF reagent during the volumetric titration process of the sample. The results were represented as free water content in the reaction mixture (wt.%). The water standard and all the studied samples were assayed in triplicates.

CHAPTER 4 :

RESULTS AND DISCUSSION

Sections in Chapter 4 have been published in the following journals;

Section 4.1;

Abd Razak, N. N., Pérès, Y., Gew, L. T., Cognet, P., & Aroua, M. K. (2020). Effect of reaction medium mixture on the lipase catalyzed synthesis of diacylglycerol. *Industrial & Engineering Chemistry Research, 59*(21), 9869-9881.

Section 4.2;

Abd Razak, N. N., Gew, L. T., Pérès, Y., Cognet, P., & Aroua, M. K. (2021). Statistical optimization and kinetic modeling of lipase-catalyzed synthesis of diacylglycerol in the mixture of acetone/tert-butanol solvent system. *Industrial & Engineering Chemistry Research, 60*(39), 14026–14037.

Section 4.3;

Abd Razak, N. N., Cognet, P., Pérès, Y., Gew, L. T., & Aroua, M. K. (2022). Kinetics and hydrodynamics of *Candida antartica* lipase-catalyzed synthesis of glycerol dioleate (GDO) in a continuous flow packed-bed millireactor. *Journal of Cleaner Production*, 373, 133816.

4.1 Preliminary study: Synthesis of glycerol oleates

The preliminary study was conducted with the aims to enhance the selectivity and yield of GDO production using enzymatic approach tested in various solvent systems and to examine the composition of glycerol oleates as the polarity and viscosity of the reaction medium changed. The effect of different types of lipase enzymes, different solvent systems (solventless, solvents and blended solvents) and temperatures on the oleic acid conversion, selectivity and yield of glycerol oleates were examined. The preliminary study also included the study on the rheological behaviours of each system mixed with substrates and thermodynamic behavior of every tested system.

4.1.1 Screening for a suitable lipase and its activity

To select the most suitable lipase for the esterification reaction, four commercially available lipases of nonspecific types were investigated under similar conditions for the synthesis of glycerol oleates through the esterification of oleic acid with glycerol. Except for CALB 2, all the lipases selected in this study have been used for the synthesis of DAG

according to the literature data (Compton *et al.*, 2006; Duan *et al.*, 2010; Mardani *et al.*, 2015). Among the lipases tested, the immobilized enzymes (CALB 1 and CALB 2) represent the suitable and active catalyst for esterification reaction of glycerol. Both enzymes produced comparable esterification yield (~56%), and free lipases showed no successful esterification. No glycerol oleates were found using the free lipases which include Amano lipase and Lecitase. Enzymes function most effectively in optimum environments. This is affected by the characteristics of the enzyme (Sarmah *et al.,* 2018). All naturally occurring enzymes eventually become inactive and denatured in the presence of organic solvents (Ahmad & Sardar, 2015). Immobilization improves a number of enzyme properties, including performance in organic solvents, pH tolerance, heat stability, or functional stability (Ismail & Baek, 2020; Remonatto *et al.,* 2022). Furthermore, due to their inflexible conformation, immobilised enzymes are typically more stable and manageable than those in their free form (Shabbir *et al.,* 2020).

Generally, CALB 1 and CALB 2 are considered as nonspecific lipases during the preparation of structured lipids. However, these enzymes' positional specificity could be affected by solvent polarity and acyl donor (Sharma & Kanwar, 2014; Kumar *et al.*, 2016). CALB 1 was immobilized in acrylic polymer resin by adsorption meanwhile CALB 2 was covalently immobilized on methacrylate polymers with epoxy functions. Since comparable yield and conversion were obtained between CALB 1 and CALB 2 employed in *tert*-butanol, CALB 1 was selected in the following studies. Furthermore, CALB 1 has been extensively studied to produce products relevant in the food industry due to its stability and recycling possibility (Vázquez *et al.*, 2016; Zhang *et al.*, 2018). As reviewed by Ortiz *et al.* (2019), CALB 1 is likely one of the most commercially available and active preparations that have permitted many studies to be performed.

Prior to the determination of the thermal stability of CALB 1 in an organic solvent, lipase activity was measured by monitoring the rate of hydrolysis of *para*-nitrophenyl

palmitate (*p*Npp). Reactions were carried out within the temperature range of 30 to 80°C. As shown in Fig. 4.1, lipase activity increased with the increase in reaction temperature. It was found that the enzyme remained active within the temperature range tested. CAL-B is known as a thermostable enzyme and able to retain its catalytic activities during the reaction even up to 90°C (Yoshida *et al.*, 2006). Thus, the suitable temperature range for the esterification reaction investigated in this study was deemed to be in which the enzyme was thermally stable without a significant loss of catalytic activity. Using 30ºC as a reference temperature, an increase in enzyme activity up to seven times was observed within the reaction temperature range studied.

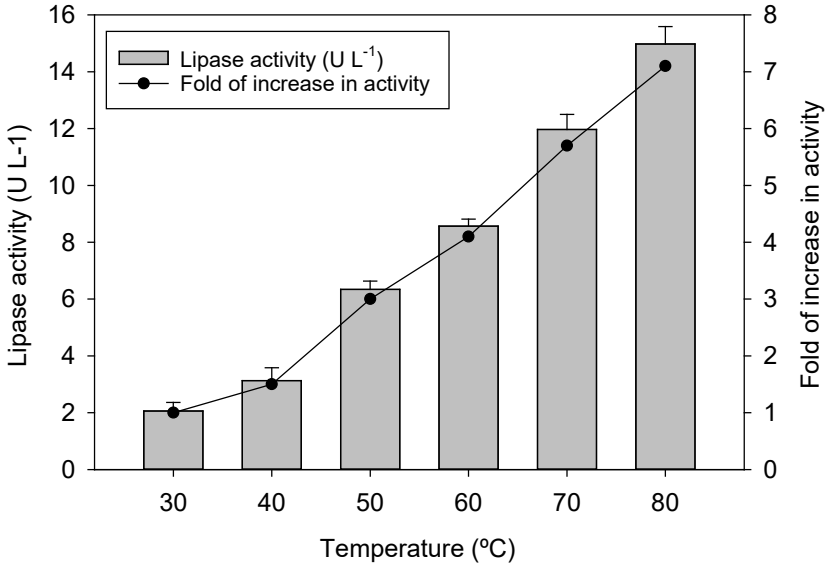

Figure 4.1. *Candida antartica* lipase B (CALB 1) activities assayed at different temperatures. *(The standard deviation of the triplicate measurements was <5 %)*

4.1.2 Rheological properties and log *P* for the solvent systems

In this reaction, solventless system was chosen as a reference reaction for all solvents tested as the industrial production of glycerol oleates are preferably carried out in such a condition (Zhong *et al.*, 2013). The rheological characteristics of the initial reaction mixture employed in the esterification of oleic acid and glycerol is shown in Table 4.1. The highest viscosity was observed in solventless media, followed by *tert*-

butanol, a blended mixture of acetone:*tert*-butanol and the least viscous was acetone. Table 4.1 shows that the viscosities of all media are influenced by temperature and continuously decrease with increasing temperature. From 35 to 65°C the viscosities of solventless and *tert*-butanol decreased to 32% (68% reduction) and 37% (63% reduction), respectively. Meanwhile for acetone:*tert*-butanol and acetone, the viscosities decreased to 85% (15% reduction) and 88% (12% reduction), respectively, from 35 to 45°C. The change in viscosity was attributed decrease of the intermolecular interactions due to an increase in the thermal motion of the molecule. Increasing temperature not only reduced the cohesive forces between molecules but also reduced the attraction forces which eventually led to reduction in viscosities (Ghotli *et al.*, 2015). At a fixed temperature, the viscosities of reaction mixtures are almost constant over the range of shear rates examined from 100 to 2000 s^{-1} indicating that viscosities of these media are independent of shear rate. Employing the Herschel-Bulkley model (Barnes *et al.*, 1989), the values of *n* were equal to almost one, which exhibited Newtonian fluid character. Newtonian fluid displays a linear relation between shear stress and shear rate. Viscosity can be an indicator for liquid properties of the reaction mixture. Besides, it provides general information on behavior of the bulk liquid medium and also the diffusivity of glycerol and oleic acid in the reaction mixture.

Densities of all mixtures exhibited temperature-dependent behavior as the values decrease with increasing temperature. The greater molecular motion at high temperatures contributes to greater expansion in volume and reduction in density. The maximum density values of glycerol and oleic acid are calculated at 1.2510 and 0.8822 g cm^{-3} respectively. As viscosity is related to the fluid's resistance to motion, it has a marked effect on diffusivity. Increasing the temperature has the effect of reducing the viscosity of the medium and lowering the resistance to particle motion, that is, glycerol or oleic acid. Table 4.1 shows that diffusivity rises with temperature which can be observed by

the significant increase of *D* values. At every temperature tested, it appears that the diffusivity of glycerol is about four times higher than that of oleic acid in the *tert*-butanol and acetone systems, meanwhile being three times higher in acetone:*tert*-butanol. The highest diffusivity coefficients of glycerol were calculated at 7.681×10^{-1} m^2 s^{-1} in the solventless system, followed by acetone (7.522×10^{-1} m^2 s^{-1}), *tert*-butanol (7.347×10^{-1} m^2 s^{-1}) and acetone:*tert*-butanol (5.179×10^{-1} m^2 s^{-1}). At the highest temperature for each tested system, the highest diffusivity of oleic acid was found in acetone, followed by *tert*-butanol, acetone:*tert*-butanol and solventless with the values of 1.909×10^{-1} m^2 s^{-1}, 1.869×10^{-1} m^2 s^{-1}, 1.639×10^{-1} m^2 s^{-1} and 1.12×10^{-1} m^2 s^{-1} respectively. Acetone has a lower viscosity than other solvent systems, which contributes to the greater diffusivity of oleic acid and glycerol in this solvent.

In this experiment, the internal diffusivity effect was studied by calculating the observable Thiele modulus and internal effectiveness factor according to Eq. (3.18) & Eq. (3.19) respectively. The initial reaction rates were calculated based on the conversion of oleic acid in different solvents and temperatures and the diameter of the support particle was taken as 0.0005 m (Denčić *et al.*, 2013). The values for all internal effectiveness factors were approaching 1. Therefore, it implies that the reaction is not influenced by mass transfer and the overall rate is solely controlled by intrinsic kinetics in all tested systems. Both mass transfer and intraparticle diffusional resistances do not influence the reaction rate. These results were in accordance with Gofferjé *et al.* (2014) who showed that Lipozyme with particle diameter of 0.0004 m practically has no effect of internal mass transfer limitations during the esterification of glycerol and free fatty acids in crude Jatropha oil.

The fundamental criterion describing the influence of polarity-hydrophobicity of organic solvents on enzymatic catalysis is log *P*. In this study the relative solubilities of the reactants in the solvents were consistent with the literature values or estimated values

of solvent polarities (log *P*). Acetone had a log *P* value of -0.23 meanwhile log *P* *tert*-butanol (log *P* = 0.80) (Narayan & Klibanov, 1993; Kuo & Parkin, 1996) and the blend of acetone and *tert*-butanol exhibited an intermediate polarity value (log P_{mix}) of 0.22.

Table 4.1. Rheological characteristics of reaction medium at different temperatures.

Media*	Temperature, T (°C)	Density, ρ (g cm^{-3})	Herschel–Bulkley model (Barnes *et al.*, 1989)				Diffusivity, D (m s^{-1})		Thiele modulus, ϕ	
			Apparent viscosity, μ (mPa.s) at 300 s^{-1}	n	k (Pa.s^n) (× 10^{-3})	τ_0 (Pa) (× 10^{-3})	OA (× 10^{-1})	Gly (× 10^{-1})	OA	Gly
Solventless	35	0.882	26.35	0.9847	29.05	17.24	0.328	2.238	1.75	0.26
	50	0.872	14.08	1.049	10.29	12.12	0.639	4.370	0.42	0.06
	65	0.861	8.38	1.014	7.651	3.552	1.12	7.681	0.23	0.03
tert-butanol	35	0.841	11.94	1.005	11.59	4.220	0.649	2.530	1.55	0.40
	50	0.831	6.87	1.005	6.68	0.190	1.175	4.586	0.31	0.08
	65	0.811	4.49	1.001	4.507	0.021	1.869	7.347	0.11	0.03
acetone	35	0.847	4.14	1.035	3.347	5.626	1.659	6.463	0.30	0.08
	40	0.837	3.97	1.026	3.406	1.201	1.747	6.843	0.21	0.05
	45	0.830	3.66	1.045	2.814	1.254	1.909	7.522	0.08	0.02
acetone: *tert*-butanol	35	0.840	6.63	1.003	6.509	0.863	1.353	4.273	0.42	0.13
	40	0.831	6.24	1.009	5.953	1.414	1.458	4.605	0.18	0.06
	45	0.831	5.63	1.025	4.834	2.829	1.639	5.179	0.15	0.05

*The media consists of the mixture of oleic, glycerol and the corresponding solvent. For acetone: *tert*-butanol a ratio of 1:1 (by weight) was used

4.1.3 Yield profile for GMO, GDO and GTO in solventless vs. solvent systems

Temperature plays a very important role in the enzymatic esterification reaction because of its influence on the reaction rate and selectivity. It was observed that at the early stage of the esterification reaction, the substrates solution separated into two phases. As the reaction progressed, glycerol and oleic acid gradually consumed and the solution became homogeneous. To improve reactant homogeneity and reduce reaction time, the reaction was conducted at different temperatures, depending on the boiling point of the solvent.

The plot evolution of yield for GMO, GDO and GTO (%) as a function of time performed at various temperatures (h) in solventless media are shown in Fig 4.2a-c. Among the glycerol oleates produced, GMO showed the lowest yield and decreased with increasing temperature. The highest GMO yield attained was only 14% at 35ºC. The GDO yield showed an excellent performance at 50ºC (59%) and slightly reduced at 65ºC (50%) but lead to a lower yield at 35ºC (26%). The curve profiles of GTO yield in solventless system were only observed after 2 h of reaction and displayed the highest yield at the highest temperature tested. At 50ºC, GTO yield increased drastically which proves that the formation of GTO in the solventless system is only favorable at high temperature. As reported by Lortie *et al.* (1993) GTO yield increased with temperature. For all products GMO, GDO, and GTO, the yield did not further increase after 6 h reaction time.

In the case of *tert*-butanol (log P = 0.80) GMO yield was higher than GDO and GTO yield at 35ºC (Fig. 4.2d-f). This result showed that, at lower temperature, the physical properties of *tert*-butanol had more significant effect on GMO yield. It was observed that *tert*-butanol naturally tends to crystallize at low temperature however the solvation properties were improved once it was mixed with oleic acid and glycerol. It is postulated that MAG tends to solidify at low temperature and therefore, the esterification was subjected to the accumulation of MAG rather than the synthesis of DAG and TAG

(Xu *et al.*, 2012). The influence of the high viscosity of the reaction medium resulted in the suppression of GDO and GTO synthesis. Moreover, at low temperature, less energy is being supplied to the reaction medium to direct the reaction to the formation of GDO and GTO. This finding is in agreement with the results obtained by Damstrup *et al.* (2006) who observed that the maximum amount of MAG was obtained with solvents with a log *P* value in the range from 0.3 to 1. The author investigated tertiary alcohols, such as *tert*-butanol and *tert*-pentanol, in the glycerolysis of sunflower oil catalyzed by Novozym 435. As the temperature increases, GDO yield dominated over GMO and GTO yield, reaching the highest yield almost 60% at 50 C.

Meanwhile, at 35 and 40°C in acetone, a gradual increase of GTO yield was observed during the first 5 h of the reaction (Fig. 4.3a-b). At 45°C, GTO yield sharply increased after 1 h of incubation (Fig. 4.3c). The evident increase of the yield of GTO after 6 h at 45ºC might be primarily ascribed to a substantial occurrence of acyl migration which resulted in an increase of GTO content. Acyl migration has been held accountable for the synthesis of TAG. When high concentrations of 1,3-DAG accumulate, they undergo acyl migration to 1,2-DAG and TAG concentrations begin to increase (Watanabe *et al.*, 2003). Besides, it was hypothesized that the more polar solvents favored partially acylated glycerol species as products whereas the more apolar solvents favored a more complete acylation of glycerol (Kuo & Parkin, 1996).

Having an intermediate polarity value (log P_{mix}) of 0.22, GDO yield showed to be the highest as compared to GMO and GTO attaining almost 70% at 40ºC in the blended solvent system (Fig. 4.3d-f). A proportion of *tert*-butanol and acetone was fixed at 1:1 because Liao *et al.* (2003) showed that the optimum solvent mixtures for the lipase catalyzed synthesis of 1,3-DAG using response surface methodology was obtained with a hexane/octane ratio (v/v) of 1:1. A substantial decrease in GDO yield at 45ºC was observed accompanied by a gradual increase of GTO yield as temperature increases (Fig.

4.3e-f). Yesiloglu *et al.* (2004) obtained 39.6% of DAG using *Candida rugose* lipase, and 57% of conversion was reported by Voll *et al.* (2011). In other cases, Duan *et al.* (2010) and Krüger *et al.* (2010) achieved DAG contents of 40% and 50%, respectively. The yield obtained in this study was higher than the reported findings, which can be attributed mainly to the different solvents and temperatures investigated since reactions were carried out under experimental conditions different from the ones used in this study. Furthermore, the current study used blended solvents. This is suggested to be due to changes in the dipole moment and the dielectric constant of the solvent as a result of blending, which affects the ionization and the polarity and thus, the solvation properties **(**Reichardt, 2003). When the reactant molecules proceed to the transition state, the solvent molecules orient themselves to stabilize the transition state. If the transition state is stabilized to a greater extent than the substrate, the solubility increases and the reaction proceeds faster. If the transition state stabilizes to a lower extent, the substrate experiences less solvation and the reaction proceeds slowly **(**Reichardt, 2003).

In every tested system, the highest GDO concentration was obtained at 0.53, 0.48, 0.45 and 0.46 M in acetone:*tert*-butanol, solventless, acetone, and tert-butanol, respectively. GMO yields display similar behavior to that of *tert*-butanol media in which the highest rate and yield of GMO were obtained at 35ºC.

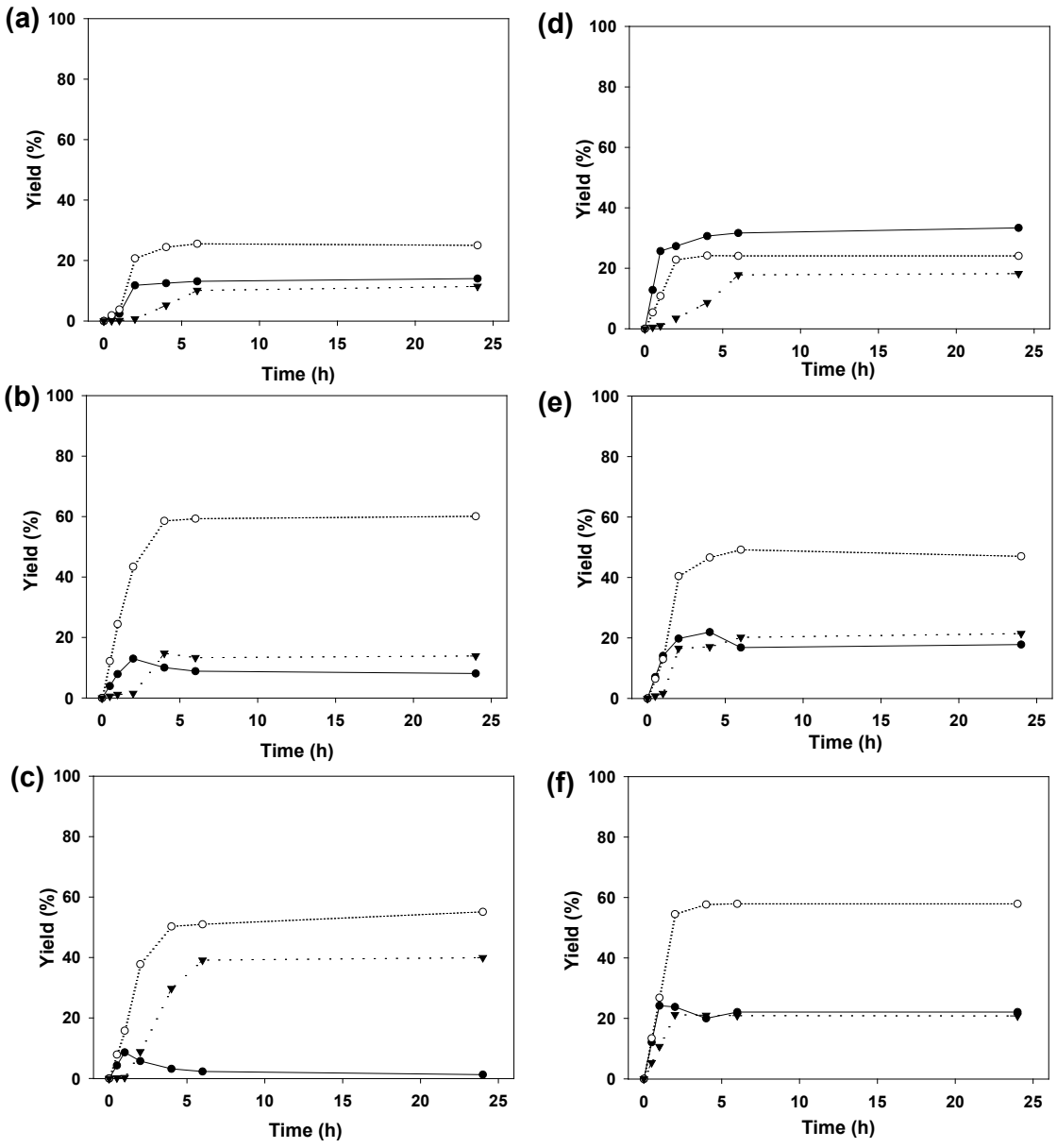

Figure 4.2. Evolution yield of GMO, GDO and GTO (%) as a function of time (h) performed in solventless (a-c) and *tert*-butanol (d-f) system at various temperatures (a, d) 35°C, (b, e) 50°C, (c, f) 65°C. Reaction conditions: 2 g of oleic acid; 0.26 g of glycerol; 1.2 g of solvent; 0.2 g of lipase enzyme; 1.28 g of 3 Å molecular sieves; and 200 rpm *(Symbol: ● yield of GMO; ○ yield of GDO; ▼ yield of GTO). (The standard deviation of the measurements of all graphs was <11 %)*

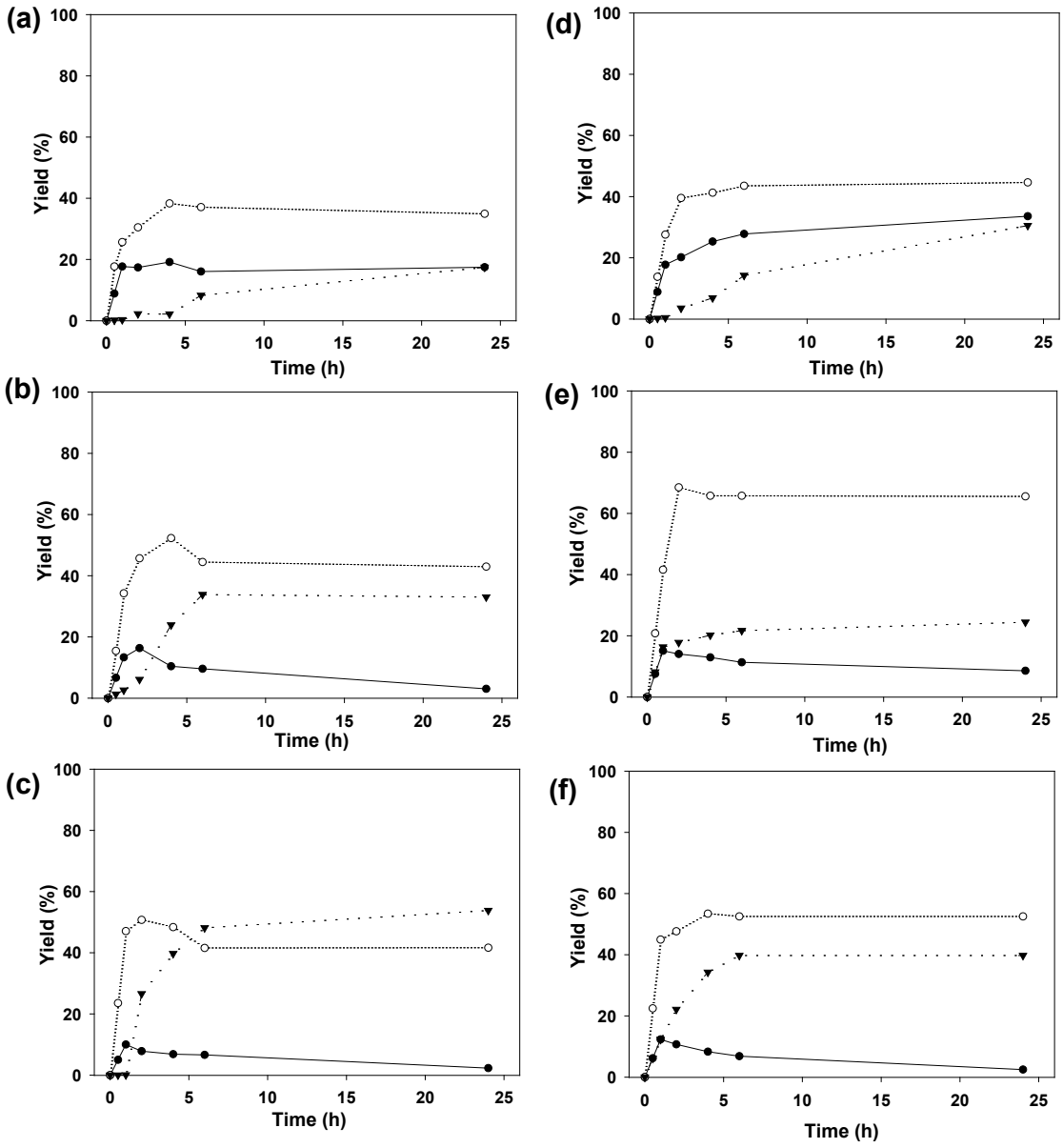

Figure 4.3. Evolution yield of GMO, GDO and GTO (%) as a function of time (h) performed in acetone (a-c) and in acetone:*tert*-butanol (d-e) at various temperatures (a, d) 35°C (b, e) 40°C (c, f) 45°C. Reaction conditions: 2 g of oleic acid; 0.26 g of glycerol; 1.2 g of solvent; 0.2 g of lipase enzyme; 1.28 g of 3 Å molecular sieves; and 200 rpm *(Symbol: ● yield of GMO; ○ yield of GDO; ▼ yield of GTO). (The standard deviation of the measurements of all graphs was <11 %)*

4.1.4 Conversion, selectivity & reaction rates of GMO, GDO and GTO

The percentage of conversion and selectivity of GMO, GDO, and GTO as a function of temperature and reaction medium is shown in Fig. 4.4. There are notable differences observed between the tested systems. A comparison of the conversion and selectivity based on solventless system shows increasing selectivity upon the addition of the acetone or *tert*-butanol particularly on GMO and GTO selectivity.

For the solventless system, the highest conversion (78%) was observed at highest temperature that is, 65°C. The highest selectivity of GMO (42%) was obtained at the lowest temperature and decreases as temperature increased. In contrast, selectivities of GDO and GTO increase with temperature and highest selectivities were achieved at 52% and 39% for GDO and GTO, respectively.

In *tert*-butanol, GMO was formed up to 64% at 35°C which was nearly about 21% higher than for the solventless system. Even though increasing the reaction temperature enhances the solubility of the substrates and products, GMO selectivity is more pronounced at low temperature. Since *tert*-butanol is a polar solvent, GTO showed the lowest selectivity among all the glycerol oleates formed at all investigated temperatures, inferior to 18%.

The highest GTO selectivity was achieved when acetone was present in the reaction attaining about 38% at 45°C which is almost similar in a solventless system at 65°C. GTO displays higher selectivity in acetone at the temperature range from 40 to 45°C, which is relatively narrow as compared to the energy supply in solventless and *tert*-butanol systems. Possible reasons for this effect are the decrease in the viscosity of the reaction system, the increase in the solubility of reaction product (Table 4.1).

The acetone: *tert*-butanol blend afforded the highest selectivity of GDO at 40 to 45°C as compared to other solventless and solvent systems corresponding to 54% and 57% respectively. These results corroborated the observed high yield obtained in Fig. 4.3.

It is worth noting that blended mixture showed intermediate effect on GTO selectivity between *tert*-butanol and acetone reaction media. In this case, GMO selectivity also exhibited similar pattern as in solventless system.

Based on Fig. 4.4, the effect of different solvent systems at various temperatures on GMO, GDO and GTO selectivity were further evaluated in the form of multiple mean comparisons. It is obvious that the increase in temperature adversely influenced the production of GMO. The selectivity of GMO in *tert*-butanol was found to be significantly different at the lowest temperature that is, 35°C between the tested solvent systems but showed no significant difference at 50 and 65°C in *tert*-butanol. Besides, the selectivity of GMO in acetone and acetone: *tert*-butanol was found to be insignificantly different between them at both 40°C and 45°C. The solventless system at 50°C showed a similar effect to acetone and acetone: *tert*-butanol at 40°C. The ANOVA test showed for each system tested that selectivity values at 35°C were found to be significantly different from that at other temperatures ($p<0.05$).

In terms of GDO selectivity, acetone: *tert*-butanol at 40°C and 45°C showed the highest selectivity followed by similar values between *tert*-butanol and solventless at 50°C and 60°C respectively. Most of the studied systems exhibited comparable values of selectivity (~46 to 48%). At 35°C, all systems were found to be significantly different between them. It can be seen that temperature had no significant effect on GDO selectivity in acetone. Because of the better solvation effect in blended mixtures of acetone: *tert*-butanol, the selectivity increased which resulted in higher formation of GDO.

An insignificant difference of GTO selectivity was observed at 35°C in all reaction media tested except for the solventless system. Temperature significantly influenced the selectivity of GTO in acetone. Further increase of temperature indicated significant changes of selectivity GTO values in all tested systems.

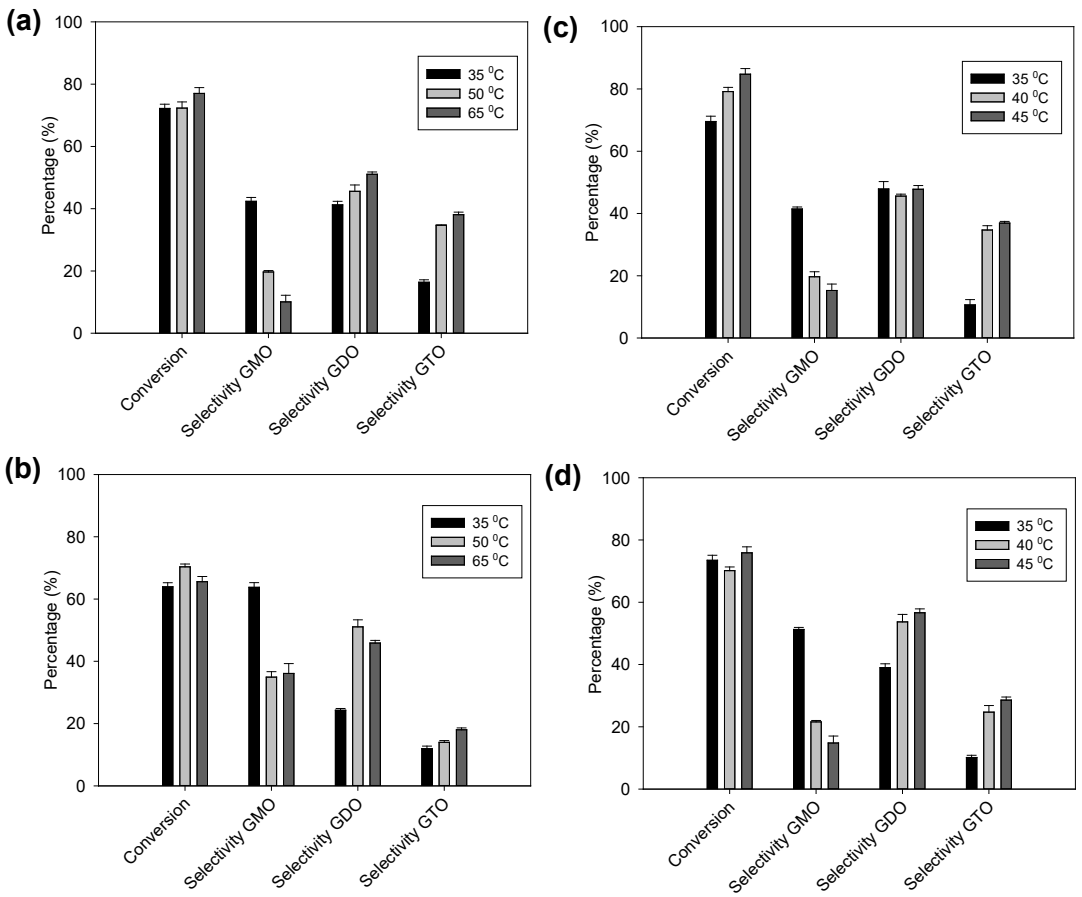

Figure 4.4. Percentage of conversion and selectivity of GMO, GDO and GTO as a function of temperature in different medium (a) solventless, (b) *tert*-butanol, (c) acetone, (d) acetone:*tert*-butanol. Reaction conditions: 2 g of oleic acid; 0.26 g of glycerol; 1.2 g of solvent; 0.2 g of lipase enzyme; 1.28 g of 3 Å molecular sieves; and 200 rpm.

The rates are interrelated concepts in process design; if the reaction rate is relatively low then a larger reactor is required to achieve the desired total productivity (Doran, 2012). The measurements were calculated according to Eq. (3.20) and Eq. (3.30) respectively for each GMO, GDO and GTO formed. The reaction rate determine how fast reactants are turned into products meanwhile productivity is useful for specifying the total output of a particular reactor. As can be seen in Fig. 4.5, GDO exhibited the highest reaction rate in acetone: *tert*-butanol at 40°C. The highest reaction rate was calculated at 0.27 M h^{-1} with the productivity value of 0.48 M h^{-1}. The comparison of individual solvents showed the GMO performance was remarkable at 35°C. Although GTO showed the worst performance, the effect is more important in the presence of acetone as both reaction rates and productivity increased rapidly with increasing temperature. It is

hypothesized that the viscosity of the other medium becomes the limiting factor affecting the maximum feasible reaction rate. Highly viscous media lessen the chances of GTO formation.

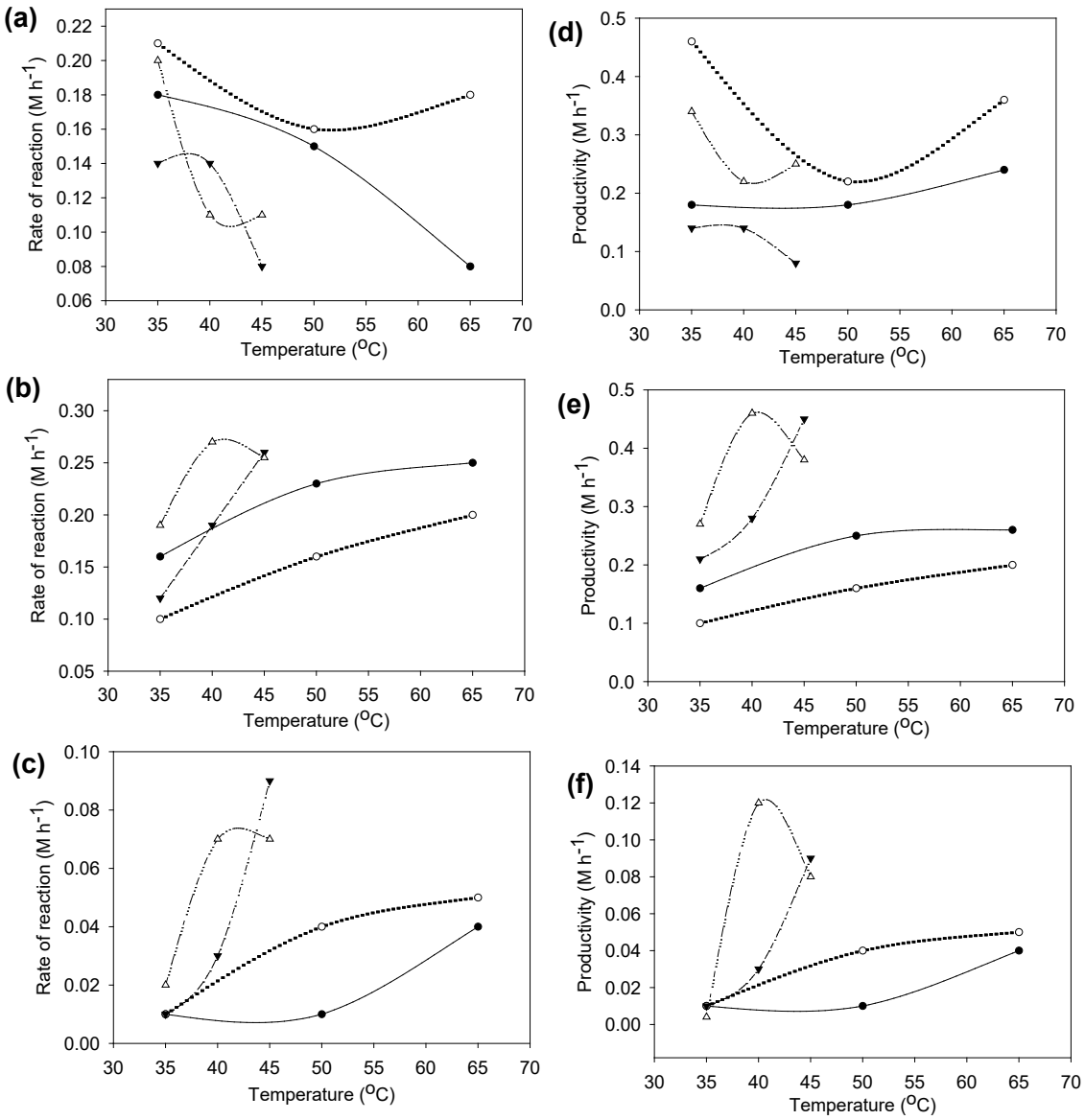

Figure 4.5. Reaction rates of glycerol oleates as a function of temperature and solvent mixture (a) GMO, (b) GDO, (c) GTO. Productivity of glycerol oleates as a function of temperature and solvent mixture (d) GMO (e) GDO f) GTO. Reaction conditions: 2 g of oleic acid; 0.26 g of glycerol; 1.2 g of solvent; 0.2 g of lipase enzyme; 1.28 g of 3 Å molecular sieves; and 200 rpm *(Symbol: ● solventless; ○ tert-butanol; ▼ acetone; Δ tert-butanol: acetone). (The standard deviation of the measurements of all graphs was <11 %)*

4.1.5 Thermochemical analysis

From this work, the K_{eq} value, enthalpy (ΔH), entropy (ΔS), and ΔG are presented in Table 4.2. The ΔH and ΔS for catalytic esterification at varied reaction temperatures were estimated from the linear Van't Hoff plot by fitting the obtained data of ln K_{eq} with the inverse of temperature. The slope and the y intercept of the straight line were calculated to determine the value of ΔH and ΔS values, respectively. The positive values of enthalpy change (ΔH) for the reactions show the endothermic nature of the esterification system, whereas the positive value of entropy change (ΔS) reflects an esterification system that is becoming increasingly disordered as the temperature increases.

As expected for endothermic reactions, K_{eq} was found to increase with temperature. Thermodynamic parameters were also affected by the solvent characteristics. Increasing the polarity resulted in an increase of enthalpy and entropy values. However, intermediate polarity of blended solvents displays the highest enthalpy and entropy values. Since the products formed are influenced by differential solvation of the substrate and transition state by the solvent, the observed effects were attributed primarily to the dispersal of GMO, GDO, and GTO and water molecules byproduct.

The values of enthalpy and entropy changes obtained subsequently were used in the calculation of Gibbs free energy change, ΔG using Eq. (3.39). Gibbs free energy reflects the favorability of reactions with respect to laws of thermodynamics and it indicates the degree of spontaneity of the esterification process. A strong negative value reflects a more energetically favorable process. As shown in Table 4.2, the esterification reaction occurs spontaneously for all solvents and solventless systems at all temperatures studied. Hence, the esterification of glycerol is an energetically favorable process, hence spontaneous in nature.

Table 4.2. Gibbs energy change (ΔG), enthalpy (ΔH) and entropy change (ΔS) as a function of temperature of the reaction

Media	**Absolute temperature, T (K)**	**Apparent K_{eq}**	**ΔG (kJ mol^{-1})**	**ΔG-$\Delta G°$ (kJ mol^{-1})**	**ΔH (kJ mol^{-1})**	**ΔS (J mol^{-1} K^{-1})**	**Van't Hoff equation**
solventless	308.15	1.04	-1.28	0.10	+259	+847	y = -31268x + 101.97
	323.15	4.84×10^{2}	-14.00	16.61			
	338.15	8.06×10^{3}	-26.72	25.29			
tert-butanol	308.15	2.89	-0.42	2.72	+303	+987	y = -36555x + 118.79
	323.15	4.43×10^{1}	-15.23	10.19			
	338.15	1.17×10^{5}	-30.05	32.82			
acetone	308.15	8.01×10^{-1}	-0.95	-0.57	+512	+1667	y = -61673x + 200.51
	313.15	1.16×10^{2}	-9.28	12.38			
	318.15	4.24×10^{2}	-17.62	16.00			
acetone*:* *tert*-butanol	308.15	1.01×10^{2}	-12.64	11.83	+768	+2536	y = -92472x + 305.02
	313.15	3.18×10^{4}	-25.32	27.00			
	318.15	1.25×10^{6}	-38.00	37.14			

As more energy in the form of heat is supplied to the system, the greater is the tendency of the system to move toward a spontaneous reaction as shown by the increase in negative value of ΔG. In the esterification of glycerol to produce monoacetin, and then monoacetin acetylation with acetic anhydride to produce triacetin at 105ºC, Liao *et al.* (2010) revealed that the reaction is preferable thermodynamically with a total Gibbs free energy value of -50.66 kJ mol^{-1}. Lower negative values obtained in this study occurred because a lower range of temperatures was applied in the reaction. From Table 4.2, the differences between the energy change for the reaction under the conditions applied in the study and the energy change for the reaction under certain defined standard conditions (ΔG - ΔG^o) showed that there was a significant surplus of energy for the temperature range studied.

4.1.6 Concluding remarks from the preliminary study

Generally, the products distribution resulting from a chemical reaction is significantly affected by solvent and temperature choice. This work was carried out to get better understanding of the choice of solvent and temperature conditions, which influence the enzymatic glycerol oleates synthesis. Nevertheless, those responses could be adjusted by changing the hydrophobicity of the reaction medium. Crucial for success of this method is the choice of the solvent or solvent mixture in which the GDO is more favorable than all of the other products. GDO was found to be dependent on intermediate polarity (log P_{mix} = 0.22) of the media, that is acetone: *tert*-butanol with 70% of yield and conversion and 54% selectivity. The thermal energy investment is minimal as the highest reaction rate and productivity for GDO was obtained at moderate temperature (40ºC). The enzymatic esterification process using blended acetone: *tert*-butanol showed the highest endothermic value and in a disordered manner. The Gibbs energy change decreased with increasing temperature. Understanding these aspects is essential for the rational design of

GDO synthesis using the enzymatic method. It has the potential to create an artificial system with functional organization found in an actual biological system, which appears to be more appealing than those made using nonenzymatic methods. Experiments comprising detailed investigations of the optimization of the proportion of solvents and reaction kinetics were further investigated in the next section.

4.2 Batch reactor study: Investigation on GDO synthesis

To further improve the selectivity of GDO production, rigorous optimization of the reaction operating variables is essential. Hence, a three-factor three-level BBD was applied in this study to optimize both conversion and selectivity of GDO production by enzymatic approach. The optimization of process variables was conducted according to the investigations concerning to the effects of solvent ratio of acetone to *tert*-butanol in the reaction mixture, reaction temperature and enzyme loading (Table 3.1). Experimental data were subjected to statistical analyses and then fitted to a regression model for optimization. The first part of the present work is to optimize the selected variables for the production of GDO through lipase-catalyzed reaction in blended solvent using RSM. Secondly, based on the optimized condition, the investigation on the reaction mechanism and the kinetic parameters has been carried out. The current study also proposes an appropriate kinetic model with the corresponding kinetic parameters.

4.2.1 Experimental data of the response surface methodology

With the objective to maximize the response variable of GDO production, RSM evaluates the strongest impact of the investigated factor and considering each individual factor effect and the interactions effects. Experimental oleic cid conversion (Y1) and GDO selectivity (Y2) values obtained from all 45 runs of the experiment with the various combinations of input variables in coded units are presented in Table 4.3.

Table 4.3. Box-Behnken Response Surface coded unit along with the experimental and predicted response of percentage of oleic acid conversion (%) and GDO selectivity (%)

Run Order	A	B	C	Y1: Conversion (%)	Y2: GDO Selectivity (%)
1	+1	0	+1	68.31	70.18
2	0	+1	+1	69.05	74.34
3	+1	-1	0	71.24	67.10
4	+1	0	+1	68.49	70.35
5	0	0	0	66.74	64.28
6	0	+1	-1	68.50	71.97
7	+1	-1	0	71.58	66.95
8	0	-1	-1	65.46	65.45
9	+1	0	-1	68.08	67.76
10	-1	0	-1	60.76	61.05
11	+1	+1	0	76.83	79.32
12	0	0	0	66.67	64.28
13	0	+1	-1	68.95	72.13
14	0	0	0	68.10	64.83
15	-1	0	-1	60.41	60.72
16	0	-1	+1	67.57	68.21
17	+1	0	-1	68.25	67.47
18	0	+1	-1	68.50	71.97
19	+1	-1	0	72.74	67.25
20	+1	0	-1	68.21	67.55
21	-1	+1	0	68.32	71.02
22	0	-1	-1	65.45	65.56
23	-1	0	+1	64.30	66.63
24	-1	+1	0	68.17	70.58
25	-1	0	+1	62.96	66.01
26	0	0	0	66.70	64.47
27	-1	-1	0	53.93	57.48
28	-1	+1	0	68.64	70.83
29	-1	0	+1	64.28	66.42
30	0	0	0	66.34	64.21
31	+1	+1	0	76.29	79.45
32	-1	0	-1	58.71	59.69
33	0	0	0	66.49	64.30
34	+1	0	+1	68.34	70.13
35	0	-1	+1	67.74	68.05
36	0	0	0	66.41	64.65
37	-1	-1	0	54.44	57.54
38	0	-1	-1	66.01	65.43
39	0	-1	+1	67.70	68.35
40	0	+1	+1	68.80	74.63
41	0	0	0	66.08	64.46
42	0	0	0	66.18	64.33
43	0	+1	+1	69.98	75.19
44	-1	-1	0	52.95	56.63
45	+1	+1	0	76.41	79.64

A = Percentage of acetone to *tert*-butanol (*v/v* %)
B = Temperature (°C)
C = Enzyme loading (g)

4.2.1.1 Data analysis and model fitting for oleic acid conversion, Y1 (%)

In order to fit a second-order polynomial regression model in Eq. (3.3), the data for conversion, Y1 was subjected to multiple regression analysis using least squares regression. The stimated regression coefficients of the fitted model for conversion for each coded value are presented in Table 4.4.

Table 4.4. Values of model coefficients of oleic acid conversion

Term	Coefficients	Value	Standard error Coefficients
Constant	β_0	66.635	0.711
A	β_1	4.87	0.436
B	β_2	2.985	0.436
C	β_3	0.843	0.436
A × A	β_{11}	-0.862	0.641
B × B	β_{22}	1.857	0.641
C × C	β_{33}	-0.681	0.641
A × B	β_{12}	-2.487	0.616
A × C	β_{13}	-0.922	0.616
B × C	β_{23}	-0.351	0.616

The positive sign of the coefficients implies a synergistic effect and an antagonistic effect on the response is indicated by the negative sign (Table 4.4). The constant 66.635 was evidently independent from any factor. Meanwhile, the linear terms A, B, and C, and a second-order terms, BB had a positive effect, which meant that if the magnitude of these factors increased, the conversion would be increased as well. Conversely, AA, CC, and all the interactive factors (AB, AC and BC) had a negative impact on conversion. The coefficients obtained in Table 4.4 were substituted into Eq. (3.3) to construct a quantitative model equation for conversion, which is given as follows;

$$\mathrm{Y1} = 66.635 + 4.87\mathrm{A} + 2.985\mathrm{B} + 0.843\mathrm{C} - 0.862\mathrm{A}^2 + 1.857\mathrm{B}^2 - 0.681\mathrm{C}^2 - 2.487\mathrm{AB} - 0.922\mathrm{AC} - 0.351\mathrm{BC} \quad (4.1)$$

The response variability was determined at 85.33%, indicated by the multiple determination coefficient value, R^2, of 0.8533. According to the variance analysis (ANOVA) results, the main factors A and B, as well as BB and AB, have a significant

effect on the response. A significant effect is presented by a *p*-value less than 0.05, whereas a non-significant effect is indicated by a *p*-value more than 0.05 (*see* Appendices Table A.1).

The Pareto chart of the standardized effects plot analysis displays the same result as the variance analysis. Fig. 4.6 shows the standardized effects (represented by the bar charts) arranged from the largest effect on the right to the smallest effect on the left, with a reference line determined at 2.03. The bars of factors A and B, followed by interaction AB and quadratic BB exceed the reference line (2.03), indicate that these effects are statistically significant.

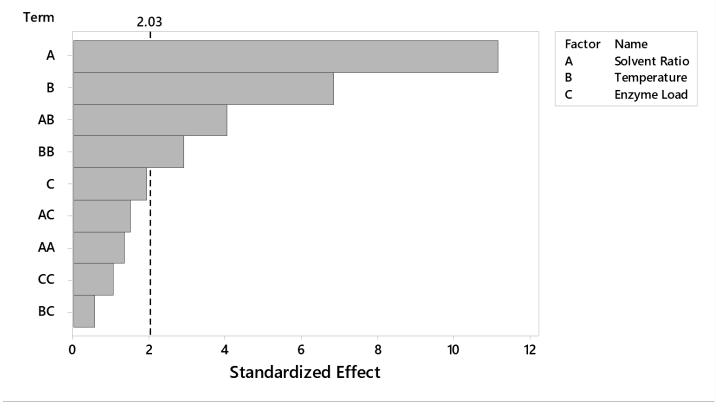

Figure 4.6. Standardized effects for oleic acid conversion (%) using a Pareto chart

Validation of the applied regression model was further perfomed through examination of residual analyses. Residual analyses assess how well a model fits the data and characteristically shown by four different graphs (Fig. 4.7). The normal probability plot (Fig. 4.7a) illustrated that as the number of runs is less than 50, the residuals were normally distributed, shown by the plots that come close to a straight-line. The histogram displayed a bell-shape curve (Fig. 4.7b), which further validated the normal probability assumption. An outlier can be seen from the bar indicated being by slightly outside from the ± 2 range (Fig. 4.7b). This error is known as a random error which is produced from the collected experimental data (Chew *et al.*, 2015). Fig. 4.7c (residuals against fitted value) showed that there was no strong evidence of systematic error as shown by a random

pattern of residuals. The lack of pattern observed in Fig 4.7d, indicates that the order in which data is collected has no impact on the data collected. In general, the residual data pattern was normally distributed and had a lower likelihood to be influenced by non-random and systematic errors.

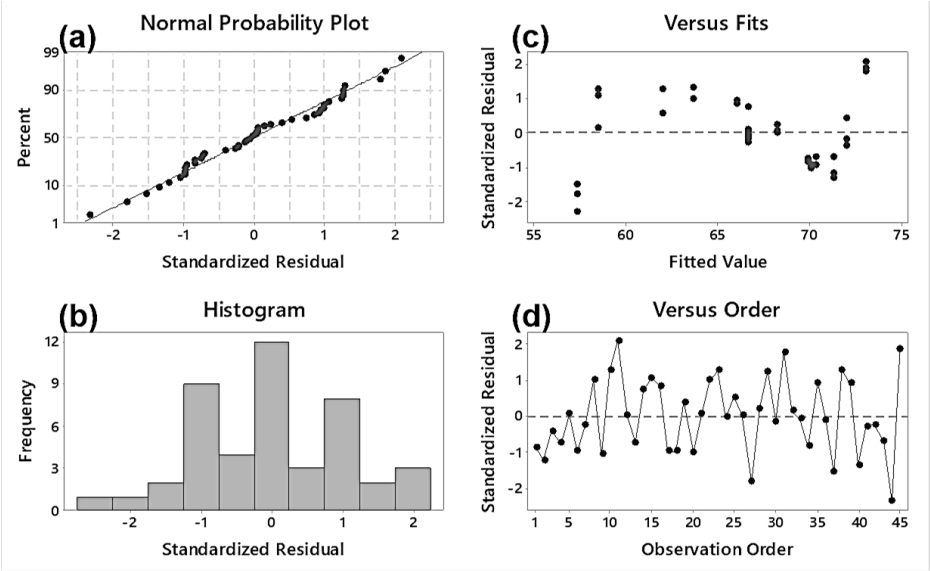

Figure 4.7. Residual plots for oleic acid conversion (%) (a) normality probability plot, (b) histogram plot, (c) standardized residual vs fitted value, and (d) standardized residual vs observation order.

4.2.1.2 Data analysis and model fitting for GDO selectivity, Y2 (%)

The experimental results for GDO selectivity are shown in Table 4.3. A full quadratic model of GDO selectivity response (%), Y2 was expressed in Eq. (4.2), whereas the coded coefficients for the main effects, the quadratic effects, and the interaction effects of the response surface of GDO selectivity (%) was generated in Table 4.5.

$$Y2 = 64.423 + 3.689A + 4.879B + 1.739C + 0.141A^2 + 4.085B^2 + 1.599C^2 - 0.306AB - 0.809AC - 0.006BC \quad (4.2)$$

The model coefficient of multiple determination, R^2 was determined at 0.9292, which describes 92.92% of the response variability. It was evident that 64.423 is constant, independent of the variables (Table 4.5) and the effect of temperature is the most important (4.879). The response was positively affected by all linear terms (A, B, and C)

as well as quadratic terms (AA, BB, and CC) however, the interaction terms (AB, AC, and BC) had a negative relationship with the response.

Table 4.5. Values of model coefficients of GDO selectivity

Term	Coefficients	Value	Standard error Coefficients
Constant	β_0	64.423	0.535
A	β_1	3.689	0.328
B	β_2	4.879	0.328
C	β_3	1.739	0.328
A × A	β_{11}	0.141	0.482
B × B	β_{22}	4.085	0.482
C × C	β_{33}	1.599	0.482
A × B	β_{12}	-0.306	0.464
A × C	β_{13}	-0.809	0.464
B × C	β_{23}	-0.006	0.464

The linear effects (A, B, and C) and quadratic effects of BB and CC are significant, as evident from the $p < 0.05$ (*see* Appendices, Table A.2). However, AA and all the interaction effects are insignificant. The p values of the quadratic regression model in ANOVA are less than 0.05, indicating that the model is significant.

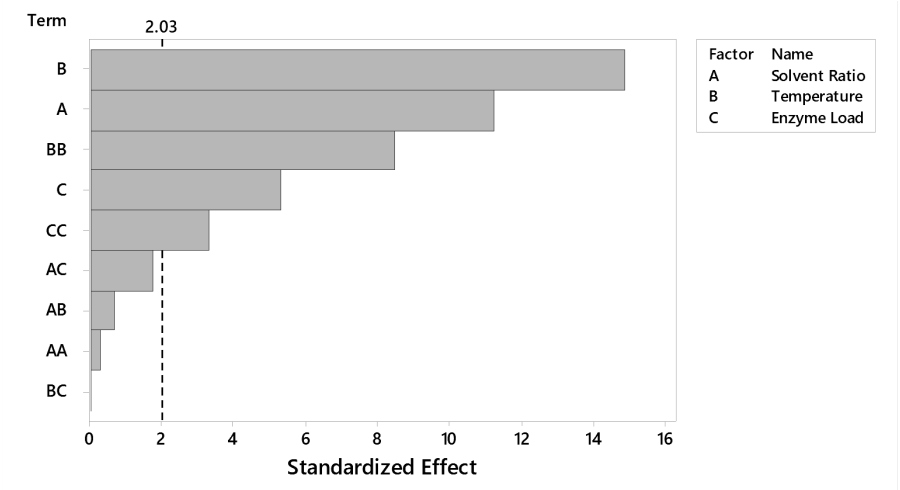

Figure 4.8. Standardized effects for GDO selectivity (%) using a Pareto chart

Fig. 4.8 shows the absolute value of the effects, which is placed at a 5% significance level. The Pareto chart shows that GDO selectivity is considerably impacted by temperature (B) and solvent ratio (A) followed by quadratics term BB, enzyme load

(C), and CC, as all these factors crossed the reference line (2.03). All the interaction terms have no profound effect on the investigated response.

The residual plots were further examined to validate the ANOVA assumption and model adequacy. In Fig. 4.9a, the data plots were narrowly scattered around the standardized line demonstrated that the underlying error distribution is normal. The histogram displayed the central tendency, symmetry, and normal shape of data distribution (Fig. 4.9b) which proved that the errors were caused solely by random error and not by a non-random factor. As can be seen in Fig. 4.9c, almost equivalent numbers of points were randomly scattered on the upper and below side of the standardized zero line. This confirms that the experimental data is absent from any systematic error. Based on the standardized residuals *vs.* observation order plot in Fig. 4.9d, the order of experiments was found to be independent with the data obtained.

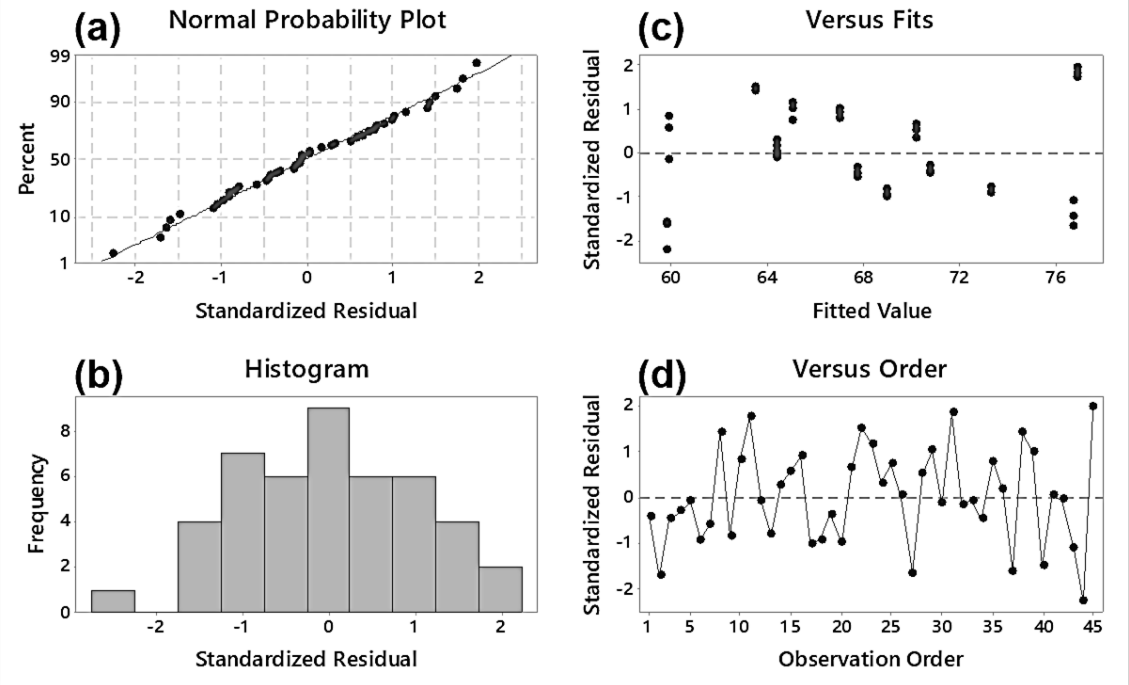

Figure 4.9. Residual plots for GDO selectivity (%) (a) normality probability plot, (b) histogram plot, (c) standardized residual vs fitted value, and (d) standardized residual vs observation order

4.2.2 Contour plot and surface plot on optimization of selected operating variables of oleic acid conversion (%) and GDO selectivity (%).

The contour plot is characterized by the contour line with factors plotted on X- and Y-axis. While surface plot is a 3-D plot surface defined by three variables, Y, X, and Z.

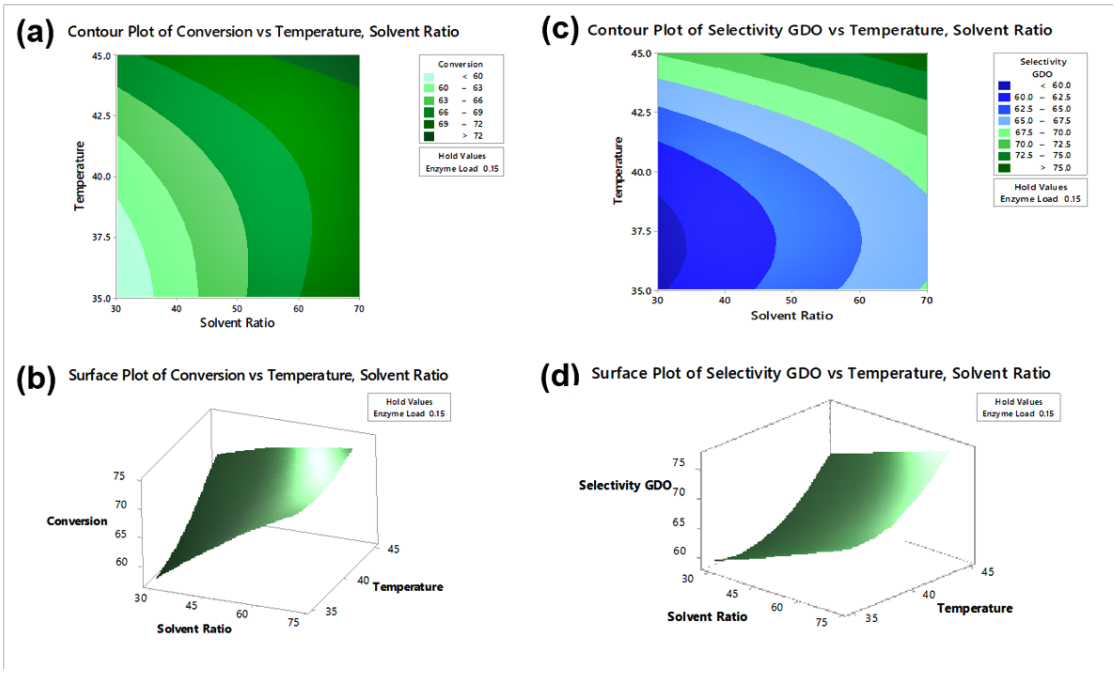

Figure 4.10. (a) Contour plot of conversion (%) (b) Surface plot of oleic conversion (%) (c) Contour plot of GDO selectivity (%) d) Surface plot of GDO selectivity (%).

The contour plot and surface plots for conversion are shown in Fig. 4.10. For the contour plot of temperature versus solvent ratio, the dark green region indicates the highest value of conversion where feasible optimization can be done (Fig. 4.10a). At constant enzyme load of 0.15 g, the highest percentage of conversion (> 70%) can be achieved at 45°C. As can be seen in the contour plot, conversion gradient tends to get higher as the temperature and solvent ratio increase simultaneously. The three-dimensional surface plot showed the relationships between conversion, temperature and solvent ratio (Fig. 4.10b). The significant effect of curvature within the model is represented in the surface plot which also showed the optimized region.

The contour plot and surface plots for GDO selectivity are shown in Fig. 4.10c. Fig. 4.10c reveals that the high predicted GDO selectivity of 75%, could be achieved by increasing the solvent ratio up to 70% of acetone to *tert*-butanol, while the temperature should be set at 45°C. GDO selectivity increased gradually with temperature and solvent ratio. Fig. 4.10d shows a response surface sloping up towards temperature (B = +1) signifying that high GDO selectivity is achieved when a substantial decrease in the viscosity of the mixture occur.

According to these results, the model equations for both conversion and selectivity can be simplified by eliminating non-statistically significant factors ($p > 0.05$). The following mathematical models were calculated as follow:

For conversion (%),

$$Y1 = 65.735 + 4.870A + 2.895B + 1.976B^2 - 2.487AB \quad (4.3)$$

For GDO selectivity (%),

$$Y2 = 64.510 + 3.689A + 4.879B + 1.739C + 4.074B^2 + 1.589C^2 \quad (4.4)$$

Where A, B and C represent the coded values of each studied factor.

4.2.3 Optimization of oleic acid conversion (%) and GDO selectivity (%) and validation of the models

Both responses, Y1 and Y2, were then subjected to optimization of variables which was done using the Response Optimizer function. The goal for optimization was to maximize the percentage of both responses considering the empirical conditions presented in Table 4.3.

Optimal conditions for dual response optimization were given as (A, B, C,) = (+1, +1, 0) corresponding to actual values of 70% of solvent ratio of acetone to *tert*-butanol, 45°C and 0.15 g of enzyme load. Under these conditions, the maximum predicted

conversion was 73 % and the GDO selectivity would be 77 %. The composite desirability was 0.86, indicating that this level could be achieved in 86 out of 100 runs.

In order to confirm the predicted optimal values obtained, additional three independent tests were executed under the predicted settings. The average percentage obtained for conversion and selectivity were 73.6 ± 0.4 % and 77.2 ± 0.5 %, respectively. Therefore, the GDO optimization considering two responses was successfully conducted as the experimental data agreeable with the model prediction.

The DAG production obtained under optimal conditions in batch reactor from other works is shown in Table 4.6. Employing statistical experimental design for maximizing DAG production, almost similar values of conversion and DAG composition were achieved by Sánchez *et al.* (2020). The authors revealed that the optimized response for the esterification of glycerol with capric acid in *n*-heptane was attained at 6 h of reaction, which is three times longer that than in this study. It can be seen that the conversion value obtained was comparable to the values reported by Duan *et al.* (2010) and Voll *et al.* (2011) and slightly lower than Zhoa *et al.* (2018). The partial hydrolysis of refined palm olein by *Lecitase Ultra* using central composite rotational design optimization achieved a relatively higher conversion at 10 h of reaction (Mardani *et al.*, 2015). It should be noted the performance of enzymatic reaction was influenced by several factors such as the origin and concentration of biocatalyst, the nature of the substrates, the reaction media composition and also the operational settings. In term of DAG composition, the selectivity of GDO attained (77%) was higher than the other reported studies using one-factor-at-a-time method. Thus, all the results in Table 4.6 were absolutely conditioned by the experimental range used in their optimization studies.

Table 4.6. Comparison of DAG production in batch system at its optimal condition.

Optimization method	Type of reaction	Solvent	Substrates	Biocatalyst (lipase)	Time (h)	Conver-sion (%)	DAG composition (%)	Reference
One-factor-at-a-time	Esterification	*tert*-butanol	oleic acid, glycerol	*Candida antarctica,* (Novozyme 435)	7	75	40	Duan *et al.* (2010)
One-factor-at-a-time	Glycerolysis	*tert*-butanol	olive oil, glycerol	*Candida antarctica,* (Novozyme 435)	12	N/A	57	Voll *et al.* (2011)
Two central composite rotational design	Partial Hydrolysis	solventless	palm oil, water	*Rhizomucor miehei* (Lipozyme®RMIM)	12	N/A	34.17	Awadallak *et al.* (2013)
Central composite rotational design	Partial Hydrolysis	solventless	refined palm olein	Lecitase Ultra	10	94.5	42.2	Mardani *et al.* (2015)
Central composite rotational design	Partial Hydrolysis	solventless	refined, bleached and deodorized palm oil (RBDPO)	*Rhizomucor miehei* (Lipozyme®RMIM)	6	N/A	29.5	Phuah *et al.* (2016b)
One-factor-at-a-time	Glycerolysis	solventless	lard, glycerol	*Rhizomucor miehei* (Lipozyme®RMIM)	4	76.68	46.91	Zhoa *et al.* (2018)
One-factor-at-a-time	Glycerolysis	solventless	algae oil from *Schizochytrium sp*, glycerol	*Candida antarctica,* (Novozyme 435)	8	N/A	48.4 (crude mixture) 75.1 (purified)	Wang *et al.* (2018)
One-factor-at-a-time	Esterification	solventless	caprylic acid, capric acid, glycerol	*Candida antarctica,* (Novozyme 435)	6	N/A	53.77 ± 3.74[a] 51.89 ± 2.60[b]	Das and Ghosh (2019)
One-factor-at-a-time	Esterification	solventless	caprylic acid, capric acid, glycerol	*Rhizomucor miehei* (Lipozyme®RMIM)	18	N/A	58.86 ± 4.05[a] 55.41 ± 3.95[b]	Das and Ghosh (2019)
One-factor-at-a-time	Glycerolysis	solventless	refined, bleached, and deodorized soybean oil	*Candida antarctica* (Novozyme 435)	12	N/A	60 - 62	Zhong *et al.* (2019)
Factorial design 2^3 with two central points	Esterification	*n*-heptane	capric acid, glycerol	*Rhizomucor miehei* (Lipozyme®RMIM)	6	73	76	Sánchez *et al.* (2020)
One-factor-at-a-time	Glycerolysis-interesterification	*tert*-butanol	palm stearin, palm olein, glycerol	*Immobilized Candida antarctica lipase B*	1	N/A	27.34	Subroto *et al.* (2020)
Box-Behnken Design	Esterification	acetone*: tert*-butanol	oleic acid, glycerol	*Candida antarctica,* (Novozyme 435)	2	73.6 ± 0.4 %	77.2 ± 0.5 %,	This work

[a]esterification of glycerol with caprylic acid, [b]esterification of glycerol with capric acid, N/A = not available

Moreover, the optimal selectivities of GMO and GTO were also tested using Response Optimizer. The optimal conditions for GMO selectivity were (A, B, C) = (-1, -0.64, -1) corresponding to actual values of 30% of acetone to *tert*-butanol, 36.8°C and 0.1 g of enzyme load. Under these conditions, the maximum predicted of GMO selectivity was 41.8%, with composite desirability of 0.9291. For GTO selectivity, the maximal selectivity of 0.11% (composite desirability at 0.84) would be achieved by input variables levels set at (A, B, C) = (0, +1, +1) corresponding to 50% of acetone to *tert*-butanol, 45°C and 0.2 g enzyme load in their actual values.

4.2.4 Proposed kinetic mechanism of GDO

For most of the enzyme reactions, the kinetic models are well represented by the Michaelis Menten equation. Considering classical kinetics, Michaelis Menten involving a two substrates reaction could be classified into a Sequential Random Bi-Bi, Sequential Ordered Bi-Bi or Ping Pong Bi-Bi mechanism. The adoption of those models is based on the evaluation and practice of the initial reaction rate method. Initial rate data are preferred because at the start of reaction, both the enzyme and substrate are more stable and accurate. The initial reaction rate, v was estimated from the changes of GDO concentration over time at different substrate concentrations (Fig. 4.11a). . In order to investigate the esterification mechanism, reactions were carried out at concentration ranges of 1.88 to 2.13 M and 0.31 to 1.32 M for oleic acid and glycerol, respectively using new enzyme samples each time at a selected temperature that is 45°C. When performing these reactions, the temperature must be constant at a value at which the lipase is physiologically active. Fig. 4.11 demonstrates that the reaction rates increased with increasing concentration of oleic acid at fixed glycerol concentration (Fig. 4.11b). A similar trend was observed when the concentrations of glycerol were varied at a fixed oleic acid concentration (Fig. 4.11c).

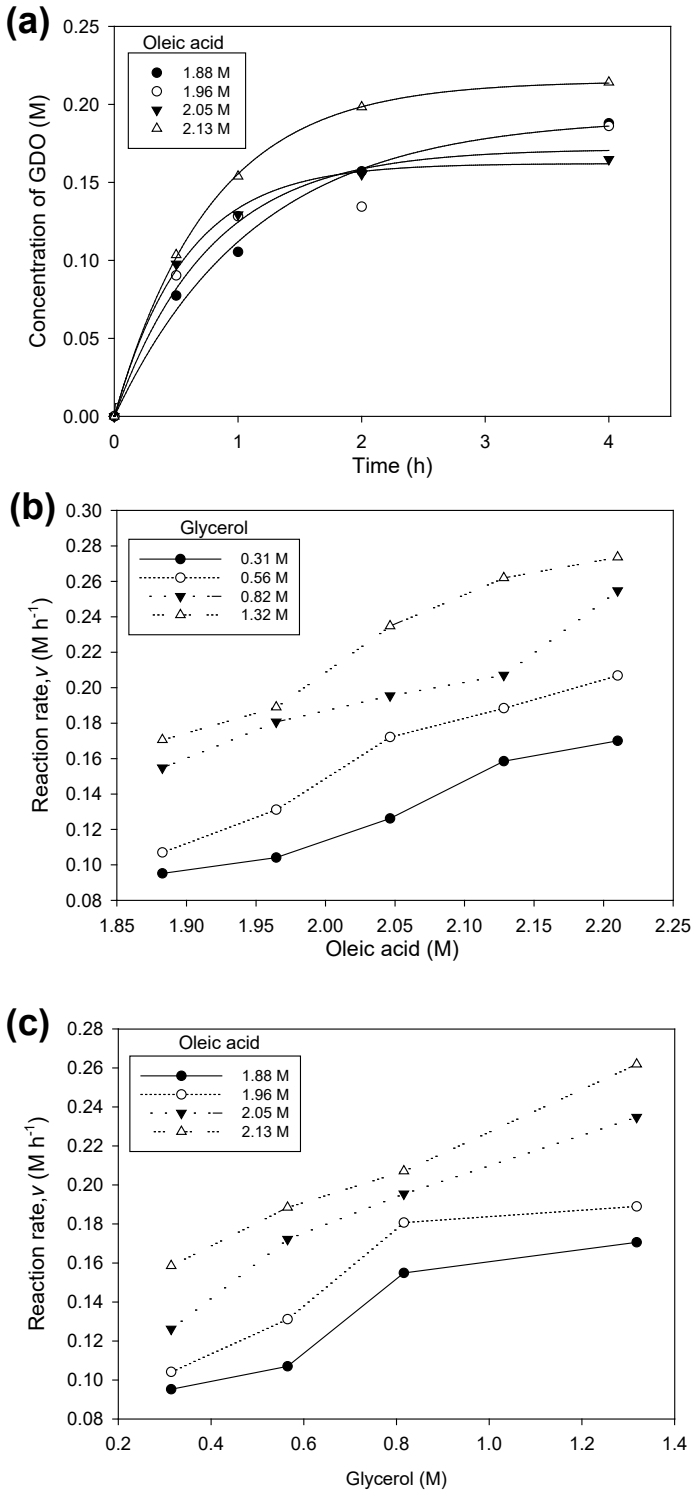

Figure 4.11. (a) Time course of GDO synthesis (M) as a function of time (h) (b) Reaction rate of GDO synthesis as a function of oleic acid concentrations (M) at fixed glycerol concentration (M) (c) Reaction rate of GDO synthesis as a function of glycerol concentrations (M) at fixed oleic acid concentrations (M). Reaction condition: 45°C, 200 rpm and 0.15 g lipase.

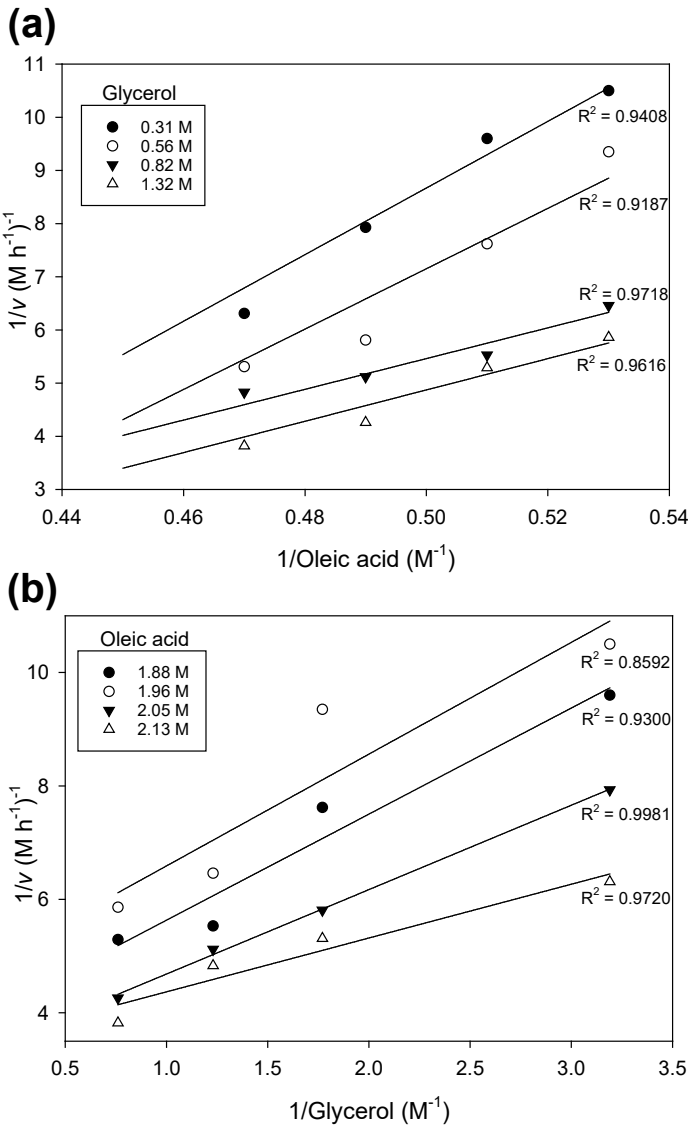

Figure 4.12. Lineweaver–Burk plots. (a) Double reciprocal plot of 1/initial reaction rates of GDO *vs* 1/oleic acid concentrations (1/*v vs* 1/*s)* at various glycerol concentrations (b) Double reciprocal plot of 1/initial reaction rates of GDO *vs* 1/glycerol concentrations (1/*v vs* 1/*s)* at various oleic acid concentrations. Reaction condition: 45°C, 200 ppm and 0.15 g lipase.

The determination of the mechanism involving bisubstrate reactions (i.e. Random, Ordered, or Ping Pong mechanism) is often presented using a Lineweaver-Burk approach (Segel, 1975; Marangoni, 2003; Cook & Cleland, 2007). The kinetic model of the GDO synthesis was initially evaluated by Lineweaver–Burk plot to understand the underlying reaction mechanism. This approach uses a linearization procedure in which a plot of 1/*v* versus 1/*s* is employed to give a straight-line plot so that the value of V_{max} and K_m could be determined and specified. Double reciprocal plots of 1/initial reaction rates of GDO *vs* 1/glycerol concentrations (1/*v vs* 1/*s)* were plotted at various oleic acid concentrations

and *vice versa*. The appearance of parallel lines can be seen with a decrease in slope as the concentration increases (Fig. 4.12a-b). It was observed that there is no common interception between the lines, which rules out the possibility of sequential mechanisms. The parallel lines in the Lineweaver–Burk plot show no upward curvatures which verified the absence of any substrate's inhibition. Even though oleic acid is present in excess, no inhibition was detected in the system. Therefore, it was concluded that the reaction follows a Ping-Pong mechanism with no inhibition.

Employing a nonlinear regression fitting with the Levenberg–Marquardt algorithm, model Ping Pong Bi-Bi model parameters were evaluated for a greater accuracy. The reaction rate equation is shown in Eq. (4.5):

$$v = \frac{V_{\max}[\mathrm{OA}][\mathrm{G}]}{K_m^{[\mathrm{G}]}[\mathrm{OA}] + K_m^{[\mathrm{OA}]}[\mathrm{G}] + [\mathrm{OA}][\mathrm{G}]} \tag{4.5}$$

where v is the reaction rate of GDO, V_{max} is the maximum reaction rate of GDO (M h^{-1}) and $K_{\mathrm{m}}^{\mathrm{OA}}$ and $K_{\mathrm{m}}^{\mathrm{G}}$ are the Michaelis constants for oleic acid [OA] and glycerol [G], respectively. However, the enzymatic esterification of glycerol with oleic acid is a multi-substrate reaction and the products produced at one reaction stage can react as the substrates for the next stage.

Based on the nonlinear regression analysis, the kinetic parameters estimated are presented in Table 4.7. With 95% confidence interval, the results were statistically valid and stable.

Table 4.7. Kinetic parameters for Ping Pong Bi-Bi model

	Parameter		
	V_{max} **(M h^{-1})**	$K_{\mathrm{m}}^{\mathrm{G}}$ **(M)**	$K_{\mathrm{m}}^{\mathrm{OA}}$ **(M)**
Predicted value	1.213	1.807	6.817
95% confidence interval	0.01	0.043	0.114

The affinity of the lipase toward glycerol was higher than that toward oleic acid, indicated by the lower K_m^G value as compared to K_m^{OA} (Table 4.7). According to the Pearson correlation coefficient, the R^2 value is 0.9075 indicating that the predicted initial rate agreeable with the experimental data (Fig. 4.13). Therefore, the lipase-catalyzed synthesis of GDO fitted to a Ping-Pong Bi-Bi mechanism was satisfactorily validated. The values of kinetic constants were then further applied in the simulation of initial rates using various oleic acid concentrations at fixed glycerol concentrations (*see* Appendices, Figure A.1).

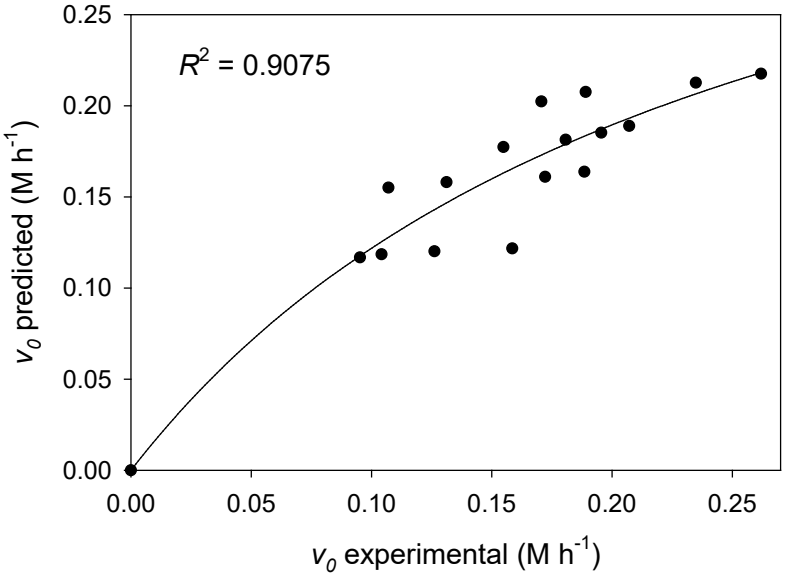

Figure 4.13. Experimental and predicted initial rates (v_0) plots utilizing Ping-Pong Bi-Bi kinetic parameters model.

Similar to substrate concentrations, other conditions such as temperature also influence the reaction rate of enzyme. Esterification and reaction rates both increase at high temperatures. The reaction was performed at an extended temperature of up to 55°C. This was done so that the rate constant and, ultimately, the activation energy of GDO production could be estimated more accurately.

Based on Fig. 4.14, the initial reaction rate increases linearly with the increased concentration of oleic acid at all temperatures. With an increase in oleic acid concentrations ranging from 2.05 to 2.13 M, the initial rates of GDO increased gradually from 0.077 to 0.122 M h^{-1}, 0.116 to 0.164 M h^{-1}, 0.155 to 0.207 M h^{-1}, 0.172 to 0.327 M h^{-1} and 0.190 to 0.447 M h^{-1} at 35°C, 40°C, 45°C, 50°C and 55°C respectively.

Increasing the temperature leads to more frequent collisions between molecules and a substantial decrease in the sample's viscosity which subsequently reduces mass transfer limitations (Al-Zuhair *et al.*, 2003; Wang *et al.*, 2010; Feltes *et al.*, 2012). As temperature increases, intensified diffusion of substrates occurs which results in an increase in the binding of substrates to the active site of the lipase. As a result, the initial reaction rate increases due to the acceleration effect at higher temperature. These results corroborate with other lipase-catalyzed esterification systems using CAL-B. It is worth noting that, Razak and Annuar (2015) reported that the initial rates and the kinetic constants of the reaction increased with increasing the temperature from 20 to 55°C in their investigation of enzymatic esterification of flavonoid with lauric acid in acetone.

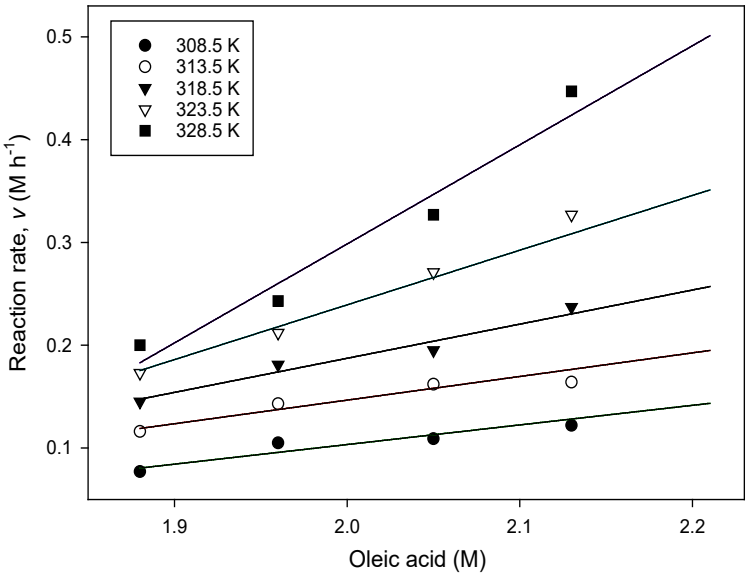

Figure 4.14. Reaction rate of GDO (M h^{-1}) at different oleic acid concentration (M) and temperatures.

Table 4.8 shows the initial reaction rates and the rate constants obtained from the slope of lines in Fig. 4.14. According to the transition state theory, an increase in temperature would magnify the effect on the kinetic constant. The slope of the reaction rate of GDO gives the rate constant, k_1'. Steeper slopes were observed as the temperature increases, which are shown by the increase in k_1' values (Table 4.8). This means that the reaction rates and oleic acid concentration are directly proportional to each other and represented as first-order behavior. First-order kinetics reflects that the reaction is dependent of the substrate concentration. A similar k_1' esterification kinetics was observed in the production of triolein by Lipozyme IM 20 (Lortie *et al.*, 1993) and also the esterification of glycerol with soybean oil and rapeseed oil by Lipozyme RM IM (Watanabe *et al.*, 2003).

Table 4.8. Reaction rate, apparent first-order rate constant, and V_{max} values obtained at different temperatures.

Temperature (°C)	**Reaction rate of GDO, v (M h^{-1})***				**Apparent first-order rate constant, k_1' (h^{-1})**	**V_{max} (M h^{-1})**
	1.88	**1.96**	**2.05**	**2.13**		
35	0.077	0.105	0.109	0.122	0.194	0.853
40	0.116	0.143	0.152	0.164	0.235	1.033
45	0.155	0.181	0.195	0.207	0.276	1.213
50	0.172	0.212	0.261	0.327	0.639	2.808
55	0.190	0.243	0.327	0.447	1.001	4.399

* at various concentrations of oleic acid (M)

The range of substrates used in this study is limited by the viscosities and solubilities of substrates. Typically, at the high substrate concentrations, initial reaction rate becomes approximately constant and less sensitive to variation in the concentration of substrates. At this range, the reaction rate at a saturation behavior is written as,

$$v = V_{max} = k_{cat}[ET] \tag{4.6}$$

Where k_{cat} is the catalytic constant ($k_{cat} = k_1$') and [ET] is the total active enzyme present in molar concentration. Assuming lipase concentration is catalytically active and

essentially constant during the reaction, V_{max} for each temperature tested is shown in Table 4.8.

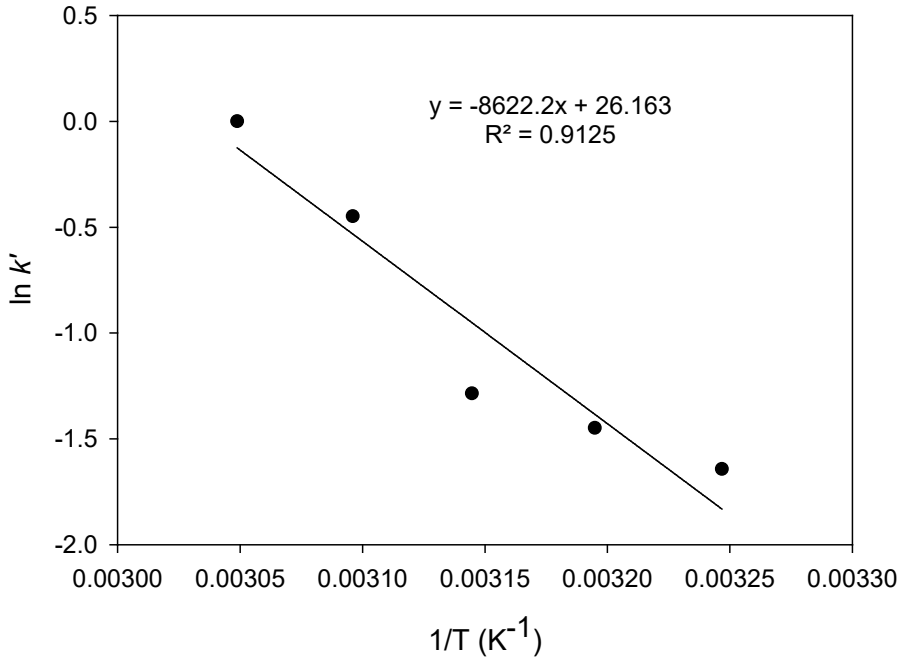

Figure 4.15. Arrhenius plot of the lipase-catalyzed synthesis of GDO.

The apparent activation energy (E_a) values were calculated using the Arrhenius plot based on the k_1' values in Table 4.8. Employing Arrhenius plot (Fig. 4.15), the estimated value of E_a was at 71 kJ mol^{-1}. This value is corroborated with the typical range of activation energy that is between 25 to 83 kJ mol^{-1} for enzymatic reactions (Dixon & Webb, 1979). The E_a value obtained in this study is comparable to the value reported by Sun *et al.* (2009) in the esterification of glycerol ferulate with oleic acid using Novozyme 435 (~67.4 kJ mol^{-1}). However, the value was lower than the values from the studies by Watanabe *et al.* (2003) and Phuah *et al.* (2012). The reaction occurs more quickly if the activation energy is lower as only a small amount of heat is necessary for the reaction to start. Watanabe *et al.* (2003) discovered that in the esterification of glycerol using a mixture of oleic and linoleic acids using *Rhizomucor meihei* as a biocatalyst, the activation energy achieved was around 13.0 to 25.5 kJ mol^{-1}. Phuah *et al.* (2012) attained

an activation energy value of 31.35 kJ mol^{-1} which is slightly higher than that of Watanabe *et al.* (2003) using the same enzyme. The reaction conditions are different as they conducted the partial hydrolysis reaction of the refined, bleached and deodorized palm oil at 55°C to obtain a mixture of DAG.

4.2.5 Concluding remarks from the batch reactor study

A response surface analysis methodology was successfully applied in this experiment to optimize the GDO production. An orthogonal array was created using the Box Behnken design utilizing three-level and three-factors namely, the solvent ratio of acetone to *tert*-butanol, temperature and enzyme loading. RSM and ANOVA were employed to determine the optimal values for both conversion and selectivity of GDO. A validation experiment was also carried out using the predicted optimal values. It was summarized that 1) the optimal conversion and GDO selectivity were achieved at 73% and 77%, respectively, 2) under optimized conditions, the operating variables are a 70:30 solvent ratio of acetone: *tert*-butanol, a temperature of 45°C and an enzyme load of 0.15 g, and 3) The lipase-catalysed reaction was represented by a Ping-Pong Bi Bi model with no substrates inhibition. The improvement of statistical and experimental techniques based on the response surface methodology provides an opportunity to develop increasingly complex models nowadays. The optimization model obtained in this work could be applied for a batch or a continuous bioreactor of the enzyme-catalysed processes, therefore saving valuable set-up time. Furthermore, the proposed kinetic model equation is useful to determine the optimal substrate concentrations in enzymatic reactions. It could be employed as the setting conditions for any practical application of GDO in food, pharmaceutical, and cosmetic industries.

4.3 Continuous flow reactor study: Investigation on GDO synthesis

This section exploited the application of the continuous flow millireactor for the synthesis of GDO using lipase enzyme. Reaction medium containing mixture of solvents of acetone: *tert*-butanol was chosen as it is more favorable towards GDO production (Abd Razak *et al.*, 2020; Abd Razak *et al.*, 2021). The effect of selected parameters (enzyme loading, flow rate and molar ratio of substrate) on the acid conversion, selectivity and yield were investigated in this study. The section is also focusing on hydrodynamic and kinetic evaluation of GDO synthesis and the effects of dimensionless parameters under continuous flow conditions were also studied parametrically.

4.3.1 Effect of enzyme concentrations and water contents

It is well known that as more enzymes present in a system mean more substrates can access to the enzyme active sites. Fig. 4.16 reveals that the conversion was enhanced with increasing enzyme concentrations up to 0.15 g and started to decrease at 0.20 to 0.25 g. GMO selectivity shows the opposite pattern with conversion and GDO selectivity. Over a range of lipase concentrations tested, the selectivity of GMO was found higher than GDO. But, at 0.15 g of lipase, comparable results of GMO and GDO selectivities (~50%) were obtained as evident from $p>0.05$. Highest GMO selectivity was calculated at 70%, obtained the lowest lipase concentration with the least amount of conversion. With increasing lipase concentration from 0.05 g to 0.15 g, the overall production increased from 11% to 54% and 30% to 50% for conversion and GDO selectivity, respectively. Similar observation was made by Šabeder *et al*., (2006). They observed that initially palmitic acid conversion increased with increasing the lipase concentration. After a certain level of lipase concentration, the amount of conversion decreased, which may have been caused by an increase in the water content of the product. The optimum water

content is a compromise between minimizing hydrolysis and maximizing enzyme activity for the esterification reaction.

GTO was not found in any of the enzyme concentrations tested. Almost similar phenomenon was also observed by Watanabe *et al.* (2005). They conducted the reaction in a packed bed reactor under a vacuum condition at 40°C using Lipozyme RM IM as a biocatalyst. They observed that GTO concentration increased at the later stage of the reaction that is after 3 to 7 h of reaction and only a minute amount of GTO (2%) was produced at 2 h of reaction at 40°C. Meanwhile in this experiment, the residence time taken was ranging from 1.5 min to 77 min with no vacuum applied. Under these experimental operating conditions with relatively short reaction time, high levels of OA, GMO and GDO were detected with no presence of GTO. It is hypothesized that esterification of GTO by lipase enzyme requires longer time and water produced in medium may become a limiting factor that affecting the synthesis of GTO.

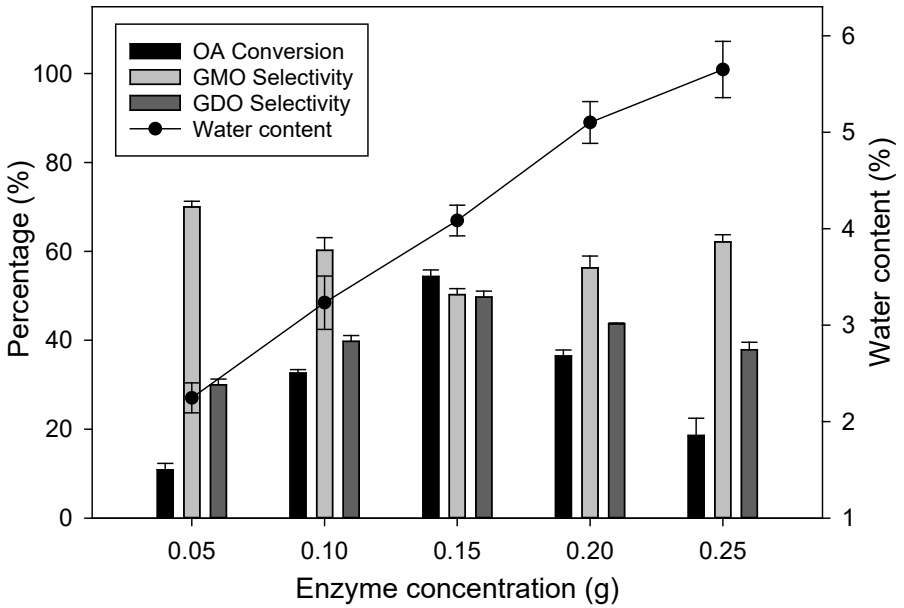

Figure 4.16. Effect of enzyme concentration and water contents on esterification of oleic acid with glycerol. Reaction conditions: ratio of oleic acid/glycerol: 2.5; 1.1 g of 3 Å molecular sieves; temperature at 45°C and flow rate of 5×10^{-5} L min^{-1}.

There is a clear change in the GO composition pattern at 0.20 to 0.25 g of lipase (Fig. 4.16). This result suggested that water produced during the synthesis of glycerol

oleates is most likely provoked a decrease in conversion and GDO production. Therefore, to confirm the inhibitory effect of water on esterification, the water content was measured using Karl-Fischer titrator. As can be seen from Fig. 4.16, the amount of water gradually increased from 2.2% to 5.6% and this by-product is thermodynamically unfavourable to esterification reaction. The results exhibited a similar inhibitory effect during the glycerolysis of palm oil for DAG production. Liu *et al.* (2014) demonstrated that when the initial water content of the substrate was greater than 5%, the DAG content decreased. Lipase-catalysed reactions are reversible and governed by the water content of the reaction mixture. The amount of water present has a significant impact on enzyme function in micro aqueous medium like organic solvent (Sarmah *et al.*, 2018). Although a small amount of water is essential to maintain enzymes active conformation, however, at higher water contents the synthesis gradually declined as the reverse reaction takes place. The finding is supported by Shimada *et al.* (1999), who reported that high water content significantly decreases ester production through an increase in hydrolysis reaction. They found that as the water content increased from 0.7% to 2%, the conversion decreased from 7.5% to 6.7%. They observed that at this point the hydrolysis reaction increased from 4.3% to 5.7%.

Various strategies have been established to eliminate water during the synthesis of DAG such as the use of such molecular sieve or silica gels as desiccating agents during the online removal of water (Wang *et al.*, 2016b), adsorption of glycerol to silica gel (Weber & Mukhrejee, 2004), the presence of a vacuum pump (Watanabe *et al.*, 2005; Diao *et al.*, 2017) and also the removal of water through evaporation under a stream of nitrogen gas (Guo *et al.*, 2007; Zhong *et al.*, 2019). In this study, the synthesis has been performed with dried solvents and also with presence of molecular sieves 4A in the column to requester the produced water. However, at enzyme load of 0.20 g and above, a larger amount of molecular sieve might be needed to shift the reaction towards

synthesis. Since this study is limited to the size of the column used, the best and suitable enzyme concentration was determined at 0.15 g for the subsequent studies.

4.3.2 Effect of substrate concentrations

With the aim to minimize the substrates concentration in the reaction in order to obtain high conversion in a short time, different ratio of oleic acid:glycerol concentrations were carried out. To counteract the hindrance caused by water produced, an excess of oleic acid also can be beneficial because it has pronounced effect on the medium homogeneity. Besides, it minimizing the diffusion limitation especially when immobilized catalyst is employed in the systems (Guo *et al.*, 2009; Duan *et al.*, 2010, Cai *et al.*, 2016).

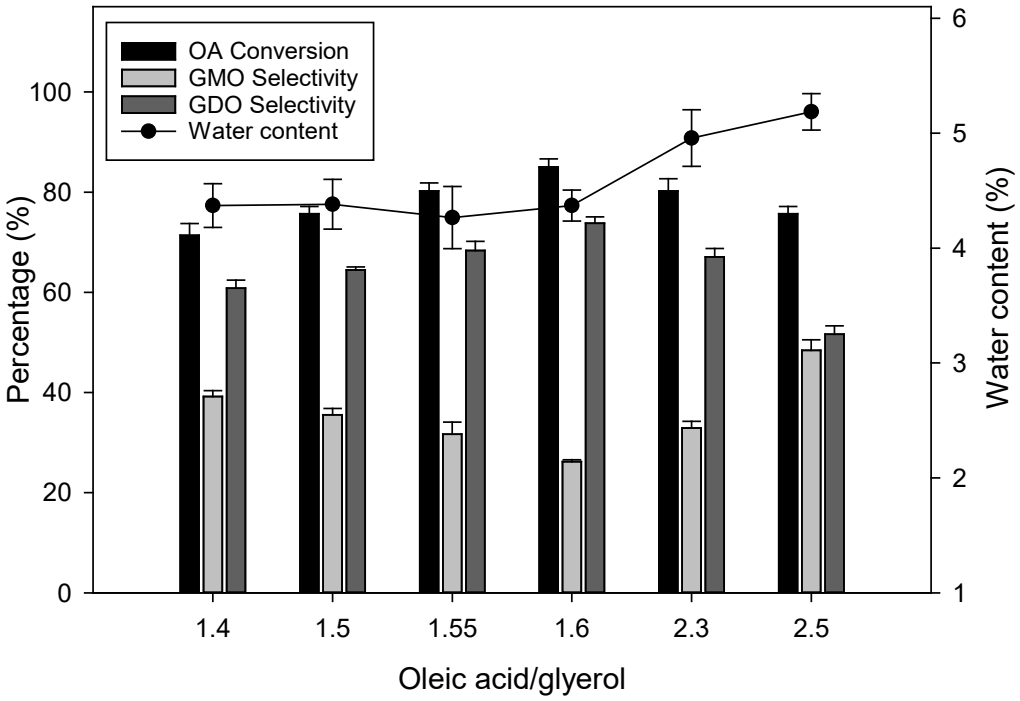

Figure 4.17. Effect of various ratio of substrates on esterification of oleic acid with glycerol. Reaction conditions: enzyme concentration at 0.15 g, 1.1 g of 3 Å molecular sieves; temperature at 45°C and flow rate of 2×10^{-5} L min^{-1}.

At a ratio of 1.6:1 (oleic acid: glycerol), highest conversion appears to take place, giving rise to higher selectivity of GDO as well. The increasing molar ratio of oleic acid:glycerol from 1.4:1 to 1.6:1 in the system led to increasing patterns in the conversion and GDO selectivity with contrary fashion of GMO selectivity (Fig. 4.17). The hypothesis that can be explained is that as CALB 1 is immobilized on a hydrophobic support (Lewatit® VP OC 1600), it requires a surplus amount of oleic acid (hydrophobic) to reach high reaction conversion. Lower oleic acid concentrations could lead to an incomplete GDO esterification. It is interesting to note that increasing in GMO selectivity was observed and at 2.5:1 molar ratio of reactants (oleic acid: glycerol), the formation of GMO and GDO were almost equivalent, reaching about 0.34 to 0.36 M at 2×10^{-5} L min^{-1}. However, further increasing the molar ratio seemed not favourable to the GDO formation. A gradual decrease was observed in the conversion and GDO selectivity was attained with the increase in molar ratio from 2.3:1 to 2.5:1 (oleic acid:glycerol). This can be associated with the water concentration in Fig. 4.18. Besides the inhibitory effects, at higher molar ratios, higher amount of water liberated and accumulated during the reaction causing poor accessibility of oleic acid to active site of lipase to form GDO. Water has a significant impact on lipase as it modifies the hydration of the enzyme or enzyme support materials. Moreover, the presence of water can indirectly affect the composition of the reaction media due to its hydrophilic characteristic (Yesiloglu & Kilic, 2004). Studies have shown that the water content in the reaction mixture should be maintained at a low level for the efficient synthesis of DAG (Watanabe *et al.*, 2005; Diao *et al.*, 2017).

4.3.3 Effect of flow rates and residence times

The contact time of the substrates with immobilized lipase is controlled by the flow rate, which is an important characteristic in a packed bed reactor. Nevertheless, it is critical to keep the residence time at a relatively short time in order to keep the water

content low. The residence time is determined by Eq. 3.4. Increase of the flow rate led to lower residence time. Fig. 4.18 shows two noticeable trends of GMO and GDO selectivities in all tested flow rates. GMO selectivity decreased with increasing residence time, meanwhile GDO selectivity increased steadily with increasing residence time and both patterns reached almost equivalent and stable selectivity at 30 min to 77 min. Almost equivalent and stable GDO selectivity reached at R_t = 31 min (5×10^{-5} L min^{-1}) and R_t = 77 min (2×10^{-5} L min^{-1}). Increased in interactions time between the substrate and enzyme led to change of final product composition in favour to GDO. The results showed both GMO and GDO selectivities did not have a significant effect the at lower flow rates ranging from 2×10^{-5} L min^{-1} (R_t = 77 min) to 5×10^{-5} L min^{-1} (R_t = 31 min). Oleic acid conversion displays the anticipated pattern; longer residence times required to accomplish higher conversion. At R_t = 77 min (2×10^{-5} L min^{-1}), the highest oleic acid conversion (85%) was obtained. The lowest oleic acid conversion was calculated at 0.5% at a very short residence time, R_t = 1 min (1.5×10^{-3} L min^{-1}).

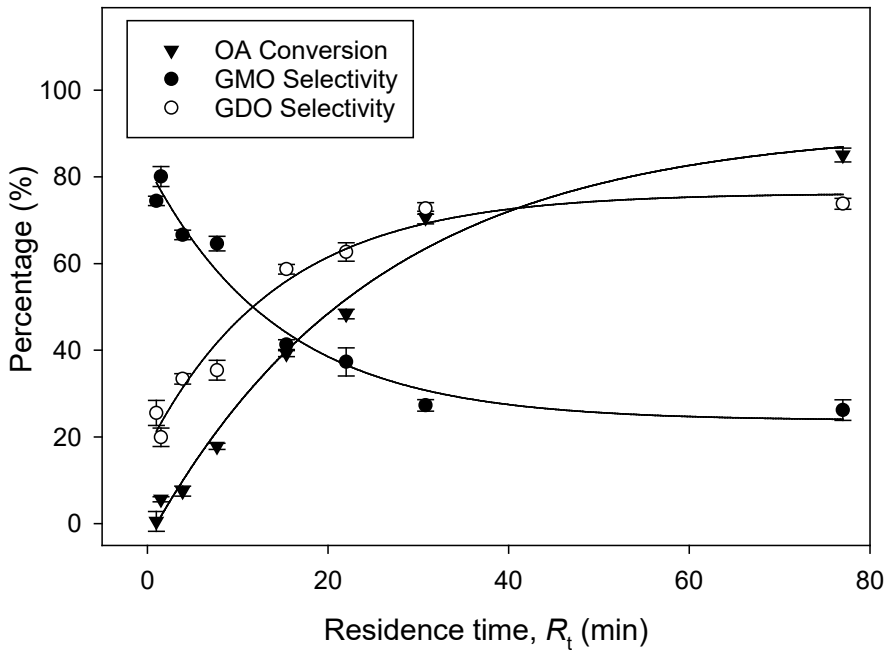

Figure 4.18. Effect of flow rate and residence time on esterification of oleic acid with glycerol. Reaction conditions: 0.15 g of lipase enzyme, molar ratio of oleic acid:glycerol at 1.6:1; 1.1 g of 3 Å molecular sieves; and temperature at 45°C.

The evolution plot of oleic acid conversion, GMO and GDO selectivities profiles depended on the residence time at various molar ratio are presented in Figs. 14.9a-c, respectively. The profiles of the increase of oleic acid conversion (Fig. 4.19a), and the decrease of GMO selectivity (Fig. 4.19b) and along with the GDO selectivity increased (Fig. 4.19c) were observed accordingly.

Oleic acid conversion showed an excellent performance at the lowest flow rate studied, in which 85% conversion was achieved at 1.6:1 molar ratio of oleic acid: glycerol (Fig. 14.9a). Furthermore, at R_t = 77 min (2×10^{-5} L min^{-1}), oleic acid conversion attaining more than 70% in all tested molar ratios. The increase in flow rate clearly had a negative impact on oleic acid conversion. Less than 10% of oleic acid conversion were obtained when the flow rates were set at 4×10^{-4} L min^{-1} (R_t = 3.9 min), to 1×10^{-3} L min^{-1} (R_t = 1.5 min), meanwhile at 1.5×10^{-3} L min^{-1} (R_t = 1 min), less than 0.6% of oleic acid conversion were achieved at all tested molar ratios.

Meanwhile, the curve profiles of GMO selectivity displayed opposite patterns with oleic acid conversion as it increased with increasing flow rates (Fig. 4.19b). It was observed that the highest GMO selectivity curve achieved at a molar ratio of 2.5, attaining about 87% at R_t = 1.5 min (1×10^{-3} L min^{-1}). At this point, GMO selectivity was formed up nearly about 6.8% higher than GDO, however only 4.2% of oleic acid was converted.

At any tested ratios, GDO increased drastically which proves that the formation of GDO is only favorable at longer residence time (Fig. 4.19c). At a molar ratio of 1.6, GDO selectivity achieved the highest and comparable values of 73-74% at R_t = 31 min (5×10^{-5} L min^{-1}) and R_t = 77 min (2×10^{-5} L min^{-1}).

Besides selectivity, it is worth estimating the yields of GMO and GDO using Eq. 3.28. As far as the longer contact time of substrates with lipase is concerned, yields of GMO and GDO increased with the decreasing flow rates. With increasing residence time from 1 to 77 min at a molar ratio of 2.5, enhancement to the extent of 0.28 % to 24% of

GMO yield in the system was noticed. It is found that GDO yield (72%) was achieved with lowest flow rates a molar ratio of 1.6. It was proven that further shortening residence time led to fewer products.

Lipase-catalyzed synthesis of GDO in blended solvents were previously investigated using the batch reactor systems (Abd Razak *et al.*, 2020; Abd Razak *et al.*, 2021). The preliminary study discovered that the synthesis of GDO is preferable in a blended solvent that contains of acetone: *tert*-butanol (Abd Razak *et al.*, 2020). Further investigation on the optimization conditions revealed that both oleic acid conversion and GDO selectivity were improved from 70 to 73% and 54 to 77%, respectively (Abd Razak *et al.*, 2021). The performance of GDO synthesis was then examined using a continuous flow system and it showed that the oleic acid conversion was further enhanced from 73 to 85% at a shorter time that is 1.3 h. As can be seen from Table 4.9, most of the studied systems exhibited comparable values of GDO selectivity (~70 to 80.3%) which is corroborated with value obtained from this study (74%). The performance of GDO production were similar to the values reported by Hu *et al.* (2013) in a packed bed reactor system. They reported a conversion of 82.3% with 77.6% of DAG content in the esterification of caprylic acid with glycerol that accomplished at 7 h of reaction. From Table 4.9, it was evident that Zhong *et al.* (2013) obtained the highest conversion and the highest DAG production that can be primarily ascribed to a substantial elimination of water which resulted in an increase of GDO synthesis. They established the operation protocol by equipped the pear-shaped flask with vacuum-driven air bubbling. However, they achieved the maximum values at 3 h of reaction, which is relatively longer that than achieved in this study. Comparing to other studies in Table 4.9, the use of continuous flow reactor millipacked bed reactor could lead to an excellent conversion and GDO selectivity within a short reaction time without any additional modification on the equipment.

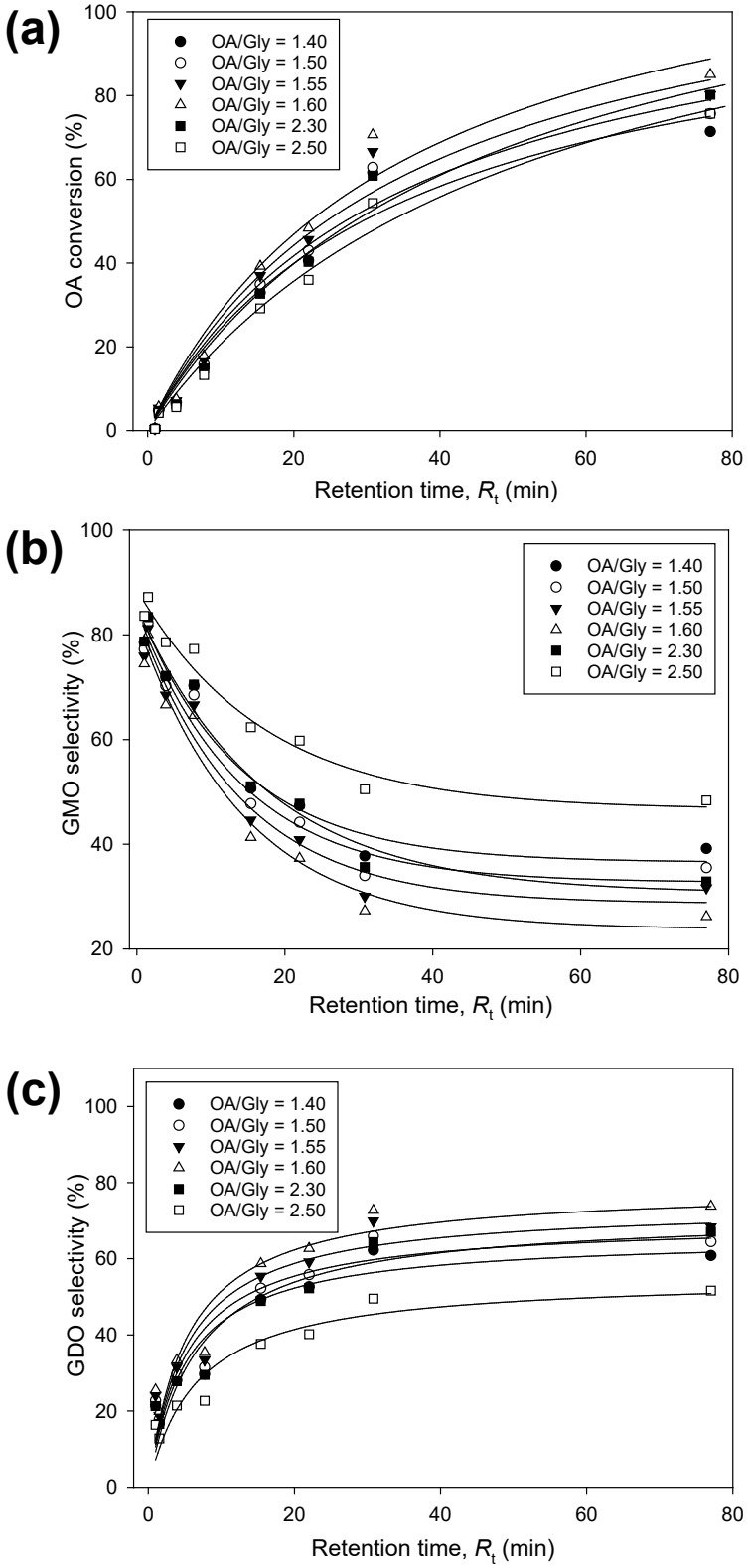

Figure 4.19. Profiles of oleic acid conversion, GMO and GDO selectivity as a function of residence time under various ratio of oleic acid:glycerol. (a) oleic acid conversion (b) GMO selectivity (c) GDO selectivity. Reaction conditions: 0.15 g of lipase enzyme, 1.1 g of 3 Å molecular sieves; and temperature at 45°C. *(The standard deviation of the measurements of all graphs was <12 %)*

Table 4.10. Comparison of DAG production at its optimal condition using various reactors. Some of the information was adapted and modified from Abd Razak *et al.* (2021).

Optimization method /	Type of reactor	Type of reaction	Reaction medium	Substrates	Biocatalyst (lipase)	Time (hr)	Conver-sion (%)	DAG composition (%)	Reference
one-factor-at-a-time	bubble column reactor with vacuum-driven air bubbling	esterification	solventless	lauric acid, glycerol	*Rhizomucor miehei*[a] (Lipozyme®RMIM)	3	95.3	80.3	Zhong *et al.* (2013)
Factorial design 2^3 with two central points	batch reactor	esterification	*n*-heptane	capric acid, glycerol	*Rhizomucor miehei*[a] (Lipozyme®RMIM)	6	73	76	Sánchez *et al.* (2020)
one-factor-at-a-time	batch reactor with ultrasonic treatment	glycerolysis	solventless	lard, glycerol	*Rhizomucor miehei*[a] (Lipozyme®RMIM)	4	76.68	46.91	Zhao *et al.* (2018)
Box–Behnken designs	batch reactor	esterification	acetone, *tert*-butanol	oleic acid, glycerol	*Candida antarctica*[a] (Novozyme 435)	2	73	77	Abd Razak *et al.* (2021)
one-factor-at-a-time	packed bed reactor with vacuum	esterification	solventless	Mixture of fatty acids, glycerol	*Rhizomucor miehei*[a] (Lipozyme®RMIM)	3	N/A	70	Watanabe *et al.* (2005)
one-factor-at-a-time	packed bed reactor	esterification	Water	Caprylic acid, glycerol	*Candida antarctica*[a] (Novozyme 435)	7	82.3	77.6	Hu *et al.* (2013)
Central Composite Rotational design	packed bed reactor	partial hydrolysis	solventless	refined, bleached and deodorized palm oil (RBDPO)	*Rhizomucor miehei*[a] (Lipozyme®RMIM)	6	N/A	29.5	Phuah *et al.* (2016b)
one-factor-at-a-time	continuous flow packed bed reactor	hydrolysis	*tert*-butanol	Hempseed oil, water	*Pseudomonas cepacia* (Amano)[b]	2	N/A	40[c]	Bavaro *et al.* (2020)
one-factor-at-a-time	continuous packed bed millireactor	esterification	acetone, *tert*-butanol	oleic acid, glycerol	*Candida antarctica*[a] (Novozyme 435)	1.3	85	74	This work

[a]commercial immobilized lipase, [b]free lipase immobilized on different carrier, [c]mixture of MAG and DAG, N/A = not available.

4.3.4 Mass transfer limitation study

Besides the estimation of the conversion of oleic acid and the production of GMO and GDO, determination values of the *Da,* and *Pe* are necessary to get an inclusive view of a continuous flow system's performance. The diffusivity and external mass transfer coefficient, K_{SL} were determined first before estimating these dimensionless numbers. Moreover, it is important to ensure that mass transfer and diffusion limitations are negligible to validate the reaction kinetics (Carberry, 2001; Shuler & Kargi, 2002). Because the reaction rate is restricted by the rate of mass transfer of reactants between the bulk fluid and the catalytic surface, many industrial reactions are conducted at high temperatures (Doran, 2012). Since the present study was experimentally executed at moderate temperature i.e. 45°C, hydrodynamic calculations were done to examine the controlling factor of the reaction rate; kinetic or diffusion. The external and internal mass transfer effects were predicted by theoretical calculations, as summarized in Table 4.10. Having a log *P* of 2.9×10^{-2}, the diffusion coefficients, D_{mix} for oleic acid and glycerol were calculated at 1.71×10^{-1} and 5.06×10^{-1} m^2 s^{-1}, respectively.

Correlations for K_{SL} were expressed using the dimensionless groups such as *Re, Sc* and *Sh*. In fluid mechanics, *Re* is used in the prediction of flow patterns in various fluid flow. Laminar flow is associated with low *Re* values (<1000), whereas turbulent flow dominates at higher *Re* numbers. *Re* numbers were calculated at 7.68×10^{-4} to 57.61×10^{-4}, indicating a laminar flow behavior for all tested flow rates, ranging from 2×10^{-5} L min^{-1} to 1.5×10^{-3} L min^{-1}. Therefore, the viscous force was dominating the flow that moving uniformly in non-turbulent condition and slight mixing in parallel layers.

Table 4.10. The influence of flow rates on the hydrodynamic parameters of GDO determined from the esterification of oleic acid with glycerol in a continuous flow reactor catalyzed by immobilized CALB 1.

Flow rate, *Q* **($\times 10^{-5}$)** **(L min^{-1})**	**Flow rate, *Q*** **($\times 10^{-10}$)** **(m^3 s^{-1})**	**Residence time (min)**	**Superficial velocity, *U*** **($\times 10^{-6}$)** **(m s^{-1})**	***Re*** **($\times 10^{-3}$)**	***Schmidt*** **($\times 10^{-5}$)**		***Sherwood*** **($\times 10^{-4}$)**		***K_{SL}*** **(m s^{-1})**		***Damköhler*** **($\times 10^{-3}$)**		***Péclet*** **($\times 10^{-6}$)**	
					OA	***Gly***	***OA***	***Gly***	***OA***	***Gly***	***OA***	***Gly***	***OA***	***Gly***
2	3.33	77.04	9.74	0.77	3.71	1.17	9.08	6.21	0.31	0.67	1.38	2.72	5.69	1.80
5	8.33	30.82	24.36	1.92			14.36	9.82	0.49	1.06	1.76	3.48	14.23	4.51
7	11.67	22.01	34.10	2.69			16.99	11.62	0.58	1.26	1.34	2.64	19.93	6.31
10	16.67	15.41	48.72	3.84			20.31	13.90	0.70	1.50	1.24	2.44	28.46	9.01
20	33.33	7.70	97.43	7.68			28.72	19.65	0.98	2.12	0.54	1.06	56.93	18.02
40	66.67	3.85	194.90	15.36			40.62	27.79	1.39	3.00	0.31	0.60	113.86	36.04
100	166.67	1.54	487.16	38.41			64.22	43.94	2.20	4.75	0.23	0.46	284.64	90.11
150	250	1.03	730.74	57.61			78.65	53.81	2.69	5.82	0.03	0.07	426.97	135.16

Having the *Sc* number of 3.71×10^{-5} and 1.25×10^{-5}, the *Sh* number were calculated at 9.08×10^{-4} to 78.65×10^{-4} and 6.21×10^{-4} to 53.81×10^{-4} for oleic acid and glycerol, respectively. *Sh* numbers obtained were then used for the estimation of K_{SL} values. From Table 4.9, K_{SL} numbers increased with increasing flow rates. Higher flow rate led to a rise in fluid velocity which resulted from the reduced resistance in the boundary layer (Matosevic *et al.*, 2011).

On the other hands, the variation of *Da* is dependent on the variation of K_{SL}, evaluated by the correlations among the *Re, Sc* and *Sh.* From Fig. 4.20, *Da* was reduced as the flow rate increases. It is interesting to note that the *Da* profile declined drastically starting from 2×10^{-5} L min^{-1} to 4×10^{-4} L min^{-1}, afterwards gradually decreased from 1×10^{-3} L min^{-1} to 1.5×10^{-3} L min^{-11}. Nonetheless, as shown in Table 4.9, increasing *U* led to the increased of K_{SL} and consequently, the value of *Da* decreased. *Da* was < 1 for all tested flow rates. The resulting *Da* values were dropped from 1.76×10^{-3} to 3.34×10^{-5} and 3.48×10^{-3} to 6.6×10^{-5} for oleic acid and glycerol, respectively. Thus, in the current study, the overall rate of the esterification of oleic acid with glycerol fall within the reaction-limited regime, indicating the diffusional rate is very fast compared to the surface reaction and the system is governed by the kinetics effect. If *Da* > 1, mass transfer rate is limiting; and the system is governed by diffusion control, and if *Da* equals to 1, the mass transfer and reaction rates are equivalent. It is desirable to keep *Da* <1 to eliminate diffusion limitations in a system (Shuler and Kargi, 2002).

Since *Da* < 1, it nevertheless seems worthwhile to further check the accuracy of the present results in term of external effectiveness factors (ηE). Employing Carberry correlation (1976), a linear relationship was observed between external effectiveness factors (ηE) and *Da* (data not shown). ηE values obtained which ranged between 0.997 to 0.999 at the flow rates of 2×10^{-5} L min^{-1} to 4×10^{-4} L min^{-1} and 2×10^{-5} L min^{-1} to 2×10^{-4} L min^{-1} for oleic acid and glycerol respectively. This confirmed that at these flow rates,

the external mass transfer effects were insignificant and can be eliminated (Table 4.11). At higher flow rates, the mass transfer and reaction rates are equal to 1.

Contrary to *Da* profile, *Pe* appears to increase linearly *U* and K_{SL} with the applied flow rate. The greater the *Pe* number, the greater the flow's influence over molecular diffusion. *Pe* was constantly < 1, which indicated that the mass transport is governed by diffusion over advection. Meanwhile if *Pe* > 1 the advection controls the mass transport over diffusion.

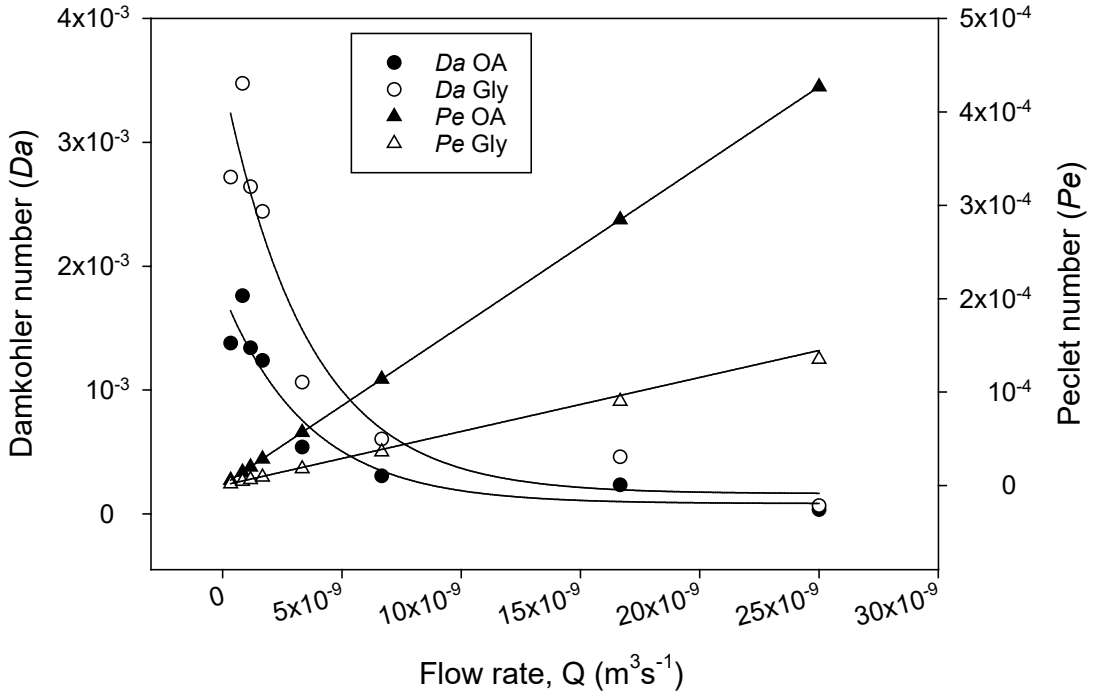

Figure. 4.20. Profiles of Damköhler and Péclet number as a function of flow rates.

Thiele modulus (ϕ) and the internal effectiveness factor (ηI) were employed to evaluate and validate the occurrence of internal mass transfer resistance. Thiele modulus should to be lower than 0.3 and the internal effectiveness factor should be equal or close to 1 to represents a system without internal limitations (Doran, 2012) Based on Table 4.11, the intra-particle diffusion is negligible, as indicated by the values of Thiele modulus and ηI achieved. Under selected process conditions, both substrates are

unrestricted by internal mass transfer systems, implying that the limiting factor is the reaction kinetics and the kinetic model generated from this experiment is valid (Section 4.3.5). These results also are in line with the published kinetic and mass transfer studies of lipase conducted in heptane (Todero *et al.*, 2015), hydrogen peroxide (Hosney *et al.*, 2020) and tetrahydrofuran (Jawale & Bhanage, 2021).

Table 4.11. Thiele modulus, external and internal effectiveness factors as a function of flow rates.

Flow rate, Q ($\times 10^{-5}$) (L min^{-1})	**Flow rate, Q ($\times 10^{-10}$) (m^3 s^{-1})**	**ϕ ($\times 10^{-7}$)**		**ηE**		**ηI**	
		OA	**Gly**	**OA**	**Gly**	**OA**	**Gly**
2	3.33	3.07	4.14	0.999	0.997	1.002	0.999
5	8.33	6.20	8.37	0.998	0.997	1.000	1.000
7	11.67	5.58	7.52	0.999	0.997	0.999	1.001
10	16.67	6.16	8.32	0.999	0.998	0.999	1.000
20	33.33	3.79	5.12	0.999	0.999	0.998	0.999
40	66.67	3.05	4.11	1.000	0.999	1.004	1.002
100	166.67	3.67	4.95	1.000	1.000	0.993	0.998
150	250	0.64	0.87	1.000	1.000	0.866	0.963

4.3.5 Kinetic parameters determination

Enzyme kinetic parameters are frequently determined by the Lilly–Hornby model that is established for packed bed reactor system that accounted for changes to hydrodynamic conditions in flow reactors. In this experiment, amount of immobilized lipase was fixed at 0.15 g and was loaded in the packed bed reactor. When working with continuous flow reaction system, flow rate playing a major role on enzyme kinetics. Therefore, the Michaelis–Menten constant, $K_{m,}$ were calculated using the experimental data achieved at different flow rates (2×10^{-5} L min^{-1} to 1.5×10^{-3} L min^{-1}) at various oleic acid concentrations (1.85 M to 2.08 M) with fixed concentration of glycerol (1.30 M). The actual concentration of oleic acid was taken at the inlet and outlet of the column. The data gathered from these set of experiments were then fitted to kinetic parameters in Eq. (3.23).

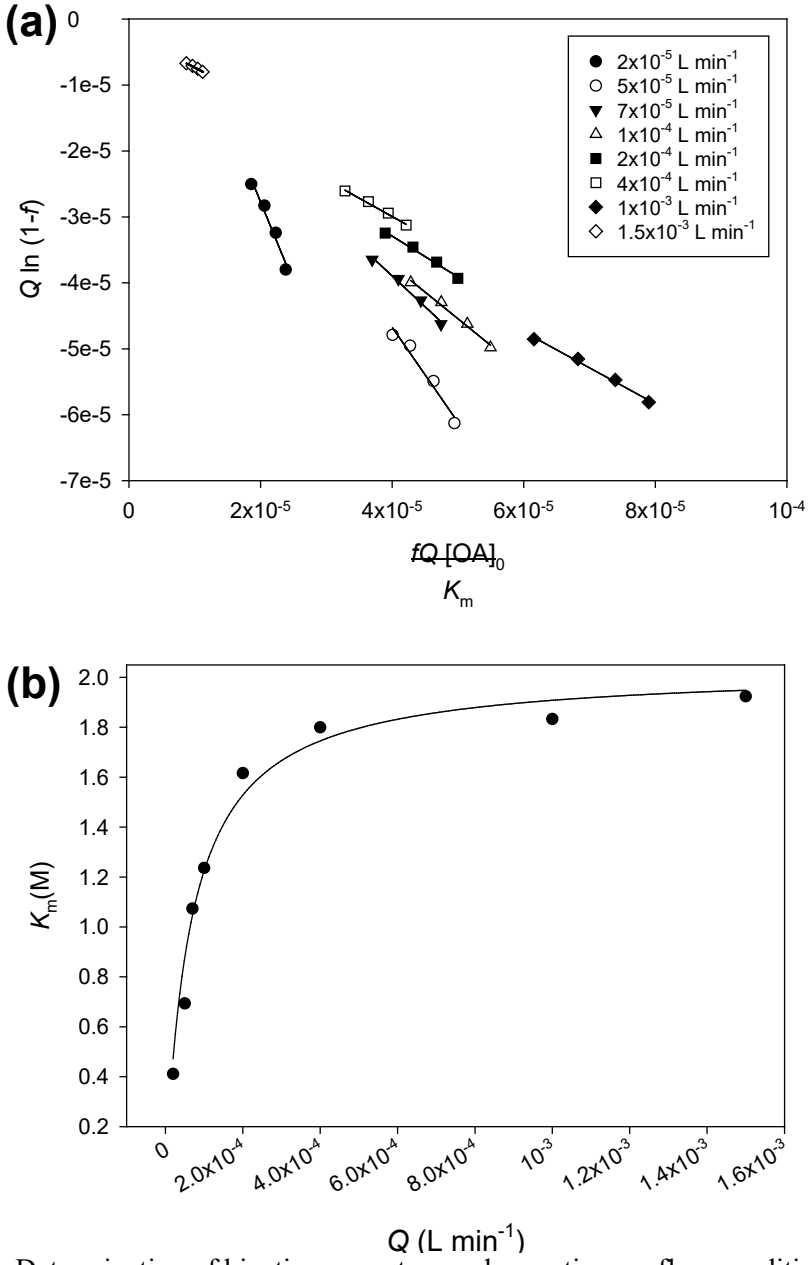

Figure 4.21. Determination of kinetic parameters under continuous flow conditions (a) plot of Q ln (1-*f*) versus $fQ[OA]_0/K_m$ (b) K_m values as a function of Q.

Fig. 4.21a shows the linear plots of Q ln(1-f) versus $fQ[OA]_0/K_m$, and K_m values were resulted from the slopes of these plots. From Table 4.12, the K_m values were in the range of 0.41 to 1.92 M. Moreover, it was observed that K_m values increased with increasing flow rates which in accordance with earlier findings (Seong *et al.*, 2003; Matsovenic *et al.,* 2011; Wang *et al.*, 2014; Liu *et al.,* 2019b). These results however, contrasts the observations of other reported kinetics by biocatalyst in packed bed reactor

(Halim *et al.*, 2013; Carvalho & Fernandes, 2015; Bhavsar and Yadav, 2018). These authors described and justified that the reason which led to a decrease affinity with the increase of flow rates was due to the occurrence of mass transfer resistances. At greater flow rates, the diffusion layer thins out until the mass transfer resistance phenomena becomes less noticeable. Therefore, earlier discussion supported and verified that the mass transfer effect observed in the present study was possibly not pronounced to influence the kinetic parameters of the enzyme reaction.

Meanwhile a rectangular hyperbolic curve was observed as the flow rate was plotted against K_m values (Fig. 4.21b). The increment of flow rate by the power of ten (10^n) which is from 10^{-5} to 10^{-3} caused a substantial variation pattern in the K_m values. At lower flow rates ranging from 2×10^{-5} L min^{-1} to 7×10^{-5} L min^{-1}, the K_m values started to incline sharply and then gradually increased when the flow rates were set at 1×10^{-4} L min^{-1} to 2×10^{-4} L min^{-1}. However, at higher flow rates (4×10^{-4} L min^{-1} to 1.5×10^{-3} L min^{-1}), K_m values obtained were almost comparable. At 2×10^{-5} L min^{-1}, the K_m was lowest, which indicated a stronger affinity and increased lipase-substrate formation efficiency. Therefore, lower flow rate ($<1\times10^{-4}$) is more preferable for the reaction under continuous flow. Given that the maximum velocity, $V_{max} = k_{cat} \times [ET]$, the reaction capacity, C_R values obtained from the intercept of the graph of all flow rates subsequently used to calculate $V_{max,}$ the reaction rate when lipase is saturated with substrate. The results show that there is no clear variation or pattern on the V_{max} of the immobilized lipase under continuous flow (Table 4.12).

Table 4.12. Kinetic parameters of oleic acid and glycerol esterification under continuous flow system.

Flow rate, Q ($\times 10^{-5}$) (L min^{-1})	**K_m (M)**	**V_{max} ($\times 10^{-3}$) (M h^{-1})**	**R^2**
2	0.41	1.92	0.9562
5	0.69	0.32	0.9794
7	1.07	2.51	0.9884
10	1.24	1.44	0.9897
20	1.62	3.02	0.9915
40	1.80	3.36	0.9921
100	1.83	4.28	0.9921
150	1.92	0.90	0.9924

4.3.6 Reusability and storage stability of *Candida antartica* lipase B (CALB 1) in the continuous flow reactor

To make the process even more sustainable and possible for practical long-term operation, esterification process was also performed by repeating the lipase enzyme. Acetone was selected as a washing solvent because it can dilute the remaining substrates and products on the surface of CALB 1 (Csajagi *et al.*, 2008). One of the advantages of packed back reactor is that, lipase can be simply unloaded from the column without any significant loss of weight as compared to the batch system (Bavaro *et al.*, 2020). At optimal conditions, it was found that CALB 1 presented an excellent recyclability and could be efficiently reused without any significant changes in conversion for 9 consecutive cycles, tested at two different flow rates, i.e. 2×10^{-5} L min^{-1} and 5×10^{-5} L min^{-1} (Fig.4.22a). Consistent values of GMO and GDO selectivities were also attained throughout the tested cycles. The obtained results were comparable with the reported literatures on the ability of CALB 1 to retain its catalytic activities during various esterification reactions, ranging from 7 to 20 cycles (Guo *et al.* 2007; Wang *et al.*, 2014,

Salvi *et al.*, 2017). Meanwhile studies on the storage stability of the reused CALB 1 revealed that the conversion was retained and stable for 5 days and gradually decreased after 8 days after being used for esterification reaction (Fig. 4.22b). At 11 days of operation, the stability of the lipase in the continuous packed bed millireactor decreased only 5 to 7%, indicating satisfying operational results and recyclability. Employment of enzyme in a continuous flow system displays several advantages over batch system, including easy and faster recovery, avoiding enzyme breakage and a lesser amount of enzyme leaching (Kundu *et al.*, 2011).

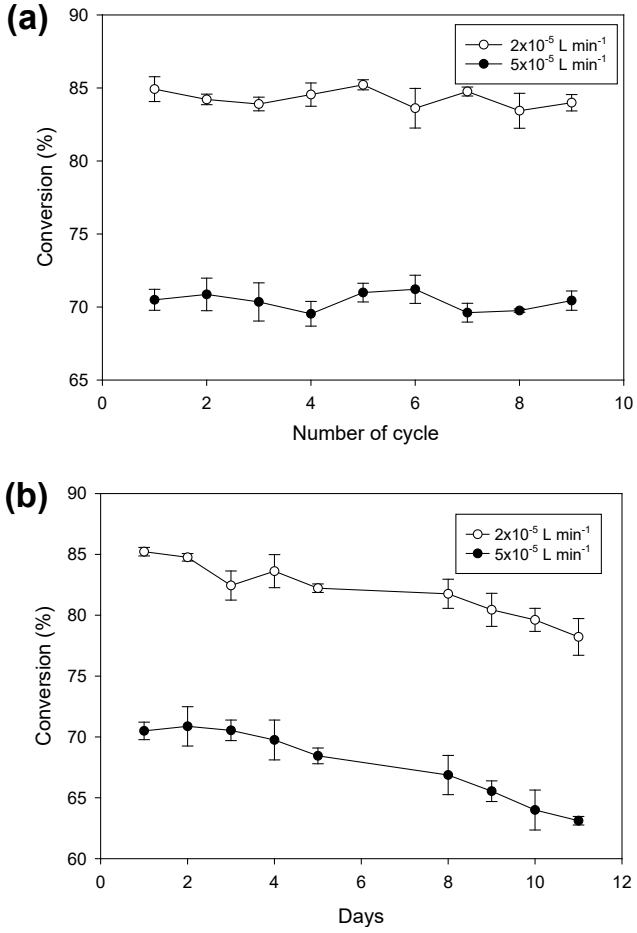

Figure 4.22. Conversion of oleic acid during esterification with glycerol. (a) Reusability of CALB 1 at Day 1 (b) Storage stability of CALB 1. Reaction conditions: 0.15 g of lipase enzyme, molar ratio of oleic acid:glycerol at 1.6:1; 1.1 g of 3 Å molecular sieves; temperature at 45°C.

4.3.7 Concluding remarks from the continuous flow reactor study

The feasibility of immobilised lipase-catalyzed synthesis of GDO in a continuous flow system was successfully established in this study, which took into account of external and internal mass transfer effects, as well as enzyme kinetics. Under the continuous flow reactor, oleic acid conversion and GDO selectivity of 85% and 74% were obtained under the best operating conditions: an enzyme loading of 0.15 g, a fixed temperature of 45ºC, a molar ratio of oleic acid:glycerol at 1.6:1, a flow rate of 2×10^{-5} L min^{-1} at a relatively short residence of 77 min. It was also observed that, GTO was not produced by lipase in a continuous flow millireactor and this would be advantageous during the recovery and separation of GDO. Under the experimental conditions applied, it is proved that the mass transfer resistance has no effect on the reaction rate. The kinetic analysis adapted from Lilly-Hornby model showed that the K_m values appeared to be flow rate dependent for all substrates. CALB 1 displays high operating stability as it can be used up to 9 successive cycles while retaining its original activity and relatively steady after 11 days. Thus, the developed process has provided an efficient and repeatable productive approach at the miniaturized scale which provides a solution to the conventional batch system. The best operating conditions, kinetic and mass transfer results acquired from this work can provide good insight for biochemical processing and allowing the procedure to be scaled up to the industrial scale.

CHAPTER 5 :

CONCLUSIONS

5.1 Conclusions

Different types of solvent systems were investigated in the esterification of glycerol with oleic acid in a batch system. It was observed that the enzymatic esterification process using blended acetone: *tert*-butanol is more favorable towards the production of GDO at 45ºC. It showed that the findings contribute to the new solvent system for GDO production, utilizing green and low temperature method.

The optimization of lipase-catalyzed synthesis of GDO has been established in the present study using batch and continuous flow reactors. It was found that the conversion of oleic acid and GDO selectivity were achieved at 73-85% and 74-77%, respectively. The optimum reaction time for esterification reaction using both batch and continuous flow reactors were established at 2 h and 1.3 h, respectively. Hence, the extended reaction time which is common in the production DAG using biocatalyst, can be circumvented.

This work also discovered that the kinetic parameter values obtained from continuous flow system were significantly difference from those determined in the conventional batch system. Under the experimental conditions applied, it is proven that the mass transfer resistance has no effect on the reaction rate in both reactors. This is an ideal feature for developing new bio-catalyzed technologies for industrial purpose.

It was found that the present study successfully established a novel process for DAG production using immobilized lipase enzyme in a continuous flow system by utilising the optimal reaction parameters. It addresses the research gap identified in Chapter 2. As compared to a batch system, the absence of GTO during the synthesis of GDO in a continuous flow system posed a significant advantage. Multiplicity of acylglycerol compounds generated during the esterification reaction will result in remarkable

complexity of recovery, separation and purification of GDO. The use of continuous flow system for GDO synthesis would help to simplify the post-separation procedure since fewer products produced from the reaction.

5.2 Study Limitations

The high viscosity and low solubility of glycerol in the reaction media was the major challenge in the non-aqueous biosynthesis of GDO. The solvent system used in this study only utilized two solvents namely acetone and *tert*-butanol for improving oleic acid conversion and GDO production. Green organic solvents capable of solubilizing adequate amounts of both polar glycerol and non-polar fatty acid substrates are rather limited.

There is a necessity to eliminate water as a by-product of the esterification. Since the size of the column used in the continuous flow system is relatively small, the reaction is limited by the amount of molecular sieve that was placed together with the lipase inside the column. It was found that the GDO content dropped when the water content in the media was larger than 5%.

The reaction time required for the optimal oleic acid conversion and GDO production from this study results are relatively shorter as compared to other common production of DAG using biocatalyst. However, in comparison to other chemical catalysts (Sakthivel *et al.*, 2007; Padzur *et al.*, 2015), the reaction using lipase enzyme takes a longer reaction time to achieve equilibrium.

5.3 Future Recommendations

The performance of the current systems could be enhanced by reducing the water content produced during the reaction. Therefore, the studies on the efficient methods to absorb water by-product were thought to be beneficial to accelerate chemical

transformation and shift the process toward DAG synthesis. Different types of dessicants or different size of molecular sieve can be considered for future studies.

Since the current work utilized the commercial lipases, it was proposed that the studies on the effective immobilization carriers for lipase are essential for future works. It should be focused on developing low-cost carriers and enhancing the lipase-carrier interaction without reducing the lipase activity. It is hypothesized that the higher amount of DAG could be obtained if the performance of lipase could be improved. Immobilization of lipase enzymes can be accomplished by using a variety of carriers, including agro-industrial wastes, nanoparticles, and metal organic frameworks. An ideal and appropriate lipase carrier will allow the esterification process to be performed under complex operating conditions due to better enzymological properties. The selection of carriers used as supports should take into consideration on the factors such sustainability, stability, reusability and safety.

It is essential to combine diverse knowledge sources and undertand the market scenario for enzymatic industrialisation. To increase the economic viability of lipase catalysed DAG synthesis, a global process integration and optimization with economic evaluation should be developed. It should incorporate all factors on upstream and downstream processing, including immobilisation of lipase, the development of bioreactors, process optimization, simulation, and techno-economic analysis.

5.4 Significance of the findings and future prospects

In the pursuit of Sustainable Development Goals, this research provides the possibility of transforming glycerol into value-added product and thus, minimizing the environmental burden to manage this compound. Currently, the vast surplus of glycerol has been produced as a by-product during the synthesis of biodiesel. It is vital to discover sustainable alternatives to volarize the glycerol so that the production of biodiesel is not

hindered by the challenges associated with utilising and discarding glycerol. The economic viability of the biodiesel sector will improve if it conforms to standards for the sustainability of the supply chain. Therefore, this work assists in opening the door to solutions for biodiesel industries by adopting this methodology in future. A fusion of biofuel technologies with innovative glycerol waste transformation could boost society's socioeconomic and environmental conditions in a positive and sustainable way. It also will help to overcome the key obstacles to the successful commercialization of biodiesel by reducing the production cost.

The findings show that lipase enzyme exhibits high catalyst productivities, recyclability and stability. It was discovered that CALB 1 had outstanding recycling abilities and could be effectively recycled for 9 cycles without experiencing any substantial conversion changes. By utilising the same enzymes in many batches, enzyme recycling increases the catalytic productivity of the enzymes as well as lowers the overall production cost. The industrial process would benefit enzyme recycling as it will bringing down the price of production to levels that can be sold. The enzymatic recycling using continuous flow system paves the way to use this technology not only to GDO synthesis, but also to other emulsifiers. It is anticipated that enzymatic recycling technology will have long-term socioeconomic benefits.

This is also a clear indication that lipase offers an effective and efficient conversion which can serve as an alternative to chemical catalyst. The substitution of chemical catalyst to biocatalyst for DAG synthesis is important from the safety point of view as well as environmental perspectives. The use of hazardous chemicals and catalysts can be eliminated and subsequently it reduces the risk of environmental pollution. The enzymes themselves are naturally harmless and being utilised in many food processing industry. With exceptional capacity to catalyse processes in both aqueous and nonaqueous settings, lipases work at milder milder temperature and pressure. This can significantly increase

operational efficiency and lowering energy consumption. Therefore, this study developed a cleaner and safer process that significantly widen the spectrum of enzyme application in industrial biotechnology, which is expected to rise in the future.

This study was also attempted to provide information on the feasibility of adopting the green reactor technology. It explores the possible use of continuous flow millireactors technology that potentially applicable to a variety of enzyme catalyzed reactions involving immiscible substrates. The optimization, kinetic and mass transfer results acquired from lipase-catalyzed synthesis of DAG can provide good insight for biochemical processing and facilitate the creation of better process intensification especially for industrial application. Therefore, the findings from this study would be beneficial to various fields such as pharmaceutical, food, fine and oleochemicals industries.

From an academic standpoint of view, this study provides a better understanding of the implication of millireactor in DAG production and the behavior of lipase in a batch reactor and under continuous flow system. It contributes to the body of knowledge on the kinetics of enzymatic reaction involving multiple substrates. The findings revealed that the synthesis of GDO shown to follow Michaelis–Menten kinetics on batch scale and milliscale and diffusion limitation seems to have no effect on the reaction.

REFERENCES

Abd Razak, N. N., Gew, L. T., Pérès, Y., Cognet, P., & Aroua, M. K. (2021). Statistical optimization and kinetic modeling of lipase-catalyzed synthesis of diacylglycerol in the mixed solvent system of acetone/*tert*-butanol. *Industrial & Engineering Chemistry Research*, *60*(39), 14026-14037.

Abd Razak, N. N., Pérès, Y., Gew, L. T., Cognet, P., & Aroua, M. K. (2020). Effect of reaction medium mixture on the lipase catalyzed synthesis of diacylglycerol. *Industrial & Engineering Chemistry Research*, *59*(21), 9869-9881.

Abd Razak, N. N., Cognet, P., Pérès, Y., Gew, L. T., & Aroua, M. K. (2022). Kinetics and hydrodynamics of *Candida antartica* lipase-catalyzed synthesis of glycerol dioleate (GDO) in a continuous flow packed-bed millireactor. *Journal of Cleaner Production*, 373, 133816.

Ahmad, R., & Sardar, M. (2015). Enzyme immobilization: an overview on nanoparticles as immobilization matrix. *Biochemistry and Analytical Biochemistry*, *4*(2), 1.

Al-Mahasneh, M., Rababah, T., & Alu'Datt, M. (2017). Effect of palm oil (PO) and distilled mono-glycerid (DMG) on oil separation and rheological properties of sesame paste. *Journal of Food Processing and Preservation*, *41*(3), e12896.

Alotaibi, M., Manayil, J. C., Greenway, G. M., Haswell, S. J., Kelly, S. M., Lee, A. F., ... & Kyriakou, G. (2018). Lipase immobilised on silica monoliths as continuous-flow microreactors for triglyceride transesterification. *Reaction Chemistry & Engineering, 3(*1), 68-74.

Al-Zuhair, S., Hasan, M., & Ramachandran, K. B. (2003). Kinetics of the enzymatic hydrolysis of palm oil by lipase. *Process Biochemistry*, *38*(8), 1155-1163.

Amini, Z., Ilham, Z., Ong, H. C., Mazaheri, H., & Chen, W. H. (2017). State of the art and prospective of lipase-catalyzed transesterification reaction for biodiesel production. *Energy Conversion and Management*, *141*, 339-353.

Anand, A., Gnanasekaran, P., Allgeier, A. M., & Weatherley, L. R. (2020). Study and deployment of methacrylate-based polymer resins for immobilized lipase catalyzed triglyceride hydrolysis. *Food and Bioproducts Processing, 123*, 164-176.

An, S., Sun, Y., Song, D., Zhang, Q., Guo, Y., & Shang, Q. (2016). Arenesulfonic acid-functionalized alkyl-bridged organosilica hollow nanospheres for selective esterification of glycerol with lauric acid to glycerol mono-and dilaurate. *Journal of Catalysis*, *342*, 40-54.

Anikisetty, M., Krishna, A. G., Panneerselvam, V., & Kamatham, A. N. (2018). Diacylglycerol (DAG) rich rice bran and sunflower oils modulate lipid profile and cardiovascular risk factors in Wistar rats. *Journal of Functional Foods*, *40*, 117-127.

Anitha, M., Kamarudin, S. K., & Kofli, N. T. (2016). The potential of glycerol as a value-added commodity. *Chemical Engineering Journal*, *295*, 119-130.

Anyaehie, U. (2009). Medicinal properties of fractionated acetone/water neem (Azadirachta indica) leaf extract from Nigeria: a review. *Nigerian journal of physiological sciences*, *24*(2).

Arpi, N., Lubis, Y. M., Supardan, M. D., & Mustapha, W. A. W. (2016). Diacylglycerol-enriched oil production using chemical glycerolysis. *European Journal of Lipid Science and Technology*, *118*(12), 1880-1890.

Arranz-Martínez, P., Corzo-Martínez, M., Vázquez, L., Reglero, G., & Torres, C. F. (2018). Lipase catalyzed glycerolysis of ratfish liver oil at stirred tank basket reactor: A kinetic approach. *Process Biochemistry*, *64*, 38-45.

Awadallak, J. A., Voll, F., Ribas, M. C., da Silva, C., Cardozo Filho, L., & da Silva, E. A. (2013). Enzymatic catalyzed palm oil hydrolysis under ultrasound irradiation: diacylglycerol synthesis. *Ultrasonics Sonochemistry*, *20*(4), 1002-1007.

Ayoub, M., & Abdullah, A. Z. (2012). Critical review on the current scenario and significance of crude glycerol resulting from biodiesel industry towards more sustainable renewable energy industry. *Renewable and Sustainable Energy Reviews*, *16*(5), 2671-2686.

Bakir, N., Ilyasoglu, H., Yucetepe, A., Kasapoglu, K. N., Demircan, E., & Ozcelik, B. (2018). Production of structured lipids from hazelnut oil with conjugated linoleic acid by lipase-catalyzed esterification: Optimization by response surface methodology. *Acta Alimentaria*, *47*(1), 1-9.

Barnes, H. A., Hutton, J. F., & Walters, K. (1989). *An Introduction to Rheology* (Vol. 3). Elsevier, Amsterdam.

Bassan, N., Rodrigues, R. H., Monti, R., Tecelão, C., Ferreira-Dias, S., & Paula, A. V. (2019). Enzymatic modification of grapeseed (Vitis vinifera L.) oil aiming to obtain dietary triacylglycerols in a batch reactor. *LWT*, *99*, 600-606.

Basso, R. C., Ribeiro, A. P. B., Masuchi, M. H., Gioielli, L. A., Gonçalves, L. A. G., dos Santos, A. O., ... & Grimaldi, R. (2010). Tripalmitin and monoacylglycerols as modifiers in the crystallisation of palm oil. *Food Chemistry*, *122*(4), 1185-1192.

Bavaro, T., Benucci, I., Pedrali, A., Marrubini, G., Esti, M., Terreni, M., ... & Ubiali, D. (2020). Lipase-mediated hydrolysis of hempseed oil in a packed-bed reactor and in-line purification of PUFA as mono-and diacylglycerols. *Food and Bioproducts Processing*, *123*, 345-353.

Bavaro, T., Pinto, A., Dall'Oglio, F., Hernáiz, M. J., Morelli, C. F., Zambelli, P., ... & Terreni, M. (2018). Flow-based biocatalysis: Application to peracetylated arabinofuranosyl-1, 5-arabinofuranose synthesis. *Process Biochemistry*, *72*, 112-118.

Bhatnagar, B. S., Sonje, J., Shalaev, E., Martin, S. W., Teagarden, D. L., & Suryanarayanan, R. (2020). A refined phase diagram of the *tert*-butanol–water system and implications on lyophilization process optimization of pharmaceuticals. *Physical Chemistry Chemical Physics*, *22*(3), 1583-1590.

Bhavsar, K. V., & Yadav, G. D. (2018). *n*-Butyl levulinate synthesis using lipase catalysis: comparison of batch reactor versus continuous flow packed bed tubular microreactor. *Journal of Flow Chemistry*, *8*(2), 97-105.

Britton, J., Majumdar, S., & Weiss, G. A. (2018). Continuous flow biocatalysis. *Chemical Society Reviews*, *47*(15), 5891-5918.

Buňková, L., Krejčí, J., Janiš, R., Kašpárková, V., Vltavská, P., Kulendová, L. and Buň ka, F. (2010). Influence of monoacylglycerols on growth inhibition of micromycetes in vitro and on bread. *European Journal of Lipid Science and Technology*, *112*,173–179.

Bushita, H., Liu, S., Ohta, T., Ito, Y., Saito, K., Nukada, Y., ... & Morita, O. (2018). Effects of dietary alpha-linolenic acid-enriched diacylglycerol oil on embryo/fetal development in rats. *Regulatory Toxicology and Pharmacology*, *98*, 108-114.

Cai, C., Gao, Y., Liu, Y., Zhong, N., & Liu, N. (2016). Immobilization of *Candida antarctica* lipase B onto SBA-15 and their application in glycerolysis for diacylglycerols synthesis. *Food Chemistry*, *212*, 205-212.

Carberry, J. J. (2001). *Chemical and catalytic reaction engineering*. Dover Publications, Mineola, N.Y.

Carrero, A., Calles, J. A., García-Moreno, L., & Vizcaíno, A. J. (2017). Production of renewable hydrogen from glycerol steam reforming over bimetallic Ni-(Cu, Co, Cr) catalysts supported on SBA-15 silica. *Catalysts*, *7*(2), 55.

Carvalho, F., & Fernandes, P. (2015). Packed bed enzyme microreactor: Application in sucrose hydrolysis as proof-of-concept. *Biochemical Engineering Journal*, *104*, 74-81.

Čech, J., Schrott, W., Slouka, Z., Přibyl, M., Brož, M., Kuncová, G., & Šnita, D. (2012). Enzyme hydrolysis of soybean oil in a slug flow microsystem. *Biochemical Engineering Journal*, *67*, 194-202.

Chen, J., Lee, W. J., Qiu, C., Wang, S., Li, G., & Wang, Y. (2020). Immobilized lipase in the synthesis of high purity medium chain diacylglycerols using a bubble column reactor: characterization and application. *Frontiers in bioengineering and biotechnology*, *8*, 466.

Cheong, L. Z., Zhang, H., Xu, Y., & Xu, X. (2009). Physical characterization of lard partial acylglycerols and their effects on melting and crystallization properties of blends with rapeseed oil. *Journal of Agricultural and Food Chemistry*, *57*(11), 5020-5027.

Chew, P. L., Annuar, M. S. M., Show, P. L., & Ling, T. C. (2015). Extractive bioconversion of poly-ϵ-caprolactone by *Burkholderia cepacia* lipase in an aqueous two-phase system. *Biochemical Engineering Journal*, *101*, 9-17.

Choi, J. H., Kim, B. H., Hong, S. I., Kim, Y., & Kim, I. H. (2012). Synthesis of structured lipids containing pinolenic acid at the sn-2 position via lipase-catalyzed acidolysis. *Journal of the American Oil Chemists' Society*, *89*(8), 1449-1454.

Choong, T. S. Y., Yeoh, C. M., Phuah, E. T., Siew, W. L., Lee, Y. Y., Tang, T. K., & Chuah Abdullah, L. (2018). Kinetic study of lipase-catalyzed glycerolysis of palm olein using Lipozyme TLIM in solvent-free system. *Plos One*, *13*(2), e0192375.

Chowdhury, A. & Mitra, D. (2015). A kinetic study on the Novozyme 435-catalyzed esterification of free fatty acids with octanol to produce octyl esters. *Biotechnology Progress, 31*, 1494-1499.

Chua, L. S., Alitabarimansor, M., Lee, C. T., & Mat, R. (2012). Hydrolysis of virgin coconut oil using immobilized lipase in a batch reactor. *Enzyme Research*, *2012*.

Ciriminna, R., Pina, C. D., Rossi, M., & Pagliaro, M. (2014). Understanding the glycerol market. *European Journal of Lipid Science and Technology*, *116*(10), 1432-1439.

Compton, D. L., Laszlo, J. A., & Berhow, M. A. (2006). Identification and quantification of feruloylated mono-, di-, and triacylglycerols from vegetable oils. *Journal of the American Oil Chemists' Society*, *83*(9), 753-758.

Cook, P. F., & Cleland, W. W. (2007). *Enzyme kinetics and mechanism*. Garland Science, New York.

Cozentino, I. D. S. C., Rodrigues, M. D. F., Mazziero, V. T., Cerri, M. O., Cavallini, D. C. U., & de Paula, A. V. (2022). Enzymatic synthesis of structured lipids from grape seed (*Vitis vinifera* L.) oil in associated packed bed reactors. *Biotechnology and Applied Biochemistry*, *69*(1), 101-109.

Csajagi, C., Szatzker, G., Tőke, E. R., Uerge, L., Darvas, F., & Poppe, L. (2008). Enantiomer selective acylation of racemic alcohols by lipases in continuous-flow bioreactors. *Tetrahedron: Asymmetry*, *19*(2), 237-246.

da Silva, J. A., Cardozo, N. S., & Petzhold, C. L. (2018). Enzymatic synthesis of andiroba oil based polyol for the production of flexible polyurethane foams. *Industrial Crops and Products*, *113*, 55-63.

Damstrup, M. L., Jensen, T., Sparsø, F. V., Kiil, S. Z., Jensen, A. D., & Xu, X. (2006). Production of heat-sensitive monoacylglycerols by enzymatic glycerolysis in *tert*-pentanol: process optimization by response surface methodology. *Journal of the American Oil Chemists' Society*, *83*(1), 27-33.

Das, K., & Ghosh, M. (2019). Comparative qualitative assessment of DAG production from medium chain fatty acids mediated by enzymatic and chemical catalysts under individually optimized conditions. *Biocatalysis and Agricultural Biotechnology*, *22*, 101422.

De Santis, P., Meyer, L. E., & Kara, S. (2020). The rise of continuous flow biocatalysis–fundamentals, very recent developments and future perspectives. *Reaction Chemistry & Engineering*, *5*(12), 2155-2184.

Denčić, I., de Vaan, S., Noël, T., Meuldijk, J., de Croon, M., & Hessel, V. (2013). Lipase-based biocatalytic flow process in a packed-bed microreactor. *Industrial & Engineering Chemistry Research*, *52*(32), 10951-10960.

Derawi, D., Azman, N.A.Z., & Jumadi, M.F. (2017). Preliminary study on production of monoacylglycerol and diacylglycerol of virgin coconut oil via enzymatic

glycerolysis using lipase *Candida antarctica* (Novozyme 435). *Malaysian Journal of Analytical Sciences*, *21*(1), 37-45.

Diao, X., Guan, H., Kong, B., & Zhao, X. (2017). Preparation of diacylglycerol from lard by enzymatic glycerolysis and its compositional characteristics. *Korean Journal for Food Science of Animal Resources*, *37*(6), 813.

Díaz-Álvarez, A. E., Francos, J., Lastra-Barreira, B., Crochet, P., & Cadierno, V. (2011). Glycerol and derived solvents: new sustainable reaction media for organic synthesis. *Chemical Communications*, *47*(22), 6208-6227.

Dixon M., Webb E.C (1979). *Enzymes*, 3rd Edition. Longman Group Ltd: London.

do Nascimento, M. A., Gotardo, L. E., Leão, R. A., de Castro, A. M., de Souza, R. O., & Itabaiana Jr, I. (2019). Enhanced productivity in glycerol carbonate synthesis under continuous flow conditions: combination of immobilized lipases from porcine pancreas and *Candida antarctica* (CALB) on Epoxy Resins. *ACS Omega*, *4*(1), 860-869.

Doležálková, I., Máčalík, Z., Butkovičová, A., Janiš, R., & Buňková, L. (2012). Monoacylglycerols as fruit juices preservatives. *Czech Journal of Food Sciences*.

Dom, Z. M., Chuan, L. T., & Yusoff, R. (2014). Production of mediumchain acylglycerols by lipase esterification in packed bed reactor: process optimization by response surface methodology. *Journal of Engineering Science and Technology (JESTEC)*, *9*(3), 384-397.

Doran P.M. (2012). *Bioprocess Engineering Principles*. Elsevier, New York.

dos Santos, P., Meireles, M. A. A., & Martinez, J. (2017). Production of isoamyl acetate by enzymatic reactions in batch and packed bed reactors with supercritical CO2. *The Journal of Supercritical Fluids*, *127*, 71-80.

Du, L. H., & Luo, X. P. (2012). Lipase-catalyzed regioselective acylation of sugar in microreactors. *RSC Advances*, *2*(7), 2663-2665.

Duan, Z. Q., Du, W., & Liu, D. H. (2010). Novozym 435-catalyzed 1, 3-diacylglycerol preparation via esterification in *t*-butanol system. *Process Biochemistry*, *45*(12), 1923-1927.

Efthymiou, M. N., Pateraki, C., Papapostolou, H., Lin, C. S. K., & Koutinas, A. (2021). Restructuring the sunflower-based biodiesel industry into a circular bio-economy business model converting sunflower meal and crude glycerol into succinic acid and value-added co-products. *Biomass and Bioenergy*, *155*, 106265.

Farfán, M., M. J. Villalón, M. E. Ortíz, S. Nieto, & P. Bouchon. (2013). The effect of interesterification on the bioavailability of fatty acids in structured lipids. *Food Chemistry, 139*(1–4), 571–7

Feltes, M. M. C., de Oliveira, D., Block, J. M., & Ninow, J. L. (2013). The production, benefits, and applications of monoacylglycerols and diacylglycerols of nutritional interest. *Food and Bioprocess Technology*, *6*(1), 17-35.

Feltes, M. M. C., Villeneuve, P., Baréa, B., Barouh, N., De Oliveira, J. V., De Oliveira, D., & Ninow, J. L. (2012). Enzymatic production of monoacylglycerols (MAG) and

diacylglycerols (DAG) from fish oil in a solvent-free system. *Journal of the American Oil Chemists' Society*, *89*(6), 1057-1065.

Ferreira, S. C., Bruns, R. E., Ferreira, H. S., Matos, G. D., David, J. M., Brandão, G. C., ... & Dos Santos, W. N. L. (2007). Box-Behnken design: an alternative for the optimization of analytical methods. *Analytica Chimica Acta*, *597*(2), 179-186.

Fiametti, K. G., Ustra, M. K., de Oliveira, D., Corazza, M. L., Furigo Jr, A., & Oliveira, J. V. (2012). Kinetics of ultrasound-assisted lipase-catalyzed glycerolysis of olive oil in solvent-free system. *Ultrasonics Sonochemistry*, *19*(3), 440-451.

Fogler, H. S. (2016). *Essentials of Chemical Reaction Engineering*, *fifth ed.* Prentice Hall, University of Michigan.

Freitas, L., Dors, G., Carneiro, B. C., de Oliveira, P. C., & De Castro, H. F. (2013). Strategies to inhibit the lipid oxidation in the enzymatic synthesis of monoglycerides by glycerolysis of Babassu oil. *Acta Scientiarum. Technology*, *35*(3), 491-497.

Friedman, H. I., & Nylund, B. (1980). Intestinal fat digestion, absorption, and transport. A review. *American Journal of Clinical Nutrition (USA)*.

Fu, B., & Vasudevan, P. T. (2010). Effect of solvent− co-solvent mixtures on lipase-catalyzed transesterification of canola oil. *Energy & Fuels*, *24*(9), 4646-4651.

Garlapati, V. K., & Banerjee, R. (2013). Solvent-free synthesis of flavour esters through immobilized lipase mediated transesterification. *Enzyme Research*, *2013*.

Gholami, Z., Abdullah, A. Z., & Lee, K. T. (2014). Dealing with the surplus of glycerol production from biodiesel industry through catalytic upgrading to polyglycerols and other value-added products. *Renewable and Sustainable Energy Reviews*, *39*, 327-341.

Ghotli, R. A., Aziz, A. R. A., Atadashi, I. M., Hasan, D. B., San Kong, P., & Aroua, M. K. (2015). Selected physical properties of binary mixtures of crude glycerol and methanol at various temperatures. *Journal of Industrial and Engineering Chemistry*, *21*, 1039-1043.

Gofferjé, G., Stäbler, A., Herfellner, T., Schweiggert-Weisz, U., & Flöter, E. (2014). Kinetics of enzymatic esterification of glycerol and free fatty acids in crude Jatropha oil by immobilized lipase from Rhizomucor miehei. *Journal of Molecular Catalysis B: Enzymatic*, *107*, 1-7.

Gonzalez-Garay, A., Gonzalez-Miquel, M., & Guillen-Gosalbez, G. (2017). High-value propylene glycol from low-value biodiesel glycerol: a techno-economic and environmental assessment under uncertainty. *ACS Sustainable Chemistry & Engineering*, *5*(7), 5723-5732.

Gourdon, C., Elgue, S., & Prat, L. (2015). What are the needs for Process Intensification? *Oil & Gas Science and Technology–Revue d'IFP Energies nouvelles*, *70*(3), 463-473.

Gu, S., Feng, F., Li, Y., Wei, W., & Lu, R. (2016). Aspergillus oryzae lipase-catalyzed synthesis of dioleoyl; palmitoyl-rich triacylglycerols in two reactors. *Journal of the American Oil Chemists' Society*, *93*(10), 1347-1354.

Guajardo, N., Schrebler, R. A., & de María, P. D. (2019). From batch to fed-batch and to continuous packed-bed reactors: Lipase-catalyzed esterifications in low viscous deep-eutectic-solvents with buffer as cosolvent. *Bioresource technology*, *273*, 320-325.

Guebara, S. A. B., Ract, J. N. R., & Vitolo, M. (2018). Conversion of caprylic acid into mono-, di-and triglycerides using immobilized lipase. *Arabian Journal for Science and Engineering*, *43*(7), 3631-3637.

Guo, Z., & Sun, Y. (2007). Solvent-free production of 1, 3-diglyceride of CLA: strategy consideration and protocol design. *Food Chemistry*, *100*(3), 1076-1084.

Halim, A. A., Szita, N., & Baganz, F. (2013). Characterization and multi-step transketolase-ω-transaminase bioconversions in an immobilized enzyme microreactor (IEMR) with packed tube. *Journal of Biotechnology*, *168*(4), 567-575.

Hamerski, F., & Corazza, M. L. (2014). LDH-catalyzed esterification of lauric acid with glycerol in solvent-free system. *Applied Catalysis A: General*, *475*, 242-248.

Haq, M., Pendleton, P., & Chun, B. S. (2020). Utilization of Atlantic salmon by-product oil for omega-3 fatty acids rich 2-monoacylglycerol production: optimization of enzymatic reaction parameters. *Waste and Biomass Valorization*, *11*(1), 153-163.

Hares Júnior, S. J., Ract, J. N. R., Gioielli, L. A., & Vitolo, M. (2018). Conversion of triolein into mono-and diacylglycerols by immobilized lipase. *Arabian Journal for Science and Engineering*, *43*(5), 2247-2255.

Hasan, F., Shah, A. A., & Hameed, A. (2006). Industrial applications of microbial lipases. *Enzyme and Microbial Technology*, *39*(2), 235-251.

Hauerlandová, I., Lorencová, E., Buňka, F., Navrátil, J., Janečková, K., & Buňková, L. (2014). The influence of fat and monoacylglycerols on growth of spore-forming bacteria in processed cheese. *International Journal of Food Microbiology*, *182*, 37-43.

Helen, L. R., Jayesh, K., & Latha, M. S. (2017). Safety assessment of aqueous acetone extract of *Clerodendrum infortunatum L.* in Wistar rats. *Comparative Clinical Pathology*, *26*(2), 369-375.

Honda, H., Fujii, K., Yamaguchi, T., Ikeda, N., Nishiyama, N., & Kasamatsu, T. (2012). Glycidol exposure evaluation of humans who have ingested diacylglycerol oil containing glycidol fatty acid esters using hemoglobin adducts. *Food and Chemical Toxicology*, *50*(11), 4163-4168.

Honda, H., Kawamoto, T., Doi, Y., Matsumura, S., Ito, Y., Imai, N., ... & Morita, O. (2017). Alpha-linolenic acid-enriched diacylglycerol oil does not promote tumor development in tongue and gastrointestinal tract tissues in a medium-term multi-organ carcinogenesis bioassay using male F344 rat. *Food and Chemical Toxicology*, *106*, 185-192.

Hosney, H., Al-Sakkari, E. G., & Mustafa, A. (2020). Kinetics and Gibbs function studies on lipase-catalyzed production of non-phthalate plasticizer. *Journal of Oleo Science*, *69*(7), 727-735.

Hu, D. J., Chen, J. M., & Xia, Y. M. (2013). A comparative study on production of middle chain diacylglycerol through enzymatic esterification and glycerolysis. *Journal of Industrial and Engineering Chemistry*, *19*(5), 1457-1463.

Hyldgaard, M., Sutherland, D. S., Sundh, M., Mygind, T., & Meyer, R. L. (2012). Antimicrobial mechanism of monocaprylate. *Applied and Environmental Microbiology*, *78*(8), 2957-2965.

Ilham, Z., & Saka, S. (2016). Esterification of glycerol from biodiesel production to glycerol carbonate in non-catalytic supercritical dimethyl carbonate. *SpringerPlus*, *5*(1), 1-6.

Ismail, A. R., & Baek, K. H. (2020). Lipase immobilization with support materials, preparation techniques, and applications: Present and future aspects. *International Journal of Biological Macromolecules*, *163*, 1624-1639.

James, P. T. (2004). Obesity: the worldwide epidemic. *Clinics in Dermatology*, *22*(4), 276-280.

Jawale, P. V., & Bhanage, B. M. (2021). Kinetic and docking study of synthesis of glyceryl monostearate by immobilized lipase in non-aqueous media. *Biocatalysis and Biotransformation*, 1-10.

Jenab, E., Temelli, F., & Curtis, J. M. (2013). Lipase-catalysed interesterification between canola oil and fully hydrogenated canola oil in contact with supercritical carbon dioxide. *Food Chemistry*, *141*(3), 2220-2228.

Junior, I. I., Flores, M. C., Sutili, F. K., Leite, S. G., e Miranda, L. S. D. M., Leal, I. C., & de Souza, R. O. (2012). Fatty acids residue from palm oil refining process as feedstock for lipase catalyzed monoacylglicerol production under batch and continuous flow conditions. *Journal of Molecular Catalysis B: Enzymatic*, *77*, 53-58.

Kabbashi, N. A., Mohammed, N. I., Alam, M. Z., & Mirghani, M. E. S. (2015). Hydrolysis of *Jatropha curcas* oil for biodiesel synthesis using immobilized Candida cylindracea lipase. *Journal of Molecular Catalysis B: Enzymatic*, *116*, 95-100.

Kahveci, D., Guo, Z., Özçelik, B., & Xu, X. (2010). Optimisation of enzymatic synthesis of diacylglycerols in binary medium systems containing ionic liquids. *Food Chemistry*, *119*(3), 880-885.

Kang, I., Bang, H. J., Kim, I. H., Choi, H. D., & Kim, B. H. (2015). Synthesis of trans-10, cis-12 conjugated linoleic acid-enriched triacylglycerols via two-step lipase-catalyzed esterification. *LWT-Food Science and Technology*, *62*(1), 249-256. (INGU)

Kecskemeti, A., & Gaspar, A. (2018). Particle-based immobilized enzymatic reactors in microfluidic chips. *Talanta*, *180*, 211-228.

Kim, B. H., & Akoh, C. C. (2015). Recent research trends on the enzymatic synthesis of structured lipids. *Journal of Food Science*, *80*(8), C1713-C1724.

Kim, J., Chung, M. Y., Choi, H. D., Choi, I. W., & Kim, B. H. (2018). Enzymatic synthesis of structured monogalactosyldiacylglycerols enriched in pinolenic acid. *Journal of Agricultural and Food Chemistry*, *66*(30), 8079-8085.

Kong, P. S., Cognet, P., Pérès, Y., Esvan, J., Daud, W. M. A. W., & Aroua, M. K. (2018). Development of a novel hydrophobic ZrO_2–SiO_2 based acid catalyst for catalytic esterification of glycerol with oleic acid. *Industrial & Engineering Chemistry Research*, 57(29), 9386-9399.

Kopelman, P. G. (2000). Obesity as a medical problem. *Nature*, *404*(6778), 635-643.

Koranian, P., Huang, Q., Dalai, A. K., & Sammynaiken, R. (2022). Chemicals Production from Glycerol through Heterogeneous Catalysis: A Review. *Catalysts, 12*(8), 897.

Kostyniuk, A., Bajec, D., & Likozar, B. (2020). One-step synthesis of ethanol from glycerol in a gas phase packed bed reactor over hierarchical alkali-treated zeolite catalyst materials. *Green Chemistry*, *22*(3), 753-765.

Krog, N. (2018). Food emulsifiers. In *Lipid technologies and applications* (pp. 521-534). Routledge.

Krüger, R. L., Valério, A., Balen, M., Ninow, J. L., Vladimir Oliveira, J., de Oliveira, D., & Corazza, M. L. (2010). Improvement of mono and diacylglycerol production via enzymatic glycerolysis in *tert*-butanol system. *European Journal of Lipid Science and Technology*, *112*(8), 921-927.

Kumar, A., Dhar, K., Kanwar, S. S., & Arora, P. K. (2016). Lipase catalysis in organic solvents: advantages and applications. *Biological Procedures Online*, *18*(1), 1-11.

Kundu, S., Bhangale, A. S., Wallace, W. E., Flynn, K. M., Guttman, C. M., Gross, R. A., & Beers, K. L. (2011). Continuous flow enzyme-catalyzed polymerization in a microreactor. *Journal of the American Chemical Society*, *133*(15), 6006-6011.

Kunz, C., Schuldt-Lieb, S., & Gieseler, H. (2018). Freeze-drying from organic cosolvent systems, part 1: thermal analysis of cosolvent-based placebo formulations in the frozen State. *Journal of Pharmaceutical Sciences*, *107*(3), 887-896.

Kunz, C., Schuldt-Lieb, S., & Gieseler, H. (2019). Freeze-drying from organic co-solvent systems, part 2: process modifications to reduce residual solvent levels and improve product quality attributes. *Journal of Pharmaceutical Sciences*, *108*(1), 399-415.

Kuo, S. J., & Parkin, K. L. (1996). Solvent polarity influences product selectivity of lipase-mediated esterification reactions in microaqueous media. *Journal of the American Oil Chemists' Society*, *73*(11), 1427-1433.

Laane, C., Boeren, S., Vos, K., & Veeger, C. (1987). Rules for optimization of biocatalysis in organic solvents. *Biotechnology and Bioengineering*, *30*(1), 81-87.

Lakshmnarayanan, S., Shereen, M. F., Niraimathi, K. L., Brindha, P., & Arumugam, A. (2021). One-pot green synthesis of iron oxide nanoparticles from *Bauhinia tomentosa*: Characterization and application towards synthesis of 1, 3 diolein. *Scientific Reports*, *11*(1), 1-13.

Lee, A., Yoo, H. J., Kim, M., Kim, M., Choi, J. H., Lee, C., & Lee, J. H. (2019). Effects of equivalent medium-chain diacylglycerol or long-chain triacylglycerol oil intake

via muffins on postprandial triglycerides and plasma fatty acids levels. *Journal of Functional Foods*, *53*, 299-305.

Lee, K. W. Y., Porter, C. J., & Boyd, B. J. (2013). A simple quantitative approach for the determination of long and medium chain lipids in bio-relevant matrices by high performance liquid chromatography with refractive index detection. *Aaps Pharmscitech*, *14*(3), 927-934.

Lee, Y. Y., Tang, T. K., Phuah, E. T., Karim, N. A. A., Alwi, S. M. M., & Lai, O. M. (2015). Palm-based medium-and-long-chain triacylglycerol (P-MLCT): Production via enzymatic interesterification and optimization using response surface methodology (RSM). *Journal of Food Science and Technology*, *52*(2), 685-696.

Lega, I. C., & Lipscombe, L. L. (2020). Diabetes, obesity, and cancer-pathophysiology and clinical implications. *Endocrine Reviews*, *41*(1), 33-52.

Lei, M., Zhang, N., Lee, W. J., Tan, C. P., Lai, O. M., Wang, Y., & Qiu, C. (2020). Non-aqueous foams formed by whipping diacylglycerol stabilized oleogel. *Food Chemistry*, *312*, 126047

Li, Q., Cai, L., Cui, W., Wang, G., He, J., & Golden, A. R. (2018). Economic burden of obesity and four obesity-related chronic diseases in rural Yunnan Province, China. *Public Health*, *164*, 91-98.

Li, D., Zhong, X., Faiza, M., Wang, W., Lian, W., Liu, N., & Wang, Y. (2021). Simultaneous preparation of edible quality medium and high purity diacylglycerol by a novel combined approach. *LWT*, 111949.

Liao, X., Zhu, Y., Wang, S. G., Chen, H., & Li, Y. (2010). Theoretical elucidation of acetylating glycerol with acetic acid and acetic anhydride. *Applied Catalysis B: Environmental*, *94*(1-2), 64-70.

Lilly, M. D., Hornby, W. E., & Crook, E. M. (1966). The kinetics of carboxymethylcellulose-ficin in packed beds. *Biochemical Journal*, *100*(3), 718.

Lima, P. J. M., da Silva, R. M., Neto, C. A. C. G., Gomes e Silva, N. C., Souza, J. E. D. S., Nunes, Y. L., & Sousa dos Santos, J. C. (2021). An overview on the conversion of glycerol to value-added industrial products via chemical and biochemical routes. *Biotechnology and Applied Biochemistry* (online version).

Liu, N., Wang, Y., Zhao, Q., & Zhao, M. (2014). Production of palm oil-based diacylglycerol using Lecitase Ultra-catalyzed glycerolysis and molecular distillation. *Food Science and Biotechnology*, *23*(2), 365-371.

Liu, M., Fu, J., Teng, Y., Zhang, Z., Zhang, N., & Wang, Y. (2016). Fast production of diacylglycerol in a solvent free system via lipase catalyzed esterification using a bubble column reactor. *Journal of the American Oil Chemists' Society*, *93*(5), 637-648.

Liu, N., Cui, J., Li, G., Li, D., Chang, D., Li, C., & Chen, X. (2019a). The application of high purity diacylglycerol oil in whipped cream: effect on the emulsion properties and whipping characteristics. *CyTA-Journal of Food*, *17*(1), 60-68.

Liu, X., Meng, X. Y., Xu, Y., Dong, T., Zhang, D. Y., Guan, H. X., ... & Wang, J. (2019b). Enzymatic synthesis of 1-caffeoylglycerol with deep eutectic solvent under continuous microflow conditions. *Biochemical Engineering Journal*, *142*, 41-49.

Liu, N., Li, N., Faiza, M., Li, D., Yao, X., & Zhao, M. (2021a). Stability and in vitro digestion of high purity diacylglycerol oil-in-water emulsions. *LWT*, *148*, 111744.

Liu, X., Shi, W., Xu, L., Yang, B., Liao, S., Lan, D., ... & Wang, Y. (2021b). Two-step enzymatic synthesis of α-linolenic acid-enriched diacylglycerols with high purities from silkworm pupae oil. Bioprocess and Biosystems Engineering, 44(3), 627-634.

Lo, S. K., Tan, C. P., Long, K., Yusoff, M., Affandi, S., & Lai, O. M. (2008). Diacylglycerol oil—properties, processes and products: a review. *Food and Bioprocess Technology*, *1*(3), 223-233.

Long, Z., Zhao, M., Liu, N., Liu, D., Sun-Waterhouse, D., & Zhao, Q. (2015). Physicochemical properties of peanut oil-based diacylglycerol and their derived oil-in-water emulsions stabilized by sodium caseinate. *Food Chemistry*, *184*, 105-113.

Lortie, R., Trani, M., & Ergan, F. (1993). Kinetic study of the lipase-catalyzed synthesis of triolein. *Biotechnology and Bioengineering*, *41*(11), 1021-1026.

Lu, Y., Zou, X., Han, W., Jiang, Y., Jin, Q., Li, L., ... & Wang, X. (2016). Preparation of diacylglycerol-enriched rice bran oil by lipase-catalyzed deacidification in packed-bed reactors by continuous dehydration. *Journal of Oleo Science*, *65*(2), 151-159.

Macias-Rodriguez, B., & Marangoni, A. G. (2016). Physicochemical and rheological characterization of roll-in shortenings. *Journal of the American Oil Chemists' Society*, *93*(4), 575-585.

Mahbub, N., Gemechu, E., Zhang, H., & Kumar, A. (2019). The life cycle greenhouse gas emission benefits from alternative uses of biofuel coproducts. *Sustainable Energy Technologies and Assessments*, *34*, 173-186.

Marangoni, A. G. (2003). *Enzyme kinetics: a modern approach*. John Wiley & Sons, Hoboken, New Jersey.

Mardani, M., Farmani, J. A. M. S. H. I. D., & Esmaeilzadeh Kenari, R. (2015). Efficacy of some commercial lipases in hydrolysis of palm olein for production of free fatty acids and diacylglycerol oil. *Journal of Oil Palm Research*, *27*(3), 1-2.

Matos, L. M., Leal, I. C., & de Souza, R. O. (2011). Diacylglycerol synthesis by lipase-catalyzed partial hydrolysis of palm oil under microwave irradiation and continuous flow conditions. *Journal of Molecular Catalysis B: Enzymatic*, *72*(1-2), 36-39.

Matosevic, S., Lye, G. J., & Baganz, F. (2011). Immobilised enzyme microreactor for screening of multi-step bioconversions: Characterisation of a de novo transketolase-ω-transaminase pathway to synthesise chiral amino alcohols. *Journal of Biotechnology*, *155*(3), 320-329.

Meng, X., Zou, D., Shi, Z., Duan, Z., & Mao, Z. (2004). Dietary diacylglycerol prevents high-fat diet-induced lipid accumulation in rat liver and abdominal adipose tissue. *Lipids*, *39*(1), 37-41.

Mohamed, I. O. (2012). Lipase-catalyzed synthesis of cocoa butter equivalent from palm olein and saturated fatty acid distillate from palm oil physical refinery. *Applied biochemistry and biotechnology*, *168*(6), 1405-1415.

Mohamed, I. O. (2013). Lipase-catalyzed acidolysis of palm mid fraction oil with palmitic and stearic fatty acid mixture for production of cocoa butter equivalent. *Applied biochemistry and biotechnology*, *171*(3), 655-666.

Monteiro, M. R., Kugelmeier, C. L., Pinheiro, R. S., Batalha, M. O., & da Silva César, A. (2018). Glycerol from biodiesel production: Technological paths for sustainability. *Renewable and Sustainable Energy Reviews*, *88*, 109-122.

Moo-Young, M., & Blanch, H. W. (1981). Design of biochemical reactors mass transfer criteria for simple and complex systems. In *Reactors and Reactions*. Springer, Berlin, Heidelberg.

Morita, O., & Soni, M. G. (2009). Safety assessment of diacylglycerol oil as an edible oil: a review of the published literature. *Food and Chemical Toxicology*, *47*(1), 9-21.

Myers, R. H., Montgomery, D. C., & Anderson-Cook, C. M. (2016). *Response surface methodology: process and product optimization using designed experiments*. John Wiley & Sons, New Jersey.

Naderi, M., Farmani, J., & Rashidi, L. (2016). Structuring of chicken fat by monoacylglycerols. *Journal of the American Oil Chemists' Society*, *93*(9), 1221-1231.

Naderi, M., Farmani, J., & Rashidi, L. (2018). Physicochemical and Rheological Properties and Microstructure of Canola oil as Affected by Monoacylglycerols. *Nutrition and Food Sciences Research*, *5*(1), 31-40.

Naik, M. K., Naik, S. N., & Mohanty, S. (2014). Enzymatic glycerolysis for conversion of sunflower oil to food based emulsifiers. *Catalysis Today*, *237*, 145-149.

Narayan, V. S., & Klibanov, A. M. (1993). Are water-immiscibility and apolarity of the solvent relevant to enzyme efficiency? *Biotechnology and Bioengineering*, *41*(3), 390-393.

Nda-Umar, U. I., Ramli, I., Taufiq-Yap, Y. H., & Muhamad, E. N. (2019). An overview of recent research in the conversion of glycerol into biofuels, fuel additives and other bio-based chemicals. *Catalysts*, *9*(1), 15.

Ng, S. P., Lai, O. M., Abas, F., Lim, H. K., & Tan, C. P. (2014). Stability of a concentrated oil-in-water emulsion model prepared using palm olein-based diacylglycerol/virgin coconut oil blends: Effects of the rheological properties, droplet size distribution and microstructure. *Food Research International*, *64*, 919-930.

Olivares, R. D. O., Okoye, P. U., Ituna-Yudonago, J. F., Njoku, C. N., Hameed, B. H., Song, W., ... & Sebastian, P. J. (2020). Valorization of biodiesel byproduct glycerol to glycerol carbonate using highly reusable apatite-like catalyst derived from waste Gastropoda Mollusca. *Biomass Conversion and Biorefinery*, 1-13.

Oliveira, P. D., Rodrigues, A. M., Bezerra, C. V., & Silva, L. H. (2017). Chemical interesterification of blends with palm stearin and patawa oil. *Food Chemistry*, *215*, 369-376.

Ornla-Ied, P., Rungsang, S., Tan, C. P., Lan, D., Wang, Y., & Sonwai, S. (2022). Production of cocoa butter substitute via enzymatic interesterification of fully hydrogenated palm kernel oil, coconut oil and fully hydrogenated palm stearin blends. *Journal of Oleo Science*, *71*(3), 343-351.

Ortiz, C., Ferreira, M. L., Barbosa, O., dos Santos, J. C., Rodrigues, R. C., Berenguer-Murcia, Á., ... & Fernandez-Lafuente, R. (2019). Novozym 435: the "perfect" lipase immobilized biocatalyst? *Catalysis Science & Technology, 9*(10), 2380-2420.

Osório, N. M., Dubreucq, E., da Fonseca, M. M. R., & Ferreira-Dias, S. (2009). Lipase/acyltransferase-catalysed interesterification of fat blends containing n-3 polyunsaturated fatty acids. *European Journal of Lipid Science and Technology*, *111*(2), 120-134.

Pala Rosas, I., Contreras, J. L., Salmones, J., Tapia, C., Zeifert, B., Navarrete, J., ... & García, D. C. (2017). Catalytic dehydration of glycerol to acrolein over a catalyst of Pd/LaY zeolite and comparison with the chemical equilibrium. *Catalysts*, *7*(3), 73.

Pang, M., Ge, Y., Cao, L., Cheng, J., & Jiang, S. (2019). Physicochemical properties, crystallization behavior and oxidative stabilities of enzymatic interesterified fats of beef tallow, palm stearin and camellia oil blends. *Journal of Oleo Science*, *68*(2), 131-139.

Paula, A. V., Nunes, G. F., Osório, N. M., Santos, J. C., de Castro, H. F., & Ferreira-Dias, S. (2015a). Continuous enzymatic interesterification of milkfat with soybean oil produces a highly spreadable product rich in polyunsaturated fatty acids. *European Journal of Lipid Science and Technology*, *117*(5), 608-619.

Paula, A. V., Nunes, G. F., de Castro, H. F., & Santos, J. C. (2015b). Synthesis of structured lipids by enzymatic interesterification of milkfat and soybean oil in a basket-type stirred tank reactor. *Industrial & Engineering Chemistry Research*, *54*(6), 1731-1737.

Pazdur, Ł., Geuens, J., Sels, H., & Tavernier, S. M. (2015). Low-temperature chemical synthesis of high-purity diacylglycerols (DAG) from monoacylglycerols (MAG). *Lipids*, *50*(2), 219-226.

Pedro, K. C., Parreira, J. M., Correia, I. N., Henriques, C. A., & Langone, M. A. (2018). Enzymatic biodiesel synthesis from acid oil using a lipase mixture. *Química Nova*, *41*, 284-291.

Pencreac'h, G., & Baratti, J. C. (1996). Hydrolysis of p-nitrophenyl palmitate in n-heptane by the Pseudomonas cepacia lipase: a simple test for the determination of lipase activity in organic media. *Enzyme and Microbial Technology*, *18*(6), 417-422.

Phuah, E. T., Lai, O. M., Choong, T. S. Y., Tan, C. P., & Lo, S. K. (2012). Kinetic study on partial hydrolysis of palm oil catalyzed by *Rhizomucor miehei* lipase. *Journal of Molecular Catalysis B: Enzymatic*, *78*, 91-97.

Phuah, E. T., Tang, T. K., Lee, Y. Y., Choong, T. S. Y., Tan, C. P., & Lai, O. M. (2015). Review on the current state of diacylglycerol production using enzymatic approach. *Food and Bioprocess Technology*, *8*(6), 1169-1186.

Phuah, E. T., Beh, B. K., Lim, C. S. Y., Tang, T. K., Lee, Y. Y., & Lai, O. M. (2016a). Rheological properties, textural properties, and storage stability of palm kernel-based diacylglycerol-enriched mayonnaise. *European Journal of Lipid Science and Technology*, *118*(2), 185-194.

Phuah, E. T., Lee, Y. Y., Tang, T. K., Lai, O. M., Choong, T. S. Y., Tan, C. P., ... & Lo, S. K. (2016b). Modeling and optimization of lipase-catalyzed partial hydrolysis for diacylglycerol production in packed bed reactor. *International Journal of Food Engineering*, *12*(7), 681-689.

Razak, N., & Annuar, M. (2015). Enzymatic synthesis of flavonoid ester: elucidation of its kinetic mechanism and equilibrium thermodynamic behavior. *Industrial & Engineering Chemistry Research*, *54*(21), 5604-5612.

Reichardt, C. (2003). *Solvent effects in organic chemistry*, Wiley-VCH: Marburg,

Remonatto, D., Júnior, R. H. M., Monti, R., Bassan, J. C., & de Paula, A. V. (2022). Applications of immobilized lipases in enzymatic reactors: A review. *Process Biochemistry*, *114*, 1-20.

Ribeiro, B. D., Castro, A. M. D., Coelho, M. A. Z., & Freire, D. M. G. (2011). Production and use of lipases in bioenergy: a review from the feedstocks to biodiesel production. *Enzyme Research*, *2011*.

Rodríguez, A., Esteban, L., Martín, L., Jiménez, M. J., Hita, E., Castillo, B., ... & Robles, A. (2012). Synthesis of 2-monoacylglycerols and structured triacylglycerols rich in polyunsaturated fatty acids by enzyme catalyzed reactions. *Enzyme and microbial technology*, *51*(3), 148-155.

Romain, V., Ngakegni-Limbili, A. C., Mouloungui, Z., & Ouamba, J. M. (2013). Thermal properties of monoglycerides from *Nephelium lappaceum* L. Oil, as a natural source of saturated and monounsaturated fatty acids. *Industrial & Engineering Chemistry Research*, *52*(39), 14089-14098.

Rønne, T. H., Yang, T., Mu, H., Jacobsen, C., & Xu, X. (2005). Enzymatic interesterification of butterfat with rapeseed oil in a continuous packed bed reactor. *Journal of Agricultural and Food Chemistry*, *53*(14), 5617-5624.

Ruela, H. S., Sutili, F. K., Leal, I. C., Carvalho, N. M., Miranda, L. S., & de Souza, R. O. (2013). Lipase-catalyzed synthesis of secondary glucose esters under continuous flow conditions. *European Journal of Lipid Science and Technology*, *115*(4), 464-467.

Saadi, S., Ariffin, A. A., Ghazali, H. M., Abdulkarim, M. S., Boo, H. C., & Miskandar, M. S. (2012). Crystallisation regime of w/o emulsion [eg multipurpose margarine] models during storage. *Food Chemistry*, *133*(4), 1485-1493.

Saat, M. N., & Annuar, M. S. M. (2020). Statistical analysis of one-pot lipase-catalyzed esterification of ϵ-caprolactone with methyl-d-glucopyranoside and its extension. *Biocatalysis and Agricultural Biotechnology*, *23*, 101464.

Šabeder, S., Habulin, M., & Knez, Ž. (2006). Lipase-catalyzed synthesis of fatty acid fructose esters. *Journal of Food Engineering*, *77*(4), 880-886.

Saberi, A. H., Chin-Ping, T., & Oi-Ming, L. (2011). Phase behavior of palm oil in blends with palm-based diacylglycerol. *Journal of the American oil chemists' society*, *88*(12), 1857-1865.

Saberi, A. H., Kee, B. B., Oi-Ming, L., & Miskandar, M. S. (2011). Physico-chemical properties of various palm-based diacylglycerol oils in comparison with their corresponding palm-based oils. *Food Chemistry*, *127*(3), 1031-1038.

Saberi, A. H., Lai, O. M., & Miskandar, M. S. (2012). Melting and solidification properties of palm-based diacylglycerol, palm kernel olein, and sunflower oil in the preparation of palm-based diacylglycerol-enriched soft tub margarine. *Food and Bioprocess Technology*, *5*(5), 1674-1685.

Safi, A., Nicolas, C., Neau, E., & Chevalier, J. L. (2007). Diffusion coefficients of aromatic compounds at infinite dilution in binary mixtures at 298.15 K. *Journal of Chemical & Engineering Data*, *52*(1), 126-130.

Said, K. A. M., & Amin, M. A. M. (2015). Overview on the response surface methodology (RSM) in extraction processes. *Journal of Applied Science & Process Engineering*, *2*(1), 8-17.

Saitou, K., Mitsui, Y., Shimizu, M., Kudo, N., Katsuragi, Y., & Sato, K. (2012). Crystallization behavior of diacylglycerol-rich oils produced from rapeseed oil. *Journal of the American Oil Chemists' Society*, *89*(7), 1231-1239.

Sakthivel, A., Nakamura, R., Komura, K., & Sugi, Y. (2007). Esterification of glycerol by lauric acid over aluminium and zirconium containing mesoporous molecular sieves in supercritical carbon dioxide medium. *The Journal of Supercritical Fluids*, *42*(2), 219-225.

Šalić, A., Tušek, A. J., Sander, A., & Zelić, B. (2018). Lipase catalysed biodiesel synthesis with integrated glycerol separation in continuously operated microchips connected in series. *New Botechnology*, *47*, 80-88

Salsinha, A. S., Rodríguez-Alcalá, L. M., Relvas, J. B., & Pintado, M. E. (2021). Fatty acids role on obesity induced hypothalamus inflammation: From problem to solution-A review. *Trends in Food Science & Technology*, *112*, 592-607.

Salvi, H. M., Kamble, M. P., & Yadav, G. D. (2018). Synthesis of geraniol esters in a continuous-flow packed-bed reactor of immobilized lipase: Optimization of process parameters and kinetic modeling. *Applied Biochemistry and Biotechnology*, *184*(2), 630-643.

Samul, D., Leja, K., & Grajek, W. (2014). Impurities of crude glycerol and their effect on metabolite production. *Annals of Microbiology*, *64*(3), 891-898.

Sánchez, D. A., Tonetto, G. M., & Ferreira, M. L. (2020). Valorization of glycerol through the enzymatic synthesis of acylglycerides with high nutritional value. *Catalysts*, *10*(1), 116.

Sarmah, N., Revathi, D., Sheelu, G., Yamuna Rani, K., Sridhar, S., Mehtab, V., & Sumana, C. (2018). Recent advances on sources and industrial applications of lipases. *Biotechnology progress*, *34*(1), 5-28.

Sarmah, N., Revathi, D., Sheelu, G., Yamuna Rani, K., Sridhar, S., Mehtab, V., & Sumana, C. (2018). Recent advances on sources and industrial applications of lipases. *Biotechnology Progress*, *34*(1), 5-28.

Satyawali, Y., Cauwenberghs, L., Maesen, M., & Dejonghe, W. (2021). Lipase catalyzed solvent free synthesis of monoacylglycerols in various reaction systems and coupling reaction with pervaporation for in situ water removal. *Chemical Engineering and Processing-Process Intensification*, *166*, 108475.

Savaghebi, D., Safari, M., Rezaei, K., Ashtari, P., & Farmani, J. (2012). Structured lipids produced through lipase-catalyzed acidolysis of canola oil. *Journal of Agricultural Science and Technology, 14*(3), 1297-1310.

Savickaite, A., Sadauskas, M., & Gudiukaite, R. (2021). Immobilized GDEst-95, GDEst-lip and GD-95RM lipolytic enzymes for continuous flow hydrolysis and transesterification reactions. *International Journal of Biological Macromolecules*, *173*, 421-434.

Saw, M. H., & Siew, W. L. (2014). The effectiveness of immobilized lipase Thermomyces lanuginosa in catalyzing interesterification of palm olein in batch reaction. *Journal of Oleo Science*, *63*(3), 295-302.

Schmid, R. D., & Verger, R. (1998). Lipases: interfacial enzymes with attractive applications. *Angewandte Chemie International Edition*, *37*(12), 1608-1633.

Segel I. H. (1975). *Enzyme kinetics: Behavior and analysis of rapid equilibrium and steady state enzyme systems.* John Wiley & Sons Inc, New York.

Sengupta, A., Roy, S., Mukherjee, S., & Ghosh, M. (2015). Production of medium chain fatty acid rich mustard oil using packed bed bioreactor. *Journal of Oleo Science*, *64*(2), 153-159.

Seong, G. H., Heo, J., & Crooks, R. M. (2003). Measurement of enzyme kinetics using a continuous-flow microfluidic system. *Analytical Chemistry*, *75*(13), 3161-3167.

Shabbir, A., Mukhtar, H., Mumtaz, M. W., & Rashid, U. (2020). Green synthesis of biodiesel using microbial lipases. *Applications of Nanotechnology for Green Synthesis*, 407-433.

Shakerardekani, A., Karim, R., Ghazali, H. M., & Chin, N. L. (2013). The effect of monoglyceride addition on the rheological properties of pistachio spread. *Journal of the American Oil Chemists' Society*, *90*(10), 1517-1521.

Sharma, S., & Kanwar, S. S. (2014). Organic solvent tolerant lipases and applications. *The Scientific World Journal*, *2014*.

Sharma, R. K., O'Neill, C. A., Ramos, H. A., Thapa, B., Barcelo-Bovea, V. C., Gaur, K., & Griebenow, K. (2019). Candida rugosa lipase nanoparticles as robust catalyst for biodiesel production in organic solvents. *Biofuel Research Journal*, *6*(3), 1025.

Sheldon, R. A., & van Pelt, S. (2013). Enzyme immobilisation in biocatalysis: why, what and how. *Chemical Society Reviews*, *42*(15), 6223-6235.

Shimada, Y., Watanabe, Y., Samukawa, T., Sugihara, A., Noda, H., Fukuda, H., & Tominaga, Y. (1999). Conversion of vegetable oil to biodiesel using immobilized *Candida antarctica* lipase. *Journal of the American Oil Chemists' Society*, *76*(7), 789-793.

Shin, J. A., Yang, D., Gan, L., Hong, S. T., Lee, E. S., Park, S. H., & Lee, K. T. (2013). Preparation of Recombined Milk Using Modified Butterfats Containing α-Linolenic Acid. *Journal of food science*, *78*(1), C17-C24.

Shuler, M.L. & Kargi, F. (2002). *Bioprocess Engineering Basic Concepts,* Prentice-Hall, New Jersey.

Siriwardhana, N., Kalupahana, N. S., & Moustaid-Moussa, N. (2012). Health benefits of n-3 polyunsaturated fatty acids: eicosapentaenoic acid and docosahexaenoic acid. *Advances in Food and Nutrition Research*, *65*, 211-222.

Skliar, V., Krusir, G., & Zakharchuk, V. (2020). Investigation of enzymatic hydrolysis of fatty waste processing of sunflower seeds by immobilized lipase. *Grain Products and Mixed Fodder's*, *20*(1), 5-11.

Song, Z., Liu, Y., Jin, Q., Li, L., Wang, X., Huang, J., & Liu, R. (2012). Lipase-catalyzed preparation of diacylglycerol-enriched oil from high-acid rice bran oil in solvent-free system. *Applied biochemistry and biotechnology*, *168*(2), 364-374.

Sonntag, N. O. (1982). Glycerolysis of fats and methyl esters - Status, review and critique. *Journal of the American Oil Chemists' Society*, *59*(10), 795A-802A.

Staniewski, B, Dorota O., Katarzyna, & Jarosław K. The effect of triacylglycerol and fatty acid composition on the rheological properties of butter. *International Dairy Journal*, 114*(2021),* 104913.

Stankiewicz, A., & Moulijn, J. A. (2002). Process intensification. *Industrial & Engineering Chemistry Research*, *41*(8), 1920-1924.

Subroto, E. (2020). Monoacylglycerols and diacylglycerols for fat-based food products: a review. *Food Research*, *4*(4), 932-943.

Subroto, E., Wisamputri, M. F., Utami, T., & Hidayat, C. (2020). Enzymatic and chemical synthesis of high mono-and diacylglycerol from palm stearin and olein blend at different type of reactor stirrers. *Journal of the Saudi Society of Agricultural Sciences*, *19*(1), 31-36.

Sun, Y., Hu, J., An, S., Zhang, Q., Guo, Y., Song, D., & Shang, Q. (2017). Selective esterification of glycerol with acetic acid or lauric acid over rod-like carbon-based sulfonic acid functionalized ionic liquids. *Fuel*, *207*, 136-145.

Sutili, F. K., Ruela, H. S., Leite, S. G., Miranda, L. S. D. M., Leal, I. C., & de Souza, R. O. (2013). Lipase-catalyzed esterification of steric hindered fructose derivative by continuous flow and batch conditions. *Journal of Molecular Catalysis B: Enzymatic*, *85*, 37-42.

Tamborini, L., Fernandes, P., Paradisi, F., & Molinari, F. (2018). Flow bioreactors as complementary tools for biocatalytic process intensification. *Trends in Biotechnology*, *36*(1), 73-88.

Teixeira, L. F., Bôas, R. V., Oliveira, P. C., & de Castro, H. F. (2014). Effect of natural antioxidants on the lipase activity in the course of batch and continuous glycerolysis of babassu oil. *Bioprocess and Biosystems Engineering*, *37*(9), 1717-1725.

Telle-Hansen, V. H., Narverud, I., Retterstøl, K., Wesseltoft-Rao, N., Mosdøl, A., Granlund, L., ... & Ulven, S. M. (2012). Substitution of TAG oil with diacylglycerol oil in food items improves the predicted 10 years cardiovascular risk score in healthy, overweight subjects. *Journal of Nutritional Science*, *1*.

Tentori, F., Brenna, E., Crotti, M., Pedrocchi-Fantoni, G., Ghezzi, M. C., & Tessaro, D. (2020). Continuous-flow biocatalytic process for the synthesis of the best stereoisomers of the commercial fragrances leather cyclohexanol (4-isopropylcyclohexanol) and woody acetate (4-(*tert*-butyl) cyclohexyl acetate). *Catalysts*, *10*(1), 102.

Tian, M., Wang, Z. Y., Fu, J. Y., Li, H. W., Zhang, J., Zhang, X. F., ... & Lv, P. M. (2021). Crude glycerol impurities improve *Rhizomucor miehei* lipase production by Pichia pastoris. *Preparative Biochemistry & Biotechnology*, *51*(9), 860-870.

Todero, L. M., Bassi, J. J., Lage, F. A., Corradini, M. C. C., Barboza, J., Hirata, D. B., & Mendes, A. A. (2015). Enzymatic synthesis of isoamyl butyrate catalyzed by immobilized lipase on poly-methacrylate particles: optimization, reusability and mass transfer studies. *Bioprocess and Biosystems Engineering*, *38*(8), 1601-1613.

Trasande, L., & Elbel, B. (2012). The economic burden placed on healthcare systems by childhood obesity. *Expert Review of Pharmacoeconomics & Outcomes Research*, *12*(1), 39-45.

Tripathi, V., Trivedi, R., & Singh, R. P. (2006). Lipase-catalyzed synthesis of diacylglycerol and monoacylglycerol from unsaturated fatty acid in organic solvent system. *Journal of Oleo Science*, *55*(2), 65-69.

Truong, T., Prakash, S., & Bhandari, B. (2019). Effects of crystallisation of native phytosterols and monoacylglycerols on foaming properties of whipped oleogels. *Food Chemistry*, *285*, 86-93.

Utama, Q. D., Sitanggang, A. B., Adawiyah, D. R., & Hariyadi, P. (2022). Lipase-catalyzed transesterification of medium-long-medium structured lipid (MLM-SL) using palm olein and palm kernel oil in batch and continuous systems. *Journal of Microbiology, Biotechnology and Food Sciences*, e3742-e3742.

Valerio, O., Horvath, T., Pond, C., Misra, M., & Mohanty, A. (2015). Improved utilization of crude glycerol from biodiesel industries: Synthesis and characterization of sustainable biobased polyesters. *Industrial Crops and Products*, *78*, 141-147.

Valerio, O., Misra, M., & Mohanty, A. K. (2018). Poly (glycerol-co-diacids) polyesters: from glycerol biorefinery to sustainable engineering applications, a review. *ACS Sustainable Chemistry & Engineering*, *6*(5), 5681-5693.

Vázquez, L., González, N., Reglero, G., & Torres, C. (2016). Solvent-free lipase-catalyzed synthesis of diacylgycerols as low-calorie food ingredients. *Frontiers in Bioengineering and Biotechnology*, *4*, 6.

Vereecken, J., Foubert, I., Meeussen, W., Lesaffer, A., & Dewettinck, K. (2009). Fat structuring with partial acylglycerols: Effect on solid fat profiles. *European Journal of Lipid Science and Technology*, *111*(3), 259-272.

Vereecken, J., De Graef, V., Smith, K. W., Wouters, J., & Dewettinck, K. (2010). Effect of TAG composition on the crystallization behaviour of model fat blends with the same saturated fat content. *Food Research International*, *43*(8), 2057-2067.

Verstringe, S., Danthine, S., Blecker, C., Depypere, F., & Dewettinck, K. (2013). Influence of monopalmitin on the isothermal crystallization mechanism of palm oil. *Food Research International*, *51*(1), 344-353.

Vilas Boas, R. N., Lima, R., Silva, M. V., Freitas, L., Aguiar, L. G., & de Castro, H. F. (2021). Continuous production of monoacylglycerol via glycerolysis of babassu oil by immobilized Burkholderia cepacia lipase in a packed bed reactor. *Bioprocess and Biosystems Engineering*, *44*(10), 2205-2215.

Vivek, N., Sindhu, R., Madhavan, A., Anju, A. J., Castro, E., Faraco, V., ... & Binod, P. (2017). Recent advances in the production of value added chemicals and lipids utilizing biodiesel industry generated crude glycerol as a substrate - metabolic aspects, challenges and possibilities: an overview. *Bioresource Technology*, *239*, 507-517.

Voll, F., Krüger, R. L., de Castilhos, F., Cardozo Filho, L., Cabral, V., Ninow, J., & Corazza, M. L. (2011). Kinetic modeling of lipase-catalyzed glycerolysis of olive oil. *Biochemical Engineering Journal*, *56*(3), 107-115.

Vucenik, I., & Stains, J. P. (2012). Obesity and cancer risk: evidence, mechanisms, and recommendations. *Annals of the New York Academy of Sciences*, *1271*(1), 37-43.

Wang, Y., Zhao, M., Song, K., Wang, L., Tang, S., & Riley, W. W. (2010). Partial hydrolysis of soybean oil by phospholipase A1 (Lecitase Ultra). *Food Chemistry*, *121*(4), 1066-1072.

Wang, J., Gu, S. S., Cui, H. S., Wu, X. Y., & Wu, F. A. (2014). A novel continuous flow biosynthesis of caffeic acid phenethyl ester from alkyl caffeate and phenethanol in a packed bed microreactor. *Bioresource Technology*, *158*, 39-47.

Wang, J., Liu, X., Wang, X. D., Dong, T., Zhao, X. Y., Zhu, D., ... & Wu, G. H. (2016a). Selective synthesis of human milk fat-style structured triglycerides from microalgal oil in a microfluidic reactor packed with immobilized lipase. *Bioresource Technology*, *220*, 132-141.

Wang, Z., Du, W., Dai, L., & Liu, D. (2016b). Study on Lipozyme TL IM-catalyzed esterification of oleic acid and glycerol for 1, 3-diolein preparation. *Journal of Molecular Catalysis B: Enzymatic*, *127*, 11-17. (not found)

Wang, X., Wang, X., Wang, W., Jin, Q., & Wang, X. (2018). Synthesis of docosapentaenoic acid-enriched diacylglycerols by enzymatic glycerolysis of *Schizochytrium* sp. oil. *Bioresource Technology*, *262*, 278-283.

Wang, S., Lee, W. J., Wang, Y., Tan, C. P., Lai, O. M., & Wang, Y. (2020a). Effect of purification methods on the physicochemical and thermodynamic properties and crystallization kinetics of medium-chain, medium–long-chain, and long-chain diacylglycerols. *Journal of Agricultural and Food Chemistry*, *68*(31), 8391-8403.

Wang, J. Z., Liu, X., Li, W. J., Song, W. M., Herman, R. A., Sheng, S., ... & Wang, J. (2020b). One hour enzymatic synthesis of structure lipids enriched unsaturated fatty acids from silkworm pupae oil under microwave irradiation. *Journal of Chemical Technology & Biotechnology*, *95*(2), 363-372.

Waraho, T., Cardenia, V., Nishino, Y., Seneviratne, K. N., Rodriguez-Estrada, M. T., McClements, D. J., & Decker, E. A. (2012). Antioxidant effects of mono-and diacylglycerols in non-stripped and stripped soybean oil-in-water emulsions. *Food Research International*, *48*(2), 353-358.

Watanabe, Y., Miyawaki, Y., Adachi, S., Nakanishi, K., & Matsuno, R. (2001). Continuous production of acyl mannoses by immobilized lipase using a packed-bed reactor and their surfactant properties. *Biochemical Engineering Journal*, *8*(3), 213-216.

Watanabe, T., Shimizu, M., Sugiura, M., Sato, M., Kohori, J., Yamada, N., & Nakanishi, K. (2003). Optimization of reaction conditions for the production of DAG using immobilized 1, 3-regiospecific lipase lipozyme RM IM. *Journal of the American Oil Chemists' Society*, *80*(12), 1201.

Watanabe, T., Sugiura, M., Sato, M., Yamada, N., & Nakanishi, K. (2005). Diacylglycerol production in a packed bed bioreactor. *Process Biochemistry, 40*(2), 637-643.

Weber, N., & Mukherjee, K. D. (2004). Solvent-free lipase-catalyzed preparation of diacylglycerols. *Journal of Agricultural and Food Chemistry*, *52*(17), 5347-5353.

Wilke, C. R., & Chang, P. (1955). Correlation of diffusion coefficients in dilute solutions. *AIChE Journal*, *1*(2), 264-270.

Woodley, J. M. (2019). Accelerating the implementation of biocatalysis in industry. *Applied Microbiology and Biotechnology*, *103*(12), 4733-4739.

World Health Organization,Obesity and overweight; https://www.670 who.int/news-room/fact-sheets/detail/obesity-and-overweight, 2020. 671 (accessed on 25 February 2021).

Xiao, F., Li, Z., & Pan, L. (2018). Application of microbial lipase and its research progress. *Progress in Applied Microbiology*, *1*(1).

Xu, D., Sun, L., Chen, H., Lan, D., Wang, Y., & Yang, B. (2012). Enzymatic synthesis of diacylglycerols enriched with conjugated linoleic acid by a novel lipase from Malassezia globosa. *Journal of the American Oil Chemists' Society*, *89*(7), 1259-1266.

Xu, Y., & Dong, C. (2017). Thermal and kinetic behaviors and microscopic characteristics of diacylglycerol-enriched palm-based oils blends. *European Journal of Lipid Science and Technology*, *119*(9), 1600491.

Xue, X., Dong, J., He, H., Wang, J., Kong, D., & Wang, L. (2021). Emulsification and stabilization of diacylglycerol-in-water pickering emulsions stabilized by ultrafine grinding oat bran insoluble fiber-gelatinized starch hybrid granules. *Food Hydrocolloids*, *112*, 106322.

Xue, X., He, H., Liu, C., Wang, L., Wang, L., Wang, Y., ... & Hou, R. (2022). L-Theanine improves emulsification stability and antioxidant capacity of diacylglycerol by hydrophobic binding β-lactoglobulin as emulsion surface stabilizer. *Food Chemistry*, *366*, 130557.

Yadav, M. G., Kavadia, M. R., Vadgama, R. N., Odaneth, A. A., & Lali, A. M. (2017). Green enzymatic production of glyceryl monoundecylenate using immobilized *Candida antarctica* lipase B. *Preparative Biochemistry and Biotechnology*, *47*(10), 1050-1058.

Yanai, H., Tomono, Y., Ito, K., Furutani, N., Yoshida, H., & Tada, N. (2007). Diacylglycerol oil for the metabolic syndrome. *Nutrition Journal*, *6*(1), 1-6.

Yang, F., Hanna, M. A., & Sun, R. (2012). Value-added uses for crude glycerol--a byproduct of biodiesel production. *Biotechnology for Biofuels*, *5*(1), 1-10.

Yang, J., Qiu, C., Li, G., Lee, W. J., Tan, C. P., Lai, O. M., & Wang, Y. (2020). Effect of diacylglycerol interfacial crystallization on the physical stability of water-in-oil emulsions. *Food Chemistry*, *327*, 127014.

Yang, Y. C., Vali, S. R., & Ju, Y. H. (2003). A process for synthesizing high purity monoglyceride. *Journal of the Chinese Institute of Chemical Engineers*, *34*(6), 617-623.

Yanık, D. K., Keskin, H., Fadıloğlu, S., & Göğüş, F. (2016). Acidolysis of terebinth fruit oil with palmitic and caprylic acids in a recirculating packed bed reactor: optimization using response surface methodology. *Grasas y Aceites*, *67*(2), e131-e131.

Ye, R., & Hayes, D. G. (2012). Solvent-free lipase-catalysed synthesis of saccharide-fatty acid esters: closed-loop bioreactor system with in situ formation of metastable suspensions. *Biocatalysis and Biotransformation*, *30*(2), 209-216.

Yesiloglu, Y., & Kilic, I. (2004). Lipase-catalyzed esterification of glycerol and oleic acid. *Journal of the American Oil Chemists' Society*, *81*(3), 281-284.

Yoshida, Y., Kimura, Y., Kadota, M., Tsuno, T., & Adachi, S. (2006). Continuous synthesis of alkyl ferulate by immobilized Candida antarctica lipase at high temperature. *Biotechnology Letters*, *28*(18), 1471-1474.

Yücel, S., Terzioğlu, P., & Özçimen, D. (2012). Lipase applications in biodiesel production. *Biodiesel-Feedstocks, Production and Applications. InTech, Croatia*, 209-250.

Zambelli, P., Tamborini, L., Cazzamalli, S., Pinto, A., Arioli, S., Balzaretti, S., ... & Romano, D. (2016). An efficient continuous flow process for the synthesis of a non-conventional mixture of fructooligosaccharides. *Food Chemistry*, *190*, 607-613.

Zhang, N., Yang, X., Fu, J., Chen, Q., Song, Z., & Wang, Y. (2016). Production of diacylglycerol-enriched oil by glycerolysis of soybean oil using a bubble column reactor in a solvent-free system. *Journal of Oleo Science*, ess15241.

Zhang, Y., Wang, X., Xie, D., Zou, S., Jin, Q., & Wang, X. (2018). Synthesis and concentration of 2-monoacylglycerols rich in polyunsaturated fatty acids. *Food Chemistry*, *250*, 60-66.

Zhang, Z., Song, J., Lee, W. J., Xie, X., & Wang, Y. (2020a). Characterization of enzymatically interesterified palm oil-based fats and its potential application as cocoa butter substitute. *Food Chemistry*, *318*, 126518.

Zhang, Z., Zhang, S., Lee, W. J., Lai, O. M., Tan, C. P., & Wang, Y. (2020b). Production of Structured triacylglycerol via enzymatic interesterification of medium-chain triacylglycerol and soybean oil using a pilot-scale solvent-free packed bed reactor. *Journal of the American Oil Chemists' Society*, *97*(3), 271-280.

Zhang, Z., Lee, W. J., Xie, X., Ye, J., Tan, C. P., Lai, O. M., ... & Wang, Y. (2021a). Enzymatic interesterification of palm stearin and palm olein blend catalyzed by *sn*-1, 3-specific lipase: Interesterification degree, acyl migration, and physical properties. *Journal of Agricultural and Food Chemistry*, *69*(32), 9056-9066.

Zhang, Z., Ye, J., Lee, W. J., Akoh, C. C., Li, A., & Wang, Y. (2021b). Modification of palm-based oil blend via interesterification: Physicochemical properties, crystallization behaviors and oxidative stabilities. *Food Chemistry*, *347*, 129070.

Zhao, J. F., Lin, J. P., Yang, L. R., & Wu, M. B. (2019). Preparation of high-purity 1, 3-diacylglycerol using performance-enhanced lipase immobilized on nanosized magnetite particles. *Biotechnology and Bioprocess Engineering*, *24*(2), 326-336.

Zhao, X., Sun, Q., Qin, Z., Liu, Q., & Kong, B. (2018). Ultrasonic pretreatment promotes diacylglycerol production from lard by lipase-catalysed glycerolysis and its physicochemical properties. *Ultrasonics Sonochemistry*, *48*, 11-18.

Zhong, N., Gui, Z., Xu, L., Huang, J., Hu, K., Gao, Y., ... & Li, B. (2013). Solvent-free enzymatic synthesis of 1, 3-Diacylglycerols by direct esterification of glycerol with saturated fatty acids. *Lipids in Health and Disease*, *12*(1), 1-7.

Zhong, N., Kou, M., Zhao, F., Yang, K., & Lin, S. (2019). Enzymatic production of diacylglycerols from high-acid soybean oil. *Journal of the American Oil Chemists' Society*, *96*(8), 967-974.

Zou, X., Jiang, X., Wen, Y., Wu, S., Nadege, K., Ninette, I., ... & Wang, X. (2020a). Enzymatic synthesis of structured lipids enriched with conjugated linoleic acid and butyric acid: strategy consideration and parameter optimization. *Bioprocess and Biosystems Engineering*, *43*(2), 273-282.

Zou, X., Nadege, K., Ninette, I., Wen, Y., Wu, S., Jiang, X., ... & Wang, X. (2020b). Preparation of docosahexaenoic acid-rich diacylglycerol-rich oil by lipase-catalyzed glycerolysis of microbial oil from *Schizochytrium* sp. in a solvent-free system. *Journal of the American Oil Chemists' Society*, *97*(3), 263-270.

LIST OF PUBLICATIONS & PAPERS PRESENTED

1. Abd Razak, N. N., Gew, L. T., Pérès, Y., Cognet, P., & Aroua, M. K. (2021). Statistical optimization and kinetic modeling of lipase-catalyzed synthesis of diacylglycerol in the mixture of acetone/*tert*-butanol solvent system. *Industrial & Engineering Chemistry Research, 60*(39), 14026–14037.

2. Abd Razak, N. N., Pérès, Y., Gew, L. T., Cognet, P., & Aroua, M. K. (2020). Effect of reaction medium mixture on the lipase catalyzed synthesis of diacylglycerol. *Industrial & Engineering Chemistry Research*, *59*(21), 9869-9881.

3. Abd Razak, N. N., Gew, L. T., Cognet, P., Pérès, Y., & Aroua, M. K. (2022). Kinetics and hydrodynamics of Candida antartica lipase-catalyzed synthesis of glycerol dioleate (GDO) in a continuous flow packed-bed millireactor. *Journal of Cleaner Production,* 373, 133816.

4. Abd Razak, N. N., Cognet, P., Pérès, Y., Gew, L. T., & Aroua, M. K. Application of continuous flow packed bed millireactor for the simultaneous production of mono- and diaclyglycerol using enzymatic catalysis. *International Symposium on Green Chemistry*, 16-20 May 2022, La Rochelle, France.

APPENDICES

Table A.1. Analysis of variance (ANOVA) for conversion (%)

Source	DF	Adj SS	Adj MS	*F*-Value	*P*-Value
Model	9	941.80	104.645	22.98	0.000
Linear	3	800.13	266.711	58.57	0.000
A	1	569.20	569.200	124.99	0.000
B	1	213.87	213.865	46.96	0.000
C	1	17.07	17.067	3.75	0.061
Square	3	55.77	18.591	4.08	0.014
A × A	1	8.23	8.232	1.81	0.187
B × B	1	38.19	38.190	8.39	0.006
C × C	1	5.13	5.132	1.13	0.296
2-Way Interaction	3	85.90	28.633	6.29	0.002
A × B	1	74.22	74.220	16.30	0.000
A × C	1	10.20	10.200	2.24	0.143
B × C	1	1.48	1.481	0.33	0.572
Error	35	159.39	4.554		
Lack-of-Fit	3	149.16	49.719	155.44	0.000
Pure Error	32	10.24	0.320		
Total	44	1101.20			

DF = Degrees of freedom; Adj SS = Adjusted sum of squares; Adj MS = Adjusted mean of squares; F: *F*-statistic; P: *P*-statistic

Table A.2. Analysis of variance (ANOVA) for GDO selectivity (%)

Source	DF	Adj SS	Adj MS	*F*-Value	*P*-Value
Model	9	1183.53	131.503	51.01	0.000
Linear	3	970.52	323.506	125.48	0.000
A	1	326.65	326.650	126.70	0.000
B	1	571.27	571.267	221.58	0.000
C	1	72.60	72.601	28.16	0.000
Square	3	204.04	68.012	26.38	0.000
A × A	1	0.22	0.220	0.09	0.772
B × B	1	184.85	184.846	71.70	0.000
C × C	1	28.33	28.334	10.99	0.002
2-Way Interaction	3	8.97	2.990	1.16	0.339
A × B	1	1.12	1.121	0.43	0.514
A × C	1	7.85	7.850	3.04	0.090
B × C	1	0.00	0.000	0.00	0.990
Error	35	90.24	2.578		
Lack-of-Fit	3	87.48	29.161	338.71	0.000
Pure Error	32	2.75	0.086		
Total	44	1273.76			

DF = Degrees of freedom; Adj SS = Adjusted sum of squares; Adj MS = Adjusted mean of squares; F: *F*-statistic; P: *P*-statistic

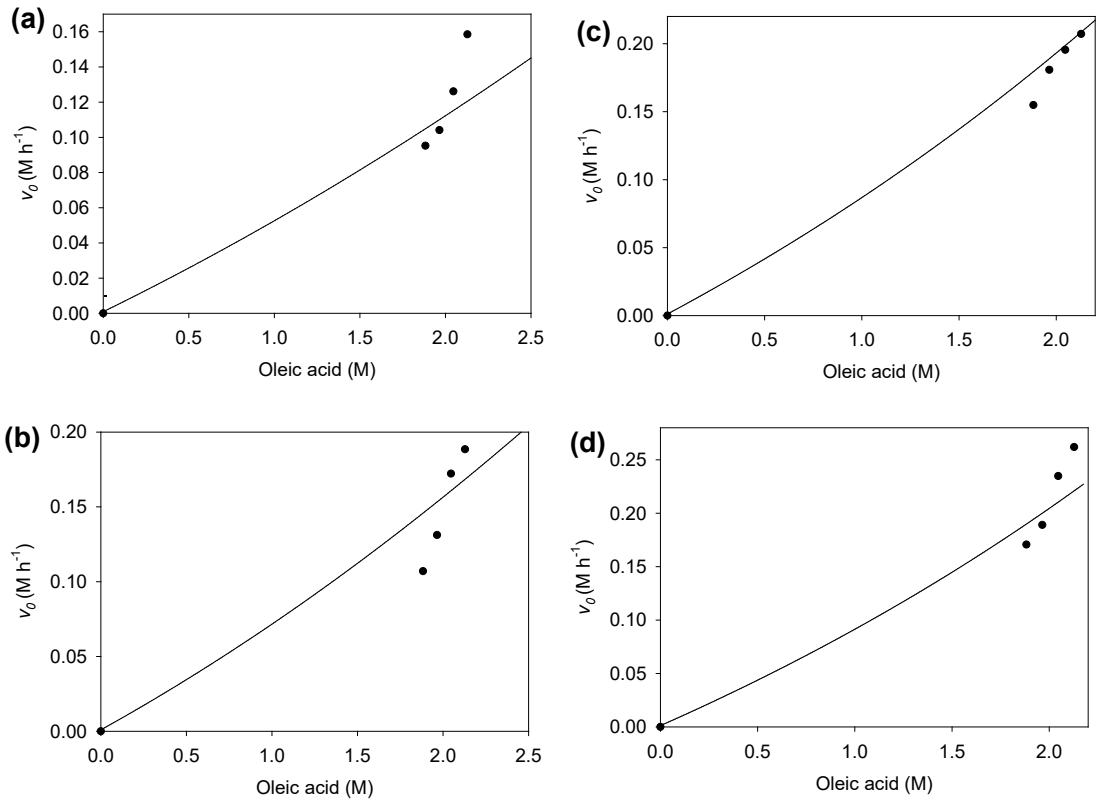

Figure A.1. Experimental and predicted initial rates (v_0) plots at different oleic acid concentrations with fixed glycerol concentrations (a) 0.31 M glycerol (b) 0.56 M glycerol (c) 0.82 M glycerol (d) 1.31 M glycerol. Symbols: (●) v_0 Experimental; (-) v_0 Predicted. Reaction condition: 45°C, 0.15 g enzyme and 200 ppm.

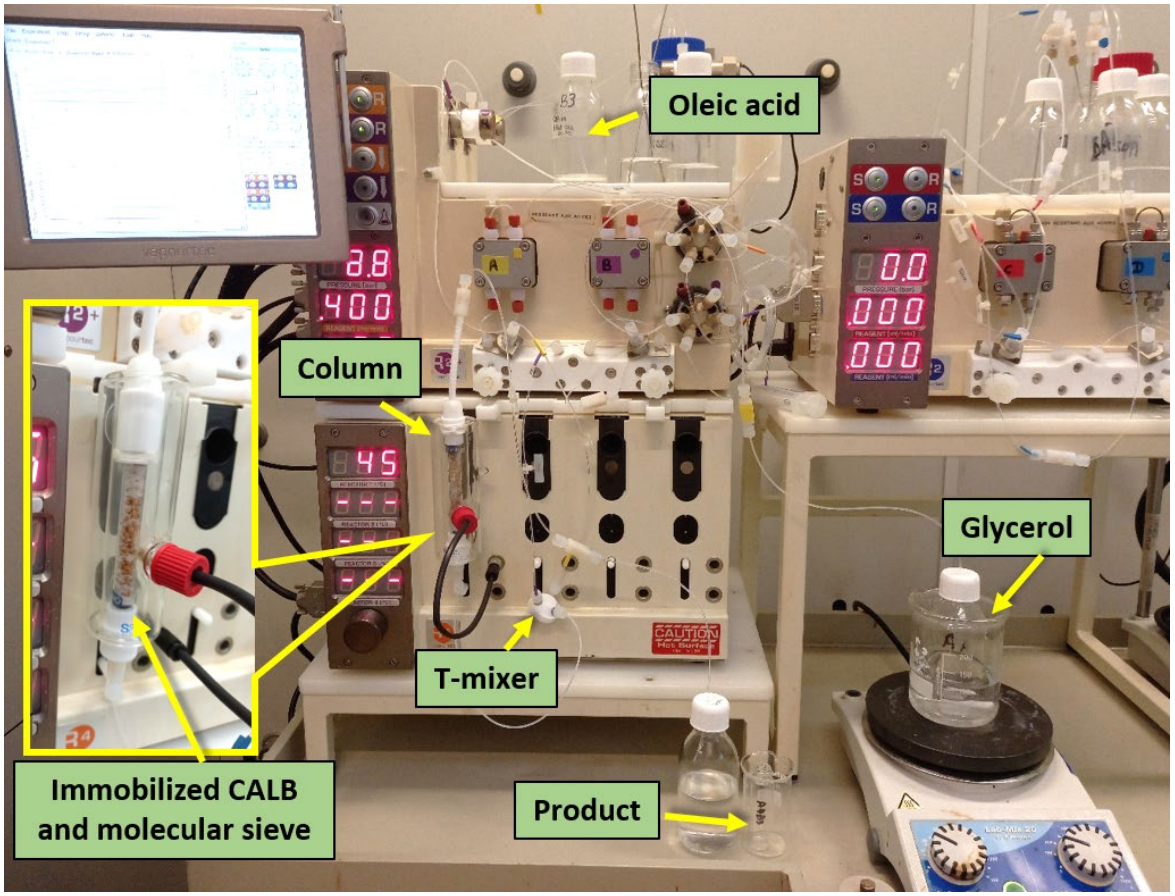

Figure A.2. Experimental set up for continuous flow reactor using an instrument namely VapourTech.



Figure A.3. Jacketed packed bed column (Omnifit) filled with lipase and molecular sieve